Energy efficient communications: from resource allocations to machine learning

Philippe Mary

Energy efficient communications : from resource allocations to machine learning

Présentée devant

l'Université de Rennes 1

pour obtenir

L'habilitation à diriger des recherches

Par

Philippe MARY

Maître de conférence INSA de Rennes, Laboratoire IETR UMR 6164

Spécialité : Traitement du signal et de l'image

Soutenue le 11 janvier 2018 devant la Commission d'examen

Président du Jury		
	Mr Pierre DUHAMEL	Senior research director CNRS, France
Rapporteurs		
	Mr Philippe CIBLAT	Professor Telecom ParisTech, France
	Mrs Laura COTTATELLUCCI	Professor FAU Erlangen-Nürnberg, Germany
	Mr Visa KOIVUNEN	Professor Aalto University, Finland
Examinateurs		
	Mr Jean-Marc BROSSIER	Professor Grenoble-INP, France
	Mr Marco DI RENZO	Researcher (HDR) CNRS, France
	Mme Maryline HÉLARD	Professor INSA Rennes, France
	Mr Christophe MOY	Professor University of Rennes 1, France

Remerciements

Il y a presque 10 ans, je soutenais ma thèse préparée à France Telecom R&D, à Grenoble et au Laboratoire CITI de l'INSA de Lyon et au moment de mettre un point final à ce manuscrit, je ne peux m'empêcher de me retourner pour contempler le chemin parcouru et adresser des remerciements à un certain nombre de personnes qui m'ont accompagnées et qui le feront sans doute encore dans les années à venir. Mes remerciements les plus chaleureux vont à ma famille pour tous les moments partagés et leur soutien ; Sophie qui m'a toujours soutenue et a enduré encore une fois un été de rédaction intense, ainsi qu'à Gabrielle et Léo qui ont dû passer une bonne partie des vacances « sans papa ».

Je tiens à remercier les personnes avec qui j'ai le plaisir de travailler à l'INSA de Rennes et au laboratoire IETR depuis mon recrutement comme Maître de Conférences en 2009 ; Maryline et Jean-François qui m'ont fourni un environnement de travail productif pour démarrer ma recherche rapidement ; arriver dans un laboratoire dans ces conditions facilite grandement l'émancipation d'un jeune chercheur. Merci également aux autres collègues, de l'IETR ou d'ailleurs, Matthieu, Jean-Yves, Christophe, Xavier, qui ont encadré avec moi les étudiants et pour les thématiques de recherche que ces collaborations ont apportées et que je n'aurais probablement pas explorées sans eux. Je n'oublie pas mes autres collègues du département SRC, permanents comme ceux de passage, pour les moments partagés qui font la vie d'un laboratoire et d'un département : qu'ils soient tous remerciés ici. Je tiens à remercier aussi les supports administratifs et techniques du département et laboratoire pour leur aide précieuse et leur disponibilité.

Merci également à Jean-Marie Gorce pour l'invitation à Princeton en 2014 qui a permis d'initier les travaux sur les paquets courts sans lesquels les perspectives de ce manuscrit seraient bien différentes aujourd'hui, ainsi qu'à Laurent Clavier pour le beau projet que l'on a su monter tous les trois et qui est tombé à point nommé pour l'écriture de ce document.

Une habilitation à diriger les recherches ne peut s'accomplir sans étudiants. Je voudrais donc remercier ici mes anciens doctorants Mohamad, Samih, Hiba, Ahmad, Navik pour la qualité de leur travail et les choses qu'ils m'ont apprises. Je n'oublie pas les étudiants de Master qui m'ont permis de tester ce qu'il me passait par la tête, en particulier les travaux autour du moment angulaire orbital pour les communications. Merci également aux étudiants de la formation SRC, qui sont le réceptacle des connaissances que nous engrangeons.

J'adresse toute ma gratitude aux trois rapporteurs qui ont acceptés d'expertiser ce manuscrit et ce dès le premier contact. Thanks to Laura Cottatellucci who accepted to review this manuscript while moving from Eurecom to FAU Erlangen and whom achievements on resource allocations shed the light on the work presented here. Thanks to Visa Koivunen, firstly met at Princeton in 2014 and whom renowned contributions in reinforcement learning approaches made him a relevant choice for reviewing these works. Merci à Philippe Ciblat, dont les compétences en traitement du signal et optimisation ont permis d'avoir une discussion des plus intéressantes autour de ces travaux lors de la soutenance. Je n'oublie pas également les autres membres du Jury qui ont accepté d'examiner ce travail avec attention : Maryline Hélard et Christophe Moy pour la partie locale, et une fois encore Maryline pour sa relecture attentive du manuscrit et les conseils prodigués lors de la finalisation du document ; Marco Di Renzo pour la discussion autour de la géométrie stochastique, merci à Jean-Marc Brossier et Pierre Duhamel qui, 10 ans après avoir examiné mes travaux de thèse, ont à nouveau accepté de se prêter à l'exercice pour l'HDR.

A Sophie, Gabrielle et Léo

Contents

Acronyms

We remind here abbreviations of the terms the most often used in the manuscript. The acronyms are defined when firstly encountered after the extended curriculum vitae. In the first part, some abbreviations are used but not reported in the list below. This is because they are used once and they are defined with a footnote on the page they are used.

AF	Amplify and Forward
ARAA	Adaptive Rate Allocation Algorithm
ARABBSP	Adaptive Rate Allocation with Branch and Bound and Signomial Programming
ARASP	Adaptive Rate Allocation with Signomial Programming
(A)SE	(Area) Spectral Efficiency
N/ACK	Non / acknowledgement
(H)ARQ	(Hybrid) automatic repeat request
ACNC	Address Correlated Network Coding
AWGN	Additive White Gaussian Noise
BC	Broadcast channel
BCSD	Basic Covering Set Discovery
BER	Bit Error Rate
BR	Broadcast Receiver
BS	Base Station
BT	Broadcast Transmitter
CCI	Co-Channel Interference
CDMA	Code Division Multiple Access
CR	Cognitive Radio
CRC	Cyclic Redundancy Check
CSI	Channel State Information
DF	Decode and Forward
DSSS	Direct Sequence Spread Spectrum
DVB	Digital Video Broadcasting
EE	Energy-Efficiency
FEC	Forward Error Correction
ICT	Information and Communications Technologies
i.i.d.	independently and identically distributed
IoT	Internet of Things
IRR	Immediate Repeat Request
ISR	Interference to Signal Ratio
LTE	Long Term Evolution
MAB	Multi-Armed Bandit
MAC	Multiple Access Channel

MAI	Multiple Access Interference
MCS	Modulation and Coding Scheme
MIMO	Multiple-Input Multiple-Output
MISO	Multiple-Input Single-Output
MMSE	Minimum Mean Square Error
M-PAM	M-ary Pulse Amplitude Modulation
M-PSK	M-ary Phase Shift Keying
M-QAM	M-ary Quadrature Shift Keying
MR	Mobile Receiver
NC	Network Coding
OAM	Orbital Angular Momentum
OSA	Opportunistic Spectrum Access
OSI	Open System Interconnexion
PEO	Packet Error Outage
PER	Packet Error Rate
PHY	PHYsical layer
PPP	Poisson Point Process
PSD	Power Spectral Density
PU	Primary User
QoS	Quality of Service
SEO	Symbol Error Outage
SER	Symbol Error Rate
SISO	Single-Input-Single-Output
OFDM	Orthogonal Frequency Division Multiplexing
OFDMA	Orthogonal Frequency Division Multiple Access
RB	Ressource Block
RF	Radio Frequency
RL	Reinforcement Learning
SINR	Signal to Interference and Noise Ratio
SLNR	Signal to Leakage plus Noise Ratio
SNR	Signal to Noise Ratio
STBC	Space-Time Block Code
SU	Secondary User
(D)THC	(Developed) Time Hopping Code
TH-UWB	Time Hopping Ultra Wide Band
UCB	Upper Confidence Bound
WLAN	Wireless Local Area Network
ZF	Zero Forcing

Foreword

This manuscript summarizes my career path since I has been recruited as Associate Professor at INSA Rennes in 2009 and my contributions to researches in telecommunications at the Institute of Electronics and Telecommunications of Rennes (IETR). This document is submitted as a partial fulfillment of the requirements for the *habilitation à diriger les recherches* degree of University of Rennes 1.

Even if an (short) Era comes to an end, I do not consider this achievement as a finality in itself. It is a milestone for sure, but an instantaneous photography at a time instant, that should be replaced in a moving context made of opportunities, successes and failures. Research is done with fundings that depend on several other factors than only the researcher will, like accepted projects, industrial collaborations and opportunities for instance. However, I think it is the duty of the academic researcher to do his/her best for seeking collaborations and projects that serve a longer term vision. From my part and thanks to an inspiring environment, I had the opportunity to conduct my researches where I wanted to, and I have tried, with this document, to show the common thread I followed, i.e. optimization of wireless network energy-efficiency. This document does not exhaustively present all my contributions, but I have tried to make this dissertation the most self-content as possible. To this end, I made the choice to present the results obtained with the five PhD students I had the luck to co-supervise so far. For each contribution, I have given the problem addressed, the related state of the art and the main achievements with theoretical or simulation results. The scientific contribution part may contain relatively detailed elements, but each chapter ends with a summary of the contributions and open issues in order to allow the bored reader to skip all equations but still catching the take-home message.

This document is divided into two parts. The first one summarizes my teaching and research activities as Associate Professor. This part contains three chapters; the first one is an extended curriculum vitae, with an exhaustive publication list at this time, the second chapter focuses on my teaching activities and provides the description of the courses I taught and the ones I am currently teaching, with some quantified data on my teaching service. The third chapter summarizes my research activities. First, the contributions of my PhD thesis are briefly reported and the main research paths I am investigating since 2009 are presented. The second part of the manuscript is dedicated to the scientific contributions achieved with the PhD students I have co-supervised and is divided in four chapters. The first one summarizes three contributions on resource allocations for multi-user communications. The second chapter focuses on network energy-efficiency through stochastic geometry and machine learning tools. The third chapter comes a bit aside from the previous studies and deals with protocols for network coding but where expertise on mathematical optimization has been re-used. The last chapter of this part is dedicated to the research perspectives I intended to follow for mid and long-term researches.

Part I

Professional career

CHAPTER

1 Extended curriculum vitae

1.1 Civil status

Philippe Mary
Born the March 27th 1979, Avignon, France
Married, 2 children

Associate Professor (Maître de conférences, CNU 61, classe normale)
Institut National des Sciences Appliquées (INSA) de Rennes
Communication Systems and Networking (CSN) Department
Research team Communication Systems (SYSCOM), Laboratory IETR UMR 6164
20 avenue des Buttes de Coësmes, 35708 RENNES

Phone : +332 23 23 85 92
Email : philippe.mary@insa-rennes.fr
Web site : http://pmary.perso.insa-rennes.fr

1.2 Academic cursus

2004-2008 **PhD** in Electrical Engineering, **INSA Lyon**.
Title: “Analytical performance study of wireless communication systems experiencing fading and shadowing" (in French)
Jury composition:

President	
Mr Pierre Duhamel	Research Director, CNRS, L2S Laboratory
Reviewers	
Mme Inbar Fijalkow	Professor ENSEA, Cergy-Pontoise
Mr Jean-Claude Belfiore	Professor ENST, Paris
Examiners	
Mr. Jean-Marc Brossier	Professor INPG, Grenoble
Mr. Guillaume Villemaud	Associate Professor INSA, Lyon
Supervision	
Mr. Mischa Dohler	Doctor France Telecom R&D, Grenoble
Mr. Jean-Marie Gorce	Associate Professor INSA, Lyon
Mr. Christian Gontrand	Professor INSA, Lyon

2004 **MSc** in Signal Processing and Digital Communications. **University of Nice Sophia-Antipolis**.

1999-2004 **Engineer Degree** in Electrical Engineering **Polytech'Nice, University of Nice Sophia-Antipolis**.

1998-1999 Preparatory classes for "Grandes Ecoles", Mathématiques Supérieures PCSI, **Ecole des Pupilles de l'Air, Grenoble**

1998 High school graduation, Scientific section.

1.3 Career

Since 2009 **Associate Professor (Maître de conférences, CNU 61) : INSA Rennes, IETR Laboratory**.
Research : Resource allocation, cooperative communications, signal processing for wireless communications.
Teaching : Deterministic analog and digital signal processing, random signal processing, wireless communications. **Systems and Communication Networks department, INSA Rennes**.

2008-2009 **Post-doc researcher at ETIS - UMR 8051 ENSEA Cergy-Pontoise. Granted by ANR RISC**.
Research : Resource allocation for TH-UWB ad-hoc networks.
Teaching : Optimization and wireless communications. **University of Cergy-Pontoise.**

2004-2008 **PhD candidate working with France Telecom R&D**.
Research : Analytical performance study of wireless communication systems.
Teaching : Smart antennas, MIMO, equalization / synchronization, mathematics. **INSA Lyon and IUT R&T Grenoble.**

2004 **MSc internship : Newlogic Technologies (Sophia Antipolis, France), University of Nice Sophia-Antipolis**.
Study of two UWB proposals for high data rate PAN and synchronization techniques for multi-band OFDM.

1.4 Expert assessments

- Reviewer for National Agency for Research (ANR) (2017)
- Reviewer for research projects funding by Mines-Télécom Institute (2014)
- Reviewer for International Journals (1 per quarter in average)

IEEE Transactions on Communications
IEEE Transactions on Wireless Communications
IEEE Transactions on Vehicular Technology
IEEE Communications Letters
EURASIP Journal on Wireless Communications and Networking

- Technical Program Committee member for International Conferences
  IEEE International Conference on Communications (ICC'11, 13, 14, 15, 16)
  IEEE Global Conference on Communications (Globecom'14, 15, 17)
  IEEE Personal Indoor and Mobile Radio Communications (PIMRC'12, 13, 14, 17)
  IEEE International Conference on Telecommunications (ICT'18)
  IEEE International Conference on Computer and Information Technology (ICCIT 2013)
  And other smaller conferences
- Chairman at IEEE PIMRC 2014, Washington DC, USA
  — Cooperative Communications I (Track: Fundamentals and PHY)
  — Resource Allocation (Track: Fundamentals and PHY)
- Committee member for tenure-track position, CNU 61, INSA Lyon (2014)
- Jury member for PhD defense
  — **Mr Vinh Tran** *Energy efficient cooperative relay protocols for wireless sensor networks*, ENSSAT Lannion, France, December 2012
  — **Mr Xin Yan** *Robustesse aux interférences dans les réseaux de capteurs*, Mines-Telecom Institute, Lille, France, December 2015
- Member of PhD thesis follow-up committee:
  — **Mrs Shanshan Wang** *Modeling and performance evaluation of spatially-correlated multi-tier heterogeneous cellular networks*, Thesis director **Marco Di Renzo**, CentraleSupélec, Gif-Sur-Yvette, France.
  — **Mr Rémi Bonnefoi** *Utilisation de la radio intelligente pour le réseau électrique intelligent*, Thesis directors **Yves Louët** and **Christophe Moy**, CentraleSupélec, Rennes, France.
  — **Mr Ali Mokh** *Spatial Modulation for Connected Object*, Thesis directors **Maryline Hélard** and **Matthieu Crussière**, INSA, Rennes, France.
  — **Mr Ahmad Shokair** *Stochastic geometry for data routing in hybrid broadcast/broadband networks*, Thesis directors **Jean-François Hélard** and **Matthieu Crussière**, INSA, Rennes, France.

1.5 Administrative duties

Since 2011, I share the responsibility of international exchange of Communication Systems and Networking department with Maryline Hélard. I handle the academic semester of students in Universities abroad, i.e. inside and outside Europe, and the semesters of students coming from abroad. This task is credited about 20 HDW [1] on my academic duty.

1.6 Supervision

1.6.1 Post-docs

Mohamad Maaz **Title**: *Communication techniques with low energy consumption*
Date: October 2013 - September 2015

1. Equivalent hour of directed works cf. definition in Chapter 2

Supervision: Maryline Hélard (INSA Rennes) 50%, Philippe Mary 50%
Fundings: Orange Labs
Results: 1 journal paper, 1 conference paper
Current situation: Post-doc at Orange Labs, Paris

1.6.2 PhD students

Dadja Toussaint Anade Akpo

Title: *Non-asymptotic fundamental limits of dense and impulsive IoT networks*
Date: October 2017 - September 2020
Supervision: Jean-Marie Gorce (INSA Lyon) 50% and Philippe Mary 50%
Fundings: ANR ARBurst

Navikkumar Modi

Title: *Machine Learning and Statistical Decision Making for Green Radio*
Date: February 2014 - May 2017
Supervision: Christophe Moy (CentraleSupélec) 50% and Philippe Mary 50%
Fundings: Labex Cominlabs
Results: 3 journal papers, 1 patent and 6 conference papers
Current situation: Research engineer at Skyline, Belgium

Ahmad Mahbubul Alam

Title: *Energy Efficiency Spectral Efficiency Tradeoff in Interference limited Networks*
Date: January 2014 - March 2017
Supervision: Xavier Lagrange (IMT) 33%, Jean-Yves Baudais (CNRS) 33%, Philippe Mary 33%
Fundings: Labex Cominlabs
Results: 1 journal paper, 3 conference papers
Current situation: Post-doc at Orange Labs, Paris

Hiba Bawab

Title: *Power Allocation in Overlaid DVB-LTE Systems*
Date: January 2012 - December 2015
Supervision: Jean-François Hélard (INSA Rennes) 30%, Oussama Bazzi (UL) 15%, Youssef Nasser 15%, Philippe Mary 40%
Fundings: ANR project M^3
Results: 1 journal paper (in revision), 3 conference papers
Current situation: Post-doc at Orange Labs, Rennes

Samih Abdul-Nabi

Title: *Centralized and Distributed Address Correlated Network Coding Protocols*
Date: November 2012 - September 2015
Supervision: Jean-François Hélard (INSA Rennes) 30%, Ayman Khalil (IUL) 30%, Philippe Mary 40%
Fundings: Libanese University and INSA de Rennes
Results: 2 journal papers, 2 conference papers
Current situation: Professor at LIU, Lebanon

Mohamad Maaz

Title: *Resource Allocation and Performance Metrics Analysis in Cooperative Cellular Networks*

Date: October 2010 - December 2013
Supervision: Maryline Hélard (INSA Rennes) 35%, Philippe Mary 65%
Fundings: Brittany region
Results: 2 journal papers, 2 conference papers

1.6.3 Master students

Alvaro Artigas Gil — **Title:** *Information Transfert Using OAM and QAM symbols*
Date: Spring semester 2015
Supervision: Philippe Mary 100%

Abdullah Haskou — **Title**: *Detection of Orbital Angular Momentum for EM Waves*
Date: Spring semester 2013
Supervision: Philippe Mary 100%
Results: 1 patent, 1 conference paper

Mohamad Kanj — **Title**: *Scaling Law of Energy Efficiency of Wireless Networks*
Date: Spring semester 2013
Supervision: Jean-Yves Baudais (CNRS) 50%, Philippe Mary 50%

Mohamed Bouzian — **Title**: *Machine learning and statistical signal processing for green radio*
Date: Spring semester 2013
Supervision: Christophe Moy (CentraleSupélec) 50% and Philippe Mary 50%

Marwa Chami — **Title**: *Suppression d'ambiguïté dans les images SAR*
Date: Spring semester 2012
Supervision: Stéphane Méric (INSA Rennes) 33%, Jean-Yves Baudais (CNRS) 33%, Philippe Mary 33%

Soha Farhat — **Title**: *Optimization of the Number of Relays in Cooperative Wireless Networks*
Date: Spring semester 2010
Supervision: Philippe Mary 100%

1.7 Scientific interactions, scientific community organization and awards

1.7.1 Collaborations

Visiting researcher Princeton University, April 2014 in Prof. H. Vincent Poor's team. I have been interested in the impact of finite block length information theory to wireless communications. Following this visit, Prof. Jean-Marie Gorce, Prof. Laurent Clavier and myself have been granted by ANR in 2016 for a project dealing with fundamental bounds in impulsive IoT networks.

Collaboration with the Lebanese University, American University of Beirut (AUB) and Lebanese International University (LIU). I have jointly worked with Prof. Oussama Bazzi (Lebanese Univ.) and Prof. Youssef Nasser (AUB) on resource allocation for LTE and DVB convergence via the supervision of Hiba Bawab's PhD thesis

(2012-2015). My collaboration with Dr. Ayman KHALIL (LIU) took place with the supervision of Samih ABDUL-NABI's PhD thesis (2012-2015). The scientific topic was the design of protocols making network coding practical, e.g. packet service time minimisation thanks to network coding.

Collaboration with the Mines-Telecom Institute Atlantique and ENSSAT Lannion. In the Labex Cominlabs framework, I have collaborated with Prof. Xavier LAGRANGE (IMT Atlantique) on the energy-efficiency spectral-efficiency tradeoff in random wireless networks via the supervision of Ahmad MAHBUBUL ALAM's PhD thesis (2014-2017). During the period 2010-2012, I have interacted with Prof. Charlotte LANGLAIS (IMT Atlantique) and Prof. Olivier BERDER (ENSSAT) in the regional project COMCOOP on cooperative communications.

Collaboration with CentraleSupélec with Prof. Christophe MOY in the Labex Cominlabs via the supervision of Navikkumar MODI's PhD thesis (2014-2017) dealing with reinforcement learning with multi-armed bandit framework.

Collaboration with University of Rennes 1 with Prof. Christian BROUSSEAU on the use of the Orbital Angular Momemtum (OAM) for encoding information and its wireless transfer.

Collaboration with INSA Lyon and IMT Lille. I am currently in a close collaboration with Prof. Jean-Marie GORCE at INSA Lyon and Prof. Laurent CLAVIER at IMT Lille in the ANR project ARBurst. The project aims at deriving fundamental bounds for impulsive IoT networks. Moreover, a dedicated workshop on mathematical models for IoT networks is being organized in collaboration with INSA Lyon and IMT Lille.

1.7.2 Scientific seminars and conferences

I have participated to two workshops (one as organizator) in the *Research Task Group* (GdR) ISIS (Information, Signal, Image and viSion), a structure informally gathering researchers in Information and communications sciences, funded by CNRS. Moreover, I gave some talks in some French Universities or abroad. In 2011, I have also been involved in the third international workshop on cross-layer design as technical program chair.

International conference	**Title:** *Third international workshop on cross-layer design (IWCLD'11)* **Date and place:** November 30th- December 1st at INSA Rennes, France **Role:** Technical program chair with Dr. Matthieu CRUSSIÈRE **Audience:** 50 people
GdR ISIS	**Title:** *Mathematical tools and methods for IoT network modelization* **Date and place:** November 2017 at Telecom ParisTech, Paris, France **Role:** Organizer 33% with Anne SAVARD, IMT Lille and Claire GOURSAUD, INSA Lyon **Audience:** 60 people
	Title: *UWB signal processing: Applications in communications and localization*

Date and place: January 2013 at Telecom ParisTech, Paris, France
Role: Speaker, title: *Multi-Rate Resource Allocations for TH-UWB Wireless Communications*
Audience: 30 people

Seminars

Title: *Finite Block Length Information Theory: What Are the Practical Impacts on Wireless Communications?*
Date and place: June 2015 at IRCICA, Lille, France

Title: *Error and Delay Outage Probability Analysis in Fading and Shadowing Environments*
Date and place: April 2014 at Princeton University, New Jersey, USA

Title: *Reliability of radio-mobile systems considering fading and shadowing channels*
Date and place: In 2009 at Eurecom and I3S both in Sophia-Antipolis and in 2010 at CentraleSupélec, Rennes France

1.7.3 Awards

- Best paper award at the 6th International Congress on Ultra Modern Telecommunications and Control Systems (ICUMT 2014), St. Petersbourg, Russia
- Owner of the research prime (PEDR) since 2016 (ranked A by the national committee).

1.8 Research projects

ANR project ARBurst

Title: *Achievable Region of bursty multi-user wireless communications*
fundings: Research national agency (ANR)
Dates: 2016-2021
Role: Scientific leader for INSA Rennes
Partners: INSA Lyon (Project leader), IMT Lille
Goal: Deriving achievable and converse bounds for hyper dense and bursty IoT-like wireless networks by using non-asymptotic information theory, stochastic geometry and non-gaussian models for interference.

Labex Cominlabs TEPN

Title: *Toward Energy Proportional Network*
fundings: National program Laboratory of Excellence (Labex) "Investing for the future"
Dates: 2013-2017
Role: Scientific leader for INSA Rennes
Partners: IMT Atlantique, CentraleSupélec Rennes, INRIA, CNRS
Goal: The scientific issues addressed in this project were energy efficiency scaling law of randomly deployed wireless networks, reinforcement learning to dynamically switch off high-consuming base stations, amplifier linearization, energy-efficient waveforms and energy oriented protocols.

Bilateral research project with Orange Labs

Title: *Communication techniques with low energy consumption*
fundings: Orange Labs
Dates: 2013-2015
Role: in charge of cooperative techniques and HARQ
Goal: Study promising communication techniques likely appealing to improve the energy efficiency of communication schemes like time reversal, massive MIMO, Relaying communications and HARQ techniques.

COMCOOP Project

Title: *Cooperative Communications*
fundings: Brittany region
Dates: 2010-2012
Role: Scientific leader for INSA Rennes
Partners: IMT Atlantique and ENSSAT Lannion
Goal: Investigating several distributed coded schemes in relay networks and their influence on the tradeoff between packet delivery and energy consumption with HARQ as well as resource allocation in multi-user cooperative networks.

ANR project RISC

Title: *Intelligent Network for Emergency Situations*
fundings: Research national agency (ANR)
Dates: 2007-2010
Role: post-doctoral researcher on ressource allocations during the year 2008-2009
Partners: THALES Communications (leader), ETIS, CRESTIC-URCA, ENST Paris, LIFL, AEC-RTS
Goal: Designing new PHY layer and protocols for ad-hoc wireless networks deployed in crisis situation, e.g. earthquake.

1.9 Publications

1.9.1 Submitted international journals peer-to-peer reviewed

[1] N. Modi, P. Mary, C. Moy, "**TRQoS-UCB: A Transfer Restless QoS-UCB Policy for Energy Efficient Heterogeneous Cellular Networks**", *Submitted to IET*, 2017.

1.9.2 Accepted international journals peer-to-peer reviewed

[14] H. Bawab, P. Mary, J. F. Hélard, Y. Nasser, O. Bazzi, "**Spectral Overlap Optimization for DVB-T2 and LTE Coexistence**", *Accepted to IEEE Transactions on Broadcasting* 2017.

[13] A. Mahbubul Alam, P. Mary, Jean-Yves Baudais, X. Lagrange, "**Asymptotic Analysis of Area Spectral Efficiency and Energy Efficiency in PPP Networks with SLNR Precoder**", *IEEE Transactions on Communications*, DOI 10.1109/TCOMM.2017.2699192, Vol. 65, no. 7, July 2017

[12] N. Modi, P. Mary, C. Moy, "**QoS driven Channel Selection Algorithm for Cognitive Radio Network: Multi-User Multi-armed Bandit Approach**", *IEEE Transactions on Cognitive Communications and Networking*, Vol. 3, no. 1, March 2017.

[11] S. Abdul-Nabi, A. Khalil, P. Mary, J. F. Hélard, "**Efficient Network Coding Solutions for Limiting the Effect of Packet Loss**", *EURASIP Journal on Wireless Communications and Networking*, (2017) 2017: 35. DOI 10.1186/s13638-017-0817-3.

[10] M. Maaz, P. Mary, M. Hélard, "**Energy Minimization in HARQ-I Relay-Assisted Networks with Delay-Limited Users**", *IEEE Transactions on Vehicular Technology*, Vol. 66, no. 8, August 2017.

[9] N. Modi, P. Mary, C. Moy, "**Efficient Learning in Stationary and Non-stationary OSA Scenario with QoS Guaranty**", *EAI Endorsed Transactions on Wireless Spectrum*, 17(11), doi:10.4108/eai.9-1-2017.152098, 2017.

[8] M. Maaz, J. Lorandel, P. Mary, J. C. Prévotet, M. Hélard, "**Energy Efficiency Analysis of Hybrid-ARQ Relay-Assisted Schemes in LTE Based Systems**", *EURASIP Journal of Wireless Communications and Networking* (2016), 2016:22. doi:10.1186/s13638-016-0520-9

[7] S. Abdul-Nabi, A. Khalil, P. Mary, J. F. Hélard, "**Aging in Network Coding**", *IEEE Wireless Communications Letters*, Vol. 4, No. 1, pp 78-81, Feb. 2015.

[6] M. Maaz, P. Mary, M. Hélard, "**Delay Outage Probability in Block Fading Channel and Relay-Assisted Hybrid-ARQ Network**", *IEEE Wireless Communications Letters*, Vol. 3, No. 2, pp 129-132, April 2014.

[5] P. Mary, I. Fijalkow, C. Poulliat, "**Multi-Rate Resource Allocations for TH-UWB Wireless Communications**", *IEEE Transactions on Wireless Communications*, Vol. 11, No. 12, Dec. 2012, pp 4470-4481.

Papers related to my PhD thesis work

[4] P. Mary, M. Dohler, J.-M. Gorce, G. Villemaud, "**Packet Error Outage for Coded Systems Experiencing Fast Fading and Shadowing**", *IEEE Transactions on Wireless Communications*, Vol. 12, No. 2, Feb. 2013, pp 574 ? 585.

[3] P. Mary, M. Dohler, J.-M. Gorce, G. Villemaud, "**Symbol Error Outage Analysis of MIMO OSTBC Systems over Rice Fading Channels in Shadowing Environments**", *IEEE Transactions on Wireless Communications*, Vol. 10, No. 4, Apr. 2011, pp. 1009-1014.

[2] P. Mary, M. Dohler, J.-M. Gorce, G. Villemaud, M. Arndt, "**M-ary Symbol Error Outage Over Nakagami-m Fading Channels in Shadowing Environments**", *IEEE Transactions on Communications*, Vol. 57, No. 10, Oct. 2009, pp. 2876-2879.

[1] P. Mary, M. Dohler, J.-M. Gorce, G. Villemaud, M. Arndt, "**BPSK Bit Error Outage over Nakagami-m Fading Channels in Lognormal Shadowing Environments**", *IEEE Communications Letters*, Vol. 11, No. 7, July 2007, pp. 565-567.

1.9.3 Patents

[2] N. Modi, C. Moy, P. Mary, "**Procédé d'accès opportuniste au spectre**", Patent no WO 2017013088 A1, January 2017.

[1] P. Mary, A. Haskou, C. Brousseau, "**Method for Transmitting a Sequence of Data Symbols, Transmission Device, Signal, Receiving Method, Corresponding Receiving Device and Corresponding Computer Program**", Patent no WO2015079020A1; FR3014271A1, 2013.

1.9.4 International conferences peer-to-peer reviewed with proceedings

[22] N. Modi, P. Mary, C. Moy, S. Darak, J. Palicot, "**Proof-of-Concept: Spectrum and Energy Efficient Multi-User CR Network via Vacancy and Quality based Channel Selection**", *In Proc. of the 32nd URSI GASS*, Montreal, Canada, August 2017.

[21] P. Mary, J. M. Gorce, A. Unsal, H. V. Poor, "**Finite Blocklength Information Theory: What is the Practical Impact on Wireless Communications?**", *In Proc. Globecom'16 Workshop, Low-Layer Implementation and Protocol Design for IoT Applications (IOTLINK)* 2016, Washington D.C., USA.

[20] A. Mahbubul-Alam, P. Mary, J.-Y. Baudais, X. Lagrange, "**Energy Efficiency-Area Spectral Efficiency Tradeoff in PPP Network with SLNR Precoder**", *In proc. of the 17th IEEE international workshop on Signal Processing Advances in Wireless Communications*, SPAWC 2016, Edinburgh, Scotland.

[19] N. Modi, C. Moy, P. Mary, J. Palicot, "**A New Evaluation Criteria for Learning Capability in OSA Context**", *In Proc. Crowncom 2016* Vol. 172, Grenoble, France.

[18] N. Modi, P. Mary, C. Moy, "**QoS driven Channel Selection Algorithm for Opportunistic Spectrum Access**", *In Proc. of IEEE International Workshop on Advances in Software Defined Radio Access Networks and Context-aware Cognitive Networks, SDRANCAN*, Globecom Workhop 2015, San Diego, CA, USA.

[17] S. Abdul-Nabi, P. Mary, J. F. Hélard, A. Khalil, "**Fault-tolerant minimal retransmission mechanism with network coding**", *In Proc. of the 23rd International Conference on Software, Telecommunications and Computer Networks*, SoftCom 2015, Split, Croatia.

[16] A. Mahbubul-Alam, P. Mary, J.-Y. Baudais, X. Lagrange, "**Energy Efficiency-Spectral Efficiency Tradeoff in Interference-Limited Wireless Networks with Shadowing**", *In Proc. of IEEE Vehicular Technology Conference, VTC-Fall 2015*, Boston, USA.

[15] M. Maaz, M. Hélard, P. Mary, M. Liu, "**Performance Analysis of Time-Reversal Based Precoding Schemes in MISO-OFDM Systems**", *In Proc. of the 80th IEEE Vehicular Technology Conference, VTC-Spring 2015*, Glasgow, Scotland.

[14] S. Abdul-Nabi, P. Mary, A. Khalil, J. F. Hélard, "**Novel Distributed Decoding Scheme for Efficient Resource Utilization in Network Coding**", *In Proc. of the IEEE Wireless Communications and Networking Conference*, WCNC 2015, New Orleans, USA.

[13] N. Modi, C. Moy, P. Mary, "**Experimental Performance Comparison and Analysis for Various MAB Problems under Cognitive Radio Framework**", *In Proc. of the Wireless Innovation Forum European Conference*, WinnComm-Europe, Nov 2014, Rome, Italy.

[12] M. Ghanem, H. Bawab, O. Bazzi, Y. Nasser, P. Mary, J.- F. Hélard, "**Closed-Form Expression of the Ergodic Capacity in a Cognitive Radio Link under Power Constraints**", *In Proc. of the 6th International Congress on Ultra Modern Telecommunications and Control Systems (ICUMT 2014)*, Saint Petersbourg, Russia.

[11] H. Bawab, P. Mary, J.- F. Hélard, Y. Nasser, O. Bazzi, "**Ergodic Capacity Optimization in Coexisting DVB-LTE-Like Systems**", *In Proc. of the 6th International Congress on Ultra Modern Telecommunications and Control Systems (ICUMT 2014)*, Saint Petersbourg, Russia. BEST PAPER AWARD

[10] A. Haskou, P. Mary, M. Hélard, **Error Probability on the Orbital Angular Momentum Detection**", *In Proc. of the 25th International Symposium on Personal Indoor and Mobile Radio Communications (PIMRC'14)*, Washington, USA.

[9] H. Bawab, P. Mary, J.- F. Hélard, Y. Nasser, O. Bazzi, "**Global Ergodic Capacity Closed-Form Expression of Coexisting DVB-LTE-Like Systems**", *In Proc. of the 79th IEEE Vehicular Technology Conference Spring (VTC Spring'14)*, VTC 2014, Seoul, Korea.

[8] M. Maaz, P. Mary, M. Hélard, "**Energy Efficiency Analysis in Relay Assisted Hybrid-ARQ Communications**", *In Proc. of the 23rd International Symposium on Personal Indoor and Mobile Radio Communications (PIMRC'12)*, Sydney, Australia.

[7] M. Maaz, P. Mary, M. Hélard, "**Resource Allocation for QoS Aware Relay-Assisted OFDMA Cellular Networks**", *In Proc. of the third International Workshop on Cross-Layer Design 2011*, IWCLD 2011, Rennes, France.

[6] P. Mary, I. Fijalkow, C. Poulliat, "**Adaptive Rate Allocation Scheme for Uplink TH-UWB Networks**", *In proc. of IEEE International Conference on Communications 2011*, ICC 2011, Kyoto, Japan.

[5] P. Mary, I. Fijalkow, C. Poulliat, "**Time Slot Allocation for TDMA/CDMA TH-UWB Ad-Hoc Networks**", *In Proc. of the 11th IEEE Workshop on Signal Processing Advances in Wireless Communications 2010*, Spawc 2010, Marrakech, Morocco.

Papers related to my PhD thesis work

[4] P. Mary, M. Dohler, J.-M. Gorce, G. Villemaud, "**Symbol Error Outage for Spatial Multiplexing Systems in Rayleigh Fading Channel and Lognormal Shadowing**", *In Proc. of the 10th IEEE Workshop on Signal Processing Advances in Wireless Communications 2009*, Spawc 2009, Perugia, Italy.

[3] P. Mary, J.-M. Gorce, G. Villemaud, M. Dohler, M. Arndt, "**Reduced Complexity MUD-MLSE Receiver for Partially-Overlapping WLAN-Like Interference**", *In Proc. of the*

65th IEEE Vehicular Technology Conference, 2007. VTCspring 2007, Page(s) :1876-1880, Dublin Ireland, 2007.

[2] P. Mary, J.-M. Gorce, G. Villemaud, M. Dohler, M. Arndt, "**Performance Analysis of Mitigated Asynchronous Spectrally-Overlapping WLAN Interference**", *In Proc. of the IEEE Wireless Communications and Networking Conference, 2007.* WCNC 2007, Page(s) :2097-2102, Hong Kong, 2007.

[1] P.-F. Morlat, P. Mary, G. Villemaud, J.-M. Gorce, M. Arndt, "**Performance Validation of a Multi-Standard and Multi-Antenna Receiver**", *In Proc. European Conference on Antennas and Propagation : EuCAP 2006 (ESA SP-626)*, Nice, France 2006.

1.9.5 National conferences peer-to-peer reviewed with proceedings

[6] N. Modi, P. Mary, C. Moy, "**Apprentissage machine pour l'optimisation énergétique des réseaux cellulaires hétérogènes sans-fil : une approche bandit à bras multiples**", *In Proc. GRETSI'17*, Juean-Les-Pins, France, 2017.

[5] A. Mahbubul-Alam, P. Mary, J.-Y. Baudais, X. Lagrange, "**Compromis efficacités énergétique et spectrale du précodeur SLNR dans un réseau cellulaire aléatoire**", *In Proc. GRETSI'17* 2017, Juean-Les-Pins, France, 2017.

[4] N. Modi, C. Moy, P. Mary, "**Machine Learning for Opportunistic Spectrum Access with Energy Consumption Constraint**", *In Proc. URSI France, Energie et Radiosciences*, CentraleSupélec, Cesson-Sévigné, France, 2016.

[3] N. Modi, P. Mary, C. Moy, "**Apprentissage machine orienté QoS pour l'accès opportuniste au spectre**", *In Proc. GRETSI'15*, Lyon, France, 2015.

[2] P. Mary, I. Fijalkow, C. Poulliat, "**Allocation de ressources multi-débit pour la radio ULB impulsionnelle**", *In Proc. GRETSI'13*, Brest, France, 2013.

[1] P. Mary, M. Dohler, J.-M. Gorce, G. Villemaud, M. Arndt, "**Estimation du taux de coupure d'une liaison radio MIMO dans un canal de Nakagami avec effet de masque**", *In Proc. GRETSI'07*, Troyes, France, 2007.

1.9.6 Technical project reports

[5] M. Maaz, J. Lorandel, P. Mary, J.-C. Prévotet, M. Hélard, "**Modèles de consommation de puissance des techniques à relais**", Deliverable L2.2 CRE Orange-Labs no. C09214, Dec. 2014.

[4] M. Maaz, P. Mary, M. Hélard, "**Analyse des Techniques de Transmission à Relais et Performances**", Deliverable L1.2 CRE Orange-Labs no. C09214, June. 2014.

[3] M. Maaz, J. Lorandel, M. Liu, P. Mary, J.-C. Prévotet, M. Hélard, "**Performances of MIMO Technique with Time Reversal in LTE-A and IEEE 802.16m Context**", Deliverable L1.1 CRE Orange-Labs no. C09214, Jan. 2014.

[2] M. Maaz, P. Mary, M. Helard, "**Resource Allocation Techniques for Future Cellular Networks**", Deliverable EPT COMCOOP, Jan. 2013.

[1] P. Mary, I. Fijalkow, C. Poulliat, "**Allocation de ressource pour réseaux ad-hoc UWB**", Deliverable ANR RISC project, Sept. 2009.

1.9.7 Thesis

[2] P. Mary, "**Etude analytique des performances des systèmes radio-mobiles en présence d'évanouissements et d'effet de masque**", *PhD dissertation, INSA Lyon*, February 2008.

[1] P. Mary, "**Study of two IEEE emerging standards for wireless communications in UWB**", *MSc dissertation, University of Nice Sophia-Antipolis*, September 2004.

CHAPTER

2 Teaching activities

2.1 Introduction

This chapter is mainly devoted to describe my teaching activities since I have been recruited as Associate Professor (Maître de Conférences) at INSA Rennes. In Section 2.2 however, I summarize the teaching classes I gave during my PhD and post-doctoral positions while Section 2.3 details my teaching activities since I am Associate Professor at INSA Rennes. The teaching activities are separated in lectures (L) [1], directed works (DW) [2] and labworks (LW) [3]. The amount of hours are given in hour of directed works (HDW), i.e. 1 hour of lecture = 1.5 HDW and 1 HDW = 1 HLW.

1. Classical teaching given in amphitheater with the whole promotion
2. Set of exercises and problems done in small groups
3. Experimental activities in small groups done in laboratory using softwares or hardware equipments

2.2 Teaching activities during PhD and post-doc

Although my PhD took place in part in a company, i.e. Orange Labs (ex-France Telecom R&D), I have always taken care to maintain a teaching activity in order to be qualified for an academic career. During the 2005-2008 period, I have been temporary lecturer at INSA Lyon, Institut Universitaire Technologique (IUT) *Network and Telecommunications* in Grenoble. In 2008-2009, I have been temporary lecturer at Cergy-Pontoise University (UCP) and Ecole National Supérieure de l'Electronique et de ses Applications (ENSEA) also at Cergy-Pontoise. The studies at College comprise 5 years, excepting doctoral programs, and two graduations, i.e. *License* and *Master*. License level comprises 3 years, denoted L1, L2, L3 in the following and Master level 2 years, i.e. M1 and M2. Table 2.1 below summarizes my teaching experience as temporary lecturer.

Year	Institution	Level	Topic	Type	Volume
08-09	UCP	M2	Optimization	LW	6
07-08	IUT	L1/L2	Mathematics	DW	58,5
	INSA Lyon	M2	Advanced communications	L	6
06-07	INSA Lyon	M2	Advanced communications	L	6
	INSA Lyon	M2	Digital communications	L	15
05-06	INSA Lyon	L3	Communication systems	LW	8
	INSA Lyon	M1	Digital communications	L	3
	INSA Lyon	M2	Advanced communications	L	3
05-09			Total in HDW		122

Table 2.1 – Teaching activities during PhD and post-doc

Teaching description

(i) Optimization:

I taught this labwork in the research Master entitled Systèmes Intelligents et Communicants. We presented the quadratic criterium that aims at minimizing the error between a reference signal and the temporal or spatial observation. Students were asked to implement the Wiener's filter, an adaptive algorithm, i.e. the least mean square algorithm. The RLS [4] algorithm was also tackled.

(ii) Mathematics:

I was in charge of some DW in mathematics for L1 and L2 at IUT in Grenoble in 2008. In L1, I gave DW on linear algebra, i.e. matrix product, linear equation systems, and DW in analysis, i.e. periodic signal, Fourier series, Fourier transform, application to signal processing: modulation and sampling. In L2, I gave DW in probabilities, i.e. combinatory, cumulative distribution function, probability density function, law of large numbers, statistical moments.

(iii) Advanced communications:

This lecture aimed at introducing multi-antenna systems. The first part was dedicated to smart antenna systems and their application to spatial filtering, i.e. spatial adapted filter, ambiguity, Woodward's theorem. In a second part, we moved to multi-antenna processing in communications, e.g. Maximum Ratio Combining, Selection Combining, RAKE 2D. The multiple input multiple output (MIMO) channel

4. recursive least square

capacity is introduced and the water-filling technique to achieve it. The precoding V-BLAST [5] and Alamouti space-time block code were introduced as well.

(iv) Digital communications:
The baseband transceiver chain was presented in this course. We first started by the optimal receiver in additive white gaussian noise (AWGN) and continued on the effect of a multipath channel on the received signal. The non inter-symbol interference criterium was introduced. The maximum likelihood receiver under the Ungerboeck's formulation was presented and Viterbi's algorithm as well. Simulation results of a suboptimal solution, i.e. minimum mean square (MMSE), were finally presented.

(v) Communications systems:
In this labwork, students designed an ADSL [6] transceiver chain on Simulink, gathering all their knowledge in signal transmission. They implemented a channel encoder, digital mapping, multi-tone modulator, propagation channel and the whole receiver chain.

Supervision:

During my PhD, I have supervised two students for their M2 research internship. The topic and supervision rate are reminded in the table below.

2007	Anya Apavatjrut	INSA Lyon
Title	**Interference rejection for heterogeneous signals**	
Rate	50% with Jean-Marie Gorce	

2006	Jordi Vila Valls	ENSERG
Title	**Signal processing for interference rejection in WLAN**	
Rate	100%	

The first student, Jordi, I have supervised in 2006 was in double cursus between Universitat Politècnica de Catalunya (UPC) and ENSERG, Grenoble. His internship took place at France Telecom R&D and aimed at exploiting the signal cyclostationarity properties for interference rejection of spectrally overlapping signals in heterogeneous wireless local area network (WLAN), e.g. direct sequence spread spectrum (DSSS) and orthogonal frequency division multiplexing (OFDM) waveforms. The second student, Anya, has studied successive and parallel interference cancellation receivers in the same context, i.e. heterogeneous WLAN signals.

2.3 Teaching activities since 2009

I exclusively teach at INSA Rennes, a 5 years engineering school after "baccalauréat". The studies are divided into two main parts, 2 years in preparatory cycle (PC) and 3 years in an engineering speciality. I essentially teach in Communication Systems and Networks (CSN) department in the initial formation. Since the year 2016-2017, I take part in the professional formation cursus, in the design and development of innovative technologies (DDIT) speciality. I am also handling a course for students in the 2nd year of preparatory cycle for raising awareness of the department courses among the PC's students. When I have been recruited, I have been released of 60 hours of teaching duty during the first two years. Table 2.2 below summarized the amount of teaching hours in face-to-face since 2009

5. Vertical-Bell Laboratories Layered Space Time
6. Asymmetric Digital Subscriber Line

in HDW. In the next sections, I detail the courses I give to the students. The audience and the level of courses I teach is then denoted with the speciality department followed by the year, ranging from 1 to 5. For instance *CSN5* means the last year of the engineering school (equivalent to M2) in the department CSN.

Year	09-10	10-11	11-12	12-13	13-14	14-15	15-16	16-17
h eq. DW	141	147	195	218	179	203	206	207

Table 2.2 – Teaching hours sum-up since 2009

2.3.1 PC department - Initial formation - PC2

Speciality Discovery and Specialized Individual Courses **15 HDW**

These courses are dedicated to students in PC2 to help them to choose one speciality department between 8 at INSA Rennes. For the CSN department, we choose to show what are the main topics with a series of experiment summarized below:

- Electronic: design of a device able to demodulate a digital video broadcasting (DVB) signal on an oscilloscope's screen
- Hyperfrequency and propagation: illustration of radiating principles with some antennas and spectrum analyzer
- Signal processing and communications: modulation and demodulation of a music sample using a digital signal processor
- Network: illustration of the main protocols at layers 2 and 3 and design of a local network

I am in charge of these labworks. I mainly teach on the signal processing and communications activity. Besides, I give with two other persons a vulgarization conference on a "packet life" where we follow the trip of a packet through the network, where a user accesses to a server in Wi-Fi. This allows us to go through all scientific and technical notions, from protocols to RF electronic, passing by baseband signal processing, that will be seen in CSN department.

2.3.2 CSN department - Initial formation - CSN3

During my career, the contents and name of some courses have been changed. In particular, some courses that used to be taught in CSN4 have been split and some parts retrograded in CSN3 following some amendments. The consequence is that I essentially teach in CSN3 nowadays while my duty was a little bit more balanced between CSN3 and 4 in the early years. In the following, the courses are denoted with their latest content and name even they did not exist in this form in the early years; thus this is a picture of my teaching at this time. I also mention the total number of hours each course is taught in HDW, averaged over the years. For DW and LW, the whole promotion is split in two groups of 24 students each.

Signal Processing Basics (SPB) **30 HDW**

This course aims at introducing the basic tools needed for deterministic signal processing. During 2009-2015, the course mainly focused on analog signals but since 2015-2016 the course also deals with discrete signals and related notions which used to be seen in CSN4 before. The following notions are addressed:

- Signal classification, i.e. finite/infinite power or energy

- Signal space representation
- Continuous time Fourier analysis (Fourier series, harmonic signal analysis, Fourier transform and distributions, energy and power spectrum)
- Discrete time Fourier analysis (sampling, discrete sequences, Fourier transform of a sequence, discrete Fourier transform)

I am in charge of labworks (19 HDW in average) where students work on Matlab. As prerequisite, students are taught Matlab in 3 slots of 2 hours (for each group) that I have created. Moreover, I have contributed to make the labworks evolve when discrete signals have been integrated to the course. I also give exercise sessions (11 HDW in average).

Digital Linear Systems (DLS) — 16 HDW

In this course, students become familiar with digital signals, i.e. sequences, and their processing through finite and infinite impulsive response filtering. My teaching in this course is limited to labworks sessions in Matlab **for which I am in charge**. The following notions are addressed:

- Z transform (and its inverse) of a sequence and stability conditions (causal and non-causal sequences)
- Particular filters (linear-phase network, pure phase-shifting network, minimal phase network), filter structures
- Finite and infinite impulse response filtering
- IIR [7] and FIR [8] synthesis (window method, bilinear transform)

Statistical Signal Processing Basics (SSPB) — 34 HDW

This course aims at introducing the basic concepts for dealing with random signals. During the period 2009-2011, I gave only exercice and labworks sessions but since 2011, I am also in charge of lectures. The concepts that are addressed in this course are:

- Probability prerequisite (combinatory, random event, general axioms and definitions of probabilities)
- Scalar random variables (cumulative and probability distribution functions, statistical moments, multi-variate description)
- Discrete and continuous random processes (definitions, temporal and statistical moments, stationarity and ergodicity, power spectral density (PSD))
- Filtering of random processes (conservation of stationarity, PSD, inter-spectral formula)
- Cyclostationary process (definitions, cyclostationary time series, cyclic spectrum)
- Markov chains (fundamental properties, state classification, long term behavior, ergodic chain, birth and death process)

I am in charge of this course and I have evolved the handout. In particular, I added chapters on cyclostationary process and Markov chains. I teach 12 hours of lectures to the whole promotion for which I produced the slides and 10 HDW and 8 HLW in average. Concerning LW, I have entirely built labworks exercises on Matlab.

Communications Systems (COMSYS) — 19 HDW

This course aims at studying a communication chain from modulation/demodulation point of view. During the period 2009-2015, only analog modulations were seen (DSB, SSB, AM,

7. Infinite impulse response
8. Finite impulse response

FM, PM [9]) and since 2015, digital communications have been introduced through line codes and mapping. The study of analog modulation may seem a little bit dusty, however, the objective is to make the students understand the universal principle of frequency transposition, the complex envelop notion and I&Q components. Moreover, a much more complete course on digital communications is taught in CSN4. The course addresses the following notions:

- Fundamental tools and notions (complex envelop, RF signal, analytic signal, Rice components)
- Linear modulations (DSB, AM, SSB, QAM [10] coherent demodulation, envelop detector, performances)
- Angular modulations (FM, PM, PLL [11], frequency discriminator)
- Line codes (NRZ, RZ, AMI [12], Manchester), PSD of line codes
- Impulsive modulations
- Digital QAM

From 2010 to 2013, I used to teach 14 hours of DW in average and 12 hours of LW in average. Since 2013, I have only been involved in LW, due to the sharing with another professor, for 14 hours in average. Moreover, **I produced the labworks in Matlab for the digital part.**

Computer Sciences **22 HDW**

During the academic year 2009-2010, I taught labworks on C language (22 HDW). Moreover, I supervised time to time a group of 3 or 4 students on a project in C language. Here some project examples:

- Aloha and CSMA [13] protocols emulation (implement CSMA and aloha protocols for distributed users)
- Impulsive ultra wide band communications (implement gaussian pulses, data structure with chips and frames, error probability in AWGN)
- Relativistic flight simulator (program and simulate relativistic aberration of starlights)
- Voronoï tesselation (program Voronoï tesselation and Delaunay graph for 2D area from a Poisson point process (PPP))

2.3.3 CSN department - Initial formation - CSN4

Digital Communications **22 HDW**

In this course, students become familiar with the main blocks of single and multi-carrier communication systems. The main notions that are studied in this course are:

- Pulse shaping and band-limited communication
- Digital mapping
- Synchronization (symbol, frame and frequency offset)
- Channel estimation and equalization
- OFDM

I am only involved in labworks which have radically changed since 2009. From 2009 to 2012, labworks were done on electronic cards, with integrated components. The material

9. double side band, single side band, frequency modulation, phase modulation
10. quadrature amplitude modulation
11. phase locked loop
12. non return to zero, return to zero, alternate mark inversion
13. carrier sense multiple access

was rather old and not really "student-proof"; lot of electronic components burned out because charge inversion or components plugged upside-down. From 2012, we decided to move digital communication labworks under software defined radio equipment with Ettus cards. The card are running with Labview but students develop their own code on Mathscript node, i.e. kind of Matlab code that can be interfaced into a Labview chain. **I have contributed to build these labs with another colleague and an engineer mastering Labview.**

2.3.4 CSN department - Initial formation - CSN5

Cross-Layer Design **15 HDW**

In 2009, **I have created a lecture on cross-layer design techniques** for the engineer students in last year. The issue of increasing communication system performance is tackled from physical (PHY), medium access control and network layers perspective through resource allocations and their impact on quality of service (QoS) metrics at different layers, e.g. packet error rate (PER), latency, spectral efficiency. The following topics are addressed in this course:

- Layered and cross-layered architecture
- Capacity region and power allocation
- Delays, hybrid automatic repeat request (HARQ)

Project supervision **60 HDW**

During Fall semester in their last engineering year, students work, in small group of 4 or 5 people during at least 60 hours, on an engineering project proposed by an industrial actor, mentioned in bold in the following. I have supervised two projects:

- 2015-2016, **Axians**: Automatisation of a processing tool for GSM-R [14] frame radio analysis
- 2016-2017, **Oya Light**: Detection of human flow in a room

The project assigned by **Axians** aimed at designing a human-machine interface under Matlab to present and analyse the data collected by Axians for the GSM-R standard. Students had to compute and present some curves on interference measurements and coverage maps for railroad applications.

The project proposed by **Oya Light** aimed at detecting and counting the number of Humans in a room and eventually at detecting their trajectory. From an infrared capture, obtained through a matrix of sensors located in the ceiling lamp, students had to design image processing algorithms on Matlab to achieve the goal fixed by the company.

During Spring semester of their last engineering year, students are asked to perform an internship, most often in industry but can be in an academic laboratory, in order to earn their Engineering degree. Every year, I follow about 3 students in their internship.

2.3.5 DDIT department - Professional formation - DDIT3

This new cursus has been created in 2016-2017 and selects apprentices to follow engineering studies in addition to a unique professional experience in a company. Students spend one month in their company and one month at INSA. If the total amount of teaching hours is the same than for students in the initial formation, the program is however quite different; apprentices have half as much scientific hours than students in the initial formation but

14. Global System Mobile - Railways

have more courses on project management and company regulations. I teach the same course on statistical signal processing that I give to the students in the initial formation. The volume is the same, i.e. 34 HDW, however due to the students' background, which is less theoretical than students in the initial formation, the cyclostationary part and Markov chains have been removed.

Moreover, I have adapted my way to teach for this audience. The course is not clearly separated in L, DW and LW, but all three are merged in each session in order to illustrate by problems and Matlab simulations the theoretical concepts seen in course.

CHAPTER

3 Research activities

In this chapter, I summarize my research activities since my PhD thesis up to now. Section 3.1 summarizes the main contributions of my PhD while Section 3.2 presents my research interests and developed expertises up to now.

3.1 PhD thesis

3.1.1 Introduction and context

My PhD work was funded by Orange Labs (ex France Telecom R&D), Grenoble, France, and hence it took place half in industrial context and half in an academic laboratory at INSA Lyon. My work was supervised by Prof. Mischa Dohler, senior researcher at Orange Labs at this time, and Prof. Jean-Marie Gorce, Professor at INSA Lyon. From that context, I benefited from an industrial issue and a strong academic expertise allowing theoretical works as well. The main topic of my thesis was the analytical study of wireless communication performance under various fading and shadowing conditions. The technical and scientific issue is that fading and shadowing are not phenomena with the same scale. While the former is due to multi-path and mobility and hence make the received signal power varying a lot during a communication call, the later is produced by large obstacles between emitter and receiver and makes the received power slowly varying during an entire call.

The combination of both effects makes the channel statistics non-ergodic so that the symbol error rate (SER), averaged over small scale fading, is not relevant since it varies from one shadowing realization to another. In this context, outage probability, i.e. probability that SER exceeds a threshold, is a quite better metric to evaluate the performance of the entire communication. In this work, we did the hypothesis that both effects are however separable, i.e. combination of fast fading and slow shadowing, making possible the computation of average SER or PER over fading, and then the computation of outage probability over the shadowing effect.

Our motivation was to express the outage probability in shadowing in fonction of the average BER or PER targeted and not only as a fonction of the signal to noise ratio (SNR) threshold, as it was done in literature. Considering that the average SNR $\overline{\gamma}_s$ is log-normal distributed of mean μ and standard deviation σ both in dB, i.e. $\overline{\gamma}_s \sim \mathcal{LN}(\mu_{dB}, \sigma_{dB})$, the symbol error outage (SEO) is expressed as

$$P_s(O|\mu) = P\left(P_s(E|\overline{\gamma}_s) \geq P_s^*(E|\overline{\gamma}_s)|\mu\right) \iff P_{\overline{\gamma}_s}(O|\mu) = P\left(\overline{\gamma}_s \leq \overline{\gamma}_{th}|\mu\right) \quad (3.1)$$

where $P_s(E \mid \overline{\gamma}_s)$ is the average SER knowing the average SNR $\overline{\gamma}_s$ and P_s^* is the targeted SER. By expressing the SNR threshold w.r.t. the targeted SER, i.e. $\overline{\gamma}_{th} = f(P_s^*(E))$ where $f(P_s^*(E)) = P_s^*(E|\overline{\gamma}_s)^{-1}$, SEO is hence:

$$P_s(O|\mu) = \int_0^{\overline{\gamma}_{th}=(P_s^*(E))^{-1}} p_{\overline{\gamma}_s}(\overline{\gamma}_s|\mu)\, d\overline{\gamma}_s = Q\left(\frac{\mu_{dB} - 10\log_{10}\overline{\gamma}_s(P_s^*(E))}{\sigma_{dB}}\right) \quad (3.2)$$

In order to have a reliable expression of SEO then a tight and invertible approximation of SER/PER is needed in various fading environments and for various PHY layers.

3.1.2 Contributions of the thesis

Outage probabilities for uncoded systems

Nakagami-m fading. I have been first interested in SEO in single input single output (SISO) and then for MIMO uncoded systems. In Nakagami-m fading channels, the error probability of M-ary phase shift keying (M-PSK) and M-ary quadrature amplitude modulation (M-QAM) signals can be expressed in a single formalism, holding for SISO and space-time block codes (STBC) MIMO systems as well.

By integrating the moment generating function of SNR in Nakagami channel, the exact SER for M-PSK and M-QAM signaling can be proved to be [1, 2]:

$$P_s^{\text{psk}}\left(E\left|\overline{\gamma}_s\right.\right) = x\left(\overline{\gamma}_s\right)^q \left(k_1 \cdot {}_2F_1\left(q, \frac{1}{2}; q+1; x\left(\overline{\gamma}_s\right)\right) + k_2 \cdot F_1\left(\frac{1}{2}, q, \frac{1}{2}-q; \frac{3}{2}; \left(1-g_{\text{psk}}\right) x\left(\overline{\gamma}_s\right), 1-g_{\text{psk}}\right)\right) \quad (3.3)$$

$$P_s^{\text{qam}}\left(E\left|\overline{\gamma}_s\right.\right) = x_1\left(\overline{\gamma}_s\right)^q k_3 \cdot {}_2F_1\left(q, \frac{1}{2}; q+1; x_1\left(\overline{\gamma}_s\right)\right) - x_2\left(\overline{\gamma}_s\right)^q k_4 \cdot F_1\left(1, q, 1; q+\frac{3}{2}; \frac{x_2\left(\overline{\gamma}_s\right)}{x_1\left(\overline{\gamma}_s\right)}, \frac{1}{2}\right) \quad (3.4)$$

where $x\left(\overline{\gamma}_s\right) = 1/\left(1 + g_{\text{psk}}\overline{\gamma}_s/\left(mn_tR\right)\right)$, $x_1\left(\overline{\gamma}_s\right) = 1/\left(1 + g_{\text{qam}}\overline{\gamma}_s/\left(mn_tR\right)\right)$, $x_2\left(\overline{\gamma}_s\right) = 1/\left(1 + 2g_{\text{qam}}\overline{\gamma}_s/\left(mn_tR\right)\right)$ and $g_{\text{psk}} = \sin^2\left(\pi/M\right)$, $g_{\text{qam}} = 3/\left(2\left(M-1\right)\right)$ with M the modulation order. In addition, ${}_2F_1$ and F_1 are Gauss and Appell hypergeometric functions respectively. Moreover, k_1, k_2, k_3 and k_4 are modulation and Nakagami distribution dependent constants and $q = mn_tn_r$ where n_t, n_r are the number of antennas at transmitter and receiver respectively and m being the fading parameter of the Nakagami distribution. Finally, R is the space-time coding rate. The SISO case is encompassed in this form and is obtained when $n_t = n_r = 1$.

In order to express the outage probability according to SER threshold, I first proposed a tight and invertible approximation of the expressions above, valuable for a wide range of SNR, that can be expressed as:

$$P_s(E|\overline{\gamma}_s) \approx k_{\text{mod}} \frac{y\left(\overline{\gamma}_s\right)^q}{\sqrt{1 - y\left(\overline{\gamma}_s\right)\tilde{t}}}; \forall \overline{\gamma}_s \quad (3.5)$$

with $\tilde{t} = q/(q+1)$, $y\left(\overline{\gamma}_s\right) = 1/\left(1 + g_{\text{mod}}\overline{\gamma}_s/\left(mn_tR\right)\right)$, g_{mod} and k_{mod} are modulation, system and Nakagami distribution dependent constants. This approximation, the tightest known in literature over a wide range of SNR, holds for M-PSK, M-QAM signals, mono and multi-antenna systems in Nakagami-m channel and has been obtained thanks to the Laplace approximation of the Gauss hypergeometric function and asymptotic derivation, i.e. $\overline{\gamma}_s \to \infty$.

From this expression, SER can be inverted w.r.t. SNR with a very good precision and takes the following form

$$\overline{\gamma}_s(P_s^*\left(E\right)) = c_0 \left(P_s^*\left(E\right)^{-\frac{1}{q}} \left(1 - c_1 P_s^*\left(E\right)^{\frac{1}{q}}\right)^{-\frac{1}{2q}} - k_{mod}^{-\frac{1}{q}}\right) \quad (3.6)$$

where c_0 and c_1 are modulation, system and Nakagami distribution dependent constants. It is worth noting that similar expressions can be derived for spatial multiplexing systems, while some adjustments though and for Rayleigh fading. These results have been published in [3–6].

Rice fading. In that case, SERs are not expressed with hypergeometric functions but with the integral of the moment generating functions of SNR. The Laplace approximation

method is directly applied on these integrals and invertible approximation of SER can be obtained leading to the following general inverse expression:

$$\overline{\gamma}_s(P_s^*(E)) = n_t R\,(1+K)\left(\frac{K}{g_{mod} W_0\left(n_t R\cdot K\,(1+K)\exp\left(-\frac{\log\frac{((1+K)n_t R)^d}{\sqrt{\pi d}P_s^*}}{d}+K\right)\right)}-\frac{1}{g_{\text{mod}}}\right) \tag{3.7}$$

where W_0 and K are the Lambert function and Rice parameter respectively and $d = n_t n_r$.

Thanks to inverse SER expressions, outage probabilities can be evaluated in shadowing environment using (3.2) and hence saving a huge amount of simulation time. Results on Rice fading have been published in [7].

Outage probabilities for coded systems

For channel coded systems, I have been interested in the packet error outage (PEO) derivation which is a step further than previous results since a highly non linear dependency between coded PER and SNR occurs. In this work, I have assumed hard decision input on channel decoder, which may perform worse than soft-decision input, but presents the advantage to be more tractable for our derivations. Reed-Solomon codes have been considered for which the word error rate (WER) can be exactly expressed as:

$$P_w\,(E) = \frac{P_s^{t+1}}{(t+1)B\,(t+1, n-t)}\,{}_2F_1\,(t+1, 1+t-n; t+2; P_s) \tag{3.8}$$

where $B\,(a,b)$ is the Beta function with parameters a and b. By considering that a packet is made of one codeword, an inverse expression of SER w.r.t. WER can be obtained in the same way than previously:

$$P_s = \left(\frac{P_w^*\,(E)\,(t+1)B\,(t+1, n-t)}{\left(1-\left[P_w^*\,(E)\,(t+1)B\,(t+1, n-t)\right]^{\frac{1}{t+1}}\tilde{y}\right)^{n-t-1}}\right)^{\frac{1}{t+1}} \tag{3.9}$$

with $\tilde{y} = (t+1)\,/\,(t+2)$, n is the block length in symbols and t is the number of errors that can be corrected. Combining this with the inverse expressions of SER w.r.t. SNR, outage probabilities of linear block coded systems in shadowing can be derived. One can extend this result to the Bose-Chaudhury-Hocquenghem kind of codes by considering the upper-bound on WER. The convolutional coded case has also been addressed but considering asymptotic analysis. These results have been published in [8].

Outage probabilities with interference and multi-user detection

The case where the signal of interest, i.e. $s_d(t)$, is jammed by another communication, i.e. $s_i(t)$, when receiver has N antennas, was addressed. The signal model considered is

$$\mathbf{y}(t) = \sqrt{P_d}\mathbf{h}_d s_d(t) + \sqrt{P_i}\mathbf{h}_i s_i\,(t-\tau) + \mathbf{w}\,(t) \tag{3.10}$$

where P_d, P_i, $\mathbf{h}_d, \mathbf{h}_i \in \mathbb{C}^{N\times 1}$ are the transmitted powers, flat fading channels of the desired and interfering signals respectively. Moreover, τ is the asynchronism of the interfering communication w.r.t. the intended receiver and $\mathbf{w}(t) \sim \mathcal{CN}\left(0, \sigma^2\mathbf{I}_N\right)$ is a multivariate

white Gaussian noise, with variance σ^2. This use-case is much more complex than the interference-free case and closed form approximations of outage probabilities have only been derived for few cases, e.g. $N = 1$ and Rayleigh/Rayleigh configuration.

In addition to these studies and due to non-tractable theoretical analysis in case of interference, I studied multi-user receivers for partial frequency overlap in heterogeneous WLANs. In particular, I proposed a method for reducing the complexity of a multi-user detector with maximum likelihood sequence estimator when multi-path channel is considered. These works have been published in [9–11].

3.2 Research interests since 2009

In this section, I sum up the researches I have been leading since my post-doctoral experience. Most of my researches has been related to energy efficient communications, through resource allocation schemes and theoretical analysis involving stochastic geometry and random matrix theory. Lastly, I have been interested in machine learning in order to increase the energy efficiency (EE) of wireless networks. One can question this interest for something that we do not actually transmit. Indeed, in some aspects this quantity is different from the spectral efficiency (SE) in the sense that this later refers to something that is directly related to user experience, i.e. data rate, over a costly resource, i.e. bandwidth. On the other hand, EE is the data rate over the power consumed to deliver this rate. However, wireless networks are connected to the grid so why searching for optimizing EE? The first clue is that even if networks are not power-critic, the operational costs for operators to run their network are increasing year-per-year [12]. Second, the CO_2 gaz emissions related to information and communications technologies (ICT) have been estimated as 2% of global CO_2 emissions in 2007 and gaz emissions of mobile communication systems alone should rise up to 0.4% of global emissions in 2020, according to the so-called FP7 EARTH project [13]. In the light of this facts, digital information appears as a costly technology not only in terms of money but also in terms of environmental resources and hence trying to use energy in the most efficient way for transmission makes sense. The structure of the second part of this manuscript will follow the research axes presented here.

3.2.1 Resource allocations for cellular wireless systems

I started working on resource allocations during my postdoctoral training, at ETIS Cergy-Pontoise, and I have continued to work on this issue after 2009. I have been interested in optimization problems arising when a finite set of physical resources, e.g. power, time, frequency, has to be shared among users. The context of my postdoctoral research was the National project RISC, cf. Section 1.8, which aimed at proposing new PHY layer and protocols for ad-hoc networks, i.e. without centralized infrastructure. I have been interested in the time scheduling of time-hopping ultra wide band (TH-UWB) communications. The first researches I supervised aimed at consolidating and developing, through new systems, the expertise skills gained during my postdoc. Since relaying technology for Long Term Evolution (LTE) systems was getting more and more attention, I oriented my first researches on resource allocation and performance analysis for orthogonal frequency division multiple access (OFDMA) systems with relays and hybrid automatic retransmission request (HARQ) mechanisms with Mohamad Maaz's PhD [14]. I pursued researches on resource allocations to optimize SE of OFDM-based systems that overlap in frequency. Under this framework, we studied in [15] the convergence issue of LTE and DVB systems. During the period 2009-2015, I investigated the following issues:

- **Multi-rate code allocation for UWB:** This research follows my earlier investigations I did during my postdoctoral training and I continued to collaborate with Prof. Inbar Fijlakow and Prof. Charly Poulliat. In TH-UWB communications, multiple users can access the channel by choosing different time-hopping codes (THC) from each others. In that scheme, the code structure is divided into N_f frames and N_c chips and a set of rules leading to an optimal code construction, i.e. minimizing the variance of interference, can be derived [16]. In the framework where users may have different data rates due to different number of frames, i.e. different N_f among users, I proposed a general expression for the variance of inter-code interference in multi-rate context. Based on this, I proposed a new algorithm to allocate various N_f to users to maximize the global data rate, under constraint of sufficient signal to interference plus noise ratio (SINR) per user [17].
- **Resource allocations for OFDM-based cellular systems:** In this theme, I first investigated power allocation for relay-aided OFDMA-based cellular systems in order to maximize SE in a single-cell environment. The study was performed considering reliable links, i.e. each user can operate at the Shannon capacity, and without considering other metrics such as delays or EE. Moreover, in LTE systems, HARQ is an important feature for delay-tolerant data transfer and should be dealt with. In real wireless scenarii, transmissions can rarely be considered reliable and non-vanishing error probability should be taken into account. Several performance metrics were analytically investigated for a single link with a relay node, i.e. PER, average delay, throughput efficiency, when using different kinds of HARQ schemes. Finally, the energy minimization problem of a single-cell multi-user OFDMA downlink communications with HARQ and relays has been investigated [18]. Moreover, a realistic study on energy efficient communication, including the baseband power consumption, has been addressed during the post-doc of Mohamad Maaz, funding by Orange Labs, Rennes. The study has been conducted with real power consumption measures on an FPGA target implementing the main blocks of LTE chain [19]. Finally, since spectrum in radio frequency bands is a rare resource, issues arising with spectral co-existence of wireless communication systems have been tackled in the framework of the ANR project Multi-Media in Mobility (M^3), with Hiba Bawab's PhD. In particular, power allocation to maximize the global data rate of frequency overlapping LTE and DVB systems was addressed. These two systems are OFDM-based signals with, however, different PHY characteristics. In consequence, the interference seen by an LTE or DVB receiver is different according to which system is viewed as the interferer. The variance of the interference seen by an LTE and DVB receiver respectively has been derived averaging over symbols, channels and asynchronism. This allows to numerically evaluate the performance of LTE transmissions impaired by a frequency-overlapped DVB signal and vice-versa [20].

3.2.2 Energy Efficiency of large networks and machine learning for green communications

The previous studies on spectral and energy efficient communications I conducted, were limited to a single cell network structure. In the framework of the project TEPN of the Laboratory of Excellence (Labex) Cominlabs, I pursued my investigations on spectral and energy efficient communications considering interfering cells and solutions to improve the network EE. I have been first interested by the scaling laws in EE of large wireless cellular networks with Ahmad Mahbubul Alam's PhD [21]. In parallel, I started work-

ing on reinforcement learning algorithms for green radio communications and networking with Navikkumar MODI's PhD co-supervised by Prof. Christophe MOY, CentraleSupélec, Rennes [22]. The following aspects have been tackled:

- **EE for large networks:** Since the seminal work of Gupta and Kumar on the achievable transport capacity (bit/s/m) of wireless ad-hoc networks [23], several works on theoretical achievable bounds for network information flows have emerged. The results in [23] state that the transport capacity per node scales in $O\left(1/\sqrt{N \log N}\right)$ with N the number of nodes. Özgür *et al.* have proved that hierarchical cooperation between nodes improve significantly the network capacity [24]. In the same idea, Rodoplu and Meng [25] defined the bits-per-joule capacity of a network as the maximum total number of bits that the network can deliver per Joule of energy deployed and studied how this quantity evolves with the size of the network. On this topic, we first studied the EE-SE tradeoff for a regular hexagonal grid network with a modified fluid model [26] that takes into account several frequency reuse factor for a single user in a cell. With a semi-analytic approach, i.e. a non-linear regressive model to fit the interference to noise ratio, we derived the $\epsilon-$EE-SE tradeoff in the hexagonal grid network for shadowing environment [27]. However, regular hexagonal deployment is far from reality and in order to cope with various network topology, we moved toward random network topology by using stochastic geometry tool [28]. The EE-SE tradeoff was investigated while considering that base stations (BSs) and users are modeled with two independent Poisson point processes (PPP) and BSs have multiple antennas. The asymptotic performance of the signal to leakage plus noise ratio (SLNR) precoder was investigated by letting the number of antennas and number of users growing to infinity by keeping a constant ratio between them [29].
- **Reinforcement learning for green communications:** One of the key feature for future communicating devices, will definitively be agility and reconfigurability. Cognitive radio, as defined by Mitola in 1999 [30], is a promising technology and decades of researches have been granted to make it a reality. In the project TEPN, we investigated a kind of reinforcement learning algorithm named upper confidence bound (UCB) algorithm. It is a policy based on trials and rewards in order to learn some parameters of a stochastic process. One of the main property of this algorithm is to have a logarithmic order regret [31]. We focused our first research on the opportunistic spectrum access (OSA) problem where we aimed at learning the best channel not only in terms of availability but also in terms of quality. The channels occupancy is modeled with the Markovian multi-armed bandit (MAB) framework, where each arm is a channel whose occupancy is governed by a Markov process while channel quality is modeled as an independent and identically distributed (i.i.d.) process. Previous works investigated the problem to take into account the quality of a channel in the learning process, e.g. [32] and references therein. These works rightly considered reward as a continuous real-valued function instead of binary-valued. However, a policy that is able to weight separately different criteria to learn on statistical properties of channels could be very interesting for various scenarii. The authors in [33] have also proposed to separate the availability and quality metrics but without characterizing the convergence rate of their policy. Our contribution in this field was to consider separate rewards for availability and quality, the later being firstly taken as interference temperature for instance, and to prove the logarithmic order regret of the modified UCB policy for restless MAB and multiple players [34]. The interesting feature of our policy is that the quality

criterium is not limited to the interference temperature but can be another metric for another scenario than OSA. Indeed in a second step, we then applied the reinforcement learning procedure developed for the OSA scenario to the dynamic network deployment problem. In this issue, we searched for the set of BSs to be switched ON or OFF in order to maximize EE of the network. An arbitrary BSs deployment is considered with a central controller able to measure EE w.r.t. trafic load variations in the cells. A near optimal configuration can be learned by the controller and the trafic load variation over the day can successfully be followed in time [35].

3.2.3 Protocols for network coding (NC)

I started this research theme with my collaboration with Ayman Khalil from LIU with Samih Abdul-Nabi's PhD [36]. I left aside a moment my studies on signal processing and PHY layer to investigate higher-layer protocols to make network coding happening. These studies did not aim at contributing on coding theory for networks, but rather proposing some protocols enhancing NC performance. My contributions on this theme are summarized below:

- **Address correlated network coding (ACNC) protocol:** The idea was to propose to use NC only on packets which present a "correlation" in their address. For instance, two packets arriving in an intermediate node in provenance from nodes A and B respectively. A being the source of one packet and the destination of the other. Similar definition holds for B. ACNC adds a layer between layers 2 and 3 in the open system interconnection (OSI) model. In general, ACNC generates a coded message made of packets coded together using XOR operation on bits of the packets. A header is added to each coded message describing each packet coded within the message and the correlation between these packets. ACNC also uses adaptive flag to steer coded messages to various destinations [37].
- **Aging concept:** In multi-hop communication networks, intermediate nodes may receive not only newly generated packets but also coded messages that need to be further coded together. We defined the message cardinality as the number of times this message has been used in a coded packet. With multiple intermediate nodes, the cardinality of all messages will increase and this calls for buffering all already transmitted and coded packets which increases the storage costs. The concept of "maturity age" has been introduced in order to limit the number of times a message is used in a coding activity. We hence showed that the cardinality remains bounded in the network and that the number of transmissions decreases with maturity [38].
- **Impact of packet loss on NC performance:** Without NC, lost packets have no impact on the delivery of other transmitted packets. With NC, the packet loss may affect the decoding of other transmitted packets thus affects the entire process of communication between nodes. We first studied the packet loss impact when decoding is performed at the end nodes. A packet loss severely affects the number of transmissions and the cardinality of coded messages. The percentage of undecoded packets increases with loss probability, without surprise, and the higher the maturity age, the higher the percentage of undecoded packets. For decoding at end nodes, two new recovery mechanisms initiated by end nodes were proposed to handle packet loss with NC; i) immediate retransmission request (IRR) mechanism that uses information extracted from the undecodable messages to request the retransmission of lost packets, ii) recovery from packet loss mechanism with a basic

covering set discovery (BCSD) that allows reducing the number of retransmissions to recover lost packets. For distributed decoding, a loss detection and recovery mechanism was studied. This technique uses network coded received messages as feedback for packet delivery and automatically adds potentially lost packets to the list of arrivals that need to be transmitted [39].

3.2.4 Non asymptotic information theory for IoT

Following my short visit at Princeton in April 2014, Prof. Jean-Marie Gorce, Prof. Laurent Clavier and I decided to present an ambitious project on fundamental bounds of Internet of things (IoT) networks, named achievable region for bursty wireless networks (ARBurst). IoT, myth or reality, is currently driving a huge amount of fundings and industrial and academic researches as well. The features of these networks, according to our vision, are the following: short packets and bursty communications, i.e. some bytes have to be transmitted time to time but not continuously. While the first hypothesis makes the use of the asymptotic Shannon theory not strictly relevant due to the finite block length of packets used in IoT [40], the second invalidates the Gaussian assumption of interferences usually made in large networks. Our project aims at defining firstly what are the relevant criteria to characterize the performances of IoT networks, e.g. end-to-end reliability, delays, nodes density an access point may support. Once the metrics defined, we aim at finding some fundamental bounds, achievability and converse, holding under finite block length and impulsive interference hypothesis. The proposed bounds will serve as a benchmark to compare existing solutions for IoT, e.g. Sigfox and Lora technologies. I have started working on this issue by first analyzing the practical impact of non asymptotic information theory on the EE-SE tradeoff in AWGN but also on the error probability in fading channels [41].

3.2.5 Supervision and projects

Up to now, I have co-supervised 5 PhD students, 1 post-doc and 6 Master students. I have participated to several projects, in collaborations with academics (IMT Atlantique, CentraleSupélec, INRIA) and industrial (Orange Labs). These experiences gave me a wide spectrum of skills in wireless communications, mainly centered around resource allocations and performance analysis in a first place, but more recently in machine learning. As exposed above, the ANR project ARBurst, for which I am the coordinator for INSA Rennes, has recently been accepted and will drive, for the next few years a large part of my research.

Part II

Scientific contributions

CHAPTER

4 Resource allocations for multi-user communications

During decades, the point-to-point scenario has been at the center of interest of researches on wired and wireless communications. With the Shannon era, engineers had a target to pursue, i.e. practical schemes to achieve the point-to-point channel capacity and the best rate compression of a source. Theoreticians have been interested very early on the best achievable regions, rate or compression, of multi-user problems, with some complete results rather recently, we may say, for some of them, e.g. multiple access and broadcast channels in 70's, cf. [42] for a good historical overview. Performance of multi-user wireless systems is closely related to the resources management in the network. This management can be centralized, like in cellular wireless networks, or distributed in case of ad-hoc networks. In the research results presented in this part, we focus on centralized management done in cellular networks and on physical resources that can be shared in a network, e.g. power or subcarriers.

In this Chapter, I expose the main researches I developed on resource allocations and mathematical optimization. I have been interested in several aspects of resource allocations, from convex optimization to integer programming. Section 4.1 summarizes my technical contributions on the problem of code provisioning in multi-rate UWB cellular communications. In Section 4.2, I move toward power allocation, relay selection and modulation and coding scheme (MCS) provisioning for multi-users OFDMA communications with delay constraints in a single cell network. Interference is the major limitation of high spectral efficiency communications and Section 4.3 deals with power allocation for overlapping OFDM signals, in the framework of LTE and DVB co-existence. Finally, Section 4.4 draws the conclusions of the Chapter, summarizes my contributions and gives some research perspectives on that subject.

4.1 Rate provisioning for uplink UWB communications

I have been first interested in resource allocation during my post-doc position at ETIS, Cergy-Pontoise. The context of my researches was the ANR project RISC that aims at designing ad-hoc networks, i.e. from PHY to network layers, for crisis situations, e.g. earthquake, chemical accident, etc. The waveform chosen for this project was TH-UWB, which consists in sending very short impulses, Gaussian shaped for instance, modulated in amplitude or in position, i.e. pulse amplitude modulation (PAM) or pulse position modulation (PPM) respectively. Moreover, TH-UWB is a code-division multiple access (CDMA) scheme by essence; multiple users can access the channel at the same time by assigning a time-hopping code to each user. A time-hopping code, is a sequence of well timely-located pulses whose positions in a frame defined the access code of a user. A symbol for one user is divided in N_f frames, also known as *processing gain*, each divided in N_c chips, and each chip has a duration of T_c seconds. In standard configuration envisaged in RISC project, N_f, N_c and T_c are fixed and an UWB symbol has the duration $T_s = N_f N_c T_c$. Fig. 4.1 illustrates the UWB symbol structure, where T_f is the frame duration.

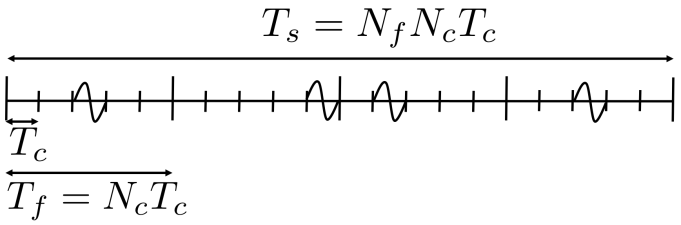

Figure 4.1 – Example of TH-UWB symbol structure, with $N_c = 5$, $N_f = 4$ and arbitrary waveform and chip duration.

The authors in [16] have derived a set of rules allowing to choose codes that minimize the multiple access interference (MAI) power for PAM and PPM modulations. These properties have been established by a careful analysis of the inter-code interference caused by multiple accesses on the channel. Moreover, due to several gigahertz bandwidth used by TH-UWB signals, power control is very difficult to realize in practical systems, if not impossible, and hence cannot be considered from a practical point of view. In this context, during my post-doc, I have first dealt with scheduling, i.e. time slot allocation, with a realistic propagation channel, based on results developed in [16], and I proposed a scheduling algorithm to maximize the network sum-rate [43].

The signal model discussed above does not allow different symbol duration among users and hence different rates. After my post-doctoral training, I pursued my investigations on resource allocations in UWB when users may have variable symbol duration, i.e. $T_s^{(u)}$, $\forall u \in \mathcal{U}$, i.e. the set of users in the network. Symbol duration may vary in several ways; in this work, I assumed that N_c remains fixed for all users and BS allocates N_f to users according to their rate demand.

Some researchers investigated the rate allocation problem in multi-rate cellular CDMA systems, e.g. [44, 45] and references therein. Authors in [44] considered the adaptive rate allocation problem in direct sequence (DS) CDMA systems, by assigning various spreading gains among users. However, the particular frame structure of TH-UWB systems with N_c chips and N_f frames implies non trivial dependency between these parameters and the global throughput. This particular structure makes the PHY layer model of [44] and the associated multi-rate resource allocation strategy unsuitable for TH-UWB systems. On the

other hand, the works dealing with multi-rate TH-UWB systems either did not focus on rate adaptation via variable processing gain allocation or considered only AWGN channel. Indeed, the authors in [46] developed an SINR model for multi-rate TH-UWB systems based on an approximation of the MAI variance. However, only AWGN and synchronous transmission have been considered and hence the variance expressions given in [46] are simpler and not as realistic as the ones which would be obtained in multipath fading environments. Moreover, the processing gain ratio between users has been considered as an integer, which significantly simplifies the inter-code interference analysis. The authors of [47] dealt with coded and uncoded TH-UWB systems with multi-rate capabilities with multi-services assignment. They effectively considered the use of various spreading gains for several rate services but without dealing with spreading gain allocation.

I first focused on the problem of an accurate model for MAI power when N_f varies among users. I have searched for a more general framework based on [16] to express the variance of MAI in multi-rate TH-UWB communication systems. For two users competing for the channel access in uplink, the interference seen by BS when decoding the signal of one user is not the same for both users, depending on the relation order between $N_f^{(1)}$ and $N_f^{(2)}$, i.e. $N_f^{(1)} \lesseqgtr N_f^{(2)}$, $N_f^{(1)}$ and $N_f^{(2)}$ being the number of frames of user 1 and 2 respectively. We tackled the processing gain allocation problem as a general mixed integer and signomial programming problem. Due to its very difficult nature, it cannot be guaranteed to find the global optimal solution. We proved that the mixed integer and signomial programming problem can be approached locally by a posynomial problem and hence can be solved via the combination of geometric programming and a branch and bound algorithm. In the following, I expose the main results obtained in this work.

4.1.1 Multi-rate TH-UWB interference analysis

Let us consider asynchronous uplink multiuser communications in a single cell network, with one BS and N_u users. By letting N_c and T_c fixed for all users in the network but allowing different $N_f^{(u)}$ among users, the UWB symbol duration of the $u-$th user is $T_s^{(u)} = N_c N_f^{(u)} T_c$ and the signal transmitted by this user is:

$$s_u(t) = \sum_i d_u(i) \sum_{j=0}^{N_c N_f^{(u)}-1} c_u(j) w\left(t - iT_s^{(u)} - jT_c - \theta_u\right), \tag{4.1}$$

where $w(t)$ is the impulse of duration $T_w \ll T_c$, d_u are the zero-mean, unit-variance PAM and θ_u is the asynchronism between users. Moreover, $c_u := \{c_u(j)\}_{j=0}^{N_c N_f^{(u)}-1}$ is the $u-$th developed time hopping code (DTHC) as defined in [16]. The UWB signal is sent through a multipath channel with N_p paths and processed at BS by a rake receiver containing L_r fingers. The signal of user u received at BS can be decomposed as [16]:

$$z^{(u)} = z_u + z_{\text{mai}} + \eta^{(u)}, \tag{4.2}$$

with:

$$z_u = \sqrt{P_u} \sum_{l=1}^{L_r} \left(A_u^l\right)^2 N_f^{(u)} d_u(0), \tag{4.3}$$

$$z_{\text{mai}} = \sum_{l=1}^{L_r} A_u^l \sum_{\substack{u'=1 \\ u' \neq u}}^{N_u} \sqrt{P_{u'}} \sum_{n=1}^{N_p} A_{u'}^n y_{u',u}^{n,l}(\theta_{u'}), \tag{4.4}$$

where:

$$y_{u',u}^{n,l}(\theta_{u'}) = \sum_i d_{u'}(i) \sum_{j=0}^{N_c N_f^{(u')}-1} \sum_{j_u=0}^{N_c N_f^{(u)}-1} c_{u'}(j) c_u(j_u) \times r_{ww}\left(iT_s^{(u')} + (j-j_u)T_c + \Delta_{u',u}^{n,l} + \theta_{u'}\right), \quad (4.5)$$

z_u and z_{mai} are the useful part of the signal and MAI respectively. Theoretically, intersymbol interference should be taken into account, which is not a trivial issue. In a first approximation, intersymbol interference is neglected by inserting a guard time at the end of each frame [16, 48, 49]. Moreover, $r_{ww}(s)$ is the autocorrelation function of the pulse waveform and $\eta^{(u)}$ is the filtered Gaussian noise [16,49]. $A_u^n = a_u^n e^{-\tau_u^n/2\gamma}$ is the $n-$th path amplitude of the $u-$th user where τ_u^n is the delay of the $n-$th path of the user u and a_u^n are zero mean random variables independent of delays and with a variance σ_a^2 [16, 50]. Moreover γ is a statistical channel parameter and is related to the channel impulse response length as defined in [50] and used in [16,49]. We also define $\Delta_{u',u}^{n,l} = \tau_{u'}^n - \tau_u^l$ as the difference between the delay of the $n-$th path of user u' and the delay of the $l-$th path of user u. Finally, P_u is the received power at the BS for the $u-$th user after path loss propagation.

In order to allocate *processing gains* to each user, average MAI should be expressed in a convenient way w.r.t. $N_f^{(u)}$, N_c and T_c and channel parameters. We first set $N_f^{(u)} = \alpha^{(u')} N_f^{(u')}$, with $\alpha^{(u')} > 0$ and $\alpha^{(u')} \in \mathbb{Q}$, i.e. the rational number set. Like in [16], the key point is to consider the Euclidean division of $\theta_{u'} + \Delta_{u',u}^{n,l}$ w.r.t. $T_s^{(u')}$ and T_c yielding to $\theta_{u'} + \Delta_{u',u}^{n,l} := Q_{u'}^{n,l} T_s^{(u')} + q_{u'}^{n,l} T_c + \epsilon_{u'}^{n,l}$ with:

$$Q_{u'}^{n,l} = \left\lfloor \frac{\theta_{u'} + \Delta_{u',u}^{n,l}}{T_s^{(u')}} \right\rfloor \in \{-\infty, \infty\}, \quad (4.6)$$

$$q_{u'}^{n,l} = \left\lfloor \frac{\theta_{u'} + \Delta_{u',u}^{n,l} - Q_{u'}^{n,l} T_s^{(u')}}{T_c} \right\rfloor \in \left\{0, \cdots, N_c N_f^{(u')} - 1\right\} \quad (4.7)$$

and $\epsilon_{u'}^{n,l} \in [0, T_c[$ is the remainder of the Euclidean division and $\lfloor \cdot \rfloor$ denotes the floor rounding. Thanks to this relationship, eq. (4.5) can be written as:

$$y_{u',u}^{n,l}(\theta_{u'}) = \sum_i d_{u'}(i) \sum_{j=0}^{N_c N_f^{(u')}-1} \sum_{j_u=0}^{N_c N_f^{(u)}-1} c_{u'}(j) c_u(j_u) \times r_{ww}\left(\left(i + Q_{u'}^{n,l}\right) T_s^{(u')} + \left(q_{u'}^{n,l} + j - j_u\right) T_c + \epsilon_{u'}^{n,l}\right) \quad (4.8)$$

4.1.2 Variance of MAI with multiple rates

The autocorrelation function r_{ww} in (4.8) can be proved to be non zero if and only if $-2 < Q_{u'}^{n,l} + i \leq \left\lceil \alpha^{(u')} \right\rceil - 1$, with $\lceil \cdot \rceil$ being the ceil rounding. One important theoretical result is stated in the following lemma, which extends and generalizes the result in [16]:

Lemma 1 *In multi-rate PAM TH-UWB communications, the multiuser interference can be written as:*

$$y_{u',u}^{n,l}(\theta_{u'}) = \sum_{k=-1}^{\left\lceil \alpha^{(u')} \right\rceil - 1} d_{u'}\left(k - Q_{u'}^{n,l}\right)\left[C_{u,u'}^{k}\left(q_{u'}^{n,l}\right) r_{ww}\left(\epsilon_{u'}^{n,l}\right) + C_{u,u'}^{k}\left(q_{u'}^{n,l}+1\right) r_{ww}\left(\epsilon_{u'}^{n,l} - T_c\right)\right] \quad (4.9)$$

Where $\forall \alpha^{(u')}$*:*

$$C_{u,u'}^{-1}(q) = \sum_{p=0}^{\min\left(q, N_c N_f^{(u)}\right)-1} c_u(p)\, c_{u'}(p-q) \quad (4.10)$$

If $\alpha^{(u')} < 1$*:*

$$C_{u,u'}^{0}(q) = \sum_{p=\min\left(q, N_c N_f^{(u)}\right)}^{N_c N_f^{(u)}-1} c_u(p)\, c_{u'}(p-q) \quad (4.11)$$

If $\alpha^{(u')} \geq 1$ *and for* $0 \leq k \leq \left\lceil \alpha^{(u')} \right\rceil - 1$ *then:*

$$C_{u,u'}^{k}(q) = \sum_{p=q+kN_cN_f^{(u')}}^{\min\left(q+(k+1)N_cN_f^{(u')}, N_cN_f^{(u)}\right)-1} c_u(p)\, c_{u'}\left(p-q-kN_cN_f^{(u')}\right) \quad (4.12)$$

Lemma 1 allows to express the pulse autocorrelation function simply with discrete cross-correlation of codes. The final expression of $y_{u',u}^{n,l}$ is however more complex than in [16] in which only two cross-correlation terms appear, i.e. $C_{u,u'}^{-}$ and $C_{u,u'}^{+}$. Here the number of cross-correlation terms depends on the ratio of processing gains. Instead of having only two UWB symbols involved in MAI in [16], we have here $\left\lceil \alpha^{(u')} \right\rceil + 1$ UWB symbols of user u' involved in MAI. Let us consider two users, u and u' with $N_f^{(u)} = 4$, $N_f^{(u')} = 2$ and $N_c = 4$. According to Lemma 1, and illustrated in Fig. 4.2, three cross-correlation terms are involved in MAI, i.e. $C_{u,u'}^{-1}(q_{u'})$, $C_{u,u'}^{0}(q_{u'})$ and $C_{u,u'}^{1}(q_{u'})$, where $q_{u'}$ is the cross-correlation delay. On this figure, DTHC associated to users u and u' are respectively $c_u = \{0,1,0,0,1,0,0,0,0,0,0,1,0,0,0,0,1\}$ and $c_{u'} = \{1,0,0,0,0,0,0,1\}$ for a lag equal to 3. Due to a smaller symbol duration, user u' has three symbols interfering with one symbol of user u leading to three cross-correlation terms in MAI expression.

In order to obtain the SINR expression, z_{mai} has to be averaged over amplitudes A_u^l, symbols d_u, asynchronism θ_u, delays τ_u as in [16], and finally over the codes. The averaged expression of z_{mai} depends on the second order moments of $C_{u,u'}^{k}$, $\forall k \in \left\{-1, \cdots, \left\lceil \alpha^{(u')} \right\rceil + 1\right\}$ which are illustrated in Fig. 4.3, for two values of $\alpha^{(u')}$, i.e. $\frac{3}{8}$ and $\frac{8}{3}$ in Fig. 4.3(a) and 4.3(b) respectively. Thanks to Lemma 1 and by averaging over the codes, the variance of MAI can be proved to be as stated in Theorem 1.

Theorem 1 (Variance of z_{mai}) *In multi-rate TH-UWB communications with PAM signals, the variance of MAI averaging over the codes is:*

$$V_{mai}^{(u)} = \Lambda \sum_{\substack{u'=1 \\ u' \neq u}}^{N_u} \frac{P_{u'}}{N_f^{(u')}} M_c(u,u'), \quad (4.13)$$

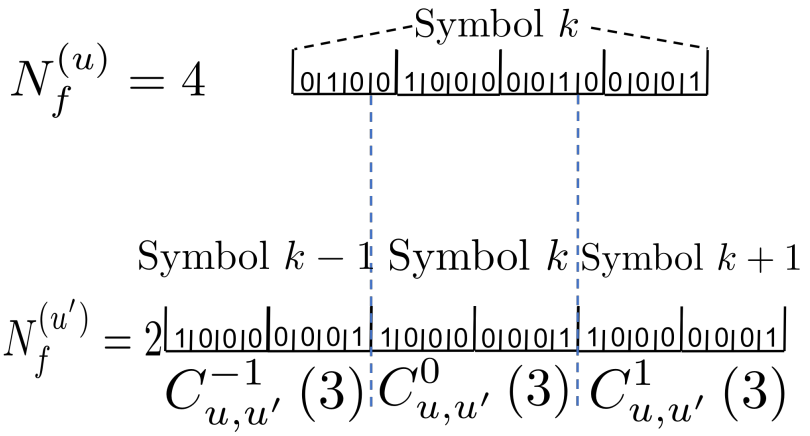

Figure 4.2 – Example of cross-correlation terms for two users when $N_f^{(u)} = 4$, $N_f^{(u')} = 2$, $N_c = 4$ and a lag equal to 3.

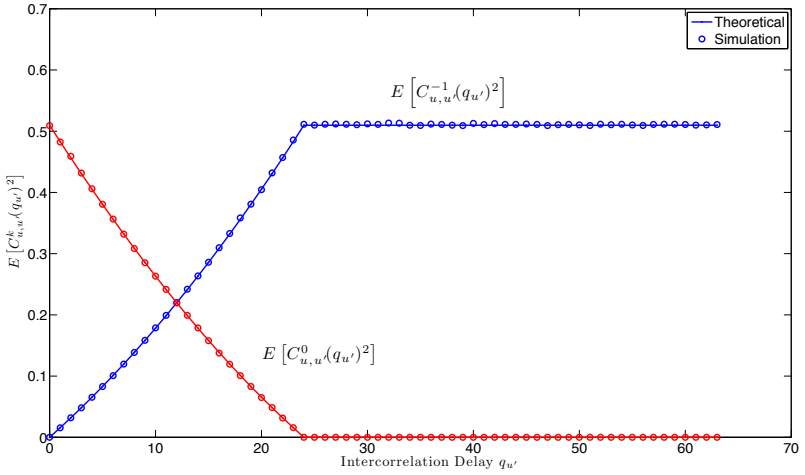

(a) $\alpha^{(u')} = \frac{3}{8}$; $N_c = 8$

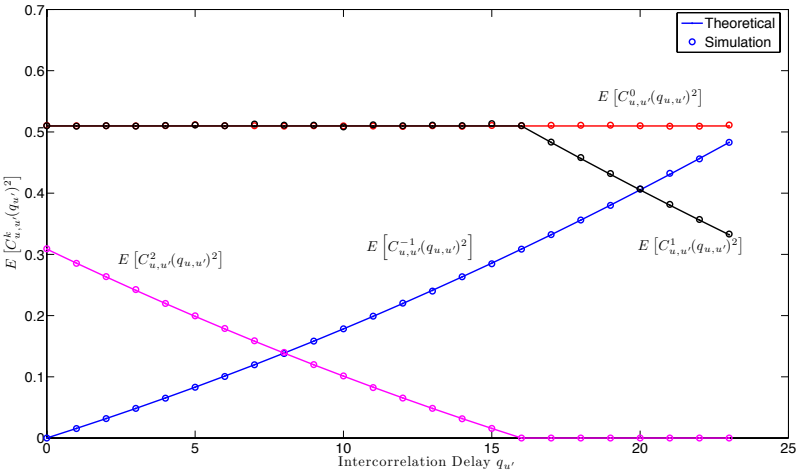

(b) $\alpha^{(u')} = \frac{8}{3}$; $N_c = 8$

Figure 4.3 – Second order moments of intercode cross-correlation functions for $\alpha^{(u')} < 1$ and for $\alpha^{(u')} \geq 1$ [17]

with, if $\alpha^{(u')} \geq 1$ *then* $M_c(u,u') := M_c^+(u,u')$*:*

$$M_c^+\left(u,u'\right) = N_f^{(u')}\left[3N_c\left(N_c^2 + N_c N_f^{(u')} - 1\right)N_f^{(u)} - N_c^2 {N_f^{(u')}}^2 + 1\right], \tag{4.14}$$

and if $\alpha^{(u')} < 1$ *then* $M_c(u,u') := M_c^-(u,u')$*:*

$$M_c^-\left(u,u'\right) = N_f^{(u)}\left[3N_c\left(N_c^2 + N_c N_f^{(u)} - 1\right)N_f^{(u')} - N_c^2 {N_f^{(u)}}^2 + 1\right]. \tag{4.15}$$

where Λ is a constant depending on channel parameters and pulse shaping. Averaging over the codes is done considering that vector $c_u\ \forall u$, is the realization of an i.i.d. random vector whose each component is a Bernoulli random variable with parameter $p = 1/N_c$ [51]. Hence, $C_{u,u'}^k(q)$ is a binomial random variable depending on k and on $\alpha^{(u')}$. The complete proofs of Lemma 1 and Theorem 1 can be found in [17] for further details.

The closed-form expression of MAI variance allows to express SINR of user u at BS as in the expression below:

$$\mathrm{SINR}_u\left(N_f^{(u)}\right) = \frac{P_u G_u {N_f^{(u)}}^2}{\Lambda\left(\sum_{\substack{u'\in\mathcal{U}_+ \\ u'\neq u}} \frac{P_{u'}}{N_f^{(u')}} M_c^+(u,u') + \sum_{v\in\mathcal{U}_-} \frac{P_v}{N_f^{(v)}} M_c^-(u,v)\right) + \frac{N_0 N_f^{(u)}}{2} V_n} \tag{4.16}$$

where G_u and V_n are the processing gain of desired user and noise enhancement due to rake receiver respectively. Moreover the following sets are defined $\mathcal{U}_+ = \left\{u' \mid \alpha^{(u')} \geq 1, u' \neq u\right\}$ and $\mathcal{U}_- = \left\{v \mid \alpha^{(v)} < 1\right\}$, such as $\mathcal{U}_+ \cup \mathcal{U}_- = \mathcal{U}$ and $\mathcal{U}_+ \cap \mathcal{U}_- = \emptyset$. The set $\mathcal{U}$ is reminded to be the set of all users in the cell. The sets $\mathcal{U}_+$ and $\mathcal{U}_-$ are the set of interfering users which have a lower or equal number of frames than the user of interest and the set of interfering users which have a strictly larger number of frames than the user of interest respectively.

The form of SINR is fundamental and exhibits a non-linear behavior that will affect the interference experienced by users when the number of frames per user changes. In the next section, I expose how handling rate allocation through the number of frames per user.

4.1.3 Rate provisioning

The interest having a closed-form expression for SINR is to express a data rate maximization problem under SINR contraints for each user. The effective throughput of user u is $D_u = 1/\left(N_c N_f^{(u)} T_c\right)$ provided that its SINR is greater than a threshold $\Gamma_{\min}$ [44]. This approach follows the Shannon philosophy, despite the data rate being not expressed with log function. Indeed, given a finite set of modulation scheme, the spectral efficiency that system may achieve is at most the spectral efficiency of the modulation, provided that SINR is above a threshold, which can be expressed as a function of the Shannon limit in E_b/N_0. If not, no coding scheme can guarantee a vanishing error probability. The maximization of global throughput, i.e. $\max \sum_u D_u$, subject to SINR constraint for each user is a highly non-convex problem and combines continuous constraints (i.e. SINR constraints) and integer constraints (i.e. $N_f^{(u)} \in \{1, \cdots, N_c\}$) [52]. This combination induces an exponential complexity, i.e. $O\left((N_c)^{N_u}\right)$, of the optimal search and cannot be envisaged for large problem (i.e. large N_c and N_u). For the sake of clarity, let us remind some definitions from literature [53] that will be used hereafter.

Definition 1 (Posynomial function) *A posynomial function with K terms is a real-valued function of n positive variables with the form*

$$f: \begin{array}{ccc} \mathbb{R}^{+n} & \longrightarrow & \mathbb{R}^{+} \\ \mathbf{x} & \longmapsto & \sum_{k=1}^{K} c_k x_1^{a_{1k}} x_2^{a_{2k}} \cdots x_n^{a_{nk}} \end{array} \tag{4.17}$$

with $c_k > 0$, $a_{ik} \in \mathbb{R}$, $\forall (i,k) \in \{1, \cdots, n\} \times \{1, \cdots, K\}$ and $\mathbf{x} = (x_1, \cdots, x_n)^T$ is the multi-dimensional variable of the function.

Definition 2 (Geometric program) *A geometric program is an optimization problem of the form*

$$\begin{array}{ll} \min\limits_{\mathbf{x}} & f_0(\mathbf{x}), \ s.t. \\ & f_i(\mathbf{x}) \leq 1, \forall i \neq 0 \end{array} \tag{4.18}$$

where f_0 and f_i $\forall i$, are posynomial functions. A geometric optimization problem can eventually includes some equality constraints with monomial functions of variables $x_1, x_2, \cdots, x_n$, i.e. functions that contain only one term of the summation in (4.17).

Definition 3 (Signomial function and program) *A signomial function is a function of the form in* (4.17) *but in which $c_k \in \mathbb{R}^*$. By extension, a signomial optimization problem is a problem of the form* (4.18) *in which the functions are signomial.*

While a global optimum can be found for geometric problems due to their convex nature, this is not the case for signomial problems where only a *local optimum* can be computed efficiently. The maximization of the global throughput can be easily proved to be equivalent to $\min \prod_{u=1}^{N_u} N_f^{(u)}$ yielding to the modified optimization problem:

$$\begin{array}{ll} \min\limits_{\mathbf{N_f}} & \prod\limits_{u=1}^{N_u} N_f^{(u)}, \text{ s.t.} \\ (c_1) & \text{if } P_u > 0 \text{ then } \frac{\Gamma_{\min}}{\mathrm{SINR}_u\left(N_f^{(u)}\right)} \leq 1, \forall u \in \mathcal{U} \\ (c_2) & N_f^{(u)} \geq 1, \forall u \in \mathcal{U}, \\ (c_3) & N_f^{(u)} \leq N_c, \forall u \in \mathcal{U}, \\ (c_4) & N_f^{(u)} \in \mathbb{N}, \forall u \in \mathcal{U}, \end{array} \tag{4.19}$$

$\mathbf{N_f} = \left(N_f^{(1)}, \cdots, N_f^{(N_u)}\right)^T$ is a vector representing the number of frames for each user. The optimization problem stated in (4.19) is a mixed integer signomial programming problem. The problem is referred as signomial because of summation of products with positive and negative coefficients in the constraint (c_1). The constraint (c_3) refers to the work of Le Martret *et al.* in [16] who have shown that there exists rigorous algebraic conditions to minimize the MAI variance of pair of codes and in particular N_f should not be greater than N_c. Due to the integer constraint on $N_f^{(u)}$, finding a global minimum is not envisageable because of prohibitive computational time.

However, the major issue of this problem comes from the form of MAI power in Theorem 1 and hence from the SINR expression in (4.16). Indeed, denominator of (4.16) presents summations over two incompatible sets, i.e. $\mathcal{U}_+$ and $\mathcal{U}_-$, whose cardinalities depend on the relative values of $N_f^{(u)}$ among users. Another way to express the denominator of (4.16) is as follows:

$$D_{\text{sinr}} = \sum_{\substack{u' \in \mathcal{U} \\ u' \neq u}} \frac{P_{u'}}{N_f^{(u')}} \left(\left[M_c^+(u,u') - M_c^-(u,u') \right] \mathbb{1}_{N_f^{(u')} \geq N_f^{(u)}} + M_c^-(u,u') \right) \tag{4.20}$$

where $\mathbb{1}_{N_f^{(u')} \geq N_f^{(u)}}$ equals to 1 if $N_f^{(u')} \geq N_f^{(u)}$ and is null otherwise. In other words, for two different vectors $\mathbf{N_f}$ and $\mathbf{N_f}'$ allocated to users, SINR experienced by each user will be different due to different repartition of users in the sets $\mathcal{U}_+$ and $\mathcal{U}_-$. Hence, any iterative algorithm attempting to solve (4.19) will imply a changing constraint (c_1) leading to non linear behavior of the algorithm.

The problem in (4.19) can however be locally converted in a geometric program by relaxing the integer constraint on $N_f^{(u)}$ in a first place and by *locally* approximating the signomial function in (c_1) by a posynomial at a particular point, and to solve the convex problem obtained and iterate on the solution. At each iteration, the original problem can be *locally* approximated by the following optimization problem:

Proposition 1 (Geometric approximation of signomial problem [17]) *The mixed integer signomial optimization problem stated in* (4.19) *can be locally approximated by the following geometric programming problem:*

$$\begin{array}{ll} \min\limits_{\mathbf{N_f}} & \prod\limits_{u=1}^{N_u} N_f^{(u)}, \ s.t. \\ (\tilde{c}_1) & \text{if } P_u > 0 \text{ then } \frac{p_u\left(\hat{\mathbf{N}}_\mathbf{f}\right)}{\beta_u \prod_{j=1}^{N_u}\left(\hat{N}_f^{(j)}\right)^{\alpha_u}} \leq 1, \forall u \in \mathcal{U} \\ (c_2) & N_f^{(u)} \geq 1, \forall u \in \mathcal{U}, \\ (c_3) & N_f^{(u)} \leq N_c, \forall u \in \mathcal{U}, \\ (\tilde{c}_4) & (1-\eta)\,\hat{N}_f^{(u)} \leq N_f^{(u)} \leq (1+\eta)\,\hat{N}_f^{(u)}, \forall u \in \mathcal{U} \end{array} \tag{4.21}$$

Constraint (c_1) in (4.19) can be expressed by a difference of two posynomials and be reformulated as $p_u\left(\hat{\mathbf{N}}_\mathbf{f}\right) \leq r_u\left(\hat{\mathbf{N}}_\mathbf{f}\right)$ where p_u and r_u are posynomials. $\beta_u \prod_{j=1}^{N_u}\left(\hat{N}_f^{(j)}\right)^{\alpha_u}$ is the best local monomial approximation around $\hat{\mathbf{N}}_\mathbf{f}$ of $r_u\left(\hat{\mathbf{N}}_\mathbf{f}\right)$, where α_u and β_u are some coefficients. The important point here is that $(\tilde{c}_1)$ is now a posynomial constraint. The optimization problem in (4.21) is a geometric programming problem and can be solved very efficiently with modern techniques [53]. Constraint $(\tilde{c}_4)$ is added in order to bound the validity of the next guess in an iterative procedure. Indeed, since (4.21) is not the original problem but just a local approximation, solving this problem without paying attention on the value returned on $\hat{\mathbf{N}}_\mathbf{f}$ may lead to non trustable solution. The real η ensures the next guess not to be too far from the current guess [53]. This allows us to find a local optimal allocation of $N_f^{(u)}$ $\forall u \in \mathcal{U}$. This idea is illustrated on Fig. 4.4 which shows a non convex function, i.e. $f_0(x)$, locally approximated by a convex function, with a validity range for estimating the next guess of the solution.

Based on this modelisation, I proposed several algorithms to solve the problem in (4.21). It is important to note that the proposed procedures are heuristics, i.e. their performance cannot be proved formally, but simulation shows interesting performance. The first algorithm proposed in [17] is named Adaptive Rate Allocation with Signomial Programming (ARASP). This scheme consists in solving (4.21) starting from a feasible point and applying a standard geometric program tool available in literature, see [53] and references therein. The solution is searched on a continuous interval, i.e. $N_f^{(u)} \in [1, N_c]$ $\forall u \in \mathcal{U}$, and not on a discrete set. Searching a feasible point, i.e. $\mathbf{N_f}$ satisfying the constraints in (4.19) is not a trivial task. It is worth mentioning that there is no analytical and general method to find such a point for a non-convex problem. Some meta-heuristics can be used such as tabu search or simulated annealing for instance, but those methods

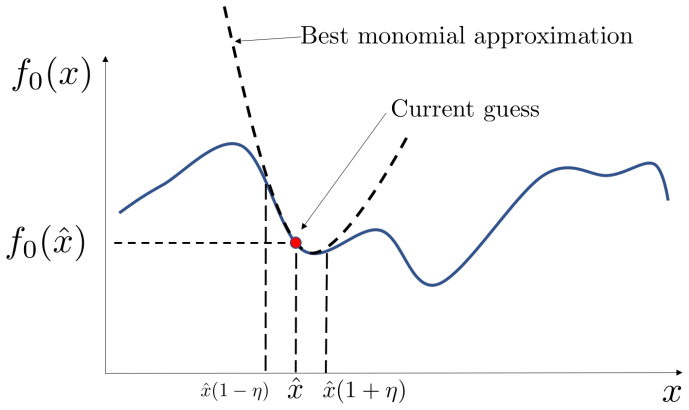

Figure 4.4 – Best local monomial approximation of a non-convex function

can be complex and computationally prohibitive just to find a feasible point. One can also used a random search to find such a point. Experience shows that a few hundred iterations are enough to find a feasible point with a random search for practical values of system parameters, e.g. $N_c = 13$ and N_u up to 20.

The second scheme proposed in [17] is named Adaptive Rate Allocation with Branch and Bound and Signomial Programming (ARABBSP). In that scheme, we aim at giving a solution in a discrete set, i.e. $N_f^{(u)} \in \{1, \cdots, N_c\}\ \forall u$. Once a feasible point is found, problem (4.21) is solved with signomial program, i.e. ARASP. Since the solution $\mathbf{N_f^*}$ belongs to $\mathbb{R}$, it is not suitable to practical systems. For a given non-integer entry in the vector $\mathbf{N_f^*}$, let say $N_f^{(j)}$, two subproblems are created, i.e. P_1 and P_2, the former with the additional constraint $N_f^{(j)} \leq \left\lfloor N_f^{(j)^*} \right\rfloor$ and the latter with $N_f^{(j)} \geq \left\lceil N_f^{(j)^*} \right\rceil$ [1] and both problems are solved with ARASP. This operation is repeated until the vector $\mathbf{N_f}$ only contains integer entries. Branch and bound procedure typically applies for non linear problems that have to be solved on the natural integer set. The principle is to start from an original problem, where the integer constraints have been released, and from the solution obtained, create subproblems integrating integer constraints by comparing the solution obtained in the real set to the floor and ceil rounding of it. The subproblems created are then solved and subproblems are again created on new solutions. A tree of subproblems is then obtained where the branches leading to satisfying solutions are kept while the others are eliminated. This is repeated until finding a unique suitable solution. When the problem is well conditioned, branch and bound performs very well. Actually, branch and bound procedure is not a heuristic, in the sense that it provides a provable upper and lower bound of the optimal solution [53]. However, let remind that our problem is not well conditioned, i.e. constraint (c_1) is changing from one iteration to another and hence even a branch and bound procedure cannot be proved to give a bound on the optimal solution, as it will be seen later. Moreover, complexity of branch and bound algorithm may be high and grows exponentially with the problem size.

The third algorithm proposed in [17, 52] is named Adaptive Rate Allocation Algorithm (ARAA), which is a much more simpler scheme than the two previous ones. The algorithm is based on the observation that the lower $N_f^{(u)}$ for user u, the larger the data rate for this user. In consequence, to maximize the data rate of the cell, $N_f^{(u)}$ should be minimized

1. It is worth noting that $N_f^{(j)^*}$ violates these new constraints

for each user. However, SINR is proportional to the square of $N_f^{(u)}$ and so the processing gain for user u should not be too small to satisfy its SINR constraint. The processing gain of a user experiencing a low received power, e.g. on the cell edge, needs to be *a priori* higher than the one for a user that is closer from BS. ARAA starts by sorting users according to their received power, i.e. from the strongest to the weakest received power at BS, and allocates $N_f^{(u)} = 1 \ \forall u \in \mathcal{U}$. SINR of each user is then computed. If some users do not fulfill their SINR constraint, the number of frames of each user is updated starting by the farthest user from BS because it experiences the lowest SINR in average. The minimum N_f for this user is computed by solving (c_1) in (4.19) which is equivalent to find the solution of a third degree polynomial equation. If a valid solution is found, the algorithm goes to the next user and so on. If no solution is found, the user is removed from the resource allocation controller and the algorithm reboots. Once all the users' processing gains have been updated, SINR of each user is checked, if all SINR constraints are fulfilled the algorithm stops. If not, the last user is removed from the network and the algorithm restarts. This algorithm has a linear complexity w.r.t. the number of users making processing gains allocation very simple.

Below are presented some simulation results that illustrate the relative performance of proposed schemes. In Fig. 4.5, the normalized average throughput and the average starved user rate for ARASP, ARABBSP and ARAA are investigated w.r.t. the number of users N_u labeled on the number of chips N_c. The normalized throughput is the global throughput of the cell, in Mbps, normalized w.r.t. the throughput which would be achieved if all users would transmit at their maximum data rate without any SINR constraint. While the average starved user rates are of the same order of magnitude between the different algorithms for a same number of chips, as it can be inferred from Fig. 4.5(b), there is an interesting behavior of the throughput of ARASP and ARABBSP revealed by Fig. 4.5(a). For $N_c = 5$, the performance of ARAA is upper and lower bounded by ARASP and ARABBSP respectively $\forall N_u$. Since ARASP solves the allocation problem in $\mathbb{R}$, the average throughput obtained is larger than the throughput of the two others. However, if the number of users and the number of chips are of the same order of magnitude, i.e. $N_c = 9$, $N_u = 9$ and $N_c = 13$, $N_u = 13$, then the throughput of ARASP and ARABBSP falls below the throughput of ARAA and increases again for an increasing number of users. This is explained by the fact that the average allocated N_f value per user with ARASP is larger than the one with ARAA and hence leads to a lower average throughput. The initial vector $\mathbf{N_f}$ for ARASP and ARRABBSP takes generally the form $\mathbf{N_f} = q \cdot \mathbf{1}$, where $q \in \{1, \cdots, N_c\}$ and $\mathbf{1}$ is a vector with all entries equal to one. It leads to a higher average number of frames per user compared to ARAA which starts with $\mathbf{N_f} = \mathbf{1}$ and computes the minimal N_f for each user. Moreover, algorithms may start from a feasible point but can become infeasible as the relative values of $N_f^{(u)}$ change between users. This behavior is due to the non linearities involved in the problem (4.21) as previously discussed. Moreover, since ARASP is based on a local convex approximation of a non-convex problem, there is no reason that a good heuristic cannot be better than ARASP.

4.1.4 Summary

At the end of my post-doctoral training, the unaddressed issue of multi-rate MAI characterization and resource allocations in that context push me to investigate more this field. This work allows me to investigate several interesting problems and to acquire some skills in mathematical optimization. First the characterization of the average MAI has been an important step and the methods developed here, even if they are not strictly applicable

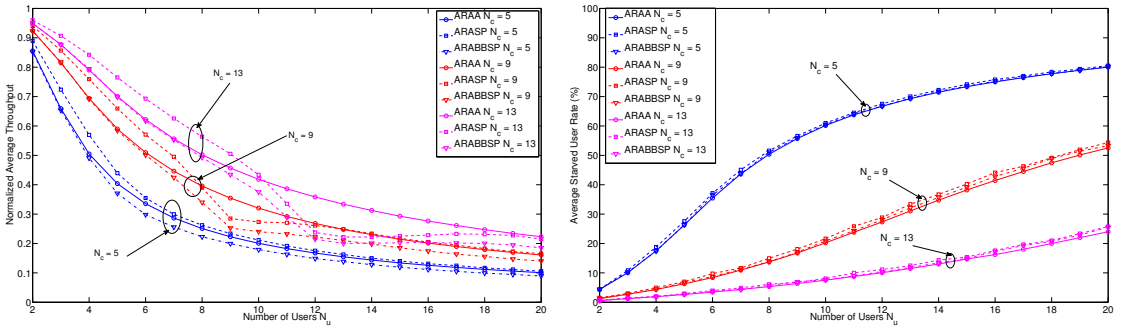

(a) Normalized Average Throughput

(b) Average Starved User Rate

Figure 4.5 – Normalized Average Throughput and Average Starvation Rate w.r.t. the number of users N_u and labeled on N_c [17]

to another system, can be used to study interference of different OFDM-based systems as we will see in Section 4.3. Moreover, non-convex optimization problems have been encountered and some methodologies used to solve them have been investigated, e.g. branch and bound algorithm. Even if the interest in impulsive UWB communications has stepped back a little few years ago, the interest for this technology for wireless communications may raise again with IoT era.

4.2 Resource allocations in relay-aided cellular OFDMA systems

In parallel to my research on resource allocations for multi-user UWB communications, I started working on resource allocations for relay-aided OFDMA cellular systems with the PhD thesis of Mohamad Maaz [14] in 2010. The context was a growing effort granted by academia and industry for the optimization of LTE-A systems including some spatial distributed processing. Since the concomitant but independent seminal works of Dohler and Laneman, [54,55], space-time distributed processings and relaying methods have drawn a huge amount of interest for cellular and sensor networks, e.g. [56] and references therein. The efforts were first mainly dedicated to obtain general performance bounds on capacity, error and outage probabilities for two-hop amplify and forward (AF) or decode and forward (DF) relaying schemes, [57–59] and references therein.

AF mainly consists in detecting the signal at relay and re-amplifying the radio frequency (RF) signal to the destination without demodulating it. In DF scheme on the other hand, RF signal is acquired, demodulated and processed in baseband before being re-encoded, RF modulated and transmitted to the destination. This scheme is hence error prone at relays. Other relaying techniques have also been developed over the years, the most important are compress and forward and compute and forward. The former consists in decoding the signal at relays and transmitting a re-modulated quantized-version of it to the destination. Actually compress and forward had been introduced very early by Cover and Gamal [60]. The later is often referred to physical network coding. Indeed, the principle of compute and forward is to perform a processing with received signals at relays, which can be viewed as interference for each others. The processing aims at re-encoding the signal to the destination in order to be interference free as much as possible [61]. In this research, we focused on AF and DF essentially.

In second step, researchers have focused on how to efficiently allocate the available resources, e.g. power, frequency bands, time slots, in multi-user relay-aided systems, see for instance [62]. The work in [63] dealt with maximizing the weighted sum rate of downlink multi-user, multi-relay OFDMA systems under total power constraint and DF protocol. However a QoS constraint, e.g. minimal SINR or data rate per user, has not been considered. Physical relays, themselves being a kind of resource, have been sought to be suitably selected by the network in order to optimize a given criterium [64]. When we started working on this topic, a resource optimization policy that jointly optimizes power, assigns subcarriers and selects optimal relays in multiuser QoS aware relay-assisted OFDMA networks was missing.

Modern wireless cellular networks include delay tolerant applications, such as downloading or web browsing, that allows for retransmission of erroneous packets. Automatic repeat request (ARQ) schemes are layer 2 mechanisms in wireless systems that retransmit a packet that would not have been correctly received at receiver. Hybrid-ARQ (HARQ) schemes include a forward error correction (FEC) block in addition to the simple retransmission of the packet. The least we can say is that literature on HARQ taxonomy is quite heterogeneous; authors often use different vocabulary to talk about the same thing. Retransmission mechanisms are denoted as simple ARQ, then HARQ of type I, II and III, i.e. HARQ-I, HARQ-II and HARQ-III respectively. When we talk about retransmissions one should distinguish operations done at transmitter and those done at receivers; sometimes different kind of processing at receiver, but with a same operation at transmitter may lead to different classification in HARQ taxonomy. Moreover, retransmission control can be done at level 2 or level 3 of the OSI model, leading to different performance metrics. One

may refer to [65] for a good overview of different schemes and associated processing. In this work, we used a subset of possible retransmission mechanisms that we define hereafter.

ARQ Layer-2 packet is sent without any encoding scheme. The receiver looks at the cyclic redundancy check (CRC) and if data are successfully decoded, an acknowledgement (ACK) is sent back to transmitter and another packet is transmitted. Otherwise, a negative ACK (NACK) is sent and the same packet is retransmitted until transmitter receives an ACK or the maximum number of allowed retransmissions $N_{\max}$ is achieved.

HARQ-I Basically the same than simple ARQ but this scheme incorporates FEC encoding at a fix rate R_0 with the retransmission.

HARQ-CC This scheme refers to a processing technique at receiver and has been introduced in [66] leading to the name *Chase combining* (CC). A coded packet like in HARQ-I is transmitted and if the packet is not correctly received, the packet at signal level, i.e. before hard decision on symbols, is stored at receiver and will be combined using a maximal ratio combining with the same packet that is retransmitted. The resulting packet at signal level is then stored at receiver and decoded. If no error, transmitter sends another packet, otherwise the same packet is sent again and combined at receiver with the resulting packet of previous transmissions. This process continues until successful decoding or maximum number of retransmissions is reached. This scheme creates temporal diversity that is fully exploited with packet combining. This scheme is often classified as belonging to type I HARQ.

HARQ-IR The drawback of HARQ-CC is that the same amount of redundancy is transmitted each round. In incremental redundancy (IR) HARQ, CRC is added to each L information bits and the resultant data packet is encoded by a rate-compatible punctured FEC encoder that generates a systematic mother code of rate R_0 [67]. By mean of a systematic puncturer, this mother code is split into $N_{\max}$ sub-codes, each of $L(n)$ bits to be associated to the n-th retransmission instant. In the first transmitted packet, the information plus some redundancy bits with the CRC header are sent. After being processed, depunctured and decoded, if no error is declared then retransmission stops and another packet is transmitted. If decoder fails to extract the correct information, this packet is stored, NACK is sent and only a part of redundancy bits are retransmitted. At receiver, they are used to decode again the information bits previously received. This process is repeated until all redundancy bits have been sent or until a successful decoding is declared. The advantage of this scheme is that channel is used more efficiently than with HARQ-CC. Indeed, only some redundancy bits are retransmitted instead of the entire PHY layer packet. This scheme is often classified as belonging to type II HARQ and is used in LTE system with a turbo code.

4.2.1 Maximum sum rate for QoS-aware relay-assisted OFDMA communications

In a first place, no retransmission mechanism is considered but a single cell made of one BS, K relay stations (RS) r_k with $k \in \mathcal{K} = \{1, \cdots, K\}$ and M mobile users u_m with $m \in \mathcal{M} = \{1, \cdots, M\}$ is considered. The multiple access scheme is OFDMA with N_F orthogonal subcarriers that can be shared between users. Two-hop DF relaying technique is adopted as depicted in Fig. 4.6. For a given user, relaying takes place in two-phases:

— Phase 1: BS transmits some subcarriers directly to users and some others to one relay selected to assist users in the second transmission phase.
— Phase 2: Relay transmits the received subcarriers to users that needs assistance.

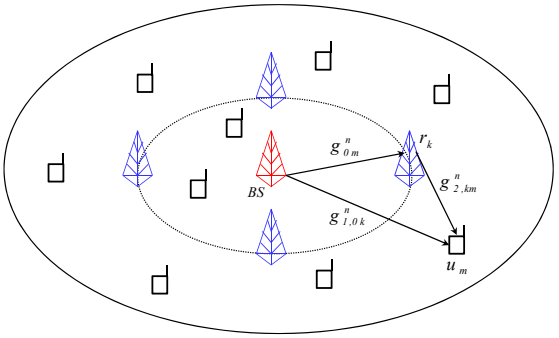

Figure 4.6 – Single cell multi-user relay-aided OFDMA system [14]

Let us denote C^n_{0m}, $C^n_{1,0k}$ and $C^n_{2,km}$ the achievable data rate on the $n-$th subcarrier between BS and user m, BS and relay k during the first phase and relay k and user m during the second phase respectively. The achievable data rate can be expressed as

$$C^n_{0m} = \log_2(1 + g^n_{0m} p^n_{0m}), \tag{4.22}$$
$$C^n_{1,0k} = \log_2(1 + g^n_{1,0k} p^n_{1,0k}), \tag{4.23}$$
$$C^n_{2,km} = \log_2(1 + g^n_{2,km} p^n_{2,km} + g^n_{0m} p^n_{1,0k}), \tag{4.24}$$

where g^n_{0m}, $g^n_{1,0k}$, $g^n_{2,km}$ are the channel gains on subcarrier n in the links BS$-u_m$, BS$-r_k$ and $r_k - u_m$ respectively. The channel gains include fading, path loss and are normalized over the noise variance, i.e. σ^2, on subcarrier n assuming to be the same for all receivers and subscript 0 denotes the base station. Moreover, p^n_{0m}, $p^n_{1,0k}$ and $p^n_{2,km}$ are the power allocated to the $n-$th subcarrier on BS-user, BS-relay first phase and relay-user second phase links respectively. For a given position of relays and users, channel gains $g^n_{i,km}$ are exponentially distributed, i.e. $g^n_{i,km} \sim \exp(\sigma^2/l^n_{i,km})$ $\forall i \in \{\emptyset, 1, 2\}$, $\forall k \in \mathcal{K} \wedge i \neq \emptyset \vee k = 0 \wedge i \in \emptyset$ and $\forall m \in \mathcal{M}$, where $\emptyset$ stands for the empty set. Finally l^n_{0m}, $l^n_{1,0k}$, $l^n_{2,km}$ are path losses on subcarrier n of links BS$-u_m$, BS$-r_k$ and r_k-u_m respectively. The channel is assumed to be invariant during both transmission phases i.e. $i = 1, 2$, which is a reasonable assumption for slow moving users and hence the instantaneous channel state information (CSI) of all relays and users are assumed to be known at BS. Expression in (4.24) indicates that direct and relay-aided signal transmissions are processed using maximal ratio combining at destination. The cell radius is equal to R and the relays are circularly located around BS at a distance $R/2$.

In order to express the problem of sum rate maximization in relay-aided OFDMA cellular network, we first invoke some basic arguments of cut-set flows. Since two time slots are needed to decode information sent through a relay, the achievable data rate of user m is [58]:

$$\frac{1}{2} \min \left\{ C^n_{1,0k}, C^n_{2,km} \right\} \tag{4.25}$$

Considering the relay-assisted mode, the end-to-end data rate at user m is maximum if

$$C^n_{1,0k} = C^n_{2,km} \tag{4.26}$$

By denoting p_{km}^n the overall power consumed in both phases, we have

$$p_{km}^n = p_{1,0k}^n + p_{2,km}^n \tag{4.27}$$

Combining (4.27) and (4.26), $p_{1,0k}^n$ and $p_{2,km}^n$ can be expressed w.r.t. p_{km}^n. In a same way, considering $g_{1,0k}^n > g_{0m}^n$, the equivalent channel gain g_{km}^n between BS and user m using relay k can be expressed as:

$$g_{km}^n = \frac{g_{2,km}^n g_{1,0k}^n}{g_{1,0k}^n + g_{2,km}^n - g_{0m}^n}. \tag{4.28}$$

The maximum achievable rate over the n-th subcarrier can be expressed with g_{km}^n and p_{km}^n:

$$C_{km}^n = \frac{1}{2}\log_2(1 + p_{km}^n g_{km}^n) \ \ \forall k = 1 \dots K. \tag{4.29}$$

According to (4.22) and (4.29), the achievable rate on the subcarrier n, under direct or indirect transmission can be written as:

$$C_{km}^n = \frac{(1+\delta(k))}{2}\log_2(1 + p_{km}^n g_{km}^n) \ \ \forall k = 0, \cdots, K, \tag{4.30}$$

where $\delta(k) = 1$ if and only if $k = 0$.

Max sum rate formulation and solution

The central controller at BS aims at performing the power, subcarriers allocation and relays selection for every user in order to maximize the global data rate. This problem can be stated in the following form:

$$\begin{aligned}
&\max_{\mathbf{S},\mathbf{P}} \ \sum_{k=0}^{K}\sum_{m=1}^{M}\sum_{n=1}^{N_F} s_{km}^n C_{km}^n \text{ s.t.} \\
(c_1) \quad &\sum_{k=0}^{K}\sum_{m=1}^{M}\sum_{n=1}^{N_F} s_{km}^n p_{km}^n \leq P_{\text{tot}} \\
(c_2) \quad &\sum_{k=0}^{K}\sum_{n=1}^{N_F} s_{km}^n C_{km}^n \geq \rho_m \ \ \forall m \in \mathcal{M} \\
(c_3) \quad &\sum_{k=0}^{K}\sum_{m=1}^{M} s_{km}^n = 1 \ \ \forall n \in \{1, \cdots, N_F\} \\
(c_4) \quad &s_{km}^n \in \{0,1\} \ \ \forall (k,m,n) \\
(c_5) \quad &p_{km}^n \geq 0 \ \ \forall (k,m,n)
\end{aligned} \tag{4.31}$$

Where s_{km}^n is the subcarrier allocation index with $s_{km}^n = 1$ if subcarrier n is allocated to the link $r_k - u_m$ and 0 otherwise. Expression in (c_1) formulates the overall power constraint P_{tot} on the whole cell, constraint (c_2) ensures that the achievable rate for each user is above or equal to a rate requirement ρ_m in bits/s/Hz. Constraint (c_3) states that subcarrier n cannot be shared among users and relays. Constraints (c_4) and (c_5) follow from the nature of variables. For each CSI hyper-matrix $\boldsymbol{G} = [g_{km}^n]_{K\times M\times N_F}$, we aim at allocating an optimal power hyper-matrix $\boldsymbol{P} = [p_{km}^n]_{K\times M\times N_F}$ and assigning a binary hyper-matrix $\boldsymbol{S} = [s_{km}^n]_{K\times M\times N_F}$ such that the rate constraint vector $\boldsymbol{\rho} = (\rho_1, \cdots, \rho_M)^T$ and the total power constraint are satisfied.

This problem, like the one we studied in UWB communications, is a combination of a non-linear continuous problem, i.e. optimization over $\mathbf{P}$ and integer programming problem, i.e. optimization over $\mathbf{S}$. A classical approach in a first place is to relax the constraint over the integer variables, i.e. assuming that $0 \leq s_{km}^n \leq 1$. By letting the change of variable $\bar{p}_{km}^n = s_{km}^n p_{km}^n$ [68], the function to be maximized in (4.31) is a multiple summation of the form:

$$g\left(s_{km}^n, \bar{p}_{km}^n\right) = s_{km}^n \log_2\left(1 + \frac{\bar{p}_{km}^n g_{km}^n}{s_{km}^n}\right) \tag{4.32}$$

This function is called the perspective function of $\log_2\left(1 + \bar{p}_{km}^n g_{km}^n\right)$ and presents the property to be concave in s_{km}^n and $\bar{p}_{km}^n$, [69, pp. 89]. Constraints in (c_2) are then also concave $\forall m \in \{1, \cdots, M\}$ and constraints (c_1) and (c_3) are affine functions and then (4.31) is a convex optimization problem for which an optimal solution can be obtained.

Writing Karush-Kuhn Tucker conditions of this problem, one may obtain the solutions on optimal powers at BS and relays and on the subcarrier-relay selection coefficient. Optimal power has a water-filling-like expression:

$$p_{km}^{n^*} = \begin{cases} \left[\frac{(1+\delta(k))(1+\gamma_m)}{2\mu} - \frac{1}{g_{km}^n}\right]^+ & \text{if } s_{km}^n = 1 \\ 0 & \text{otherwise} \end{cases} \tag{4.33}$$

where $[x]^+$ stands for $\max\{0, x\}$ and γ_m, μ are the Lagrange multipliers associated to the $m-$th rate constraint and total power constraint in (c_2) and (c_1) respectively. Differentiating w.r.t. s_{km}^n, the following is obtained:

$$\nabla_{s_{km}^n}\mathcal{L} = \frac{(1+\delta(k))(1+\gamma_m)}{2}\left(\log_2\left(1 + g_{km}^n \frac{\bar{p}_{km}^n}{s_{km}^n}\right) - s_{km}^n\left(\frac{\frac{\bar{p}_{km}^n}{\left(s_{km}^n\right)^2} g_{km}^n}{1 + \frac{\bar{p}_{km}^n}{s_{km}^n} g_{km}^n}\right)\right) - \alpha_n \tag{4.34}$$

where α_n is the Lagrange multiplier associated to the $n-$th constraint in (c_3). According to problem assumptions, if $p_{km}^n = 0$ then $s_{km}^n = 0$. However, for $s_{km}^n \neq 0$, we have:

$$\nabla_{s_{km}^n}\mathcal{L}\begin{cases} > 0 & \text{if } s_{km}^n = 1 \\ = 0 & \text{if } 0 < s_{km}^n < 1 \end{cases} \tag{4.35}$$

where (4.35) can be interpreted as follows:

— $\nabla_{s_{km}^n}\mathcal{L} = 0$ signifies that the maximum is occurred for $0 < s_{km}^n < 1$.

— In the other hand, at the boundary, i.e. $s_{km}^n = 1$, $\nabla_{s_{km}^n}\mathcal{L} \neq 0$. Hence, if $\nabla_{s_{km}^n}\mathcal{L} > 0$ then $s_{km}^n = 1$.

These conditions give a criterium to pass from a relaxed continuous variable s_{km}^n to a discrete variable. Substituting (4.33) in (4.34), one can easily obtain a criterium to choose the optimal relay for each user and subcarrier, $\forall n \in \{1, \cdots, N_F\}$:

$$\begin{aligned} (k,m)^* &= \arg\max_{(k,m)} \frac{(1+\delta(k))(1+\gamma_m)}{2}\left[\log_2\left(\frac{(1+\delta(k))(1+\gamma_m)}{2\mu} g_{km}^n\right)\right]^+ - \mu\left[\frac{(1+\delta(k))(1+\gamma_m)}{2\mu} - \frac{1}{g_{km}^n}\right]^+ \\ s_{km}^n &= \begin{cases} 1 & \forall\ (k,m) = (k,m)^* \\ 0 & \text{otherwise} \end{cases} \end{aligned} \tag{4.36}$$

Similar expression has been obtained in [68] but ours account not only for subcarrier allocation but also for relay selection. We then proposed an algorithm that jointly allocates power, subcarriers and performs relay selection [70] that is reproduced in Algorithm 1 for the sake of readability.

Algorithm 1 Joint Power, Subcarrier and Relay Selection algorithm (JPRS)

1: $\mu \leftarrow \mu_0$, $\mathcal{M} = \{1, \cdots, M\}$
2: $\gamma_m^+ \leftarrow 0$, $\gamma_m^- \leftarrow 0$, $r_{e_m}^- \leftarrow -\rho_m$, $r_{e_m}^+ \leftarrow +\rho_m \ \forall m \in \mathcal{M}$
3: **while** $r_{e_m}^- < 0, \forall m$ **do**
4: $\quad \gamma_m^+ \leftarrow \gamma_m^+ + \delta$
5: $\quad$ Apply (4.36)
6: $\quad r_{e_m}^- \leftarrow \sum_{k=0}^{K} \sum_{n=1}^{N_F} s_{km}^n C_{km}^n - \rho_m$
7: **end while**
8: **while** $r_{e_m}^+ > 0, \forall m$ **do**
9: $\quad \gamma_m^- \leftarrow \gamma_m^- - \delta$
10: $\quad r_{e_m}^+ \leftarrow \sum_{k=0}^{K} \sum_{n=1}^{N_F} s_{km}^n C_{km}^n - \rho_m$
11: **end while**
12: Find $\gamma_m^* \in [\gamma_m^-, \gamma_m^+]$ such that $f_m(\gamma_m, \mu_0) = 0 \ \forall \ m$
13: $P_{\text{tot}_{\text{req}}} \leftarrow \sum_{m=1}^{M} \sum_{k=0}^{K} \sum_{n=1}^{N_F} s_{km}^n p_{km}^n$
14: **if** $P_{\text{tot}_{\text{req}}} > P_{\text{tot}}$ **then**
15: $\quad P_{m_{\text{req}}} \leftarrow \sum_{k=0}^{K} \sum_{n=1}^{N_F} s_{km}^n p_{km}^n \quad \forall m \in \mathcal{M}$
16: $\quad m^* \leftarrow \arg\min_m \frac{\rho_m}{P_{m_{\text{req}}}}$
17: $\quad$ Update $\mathcal{M}$ by removing the user u_{m^*}
18: **else**
19: $\quad$ Find $P(\boldsymbol{\gamma}^*, \mu) = 0$, else
20: $\quad$ Update μ and go to step 2
21: **end if**

The joint power, subcarrier and relay selection algorithm attempts to search the optimal Lagrange multipliers μ and γ_m. After initializing the Lagrange multiplier for power constraint, i.e. $\mu = \mu_0$, our algorithm searches for bounding the optimal Lagrange multiplier for data rate constraint for each user, i.e. γ_m^*, in order to satisfy the rate constraint (c_2), i.e. steps from 3 to 11. Once the interval $[\gamma_m^-, \gamma_m^+]$ is defined, optimal γ_m^* is found by solving the equation $f_m(\gamma_m^*, \mu_0) = 0$ on $[\gamma_m^-, \gamma_m^+]$ with:

$$f_m(\gamma_m^*, \mu_0) = \sum_{k=1}^{K} \sum_{n=1}^{N_F} s_{km}^n \log_2 \left[\frac{(1+\delta(k))(1+\gamma_m^*) g_{km}^n}{2\mu_0} \right]^+ - \rho_m \quad \forall m \in \{1, \cdots, M\} \quad (4.37)$$

Then the power required to achieve the data rate constraints is computed in step 13. If the required power is less than P_{tot}, the algorithm updates μ and restarts updating γ_m for every user until finding $(\boldsymbol{\gamma}^*, \mu^*)$ such that $P(\boldsymbol{\gamma}^*, \mu^*) = 0$, with

$$P(\boldsymbol{\gamma}^*, \mu^*) = \sum_{k=1}^{K} \sum_{m=1}^{M} \sum_{n=1}^{N_F} s_{km}^n \left[\frac{(1+\delta(k))(1+\gamma_m^*)}{2\mu^*} - \frac{1}{g_{km}^n} \right]^+ - P_{\text{tot}} \quad (4.38)$$

If the required power exceeds the total power constraint, then user with the lowest spectral efficiency per Watt allocated is removed (step 16) and the algorithm restarts until all users be satisfied or removed.

Fig. 4.7(a) illustrates the achievable data rate with our algorithm w.r.t. the total power constraint P_{tot}. In this period, since we just started working on cooperative communications and resource allocations, we aim at verifying some advantages of relay-aided transmissions that are usually given in literature without too much details. The algorithm is compared with a power and subcarrier allocation procedure without relays, [68], and another algorithm that allocates equal power to BS and relays [71]. As expected, the data sum rate increases when the total power budget increases and exploiting full frequency-spatial diversity by selecting the suitable couple relay-subcarrier is beneficial compared to other schemes.

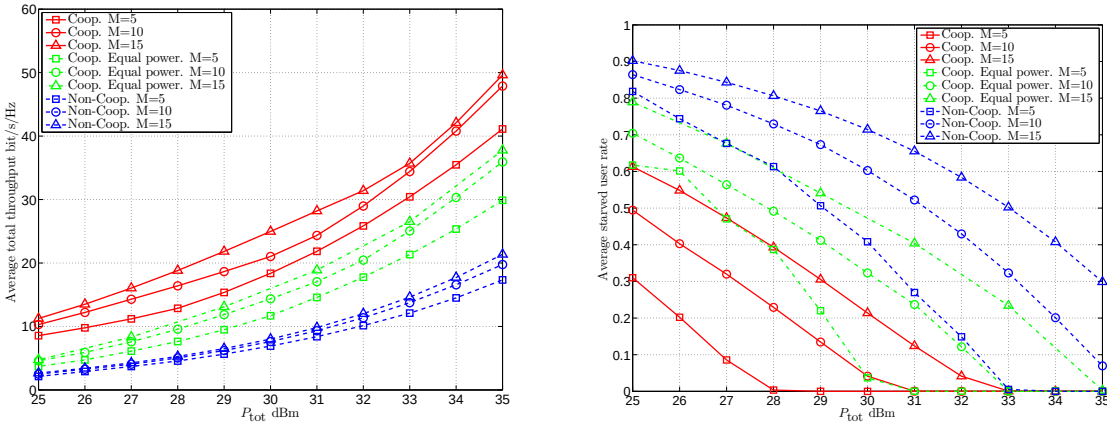

(a) Average total throughput versus P_{tot}

(b) Average starvation rate versus P_{tot}

Figure 4.7 – Average throughput and starvation rate versus P_{tot} [14]

Since the optimization problem stated in (4.31) is not necessarily feasible, depending on constraint values, some users may be in starvation, i.e. without any resources. It is hence important to monitor the starvation rate that any allocation procedure implies, like we did

for resource allocations in TH-UWB communications. For a given power constraint, relay-aided transmission with power allocation allows to serve more users than non cooperative technique in average as it can be observed in Fig. 4.7(b).

4.2.2 Energy minimisation in relay-aided OFDMA networks with HARQ

The studies detailed above did not take into account possible retransmission mechanisms available in LTE systems and did not focus on energy consumption. Our early work was instead dedicated to sum rate maximization which is, generally, not energy efficient [72, 73]. The energy efficiency can be seen as a ratio between a benefit function and a cost function. There were a tremendous amount of contributions in energy efficient communications [74], basically divided in two categories, i.e. information theoretic and pragmatic approaches respectively. The former deals with fundamental limits by studying the achievable value of a benefit function, e.g. channel capacity for a point-to-point communication for instance, over a cost function, i.e. power used to achieve this capacity. One of the earlier work was performed by Gallager in [75] who has studied the maximum achievable rate per unit energy consumed by imposing an energy constraint on code words. The binary symbol 1 representing non-zero energy input and symbol 0 representing a zero energy input, in other words silence conveys information and it costs nothing. The constraint on codeword is then equivalent to limit the number of 1's in codewords. The capacity was defined such as the limit of error exponent over the energy constraint. In [76], Verdu imposed a constraint per input, and defined what the author called the maximum number of bits that can be conveyed per channel use (c.u.) and per unit cost:

$$C = \sup_{X} \frac{I(X;Y)}{\mathrm{E}[b(X)]} \tag{4.39}$$

where X and Y are the input and output of the discrete memoryless channel, $I(X;Y)$ is the mutual information between X and Y, $\mathrm{E}[\cdot]$ stands for expectation operator and $b(X)$ is the cost function associated to the input X. In case where no cost can be associated to symbol 0, the author proved that the achievable capacity per unit cost is a function of the Kullback-Leibler divergence, i.e. $D\left(P_{Y|X=x}||P_{Y|X=0}\right)$, normalized over the cost of input x, where $P_{Y|X}$ is the channel probability distribution function. Some extensions to these early works have been performed in [77] for wide sense stationary and uncorrelated scattering channels. Since then, a lot of works have been done including more and more complex scenarii, e.g. multi-user, interference, MIMO and relay channels [78, 79].

The second kind of works deals with practical approaches of energy efficient communications. These approaches consist in defining benefit and cost functions, the same as information theoretic approaches, but these functions may depend on system parameters in a stronger way. Once the system model carefully stated, authors attempt to find optimal system parameters, e.g. powers, frequency bands, to maximize the ratio between the benefit and cost functions. In [80] the authors studied the energy efficiency for cooperative and non cooperative HARQ schemes by minimizing the energy consumed for a single user under outage probability constraint. In [81], energy efficiency of DF, AF and compress and forward relaying schemes with HARQ under outage probability and delay constraints has been investigated. It is also convenient to note an important amount of works for wireless sensor networks in which the energy consumption is of crucial importance [82]. Our contribution in this field has been to minimize the energy consumed in a single cell OFDMA network and multiple relays when HARQ-I is considered. Contrarily to previous cited works, the energy minimization is done by allocating jointly power, resource blocks and

MCS index	QAM	Coding rate ×1024	a	b	c	# of RBs
1	4	449	17.76	-1.90	4.25	15
2	4	602	17.69	-1.50	3.98	12
3	16	378	69.94	-1.64	3.65	9
4	16	490	43.34	-1.27	3.85	7
5	16	616	50.91	-1.22	2.98	6
6	64	466	76.76	-1.04	3.98	5
7	64	567	125.87	-1.16	2.49	4
8	64	666	174.46	-1.20	1.75	4
9	64	772	232.16	-1.30	0.97	3

Table 4.1 – Curve fitting parameters a, b and c for each MCS [14, 18]

MCS under power and delay-constrained users. The main challenge comes from the need of a closed-form expression of PER with HARQ in order to express the delay requirements.

System, delay and energy models

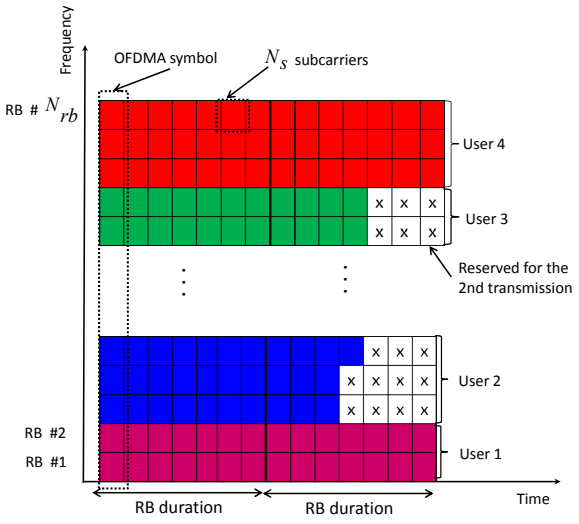

Figure 4.8 – Resource blocks sharing scheme between users [18]

The system considered is similar to the one described in Section 4.2.1 but now N_s subcarriers are grouped in one resource block (RB) like in LTE. Moreover, direct or relay-aided transmission modes are exclusive, i.e. it is one or the other but not both. The structure of OFDMA symbols and RBs is illustrated in Fig. 4.8. One of the major difference with the previous contribution, is that average channel state information is considered at BS and relays instead of instantaneous CSI. For a given MCS, the average PER in fading channels can be tightly approximated with $\Pi(\overline{\gamma}) = \left(1 - \exp\left(-a\overline{\gamma}^{b}\right)\right)^{c}$ where a, b, and c are curve fitting parameters which depend on the adopted MCS [83] and $\bar{\gamma}$ is the average SNR over the communication. The curve fitting parameters can be obtained for typical LTE turbo codes and are given in Table 4.1.

Let us assume that for user m, the scheduler has to select a certain QAM modulation order Q_m and a coding rate R_m. Therefore, according to the packet length L, the number

of required frequency or time RBs to be allocated to user m is given by

$$\mathrm{RB}_m = \left\lceil \frac{L}{R_m \log_2(Q_m) N_s} \right\rceil . \tag{4.40}$$

If user m has a delay constraint $\overline{D}_m$, in time slots, to be satisfied, where a time slot is the duration of one resource block, then the possible number of RBs to be allocated to user m varies between 1 and RB_m. Thus, the larger the number of allocated RBs for a given user, the lower its average delay due to frequency multiplexing. Therefore, for every possible combination of MCS and every selected number of RBs, the scheduler has to allocate a transmission power such that the delay constraint is guaranteed.

Delay model. It is assumed that the number of retransmission for each packet is unlimited or large enough to neglect the packet loss, [84]. Hence, the average delay per packet is only determined by PER on the considered link. Of course, this assumption is optimistic and neglects the fact that some packets will be irremediably lost affecting the user experience in real communication scenario. However, it can be used as a first hypothesis for tractability purpose. The average delay per packet depends on the selected mode, i.e. direct or relay-aided and is:

$$\overline{N}^d_{0m} = \frac{1}{1-\Pi^d_{0m}(\overline{\gamma}^d_{0m})} \qquad \text{direct transmission} \tag{4.41}$$

$$\overline{N}_{km} = \overline{N}^c_{0km} + \overline{N}^c_{km} \qquad \text{relay-aided transmission} \tag{4.42}$$

where $\overline{\gamma}^d_{0m} = g_{0m}\frac{p^d_{0m}}{\sigma^2}$, g_{0m}, p^d_{0m} and Π^d_{0m} are respectively the average received SNR, the channel gain, the allocated power and PER in the $\mathrm{BS}-u_m$ link and

$$\overline{N}^c_{0km} = \frac{1}{1-\Pi^c_{0m}(\overline{\gamma}^c_{0m})\Pi^c_{0km}(\overline{\gamma}^c_{0km})} \tag{4.43}$$

$$\overline{N}^c_{km} = \frac{\Pi^c_{om}(\overline{\gamma}^c_{0m})\left(1-\Pi^c_{0km}(\overline{\gamma}^c_{0km})\right)}{1-\Pi^c_{0m}(\overline{\gamma}^c_{0m})\Pi^c_{0km}(\overline{\gamma}^c_{0km})}\frac{1}{1-\Pi^c_{km}(\overline{\gamma}^c_{km})} \tag{4.44}$$

where $\overline{\gamma}^c_{0m} = g^c_{0m}\frac{p^c_{0km}}{\sigma^2}$, $\overline{\gamma}^c_{0km} = g^c_{0km}\frac{p^c_{0km}}{\sigma^2}$, $\overline{\gamma}^c_{km} = g^c_{km}\frac{p^c_{km}}{\sigma^2}$ and g^c_{0m}, g^c_{0km}, g^c_{km} are the average received SNRs and the channel gains in the $\mathrm{BS}-u_m$, $\mathrm{BS}-r_k$ and $r_k - u_m$ links respectively. Moreover, the allocated powers at BS and r_k are respectively p^c_{0km} and p^c_{km}. We observe that p^c_{0km} is common to delay expressions on $\mathrm{BS}-u_m$ and $\mathrm{BS}-r_k$ links. This is because when BS transmits then final user or relays can decode the packet.

Energy consumption model. The generic model for energy consumed by a transmission between a source s and a destination d, i.e. E_{sd}, is of the form $E_{sd} = f(p)\,\overline{N}_{sd}$, where $f(p)$ is a linear function of the transmit power p and $\overline{N}_{sd}$ is the average delay to transmit one packet. The linear power consumption model is widely used in works on energy-efficient communications [82, 85] and is valid in a first approximation. The energy consumed per received packet in the direct and relay-aided links is

$$\overline{E}^d_{0m} = f_1(p^d_{0m})\overline{N}^d_{0m} \tag{4.45}$$

$$\overline{E}^c_{km} = f_2(p^c_{0km})\overline{N}^c_{0km} + f_3(p^c_{km})\overline{N}^c_{km} \tag{4.46}$$

where $f_1(p^d_{0m}) = k_1 + k_2 p^d_{0m}$, $f_2(p^c_{0km}) = k_3 + k_4 p^c_{0km}$ and $f_3(p^c_{km}) = k_5 + k_6 p^c_{km}$ are the power consumed to transmit one packet in the $\mathrm{BS}-u_m$, $\mathrm{BS}-r_k$ and $r_k - u_m$ links respectively. Moreover k_i, $i = 1, \cdots, 6$, are constants depending on static power consumption,

power amplifier efficiency, modulation order, packet size, etc. This model takes into account the energy spent in sending and receiving N/ACK packets, as in [82]. For further details, the reader may refer to [18].

Energy minimization problem and solution

In this research, we aimed at minimizing the energy consumed in a single-cell relay-aided OFDMA network with multiple users, by taking into account non reliable links, i.e. non vanishing packet error probability, and HARQ-I retransmission mechanism. As indicated above, no work attempted to formulate this problem with a pragmatic approach, i.e. non information-theoretical approach, and allocate power, RBs, relay and MCS. We first searched for a procedure that allocates powers at BS and relays and selects suitable relays to help users. The minimization problem can be expressed as:

$$
\begin{aligned}
&\min_{\boldsymbol{\lambda_{km}}} \quad \sum_{m=1}^{M}\left(\left(1-\sum_{k=1}^{K}s_{km}\right)f_1(p_{0m}^{d})\overline{N}_{0m}^{d}+\sum_{k=1}^{K}s_{km}\left(f_2(p_{0km}^{c})\overline{N}_{0km}^{c}+f_3(p_{km}^{c})\overline{N}_{km}^{c}\right)\right) \text{ s. t.}\\
&(c_1)\quad \left(1-\sum_{k=1}^{K}s_{km}\right)\overline{N}_{0m}^{d}+\sum_{k=1}^{K}s_{km}\left(\overline{N}_{0km}^{c}+\overline{N}_{km}^{c}\right)\leq \overline{D}_m \;\forall m\in\mathcal{M}\\
&(c_2)\quad s_{km}=\{0,1\}\;\forall(k,m)\in\mathcal{K}\times\mathcal{M} \text{ and } \sum_{k=1}^{K}s_{km}=\{0,1\}\;\forall m\in\mathcal{M}\\
&(c_3)\quad \overline{N}_{0m}^{d}=\frac{1}{1-\Pi_{0m}^{d}(p_{0m}^{d})}\;\forall m\in\mathcal{M}\\
&(c_4)\quad \overline{N}_{0km}^{c}=\frac{1}{1-\Pi_{0m}^{c}(p_{0km}^{c})\Pi_{0km}^{c}(p_{0km}^{c})}\;\forall(k,m)\in\mathcal{K}\times\mathcal{M}\\
&(c_5)\quad \overline{N}_{km}^{c}=\frac{\Pi_{0m}^{c}(p_{0km}^{c})(1-\Pi_{0km}^{c}(p_{0km}^{c}))}{(1-\Pi_{0m}^{c}(p_{0km}^{c})\Pi_{0km}^{c}(p_{0km}^{c}))(1-\Pi_{km}^{c}(p_{km}^{c}))}\;\forall(k,m)\in\mathcal{K}\times\mathcal{M}\\
&(c_6)\quad \sum_{m=1}^{M}\left(\left(1-\sum_{k=1}^{K}s_{km}\right)p_{0m}^{d}+\sum_{k=1}^{K}s_{km}(p_{0km}^{c}+p_{km}^{c})\right)\leq P_{tot}\\
&(c_7)\quad p_{0m}^{d},\; p_{0km}^{c},\; p_{km}^{c}\geq 0
\end{aligned}
\tag{4.47}
$$

In the energetic cost function, the binary variable s_{km} is equal to 1 if the relay r_k is selected to help the user u_m and zero otherwise. The average energy consumed in the cell is the energy consumed when a group of users has been selected to communicate directly with BS, i.e. $\sum_{k=1}^{K}s_{km}=0$ plus the energy consumed by another group of users that uses a relay, i.e. the right most term in the cost function of (4.47). The constraint (c_1) ensures that the average delay is less than or equal to $\overline{D}_m$ for every user u_m, (c_2) ensures that only one relay can be selected per user and (c_6) states that the total allocated power (for BS and relays) is less than or equal to the power constraint P_{tot}. The minimization of energetic cost function under constraints (c_1), (c_2), (c_6) and (c_7) constitutes the original problem whose the solution over the variables p_{0m}^{d}, p_{0km}^{c}, p_{km}^{c} and the integer variables s_{km} is very challenging to find due to the combination of non convex functions of powers, e.g. delay $\overline{N}_{km}^{c}$, and binary constraints that make the problem intractable. Hence, it is very difficult to shown that an algorithm can achieve a global optimal solution. The problem of relay selection is overcome by relaxing the integer constraint on s_{km}, assuming it could be a time sharing factor between 0 and 1 as we did in the previous section.

In order to overcome the difficulty implied by this non convex problem, we consider that the delays $\overline{N}_{0m}^{d}$, $\overline{N}_{0km}^{c}$ and $\overline{N}_{km}^{c}$ $\forall k,m$ are also variables satisfying the new equality constraints in (c_3), (c_4) and (c_5) respectively. One can notice that energy minimization

problem in (4.47) over powers with or without (c_3), (c_4) and (c_5) is the same since delays in the energetic cost function are expressed with (4.41), (4.43) and (4.44) which are constraints (c_3), (c_4) and (c_5) respectively. Solving (4.47) is equivalent to find the optimal vector $\boldsymbol{\lambda_{km}} = \{\lambda_{km} : (k,m) \in \mathcal{K} \times \mathcal{M}\}$ with $\lambda_{km} = [s_{km}\ p^d_{0m}\ p^c_{0km}\ p^c_{km}\ \overline{N}^d_{0m}\ \overline{N}^c_{0km}\ \overline{N}^c_{km}]$.

Optimal powers. Let denote $\mathcal{L}$ the Lagrangian function of problem (4.47) whose the expression is reported in [18]. Let consider in a first place that delays and powers are independent from each others, the derivatives of the Lagrangian w.r.t. delays, i.e. $\nabla_{\overline{N}}\mathcal{L}$ where $\overline{N} \in \left\{\overline{N}^d_{0m}, \overline{N}^c_{0km}, \overline{N}^c_{km}\right\}$, are equated to zero to give power expressions:

$$p^d_{0m} = \left[\frac{\alpha^d_{0m} - \gamma_m - k_1}{k_2}\right]^+ \tag{4.48}$$

$$p^c_{0km} = \left[\frac{\alpha^c_{0km} - \gamma_m - k_3}{k_4}\right]^+ \tag{4.49}$$

$$p^c_{km} = \left[\frac{\alpha^c_{km} - \gamma_m - k_5}{k_6}\right]^+ \tag{4.50}$$

where γ_m $m \in \mathcal{M}$ are Lagrange multipliers of delay constraint (c_1) for each user and $\boldsymbol{\alpha_{km}} = \left\{(\alpha^d_{0m}, \alpha^c_{0km}, \alpha^c_{km}) : (k,m) \in \mathcal{K} \times \mathcal{M}\right\}$ are Lagrange multipliers for equality constraints (c_3) to (c_5).

Optimal delays. In a second step, the derivative of Lagrangian is taken over powers, i.e. $\nabla_p\mathcal{L}$ where $p \in \left\{p^d_{0m}, p^c_{0km}, p^c_{km}\right\}$, considering that delays do not depend on them, and nullified. Optimal $\boldsymbol{\alpha_{km}}$, i.e. $\{\boldsymbol{\alpha_{km}} \mid \nabla_p\mathcal{L}(\boldsymbol{\alpha_{km}}) = 0, \forall (k,m) \in \mathcal{K} \times \mathcal{M}\}$ are obtained with Newton-Raphson method.

Optimal powers are then obtained by solving $\nabla_p\mathcal{L} = \mathbf{0}$ to get $\boldsymbol{\alpha_{km}}^*$ and then α^{d*}_{0m}, α^{c*}_{0km}, α^{c*}_{km} are substituted in (4.48), (4.49), (4.50). The key point here was to consider delays and powers as separate variables allowing us to make one vary while keeping the other constant and then search for Lagrangian multipliers in order to satisfy constraints (c_3) to (c_5). Our algorithm cannot be proved to achieve a global optimum, due to the highly non-convex delay expressions w.r.t. powers. However it achieves necessarily at least a local optimum and the algorithm is guaranteed to finish [18]. The relay selection task is done in a similar way that the one that has been described in the previous Section.

Another contribution has been to include MCS and RBs allocations in addition to power and relay selection described above. In LTE system, the resource allocation manager selects for every user an MCS and a certain number of time/frequency resource blocks in order to satisfy the demanding QoS. We assumed that the number of possible MCS is N_{mcs} and the total number of frequency resource blocks is N_{RB}. For a given allocated power policy, the energy consumed by the system depends on MCS and RBs. The minimization of the

consumed energy can be formulated in the canonical form as follows:

$$\begin{aligned}
&\min_{\mathbf{x_{mr}^{mcs}}} \quad \sum_{m=1}^{M}\sum_{r=1}^{N_{\mathrm{RB}}}\sum_{\mathrm{mcs}=1}^{N_{\mathrm{mcs}}} \mathrm{x}_{mr}^{\mathrm{mcs}} E_{mr}^{\mathrm{mcs}} \text{ s. t:} \\
&(c_1) \quad \mathrm{x}_{mr}^{\mathrm{mcs}} \in \{0,1\} \forall (m,r,\mathrm{mcs}) \in \mathcal{M}\times\mathcal{N}_{\mathrm{RB}}\times\mathcal{N}_{\mathrm{mcs}} \\
&(c_2) \quad \sum_{r=1}^{N_{\mathrm{RB}}}\sum_{\mathrm{mcs}=1}^{N_{\mathrm{mcs}}} \mathrm{x}_{mr}^{\mathrm{mcs}} = 1 \ \forall m \in \mathcal{M} \\
&(c_3) \quad \sum_{m=1}^{M}\sum_{r=1}^{N_{\mathrm{RB}}}\sum_{\mathrm{mcs}=1}^{N_{\mathrm{mcs}}} r\mathrm{x}_{mr}^{\mathrm{mcs}} \leq N_{\mathrm{RB}} \\
&(c_4) \quad \sum_{m=1}^{M}\sum_{r=1}^{N_{\mathrm{rb}}}\sum_{\mathrm{mcs}=1}^{N_{\mathrm{mcs}}} rN_s\mathrm{x}_{mr}^{\mathrm{mcs}} p_{mr}^{\mathrm{mcs}} \leq P_{\mathrm{tot}}
\end{aligned} \tag{4.51}$$

where E_{mr}^{mcs} is the energy consumed to serve user m with the MCS mcs, and r RBs, p_{mr}^{mcs} is the power allocated per subcarrier for user m and $\mathcal{N}_{\mathrm{RB}}$, $\mathcal{N}_{\mathrm{mcs}}$ are the sets of RBs and MCS respectively. Moreover, N_s is reminded to be the number of subcarriers per RB. The problem in (4.51) is a binary-integer programming problem where (c_2) ensures that only one combination of MCS and RB is attributed for every user u_m. The constraint (c_3) ensures that the total number of allocated RBs for all users is less than or equal to N_{RB}. The constraint (c_4) states that the overall allocated power is constrained by P_{tot}.

Even if integer programming problems are in general NP-difficult to solve, some efficient algorithms can be found and perform well in practice. We used the CVX toolbox in conjunction with an integer programming solver [86, 87] in order to provide for every user, the optimal number of RBs and MCS index leading to the minimum energy consumption. The global procedure iterates the integer programming solver for each allocated power p_{mr}^{mcs} obtained with the previously described power allocation strategy, until all users are satisfied or a non feasible solution is declared. In that case, the user with the highest energy consumption goes in starvation and the algorithm restarts allocation. To the best of our knowledge, there was not in open literature a procedure that allocates powers, MCS and RBs in multi-user relay-aided OFDMA networks. In the following, we give some results obtained with practical system parameters, borrowed from LTE system and reminded in Table 4.2.

Table 4.2 – System model parameters [14, 18]

Parameters	Description	value
f_s	Sampling rate	7.68 MHz
B_w	Bandwidth	5 MHz
Δf	Subcarrier spacing	15 kHz
N_{c}	Number of subcarriers (FFT size)	512
N_{CP}	Cyclic prefix	128
N_{g}	Number of Guard subcarriers	211
N_{OFDM}	Number of OFDM symbols in a block	7
N_{RB}	Maximum number of RBs	25
L	Block length	1024
f_c	Carrier frequency	2.6 GHz
N_0	Noise spectral density	-174 dBm/Hz
β_{amp}	Power amplifier inefficiency	1

Figure 4.9 shows the overall consumed energy and starvation user rate w.r.t. the power constraint P_{tot} in dBm, in Fig. 4.9(a) and Fig. 4.9(b) respectively. Whatever the number of users considered, i.e. $M = 4, 8, 12$, relay-aided transmission is more energy efficient

than direct transmission thanks to our resource allocation scheme. In Fig. 4.9(a) the delay constraint has been fixed to 3 time slots. One can observe that the more power budget, the more energy consumption per bit due to a higher number of satisfied users, i.e. number of users without resources reduces. A stringent power budget leads to a low energy consumption but to a high number of unsatisfied users. Whatever the number of users and for unbounded power budget, the energy consumption becomes constant since all users are accepted in the network and served. While the starvation rate is nearly the same for networks with and without cooperation, this is not the case for energy consumption for which significant gains can be expected with relay-assisted communications. According to our system model, relay-assisted scheme can save about 30 % of energy compared to direct transmission for $P_{tot} = 45$ dBm. It is worth mentioning that when comparing the starvation rate of direct and relay-assisted transmissions, this should be done with a look on the consumed energy for a fixed power constraint. Since the consumed energy depends on the circuitry power consumption and the required transmission power for all users, relay-assisted network makes a better use of power than non relay-aided system, in average.

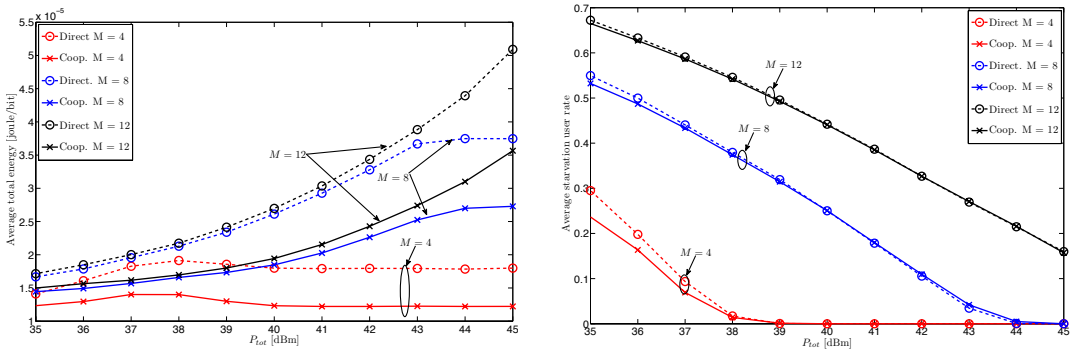

(a) Energy consumption w.r.t. power constraint (b) Starvation user rate w.r.t. power constraint

Figure 4.9 – Average energy consumption in Joule/bit and starvation rate versus P_{tot} in dBm [14, 18]

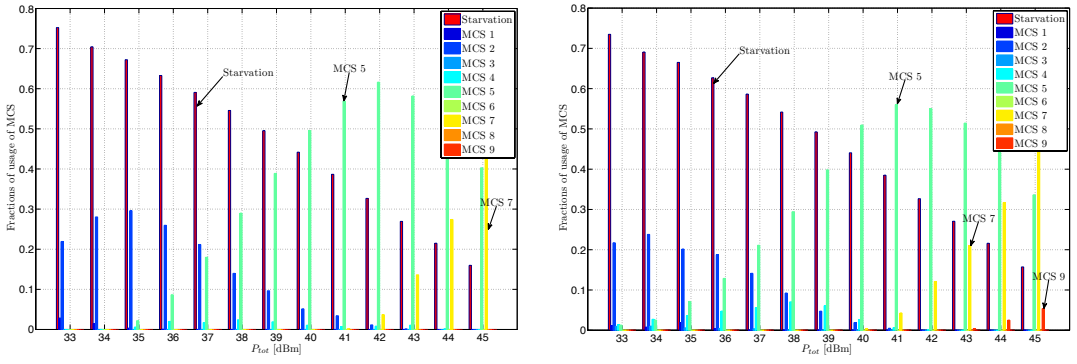

(a) MCS usage in non relay-aided network (b) MCS usage in relay-aided network

Figure 4.10 – Fractions of usage of MCS w.r.t. the power constraint with $M = 12$ and each user has a delay constraint of 3 time slots [14, 18]

Figures 4.10(a) and 4.10(b) represent the fraction of usage of different MCS as function of the total power budget, for direct and cooperative transmissions respectively and for

$M = 12$. For very stringent power constraint, a large starvation user rate can be observed as it has been previously remarked. Moreover, in this case, the most common MCS is the one with the lowest index, corresponding to a QPSK and a low coding rate inducing a low energy consumption but also a low data rate. As P_{tot} increases, the starvation rate decreases and more users can be satisfied and high MCS indexes start being used, enabling a higher spectral efficiency. It is also interesting to remark that relay-assisted scheme, Fig. 4.10(b), enables the use of MCS 9, i.e. allowing the highest spectral-efficiency, for $P_{\text{tot}} = 45$ dBm, which is not possible for a cell without relays as it can be observed from Fig. 4.10(a).

4.2.3 Summary

Finally in this research, we have tackled two different problems with two different approaches: i) maximum sum rate problem under data rate and power constraints with information-theoretic based approach, i.e. using Shannon capacity formula and ii) energy minimization problem under delay and power constraints with pragmatic approach, i.e. energy and delay functions depend on system parameters in a highly non convex way. While the first problem is convex and hence a global optimal can be found, the second one is not and heuristics have to be proposed. For the second problem, we have introduced delays as temporary variables that allows us to provide an iterative procedure to converge toward a feasible solution. Moreover, an integer programming problem has been formulated and solved to allocate MCS and RBs in addition to powers for delay-constrained users in OFDMA networks. These results can be used as benchmark to evaluate other methodologies that would minimize the energy consumption under delay constraint in relay-aided transmission for LTE or next cellular generation systems.

4.3 Power allocation in overlaid DVB-LTE systems

In previous sections, only one cell has always been considered and hence no intercell interference has been taken into account [2]. It is a necessary step to evaluate the fundamental performance of wireless systems but which cannot be sufficient in itself. Nowadays indeed, the wireless spectrum is overcrowded in the range sub gigahertz to 2 gigahertz and systems are, in the best case, located very closely in frequency inducing out-of-band interference.

I have been interested in power allocation when considering interference with the PhD of Hiba Bawab [15]. The spectrum congestion becomes a major issue for developing new wireless services on high data rate requirements. In this context, the spectral overlap of some wireless technologies is more and more envisaged. For instance in the LTE standard, the deployment of small-cells (micro, pico, femto) under the main macro cell is an envisaged mode of communication. In this mode, femto or micro cells can use a separated band from the macro cell or reuse the same band and hence create interference with the macro cell [88].

Multimedia services are more and more required by highly mobile users, e.g. Internet, data sharing, social networks, TV, etc. Future broadcasting network, like digital video broadcasting - next generation handled, is a necessary component of the future usage of the mobile web TV. Moreover, the integrated mobile broadcasting standardized by the 3GPP group can offer mobile broadcasting services to cellular subscribers. This work has been part of the research project mobile multimedia M^3, funded by the french national research foundation (ANR), that aimed at studying the possibility to merge broadcast and cellular technologies. In that context, we aimed at proposing a resource allocation scheme to optimize LTE and DVB data rates when both frequency bands overlap.

Related works

In [89, 90], the authors analyzed an adaptive resource management, i.e. power and time slots, for a secondary cognitive network using the spectrum of a primary broadcast network. The authors derived the optimal transmission time and power policies to maximize the ergodic capacity of secondary network under maximal interference constraint on primary receiver. However, they did not consider the second interfering link, i.e. from the primary transmitter to the secondary receiver, limiting the capacity of this link. The authors of [91] explored the tradeoff between opportunistic and regulated access of multiuser cognitive networks w.r.t. a primary licensed network. In particular, they showed that a non-zero interference level at the primary receivers allows lot of transmission opportunities compared to the strict zero interference requirement at the primary receivers. In [92], channel assignment and power control for cognitive users were investigated in order to maximize the number of cognitive users under a satisfactory interference level at primary receivers. A similar problem was investigated in [93, 94]. In all these works, the symmetric interfering link, i.e. from the primary users to the secondary users was not considered.

Li and Goldsmith in [95] have investigated ergodic capacity of multiuser broadcast fading channels, in particular they found the optimal power allocation policy for the code division multiple access (CDMA) scheme. In [96], the authors studied the information-theoretic limits of a secondary cognitive radio (CR) under spectrum sharing condition with an existing primary user. In their works, the ergodic capacity was studied when secondary users transmit to their secondary base stations under individual power constraint and acceptable interference level at the primary receivers. To the best of our knowledge, the

2. In Section 4.2 intra-cell interference are assumed to be inexistant due to the nature of the multiple access considered, i.e. OFDMA, which is by essence interference free in perfect condition. The UWB scheme that has been dealt with in Section 4.1 is, on the other hand, interfering by nature.

global ergodic capacity under the full interference channel in a DVB-LTE like coexistence scenario was not studied. One can also notice an important amount of more practical works in DVB-LTE interference characterization, cf. [97, 98] and references therein.

On resource allocation in multi-cell interference environment in OFDMA networks, one can mention the work of Ksairi *et al.* in [99, 100] where authors investigated the problem of minimizing the allocated power and finding the subcarriers assignment under data rate constraint and when a part of bandwidth is reused in the adjacent cell while the other remains dedicated to its own cell. Although the optimization problem was not convex, they shown that optimal solution turns to find a pivot distance within which users should use non-protected subcarriers and beyond which they should modulate only dedicated subcarriers.

Our position is rather different where two *different* OFDM-based systems are interfering due to frequency bands overlap. One macro DVB cell is assumed to geographically encompass a smaller LTE cell and a part of their spectrum is shared. In a first part, we have studied the achievable ergodic data rate under a simplified interference model between DVB and LTE. In a second part, the variance of interfering signals seen by one or the other system, i.e. LTE or DVB, has been derived and used to study the achievable data rate under LTE-DVB coexistence.

4.3.1 DVB-LTE ergodic capacity optimization in coexisting DVB-LTE like systems

System model. One considers a single LTE cell encompassed in a single DVB macro-cell as illustrated on Fig. 4.11. The broadcast system is composed of the broadcast transmitter (BT) and one broadcast receiver (BR). The mobile system consists in a single cell of one BS and one mobile receiver (MR). Of course, LTE cell contains more than one user, however since users are separated in the time/frequency grid, they are not interfering each others. Our goal is to study the influence of DVB-LTE frequency overlap, hence we assume one user in LTE cell that uses all RBs. In this model, $h^{(b)}$, $h^{(m)}$, $q^{(b)}$ and $q^{(m)}$ are the channel fading coefficients on one subcarrier of the BT-BR, BS-MR, BT-MR and BS-BR links respectively and are all complex Gaussian distributed with zero mean and unit variance. Moreover d_m is the BS-MR distance assumed to be equal to the LTE cell radius and d_b is the BT-BR distance assumed to be also equal to the DVB cell radius. Since $d_b \gg d_m$, MR can also be assumed to be located on the DVB cell-edge and hence the BT-MR interfering distance is also taken to be d_b.

Both DVB and LTE are OFDM-based systems but with different physical characteristics, e.g. subcarrier spacing is not the same for both systems and hence the number of interfering subcarriers are not the same for each system. Indeed, an LTE subcarrier is typically larger than DVB one then we consider a simplified model where R_b DVB subcarriers interfere with one LTE subcarrier. Contrarily, focusing on one subcarrier at DVB receiver, only a fraction κ of one LTE subcarrier is visible. This model does not take into account different synchronization mismatches that occurs between these two systems but this will be dealt with in the next Section.

The received signals on one subcarrier at MR and BR are respectively given by

$$y_m = \sqrt{p_m l_m} h^{(m)} x_m + \sum_{b=1}^{R_b} \sqrt{p_b l_{bm}} q^{(b)} x_b + w_m \tag{4.52}$$

$$y_b = \sqrt{p_b l_b} h^{(b)} x_b + \kappa \sqrt{p_m l_{mb}} q^{(m)} x_m + w_b \tag{4.53}$$

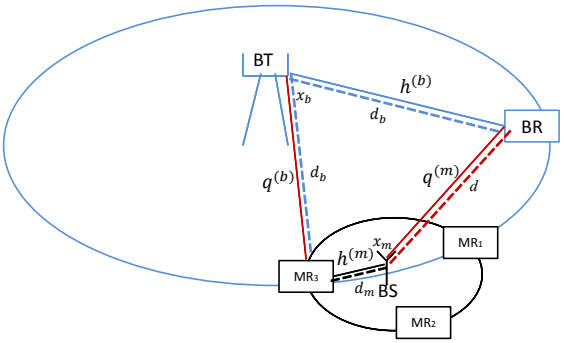

Figure 4.11 – Full interfering LTE cell in a DVB macro cell [15]

where x_m, x_b are the centered-mean information symbols of mobile and broadcast systems respectively with $\mathrm{E}\left[|x_m|^2\right] = \mathrm{E}\left[|x_b|^2\right] = 1$. Moreover, p_m, p_b and l_m, l_b, are the BS, BT transmit powers per subcarrier respectively and the path-loss attenuation in the BS-MR and BT-BR links respectively. l_{bm} and l_{mb} are path loss coefficients of BT-MR and BS-BR links. Finally, $w_m \sim \mathcal{CN}\left(0, \sigma_m^2\right)$ and $w_b \sim \mathcal{CN}\left(0, \sigma_b^2\right)$ are AWGN on one subcarrier at LTE and DVB receiver respectively.

Max sum rate or fairness?

We call the global ergodic capacity, the achievable rate of DVB system under LTE interference plus the achievable rate of LTE under DVB interference, when receivers do not deal with interference. In consequence, this sum rate is not the maximum achievable sum rate of interference channel which implies some schemes that takes into account mutual interference like Han-Kobayashi scheme [101]. By considering interference limited system, i.e. noise is neglected w.r.t. the interfering signal, and equal repartition power between subcarriers for DVB, the global ergodic capacity can be proved to be [97]

$$\begin{aligned} C_g(\beta) &= C_m(\beta) + C_b(\beta) \\ &= \frac{1}{\beta - 1}\log_2\beta + \frac{1}{\frac{A}{\beta} - 1}\log_2\frac{A}{\beta} \end{aligned} \tag{4.54}$$

where the first and second terms represent the cellular and broadcast network capacities respectively, i.e. $C_m(\beta)$ and $C_b(\beta)$. The term $A = \frac{l_{mb}l_{bm}}{R_b l_b l_m}$ is a constant depending on the system parameters and $\beta = \frac{R_b p_b l_{bm}}{p_m l_m}$ gathers the transmission powers p_m and p_b in a ratio, and (4.54) is defined for $\beta \in]0, \infty[\setminus \{1, A\}$. In consequence, C_m and C_b are convex and concave functions in β respectively. Inverting for instance, the LTE capacity w.r.t. β, we straightforwardly have:

$$\beta(C_m) = -\frac{\mathrm{W}(-2^{-C_m}C_m\log(2))}{C_m\log(2)} \tag{4.55}$$

where $\mathrm{W}(.)$ is the Lambert function. Therefore, the broadcast capacity C_b can be expressed in function of C_m as:

$$C_b(C_m) = \frac{1}{\frac{A}{\beta(C_m)} - 1}\log_2\left(\frac{A}{\beta(C_m)}\right) \tag{4.56}$$

Max sum rate. If one is interested in maximizing the global data rate, the optimal strategies would consist in drawing β toward 0, i.e. turn off DVB system, or drawing β toward infinity, i.e. turn off mobile system. The unbounded nature of C_g comes from the fact that noise has been neglected in the model. By imposing data rate constraints on LTE and DVB systems, i.e. C_{mth} and C_{bth} respectively, the max sum rate problem would be

$$\begin{array}{ll} \max\limits_{\beta} & C_g(\beta) \text{ s.t.} \\ (c_1) & C_m(\beta) \geq C_{mth} \\ (c_2) & C_b(\beta) \geq C_{bth} \end{array} \tag{4.57}$$

Since the mobile system capacity is varying in an opposite way compared to the DVB system capacity, the maximum global capacity should lie on the boundaries of β defined by both system capacities with the intersection of the constraints, i.e. C_{mth} and C_{bth}. A procedure searching for the optimal power ratio β^* maximizing C_g can be programmed and has been proposed in [98].

Fairness. Maximizing the global data rate leads to favor one system over the other, i.e. LTE because of its smaller cell-dimension compared to the DVB cell. Convex-concave procedure (CCCP) searches for the equilibrium point of a sum of convex and concave functions [102]. The Lagrangian of (4.57) is defined as:

$$\mathcal{L}(\beta, \lambda, \nu) = (1+\lambda)C_m(\beta) + (1+\nu)C_b(\beta) - \lambda C_{mth} - \nu C_{bth} \tag{4.58}$$

where $\lambda \geq 0$ and $\nu \geq 0$ are the Lagrange multipliers associated to the constraints on C_m and C_b respectively. $\mathcal{L}$ in (4.58) is composed of two terms:

$$\text{convex term: } \mathcal{L}_{\text{vex}}(\beta) = (1+\lambda)C_m(\beta) - \lambda C_{mth} \tag{4.59}$$

and

$$\text{concave term: } \mathcal{L}_{\text{cave}}(\beta) = (1+\nu)C_b(\beta) - \nu C_{bth} \tag{4.60}$$

CCCP consists in an iterative algorithm where at each iteration time t we have:

$$\nabla_\beta L_{\text{vex}}(\beta^{t+1}) = -\nabla_\beta L_{\text{cave}}(\beta^t) \tag{4.61}$$

$$\nabla_\beta C_m\left(\beta^{t+1}\right) = -\frac{1+\nu}{1+\lambda}\nabla_\beta C_b\left(\beta^t\right). \tag{4.62}$$

where ∇_β stands for the derivative w.r.t. β and β^t is the current step value of β. The implementation of CCCP procedure requires closed-form expressions of λ and ν in function of β^t, which we do not have. However, an iterative procedure can be obtained without having closed-form expressions for Lagrange multipliers [98]. The principle is to set some lower and upper bounds for λ and ν, i.e. λ_{min}, λ_{max} and ν_{min}, ν_{max} respectively and a starting point $\beta = \beta_0$. By iterating on Lagrange multipliers until data rate constraints are satisfied, β^t is updated at each iteration according to the numerical values of λ and ν obtained. The algorithm leads to the minimum global capacity but to an equilibrated data rate of broadcast and mobile systems.

Numerical results

Fig. 4.12(a) shows the optimal points reached by CCCP and max sum rate procedure for individual data rate constraints $C_{mth} = 0.5$ and $C_{bth} = 1$ bit/s/Hz. The interval of β satisfying both constraints in (4.57) is $[\beta_{\min}, \beta_{\max}]$. While the max sum rate procedure

draws optimal β to $\beta_{\max}$ leading to $C_{g\,\max}$, CCCP converges to $C_{g\,\min}$ with β^* corresponding to the equal sum rate between both systems. Max sum rate procedure favors necessarily one system over the other which may not be prejudicial if QoS constraints have been set with care. However, CCCP allows to maximize *both individual* rates at the price to minimize the global sum rate. This is also visible on Fig. 4.12(b) where global, mobile and broadcast achievable rates are given for optimal β obtained with the max sum rate and CCCP when d is varying. All capacities increase with d for both algorithms (except mobile capacity obtained with max sum rate which remains constant while d is varying). When d increases, the DVB system becomes interference-free and hence contributes to the increase of the global capacity. Second, the data rates achieved with max sum rate are higher than the ones achieved with CCCP, except for mobile capacity and very small d. However, CCCP allows to balance between both system performance.

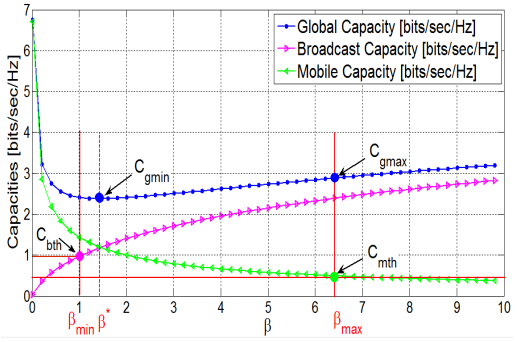

(a) Optimal C_g with max sum rate or fairness procedure, $d = 100$m, $C_{mth} = 0.5$, $C_{bth} = 1$ bits/s/Hz

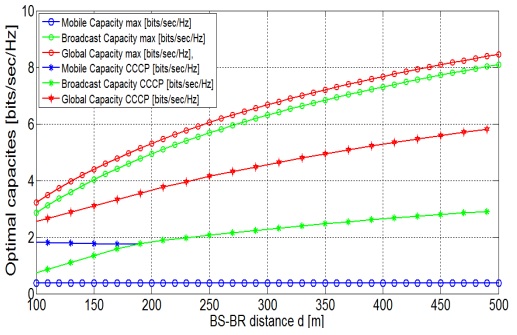

(b) Achievable rates obtained with CCCP and max sum rate procedures w.r.t. d and $C_{mth} = C_{bth} = 0.4$ bits/s/Hz

Figure 4.12 – Optimal achievable rates obtained with max sum rate and CCCP [15]

4.3.2 Spectral efficiency of DVB and LTE with realistic interference signal model

The signal model considered in the previous section, i.e. (4.52) and (4.53), is sufficient in a first approach but is far from being realistic. Because of quite different OFDM modulation characteristics, the interference seen on one subcarrier at a given receiver is composed of a complex expression of all other subcarriers of the other system and the frequency overlap. The received signal in one subcarrier of a given receiver, DVB or LTE, cannot be expressed directly in frequency domain because of non time-invariant sampled interfering signal seen by the considered receiver, due to difference in sampling frequency of DVB and LTE systems.

The system model considered is the same than that described in Fig. 4.11 where the frequency overlap may be variable as illustrated in Fig. 4.13. The spectral overlap can be represented as a ratio of the minimum bandwidth of the system as:

$$\alpha = \frac{\Delta f_0}{B_{\min}} = \frac{1+\chi}{2\chi} - \frac{\Delta f}{B_{\min}} \tag{4.63}$$

where Δf_0 is the spectral overlap between LTE and DVB bandwidths, i.e. $B^{(L)}$ and $B^{(D)}$ respectively, while f_c and f_c' are their central frequencies such as $\Delta f = |f_c - f_c'|$. The ratio χ is defined by $\chi = \frac{B_{\min}}{B_{\max}}$, $B_{\min} = \min\left\{B^{(L)}, B^{(D)}\right\}$ and $B_{\max} = \max\left\{B^{(L)}, B^{(D)}\right\}$.

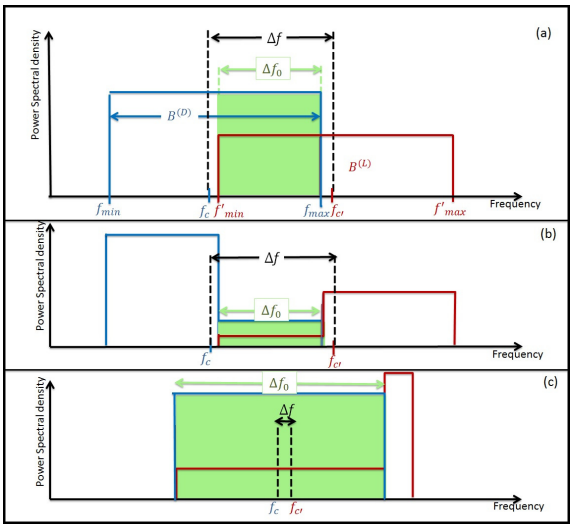

Figure 4.13 – Spectral overlap between LTE and DVB [20]

Let us define $T_s^{(L/D)}$, $T_g^{(L/D)}$, $N^{(L/D)}$ the useful part of OFDM symbol, cyclic prefix durations and the number of subcarriers of LTE/DVB systems respectively with $T^{(L/D)} = T_s^{(L/D)} + T_g^{(L/D)}$ the total symbol duration of OFDM symbols. Moreover, $\xi = \frac{T^{(D)}}{T^{(L)}} = \frac{T_s^{(D)}}{T_s^{(L)}} = \frac{T_g^{(D)}}{T_g^{(L)}} > 1$, such as $\xi \in \mathbb{Q}$. It is well known that when transmitter and receivers are perfectly synchronized the useful part of signal, i.e. without interference, received on the $p-$th subcarrier over the $m-$th OFDM data block is simply expressed as:

$$\tilde{X}_p^{(L/D)}[m] = X_p^{(L/D)}[m] H_p^{(L/D)}[m] \tag{4.64}$$

where $X_p^{(L/D)}[m]$ is the QAM symbol of the $m-$th OFDM data block transmitted over the $p-$th LTE/DVB subcarrier, $H_p^{(L/D)} = \sum_{n=1}^{L/L'} h_n^{(L/D)} e^{-j2\pi \frac{p}{T_s^{(L/D)}} \tau_n^{(L/D)}}$ is the channel frequency response coefficient on the $p-$th subcarrier of the BS-MR/BT-BR link respectively. Moreover, $h_n^{(L/D)}$ and $\tau_n^{(L/D)}$ are respectively the complex Gaussian channel coefficients and delays of the $n-$th path of the LTE/DVB channel which contains L and L' paths respectively.

Variance of interference

Considering a classical rectangular pulse shaping for OFDM waveforms, the expression of interference signals, i.e. DVB over LTE and LTE over DVB, are rather complex. A careful analysis of interfering symbols taking into account multi-paths and asynchronism has to be lead. One can represent the interfering DVB signal over LTE and vice versa as in Figs. 4.14(a) and 4.14(b) respectively.

One can prove the following two theorems on the variance of the interference caused by a DVB signal on a LTE receiver and vice versa. The expressions are derived by averaging over symbols, channel amplitudes and asynchronism (in the same way we did for UWB in Section 4.1).

Theorem 2 (DVB interference variance over the LTE receiver) *The DVB interference variance over the LTE receiver can be expressed by:*

$$V_p^{(D)} = \left(1 - \frac{T_s^{(D)}}{\xi T^{(D)}}\right) \mathrm{E}^{(1)}_{x_{k'},q_{n'}}[|I_p^{(D)}[m]|^2] + \mathrm{E}^{(2)}_{x_{k'},q_{n'},\theta^{(D)}}[|I_p^{(D)}[m]|^2] \tag{4.65}$$

where $\theta^{(D)}$ is the random asynchronism of DVB signal from MR point of view. $q_{n'}^{(D)}$ and $\tau_{n'}^{(D)}$ are respectively the BT-MR complex Gaussian distributed channel coefficient and delay of the $n'-th$ path of the DVB channel. Its frequency response on the $k'-th$ subcarrier is defined as $Q_{k'}^{(D)} = \sum_{n'=1}^{L'} q_{n'}^{(D)} e^{-j2\pi \frac{k'}{T_s^{(D)}} \tau_{n'}}$. $\mathrm{E}^{(1)}_{X_{k'},q_{n'}}[|I_p^{(D)}[m]|^2]$ and $\mathrm{E}^{(2)}_{X_{k'},q_{n'},\theta^{(D)}}[|I_p^{(D)}[m]|^2]$ can be expressed as:

$$\mathrm{E}^{(1)}_{X_{k'},q_{n'}}\left[|I_p^{(D)}[m]|^2\right] = \frac{1}{\xi} \sum_{k'=0}^{N^{(D)}-1} \left|\mathrm{sinc}\left(\pi\left(\frac{\Delta f^{(D)} T_s^{(D)}}{\xi} + \frac{k'}{\xi} - p\right)\right)\right|^2 \sum_{n'=1}^{L'} \Omega_{n'}^{(D)} \tag{4.66}$$

$$\begin{aligned}\mathrm{E}^{(2)}_{X_{k'},\theta^{(D)},q_{n'}}[|I_p^{(D)}[m]|^2] = \frac{\xi}{2\pi^3 \left(T_s^{(D)}\right)^2 T_s^{(L)}} \sum_{k'=0}^{N^{(D)}-1} \frac{1}{A(k')^3} \sum_{n'}^{L'} \Omega_{n'} \left\{ \frac{T_s^{(D)}}{\xi} + \right. \\ 2\cos\left(\pi A\left(k'\right)\left(\frac{mT^{(D)}}{\xi} + \frac{T_s^{(D)}}{\xi} - B\left(n', \frac{Ts^{(D)}}{\xi}\right) - B\left(n', 0\right)\right)\right) \times \\ \left. \cos\left(\pi A\left(k'\right)\frac{Ts^{(D)}}{\xi}\right) \sin\left(\pi A\left(k'\right)\left(B\left(n', 0\right) - B\left(n', \frac{Ts^{(D)}}{\xi}\right)\right)\right)\right\}\end{aligned} \tag{4.67}$$

where $\Omega_{n'}^{(D)} = \mathrm{E}[|q_{n'}^D|^2]$, $A(k') = \Delta f^{(D)} + \frac{k'}{T_s^{(D)}} - \frac{p}{T_s^{(L)}}$ and
$B(n', \theta^{(D)}) = l'T^{(D)} - T_g^{(D)} + \tau_{n'}^{(D)} + \theta^{(D)}$.

Theorem 3 (LTE interference variance over the DVB receiver) *The LTE interference variance over the DVB receiver can be expressed as:*

$$\begin{aligned} V_{p'}^{(L)} &= \mathrm{E}_{X_k, q_n^{(L)}, \theta^{(L)}}\left[|I_{p'}^{(L)}[m']|^2\right] \qquad (4.68) \\ &= \frac{1}{T_s^{(D)} T_s^{(L)} T^{(L)}} \sum_{k=0}^{N^{(L)}-1} \sum_{n=1}^{L} \Omega_n^{(L)} \left(\frac{1}{\pi^2 C(k)^2}(T1 + T2) + \lfloor \xi' \rfloor (T^{(L)})^3 \mathrm{sinc}^2\left(\pi C(k) T^{(L)}\right)\right) \end{aligned}$$

where $q_n^{(L)}$ is the BS-BR complex Gaussian distributed channel coefficient where $Q_k^{(L)}$ is its frequency response on the $k-th$ subcarrier defined as $Q_k^{(L)} = \sum_{n=1}^{L} q_n^{(L)} e^{-j2\pi \frac{k}{T_s^{(L)}} \tau_n^{(L)}}$. $T1$ and $T2$ are defined as:

$$T1 = \frac{1}{2}T^{(L)} + \frac{\sin\left(2\pi C(k)\left(m\xi T^{(L)} - G(n, T^{(L)})\right)\right) - \sin\left(2\pi C(k)\left(m\xi T^{(L)} - G(n, 0)\right)\right)}{4\pi C(k)} \tag{4.69}$$

$$\begin{aligned} T2 = \frac{1}{2}T^{(L)} + \frac{\sin\left(2\pi C(k)\left(\xi\left(mT^{(L)} + T_s^{(L)}\right) - \lfloor \xi' \rfloor T^{(L)} - G\left(n, T^{(L)}\right)\right)\right)}{4\pi C(k)} \\ - \frac{\sin\left(2\pi C(k)\left(\xi\left(mT^{(L)} + T_s^{(L)}\right) - \lfloor \xi' \rfloor T^{(L)} - G\left(n, 0\right)\right)\right)}{4\pi C(k)} \end{aligned} \tag{4.70}$$

where $C(k) = \Delta f^{(L)} + \frac{k}{T_s^{(L)}} - \frac{p'}{T_s^{(D)}}$, $G\left(n, \theta^{(L)}\right) = lT^{(L)} - T_g^{(L)} + \tau_n^{(L)} + \theta^{(L)}$ *and* $\theta^{(L)}$ *is the random asynchronism of LTE signal seen by BR.*

The proofs are omitted but can be found in [15, 20]. To the best of our knowledge, these expressions are the first analytical ones assessing the variance of DVB and LTE interferences over the reciprocal receiver. They allow us to study the data rate penalty imposed by a certain frequency overlap between systems and power allocation strategy.

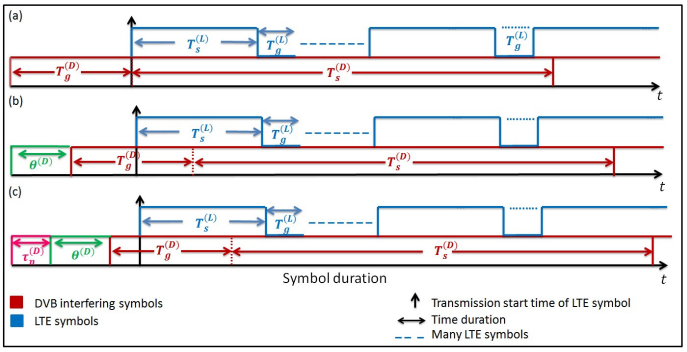

(a) Time representation of interfering DVB symbols over LTE symbol

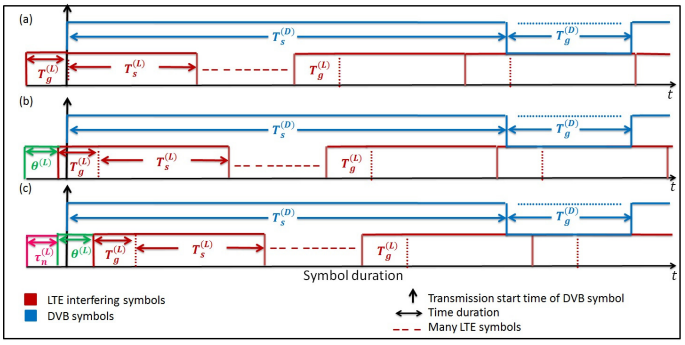

(b) Time representation of interfering LTE symbols over DVB symbol

Figure 4.14 – Chronograph of interfering signals according to the considered receiver, i.e. LTE or DVB [20]

Spectral efficiency

Due to the complexity of expressions derived, an optimization problem giving the optimal allocated power according to the overlap ratio α has not been solved up to now and remains an open issue. However, different strategies has been numerically evaluated in this work and are summarized hereafter.

Uniform allocation. Transmit powers are equally allocated to each subcarrier in both systems whatever the frequency overlap ratio. This strategy corresponds to the illustration in Fig. 4.13a. An upper bound on the global spectral efficiency can be written as

$$S_T(\alpha) = \frac{1}{B_T(\alpha)}(\hat{D}^{(D)}(\alpha) + \hat{D}^{(L)}(\alpha)) \tag{4.71}$$

where $B_T(\alpha)$ is the total used bandwidth given by $B_T(\alpha) = B_{\min}(1-\alpha) + B_{\max}$ and $\hat{D}^{(D)}(\alpha)$, $\hat{D}^{(L)}(\alpha)$ are the upper bound, obtained thanks to Jensen's inequality, of the ergodic data rate of LTE and DVB systems respectively.

Interference aware power allocation. The idea is to allocate different powers on the interfering and non-interfering part of the spectrum as illustrated on Figs. 4.13b and 4.13c. The former shows that PSD of the non interfering part of both systems are greater than the one of the interfering part. The later shows a full spectral overlap scenario where the DVB bandwidth is completely overlapped by LTE while this latter keeps a fraction of its bandwidth interference-free. In that case, only LTE is able to divide its power budget in the interfering and non-interfering parts. For the system with the lowest bandwidth, i.e. $B_{\min}$, the total transmission power can be expressed as $P_T^{\min} = (1-\beta)P_T^{\min} + \beta P_T^{\min}$ where $P_T^{\min}$ is the total transmission power over the bandwidth $B_{\min}$, $\beta \in [0,1]$ is the interference aware power allocation parameter and $\beta P_T^{\min}$ is the power allocated to the interfering part and $(1-\beta)P_T^{\min}$ is the dedicated portion for the interference free part. Therefore, the transmission powers per subcarrier in the interfering and non-interfering parts are respectively $\lambda_I^{\min} = \frac{\beta P_T^{\min}}{K_I^{\min}}$ and $\lambda^{\min} = \frac{(1-\beta)P_T^{\min}}{K}$ with $K_I^{\min} = \alpha N^{\min}$, $K = (1-\alpha)N^{\min}$ and $N^{\min}$ the total number of subcarriers in $B_{\min}$. The transmission power per one subcarrier can be re-written as:

$$\lambda_I^{\min} = \frac{\beta}{\alpha}\lambda_t^{\min} \text{ and } \lambda^{\min} = \frac{1-\beta}{1-\alpha}\lambda_t^{\min}$$

with $\lambda_t^{\min} = P_T^{\min}/N^{\min}$ is the transmission power value per subcarrier in case of uniform power allocation. On the other hand, for the system with the largest bandwidth, i.e. $B_{\max}$, the transmission powers per subcarrier in the interfering and non-interfering parts are respectively $\lambda_I^{\max} = \frac{\beta_m P_T^{\max}}{K_I^{\max}}$ and $\lambda^{\max} = \frac{(1-\beta_m)P_T^{\max}}{K}$ with $K_I^{\max} = \alpha_m N^{\max}$, $K^{\max} = (1-\alpha_m)N^{\max}$ and $\alpha_m = \chi\alpha$. Moreover, $N^{\max}$ is the total number of subcarriers in $B_{\max}$, $P_T^{\max}$ is the total transmission power over the bandwidth $B_{\max}$ and similarly than the other system, β_m is the fraction of power allocated to the interfering part of the system with the maximum bandwidth. Two strategies for the power allocation, i.e. β and β_m, can be envisaged: i) these two fractions are correlated to each other and when β is fixed, the other is immediately obtained with $\beta_m = \chi\beta$ and ii) β and β_m are let free from each other. From this model, SINR expressions of interfering and non-interfering subcarriers can be assessed and the achievable data rate of each system can be separated in a summation containing subcarriers that fully interfere and a summation without interference. However, it is worth noting that due to the non-adapted FFT sampling frequency of one system to the other, inter-carrier interference is reported over all the spectrum, cf. Theorems 2 and 3.

Fig. 4.15 illustrates the global spectral efficiency for two overlapping ratios, i.e. $\alpha = 0.3, 0.7$ w.r.t. the proportion of PSD allocated to the interfering part on both systems. We can remark that global spectral efficiency can benefit from a high spectral overlap, i.e. $\alpha = 0.7$ depending on (β, β_m), thanks to a lower occupied bandwidth and also because of the larger LTE data rate compared to the DVB rate. These results enlighten the potentiality of spectral overlap between DVB and LTE to increase the global spectral efficiency of the global system. However, both surfaces are non convex in β and β_m that leaves room for proposing simplified allocation procedure to optimize the global spectral efficiency.

4.3.3 Summary

Our contributions in this part have been "polarized" in the sense that either the problem of resource allocation in spectral overlap scenario between DVB and LTE systems, has been

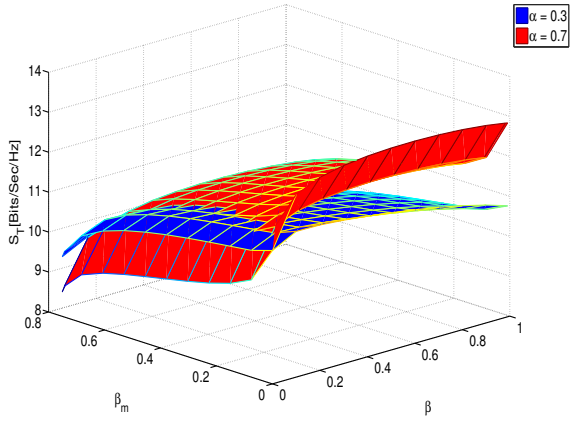

Figure 4.15 – Total spectral efficiency w.r.t. β and β_m, $d = 1$km and $\alpha = 0.3, 0.7$ [20]

solved but based on a simple interference model, or an accurate interference model has been derived but leads to a complex optimization problem to solve. However, we believe that a true interference model as it has been proposed in this part may lead to optimize the spectral overlap of DVB and LTE systems as it has been suggested by the first analysis presented above.

4.4 Conclusions, on-going work and perspectives

So far, I co-supervised two PhD students in resource allocation issues, i.e. Dr. Mohamad Maaz and Dr. Hiba Bawab, with whom I tackled quite different optimization problems, e.g. continuous convex, non-convex, integer, and search for adapted mathematical tools to solve these problems. I believe these experiences have improved my background acquired during my work on resource allocations for TH-UWB communications. My main contributions on resource allocation for wireless systems can be summarized as follows:

— **Resource allocations:** Proposition of convex and non-convex power allocation procedures in OFDMA context in relay aided networks when BSs have full CSI and when only statistical CSI are available. This has been done with the PhD of Dr. Mohamad Maaz while searching for maximizing the data rate of the cell or minimizing the energy consumed in the cell under delay constraints when HARQ is considered. These works lead to the publications [18, 70, 103]. A contribution has also been provided in non-convex power allocation with the convex-concave procedure concept when two OFDM-based systems overlap in frequency. In particular, it has been shown that CCCP achieves the minimum global data rate in this case but the maximum of both systems data rate. These researches have been published in [97, 98]. Finally, non-integer programming has been successfully used to propose frame allocation in variable rate TH-UWB communications in [17, 52] and to allocate MCS minimizing the energy consumption of the cell in OFDMA relay aided network with HARQ-I in [18].

— **Signal processing:** Performance of interfering wireless systems is greatly conditioned by the interference power seen by a given receiver. The derivation of the interference power may be rather involved according to the signal model chosen for the analysis. Two contributions have been provided on this issue, the first one relies on the derivation of multiple-access interference variance of multi-rate TH-UWB

communications, [17], and the second one relies on the derivation of the interference variance of spectrally overlapping DVB and LTE systems [20].

Moreover, these studies have opened several research issues that could be addressed in a near future with some links with the works that will be presented in the next chapters. First, it would be interesting to link my recent interest for finite block length information theory to resource allocation with HARQ schemes. Indeed, finite block length theory allows to address some fundamental bounds of practical systems without resorting with practical, often untractable, coding and modulation schemes that are used in HARQ mechanisms. In [104], authors studied the performance of HARQ-IR scheme by bounding the probability that the $m-$th transmission failed in Rayleigh quasi-static fading scenario using recent finite block length results [105]. However, finite block length description is not the more relevant in Rayleigh fading channel where the average error probability converges quickly to the traditional outage capacity defined in the framework of asymptotic information theory as it has been stated in [105] and verified in [41]. The study of [104] can be first extended to Rice channel with a high specular component and optimal power allocation could be searched in the framework of finite block length information theory.

Concerning the work of co-existence between DVB and LTE systems, we could first try to theoretically solve the optimization problem associated with the theoretical interference model developed in Section 4.3. This is a challenging task due to the complex dependence of interference power on frequency overlap ratio α. However, a more careful look on the behavior of interference variance w.r.t. α could exhibit some properties that could be exploited to approximate the expressions. In a second time, the integration of multiple LTE cells with multiple users should be taken into account. Randomization of cell deployment based on stochastic geometry would be useful to assess average performance. Broadcast cells can be considered as macro-BS and LTE cells as micro-cells and results on heterogeneous point process networks could be used to characterized the distribution of the interference seen by both systems. Obviously, the different system characteristics should be kept in order not to reduce the problem to a classical heterogeneous randomly deployed network and the expressions obtained in Section 4.3 should be averaged over network geometry.

CHAPTER

5 Energy efficiency of large cellular networks and machine learning for green communications

Currently, 3% of the world-wide energy is consumed by the ICT infrastructure which generates about 2% of the world-wide CO_2 emissions, comparable to the world-wide CO_2 emissions by all commercial airplanes. The ICT sector's carbon foot print is expected to quickly grow to 1.4 Giga ton CO_2 equivalents by 2020, nearly 2.7% of the overall carbon footprint from all human activities [1].

There was, and there is still, a huge need for developing sustainable information technologies that justified the European project FP7 EARTH that investigated the energy efficiency of mobile communications. In 2013, we have been granted by ANR, in the framework of the Labex Cominlabs, for the project entitled toward energy proportional networks (TEPN) that aims at making the networks energy consumption proportional to their load. Since we were not able to compete with EARTH project due to not the same amount of resources, in scale and fundings, our approach in TEPN was to tackle the problem under the cognitive angle. As in almost all areas of engineering in the past several decades, the design of computer and network systems aimed at delivering maximal performance without regarding to the energy efficiency. Thus, the current way of dimensioning and operating the infrastructure supporting the user services, such as cellular networks and data centers, is to dimension for peak usage. The problem with this approach is that usage is rarely at its peak. The overprovisioned systems are also aimed at delivering maximal performance, with energy efficiency being considered as something desired, but non-essential. An energy proportional network can be designed by taking intelligent decisions (based on various constraints and metrics) into the network such as switching on and off network components in order to adapt the energy consumption to the user needs.

TEPN gathered several people from different team, i.e. INSA Rennes, CentraleSupélec Rennes, IMT Atlantique, INRIA. The issues tackled in this project ranged from the design of new energy-efficient waveforms to level-2 and 3 protocols to save energy passing by peak to average power ratio (PAPR) reduction techniques and machine learning for energy-efficient networks. I co-supervised two PhD students in this project whose works and contributions are summarized in this Chapter. Section 5.1, summarizes our contributions in energy-efficiency spectral-efficiency tradeoff of large networks. An intensive use of stochastic geometry and random matrix theory have been necessary to derive computable expressions of EE and SE. Section 5.2, explains our work on machine learning for green communications by the use of MAB theory. Finally Section 5.3 draws the conclusions of the Chapter, summarizes my contributions and gives some research perspectives.

1. The Climate Group, *SMART 2020: Enabling Low Carbon Economy in Information Age*, June 2008. Available online: http://www.theclimategroup.org/publications.

5.1 EE-SE tradeoff of large cellular networks

In the previous chapter, we only have considered single cell problems, except in the last part where a macro DVB cell overlaying on a LTE cell was considered. However, the performance of communication systems in large interference-limited networks has not been addressed in the previous Chapter. In the PhD of Ahmad Mahbubul Alam [21], we have first dealt with EE-SE tradeoff in hexagonal cellular networks and single user and then moved to randomly deployed multi-cell, multi-user networks, in the downlink scenario.

A lot of energy metrics have been defined in literature; here, we used energy-efficiency which is the ratio of the achievable data rate, R in bits/s, by the consumed power, P_{tot}:

$$\eta_{EE} = \frac{R}{P_{\text{tot}}} \tag{5.1}$$

and SE itself is a ratio between the achievable data rate, over the bandwidth, w, used to achieve this rate, i.e. $\eta_{SE} = R/w$. The power consumed at BS follows a linear model as stated in Section 4.2.2 but may take into account multi-antenna systems:

$$P_{\text{tot}} = aP_t + MP_{\text{RF}} + c, \tag{5.2}$$

where a, c, M, P_{RF} and P_t are power amplifier inefficiency constant [2], non-transmission power consumption, (including cooling, baseband unit, ...), the number of RF chains, the power consumed in one RF chain and the effective transmit power respectively.

On the side of the network models existing in literature, we can find two kinds of works: the work considering regular hexagonal networks with fixed BS positions [106, 107] and the researches dealing with spatial point processes, in particular PPP, to model the BS distribution, e.g. [108–111] among others.

5.1.1 Hexagonal network

The regular hexagonal grid model has been widely used to model the cellular deployment. The whole system bandwidth is divided and allocated to a number of cells in a regular pattern, named cluster. In order to avoid as much as possible co-channel interference (CCI), a frequency is allowed to be reused only in two cells that do not belong to the same cluster. The frequency reuse factor K is then defined as the number of cells in one cluster. If r_H is the radius of the hexagonal cell, then the distance between two adjacent cell centers is $\sqrt{3}r_H$ and the frequency reuse distance is

$$l = \sqrt{3K}r_H. \tag{5.3}$$

When the cell size and the BS transmit power are the same for all BSs, then CCI only depends on the ratio between the frequency reuse distance and cell radius, which is equal to $\sqrt{3K}$ as obtained from (5.3). If K increases then CCI decreases. However, the number of cells in a cluster increases, and thus available bandwidth in a cell decreases. This has a negative effect on SE and EE as well. In this research, we aimed at studying the effect of different frequency reuse factors, i.e. K, on the EE-SE tradeoff both with and without shadowing when user is at different locations in the cell.

Hexagonal model is generally intractable to analytically derive the key performance indicators, e.g. outage probability, coverage. In order to make wireless network analysis tractable, Kelif *et al.* have proposed to replace the discrete interfering BS set by a continuum of infinitesimal interferer. This model is known as fluid model [26,112]. Thanks to this

2. The higher a, the more PA inefficient.

Parameter	Value
w	10 MHz
N_0	-168.83 dBm/Hz
r_0	1.7×10^{-4} km
r_H	0.5 km
a	14.5 [113]
b	712 W [113]
α	3.5

Table 5.1 – Parameters for hexagonal cellular network [21]

formulation, the authors derived a closed form expression for interference to signal ratio (ISR) allowing a tractable expression for outage probability in hexagonal cellular networks. However, the ISR expression provided by Kelif *et al.* [26] is limited to the case where the system bandwidth is reused in each cell. Indeed, a generic expression for ISR taking into account K, path loss exponent is challenging to find.

Let us consider a regular hexagonal network with different frequency reuse factors where each BS is equipped with a single antenna such that the power consumption model on (5.2) reduces to $P_{\text{tot}} = aP_t + b$, with b accounts for all static powers consumed in BS. We consider an OFDMA-like system, with no intra-cell interference, so the study can be done on one subcarrier. The power received by the typical k-th user at distance r_{ik} from BS $i \geq 0$ considering shadowing along with path loss is

$$P_{ik} = P_t \left(\frac{r_{ik}}{r_0} \right)^{-\alpha} Y_{ik}, \tag{5.4}$$

where r_0^α is the propagation constant, including close-in reference point, Y_{ik} is the long-term shadowing effect, log-normally (LN) distributed, i.e. $Y_{ik} \sim \mathcal{LN}(0, \sigma)$, with zero mean and σ as standard deviation in dB. The user receives interference from all BSs having the same frequency sub-band as the connected BS. The connected BS is set for $i = 0$, and the power received by the k-th user at distance r_{0k} from the connected BS is

$$P_{0k} = P_t \left(\frac{r_H v}{r_0} \right)^{-\alpha} Y_{0k}, \tag{5.5}$$

ISR [26] depends on the r.v. Y_{ik} and can be written as

$$f_s(v, \alpha) = \frac{I}{P_{0k}} = \sum_{i \geq 1} \left(\frac{r_{ik}}{r_H v} \right)^{-\alpha} \frac{Y_{ik}}{Y_{0k}}. \tag{5.6}$$

EE-SE without shadowing

After having searched for a non linear regression of ISR in (5.6), but without Y_{ik}/Y_{0k}, we have firstly characterized the EE-SE tradeoff without shadowing illustrated in Fig. 5.1, following specifications given in Table 5.1. Figure 5.1 plots EE w.r.t. SE for two normalized distances, i.e. $\nu = 0.5$ and $\nu = 0.85$, and several frequency reuse factors. The linear behavior of EE w.r.t. SE is due to the huge amount of power that is not directly used to transmit information but simply to run BS. This characteristic is somehow the payoff of the static power consumption drawback in real systems. It hence exists an optimal transmit power that maximizes both EE and SE. The sharp decrease of EE w.r.t. SE is due to the

interference-limited situation, where increasing too much P_t does not improve SE but has a certain energetic cost. Since all BSs have the same transmit power, SE converges toward the limit $\frac{1}{K}\log_2\left(1+\frac{1}{\sum_{i\geq 1}\left(\frac{r_{ik}}{r_H v}\right)^{-\alpha}}\right)$ when $P_t \to \infty$ and $\eta_{\text{EE}} \to 0$. Results illustrate also that an aggressive frequency reuse factor, i.e. $K = 1$, is beneficial for both EE and SE when users are not located on cell-edge, e.g. $v = 0.5$ but this is not the case for cell-edge user, e.g. $v = 0.85$, for which $K = 3$ leads to a better achievable performance in EE and SE than for $K = 1$ since the lower K, the higher ISR.

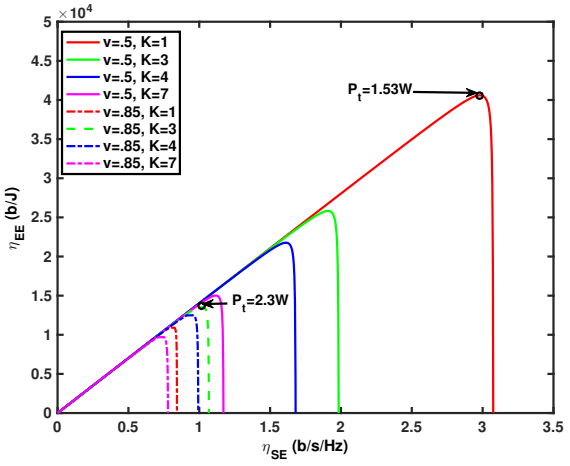

Figure 5.1 – EE-SE tradeoff without shadowing [21]

EE-SE with shadowing

With long term shadowing, global channel gain does not necessarily satisfy ergodicity property. In particular, without CSI at transmitter, it cannot be guaranteed to find a coding scheme at a given rate that ensures a vanishing error probability. In that sense, the capacity in the Shannon definition, does not hold. One may rather prefer talking about outage capacity or $\epsilon-$capacity [114] defined as:

$$\begin{aligned}\eta_{\text{SE}}^{(\epsilon)} &= \sup_R \left\{R : \mathrm{P}\left[\frac{1}{K}\log_2(1+\gamma) < R\right] \leq \epsilon\right\} \\ &= \sup_R \left\{R : F_\gamma\left(2^{KR}-1\right) \leq \epsilon\right\}, \end{aligned} \tag{5.7}$$

where F_γ is the cumulative distribution function of SINR γ, that is:

$$\gamma = \left(\frac{\frac{w}{K}N_0}{P_t\left(\frac{r_H v}{r_0}\right)^{-\alpha} Y_{0k}} + f_s(v,\alpha)\right)^{-1} \tag{5.8}$$

where w is the bandwidth of a resource block allocated to a user when frequency reuse factor is one, N_0 is the noise spectral density and $f_s(v,\alpha)$ is ISR in (5.6). Outage capacity represents the maximal allowed rate for which the probability the channel capacity falls below this rate is less than the threshold ϵ. It is worth noting that $\epsilon-$capacity is not a rate

without error but a given rate for which some errors are tolerated. Outage EE or ϵ-EE is then simply defined as $\eta_{\mathrm{EE}}^{(\epsilon)} = w\eta_{\mathrm{SE}}^{(\epsilon)}/aP_t + b$.

Using the Fenton-Wilkinson method [115], SINR can be approached as a log-normal variable, i.e. $\gamma \sim \mathcal{LN}(\mu_\gamma, \sigma_\gamma)$ where

$$\begin{cases} \mu_\gamma = \frac{1}{2d}\log\left(\frac{{\sigma_{NL}}^2+{\sigma_{FL}}^2}{(\mu_{NL}+\mu_{FL})^2}+1\right) - \frac{1}{d}\log\left(\mu_{NL}+\mu_{FL}\right) \\ \sigma_\gamma = \frac{1}{d}\sqrt{\log\left(\frac{{\sigma_{NL}}^2+{\sigma_{FL}}^2}{(\mu_{NL}+\mu_{FL})^2}+1\right)} \end{cases} \tag{5.9}$$

where

$$\begin{cases} \mu_{NL} = e^{d\mu_N + d^2\sigma^2/2}, \quad \mu_{FL} = e^{d\mu_F + d^2{\sigma_F}^2/2} \\ \sigma_{NL}^2 = e^{2d\mu_N + d^2\sigma^2}\left(e^{d^2\sigma^2}-1\right) \\ \sigma_{FL}^2 = e^{2d\mu_F + d^2{\sigma_F}^2}\left(e^{d^2{\sigma_F}^2}-1\right) \\ \mu_N = 10\log_{10}\left(\frac{w}{K}N_0\right) - 10\log_{10}\left(P_t\left(\frac{r_H v}{r_0}\right)^{-\alpha}\right) \\ \mu_F = \frac{1}{d}\left(\log f(v,\alpha) + \frac{d^2\sigma^2}{2} - \frac{1}{2}\left(\log\left[\left(e^{d^2\sigma^2}-1\right)G(v,\alpha)+1\right]\right)\right) \\ \sigma_F = \sqrt{\frac{1}{d^2}\log\left[\left(e^{d^2\sigma^2}-1\right)G(v,\alpha)+1\right] + \sigma^2} \end{cases} \tag{5.10}$$

where d is a constant, $d\sigma$ is the standard deviation of the normally distributed variable $\log r_{ik}^{-\alpha} Y_{ik}$ and $G(v,\alpha) = \frac{\sum_{i\geq 1} r_{ik}^{-2\alpha}}{\left(\sum_{i\geq 1} r_{ik}^{-\alpha}\right)^2}$. After a experimental study of $G(v,\alpha)$, an exponential behavior has been exhibited and motivated the search for a non linear regression of the form [27]:

$$G(v,\alpha) = e^{\sum\limits_{i+j\leq 5} A_{i,j}(\log v)^i \alpha^j}. \tag{5.11}$$

The optimal coefficients $A_{i,j}$ are reported in [27] where the relative error between simulation and curve fitted expression does not exceed 3% for $K = \{1,3,4,7\}$ and path loss exponent ranging from $\alpha = 2.5$ to $\alpha = 4$. $G(v,\alpha)$ may be seen as the contribution of path loss ratios of interfering BS in shadowing environment for a given couple (K,α). The higher value of G, the higher interference caused by neighboring cells, in average.

From the above, SINR can be considered as log-normally distributed, and $\epsilon-$capacity is expressed as

$$\eta_{\mathrm{SE}}^{(\epsilon)} = \sup_R \left\{ R : 1 - Q\left(\frac{10\log_{10}\left(2^{KR}-1\right) - \mu_\gamma}{\sigma_\gamma}\right) \leq \epsilon \right\}. \tag{5.12}$$

From which the maximal rate R leading to the outage probability ϵ can be found to be equal to:

$$\eta_{\mathrm{SE}}^{(\epsilon)} = \frac{1}{K}\log_2\left(10^{\frac{\sigma_\gamma Q^{-1}(1-\epsilon)+\mu_\gamma}{10}}+1\right), \tag{5.13}$$

where Q and Q^{-1} are the Gaussian error function and its inverse. Fig. 5.2 reports the EE-SE tradeoff of a hexagonal network for a user located in the middle of the cell, i.e. $v = 0.5$ Fig. 5.2(a), and a user at cell-edge, i.e. $v = 0.85$ Fig. 5.2(b), and labeled on the frequency reuse factor and outage probability. The same general shape can be observed in shadowing environment compared to non-shadowing environment. However, even for

user not at the cell boundary, $K = 1$ is no longer optimal in terms of energy and spectral efficiencies, but $K = 3$ achieves higher values. For user on cell-edge, $v = 0.85$, optimal frequency reuse factor is 7. The achievable EE-SE also depends on the outage rate that system may tolerate, i.e. the higher outage probability, the higher energy and spectral efficiencies. However, it does not mean that outage has to be set at high value, because it leads to multiple errors.

Our contribution in that part was to propose a semi-analytical approach to assess the performance in terms of energy and spectral efficiencies of interference-limited hexagonal cellular network when shadowing is taken into account and has been published in [27]. The closed-form expressions available in literature, [26, 116] reveal not to be accurate for all frequency reuse factors and path loss exponents. However, the limits of the analysis are i) only one user has been considered to be active at a time, ii) outage EE-SE tradeoff does not take into account the fact that lost data may be eventually retransmitted to complete the service. Here we implicitly assumed that lost data are not recovered. This is the case for voice application for instance where a certain amount of loss can be tolerate. However, if one may want completely recover lost packets, then retransmission is needed impacting the energy-efficiency of the system.

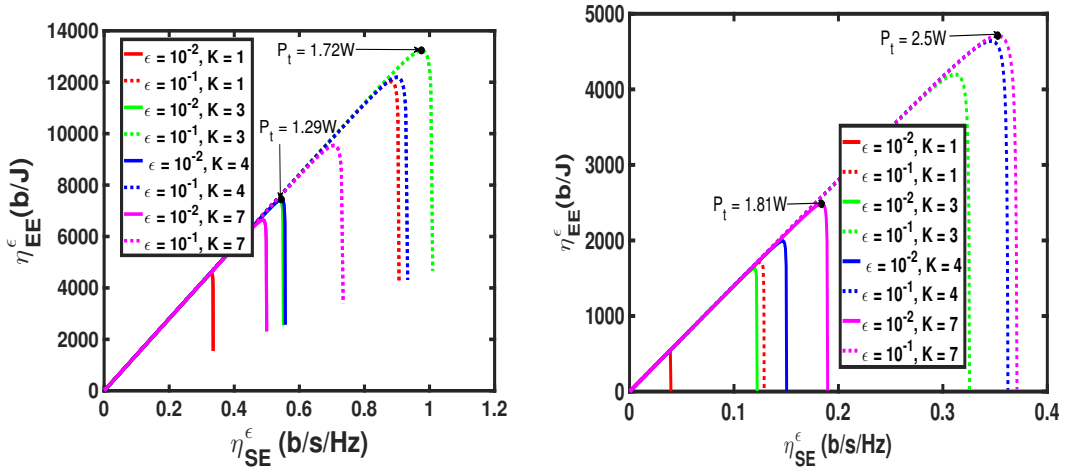

(a) $v = 0.5$ (b) $v = 0.85$

Figure 5.2 – EE-SE tradeoff with long term shadowing, labeled on frequency reuse factor K and outage probability ϵ [21].

In the next section, we explore the EE-SE tradeoff of randomly deployed BSs and users when multi-antenna is considered at BSs.

5.1.2 Randomly deployed networks

Due to the intractability of regular hexagonal model for predicting, without resorting with lengthly simulations, the performance of large cellular networks, another theoretical tool recently appeared for modeling large cellular deployment: stochastic geometry where BS deployment is considered as a spatial point process [28]. There is a lot of spatial point processes, see [117] for a compelling overview of point processes, the most common one being the homogeneous Poisson point process in $\mathbb{R}^2$ in which the number of points in a given area follows a Poisson law. A notable difference is that the area partitioning follows a general Voronoï tessellation and the cell shape is no longer regular [118]. In a

such tessellation, the cell size is not the same for all cells and becomes a random variable. The interest of such a model is the independency of BS locations, leveraging the average of a performance metric over network geometry. Typically, stochastic geometry allows to express the most relevant performance metrics, e.g. coverage probability, ergodic rate, as a function (generally an integral) of the Laplace transform of SINR at a given point of the network. Even if PPP does not correspond to a real deployment, hexagonal grid network neither and some authors showed that hexagonal model leads to optimistic performance predictions while PPP to more pessimistic predictions; experimental measurements being between both [28].

A point process can be viewed either as a *random countable set* or a *counting measure*, both being dual notions. In the first case, the point process is regarded as a random set $\Phi = \{x_1, x_2, \cdots\} \subset \mathbb{R}^d$ consisting of random variables x_i. In the other hand, point process can be characterized by counting the number of points falling in a subset $\mathcal{B} \subset \mathbb{R}^d$. This measure is denoted as $N(\mathcal{B})$ and is a random variable, e.g. Poisson distributed [117].

System model

A downlink multi-user multiple input single output (MU-MISO) cellular network is considered where BSs are equipped with M transmit antennas and users have a single receive antenna. BSs and users are modeled by two independent PPPs with density λ_b and λ_u respectively and users are connected to their nearest BS. All BSs have the same transmit power, which is equally divided among the active users in the cell. The whole system bandwidth is allocated to each user, and hence users experience both intra and inter-cell interferences. The linear power consumption model in (5.2) is used.

Rayleigh flat fading channels between BS and users are considered and perfect CSI is assumed to be available at each BS. The signal received by the k-th user from the typical 0-th BS is given by

$$y_k = \sqrt{\frac{P_t r_{0k}^{-\alpha}}{u_0}} \mathbf{h}_{0k}^H \mathbf{w}_{0k} x_{0k} + \sum_{(i,j)\in\mathcal{A}} \sqrt{\frac{P_t r_{ik}^{-\alpha}}{u_i}} \mathbf{h}_{ik}^H \mathbf{w}_{ij} x_{ij} + n_k, \tag{5.14}$$

where $\mathcal{A} = \big\{\{i,j\} \in \mathbb{N}^2 | i = 0 \wedge j \neq k \vee i \neq 0, \forall j\big\}$, r_{ik} is the distance between the i-th BS and the k-th user, $\{i,k\} \in \mathbb{N}^2$, u_i is the number of users in the i-th cell and n_k is the AWGN with zero mean and variance σ_n^2 for user k. Moreover, $\mathbf{h}_{ik} \sim \mathcal{CN}(0, \mathbf{I}_M)$ is an $M \times 1$ vector representing the complex Gaussian distributed channel between the i-th BS and the k-th user where $\mathbf{I}_M$ is an $M \times M$ identity matrix. In addition, $\mathbf{w}_{ij} \in \mathbb{C}^{M\times 1}$, x_{ij} are the precoding vector and the transmitted symbol respectively for the j-th user in the i-th cell with $\mathrm{E}[|x_{ij}|^2] = 1$. Note that $(\cdot)^H$ denotes the Hermitian (transpose-conjugate) operation.

Following the approach in [109], BSs are divided into subsets denoted as Φ_u, with $u \in [0, u_{\max}]$, and each BS in the subset Φ_u serves u users. The maximum number of users simultaneously served in a cell is limited to $u_{\max}$ in order to compare later with zero forcing (ZF) precoding. Of course the possible number of users in a cell is unbounded in PPP networks, however we assume that system chooses to serve at most $u_{\max}$ users in a resource block. The number of users in different cells is assumed to be independent, and each BS group Φ_u follows a homogeneous PPP distribution with density $\lambda_b p_N(u)$, where $p_N(u)$ is the probability mass function of the number of active users in a cell. The calculation of $p_N(u)$ requires the exact size distribution of the Poisson-Voronoi typical cell, which has been given in [119]. However, since the expression is challenging to numerically compute, a curve-fitted equation has been proposed in [120]. Using this equation, the

probability mass function of the number of active users in a cell can be expressed as in [109]:

$$p_N(u) = \begin{cases} \frac{\mu^\mu \Gamma(u+\mu)\rho^{-u}}{\Gamma(\mu)u!\left(\frac{1}{\rho}+\mu\right)^{u+\mu}} & 0 \leq u \leq u_{\max}-1 \\ \sum\limits_{n=u_{\max}}^{\infty} \frac{\mu^\mu \Gamma(n+\mu)\rho^{-n}}{\Gamma(\mu)n!\left(\frac{1}{\rho}+\mu\right)^{n+\mu}} & u = u_{\max} \end{cases} \tag{5.15}$$

where u is the number of users in a cell, $\mu = 3.5$ is a constant obtained through data fitting [120], $\rho = \frac{\lambda_b}{\lambda_u}$ is the BS-user density ratio, and $\Gamma(\cdot)$ is the gamma function. When $u \leq u_{\max} - 1$, u users are served by BS, while BS randomly chooses $u_{\max}$ users to serve when $u \geq u_{\max}$. Due to the limitation of active users to $u_{\max}$, their locations become correlated, which is very challenging to handle. In order to make the problem tractable, the simplifying assumption that the set of active users is the sum of independent PPPs with density $\lambda_b u p_N(u)$ with $u \in [1, u_{\max}]$ is made. Since the sum of independent PPPs is another PPP, the set of active users is considered as a PPP with density $\lambda_{au} = \sum_{u=1}^{u_{\max}} \lambda_b u P_N(u)$. The network is considered to be a circular disc of radius R_a, and total number of active users in this network is N_{au} which is a r.v. in a given area. However, the following asymptotic behavior holds $\lim\limits_{R_a \to \infty} N_{au}(R_a) = \lim\limits_{R_a \to \infty} \lambda_{au} \pi R_a^2$ when the network size grows to infinity.

Power received by the typical k-th user at distance r_{0k} from the 0-th BS is

$$P_{0k} = \frac{P_t}{u_0} r_{0k}^{-\alpha} \left| \mathbf{h}_{0k}^H \mathbf{w}_{0k} \right|^2, \tag{5.16}$$

where the close-in reference distance r_0 in (5.4) is one and $\left| \mathbf{h}_{0k}^H \mathbf{w}_{0k} \right|^2$ is the random channel power gain. By grouping the interfering BSs into subsets according to the number of users they have, SINR of the k-th user can be written as

$$\gamma(u_0) = \frac{\frac{P_t r_{0k}^{-\alpha}}{u_0} \left| \mathbf{h}_{0k}^H \mathbf{w}_{0k} \right|^2}{\sum\limits_{j \neq k} \frac{P_t r_{0k}^{-\alpha}}{u_0} \left| \mathbf{h}_{0k}^H \mathbf{w}_{0j} \right|^2 + \sum\limits_{u=1}^{u_{\max}} \sum\limits_{i \in \Phi_u \setminus \{0\}} \sum\limits_{j=1}^{u} \frac{P_t r_{ik}^{-\alpha}}{u} \left| \mathbf{h}_{ik}^H \mathbf{w}_{ij} \right|^2 + \sigma_n^2}. \tag{5.17}$$

According to Slivnyak's theorem [117], the set $\Phi_u \setminus \{0\}$ has the same statistics as Φ_u. At denominator, the first and second terms refer to the intra and inter-cell interferences respectively.

Scientific problem

As in Section 5.1.1, we are still interested in EE-SE tradeoff in case of random BS and users deployments. The ergodic spectral efficiency of a cell containing u_0 users is [121]

$$R_{\text{BS}}(u_0) = u_0 R_u(u_0), \tag{5.18}$$

where $R_u(u_0)$ is the ergodic rate of a typical user when there are u_0 active users in the cell. In this section, we talk about area spectral efficiency (ASE) per unit area (u.a.), in bits/s/Hz/u.a., defined as the ergodic rate of a cell, averaged over the number of active users in the cell, weighted by the BS point process intensity, that is to say:

$$\eta_{\text{ASE}} = \lambda_b \sum_{u_0=1}^{u_{\max}} u_0 R_u(u_0) p_N(u_0). \tag{5.19}$$

Three different random processes, i.e. two independent PPPs governing users and BSs locations, and fading channels are taken into account in the system model. To calculate the ergodic rate of the k-th user, we first average the rate over SINR conditioned on distance to the connected BS and then average over this random quantity. Therefore, the ergodic rate of the k-th user with u_0 users in the cell is

$$R_u(u_0) = \mathrm{E}_{r_{0k}}\left[\mathrm{E}_{\gamma}\left[\log_2\left(1+\gamma\left(u_0\right)\right)|_{r_{0k}}\right]\right], \tag{5.20}$$

where E_{γ} and $\mathrm{E}_{r_{0k}}$ denote the expectations over SINR, and the distance of the k-th user from the connected BS respectively. Calculation of (5.20) can be done using coverage probability [28] or moment generating function approaches [122]. Both these methods necessitate finding the distribution of the terms $\left|\mathbf{h}_{0k}^H\mathbf{w}_{0k}\right|^2$, $\left|\mathbf{h}_{0k}^H\mathbf{w}_{0j}\right|^2$ and $\left|\mathbf{h}_{ik}^H\mathbf{w}_{ij}\right|^2$, which are difficult to obtain.

We rather work on an upper bound of (5.20), by using Jensen's inequality on the expectation of γ only, that is to say:

$$R_u(u_0) \leq \mathrm{E}_{r_{0k}}\left[\log_2\left(1+\mathrm{E}_{\gamma}\left[\gamma(u_0)|_{r_{0k}}\right]\right)\right] = \hat{R}_u(u_0). \tag{5.21}$$

Upper bound of $R_u(u_0)$ is hence obtained with

$$\hat{R}_u(u_0) = \int_{r_{0k}\geq 0}^{\infty} \log_2\left(1+\mathrm{E}_{\gamma}\left[\gamma\left(u_0\right)|r_{0k}\right]\right) f_{r_{0k}}(r_{0k})dr_{0k}, \tag{5.22}$$

where $f_{r_{0k}}(r_{0k})$ is the probability density function of the distance of the k-th user from its connected BS, and is given by [28]

$$f_{r_{0k}}(r_{0k}) = e^{-\lambda_b\pi r_{0k}^2}2\pi\lambda_b r_{0k}. \tag{5.23}$$

With (5.22), an upper bound of ASE can be written as

$$\hat{\eta}_{\mathrm{ASE}} = \lambda_b \sum_{u_0=1}^{u_{\max}} u_0\hat{R}_u(u_0)p_N(u_0). \tag{5.24}$$

Once an expression for ASE has been obtained, EE can be easily upper-bounded with

$$\hat{\eta}_{\mathrm{EE}} = \frac{\hat{\eta}_{\mathrm{ASE}}}{P_A}, \tag{5.25}$$

where P_A is the average power consumption per unit area given by

$$P_A = \lambda_b\left(1-p_N\left(0\right)\right)\left(aP_t + MP_{\mathrm{RF}}\right) + \lambda_b c \tag{5.26}$$

where $1-p_N\left(0\right)$ is the activity probability for a BS, i.e. probability that the cell at least contains one user. Only non-transmission power is taken into account for inactive BSs, i.e. $\lambda_b c$.

We aimed at obtaining computable expressions for $\hat{\eta}_{\mathrm{EE}}$ and $\hat{\eta}_{\mathrm{ASE}}$ when considering signal to leakage plus noise ratio (SLNR) as precoding vector and comparing this with Monte-Carlo simulations.

Related works

Research on precoder maximizing the downlink network sum rate subject to a transmit power constraint receives a lot of attention during past decades. Such precoder is generally the solution of a complex non-convex problem that is not even known for situation with multi-cell interference [123]. Therefore linear precoding techniques, e.g. maximum ratio transmission, ZF, SLNR, MMSE are also of interest [124, 125]. Although the ZF precoder nulls the intra-cell interference [109–111], it is not designed to limit the inter-cell interference. Moreover, the ZF precoder imposes a restriction on the minimum number of transmit antennas at BS [126]. A generalized MMSE precoder for downlink multicell MU-MISO systems considering different average SNRs of users has been proposed in [127]. The authors have shown that MMSE achieves higher throughput compared to other linear precoders by performing Monte Carlo simulations. However, evaluating the performance of MMSE precoder is generally difficult to handle theoretically.

Authors in [128] have proposed SLNR as an optimization metric for designing precoder. SLNR does not impose any restriction on the number of BS antennas in contrast to ZF solution and moreover noise is considered. However, the previous works based on SLNR do not consider a multi-cell environment and also ignore the network geometry while computing the SLNR precoder solution [126,128–130]. The MMSE and SLNR precoders have been proved to be equivalent under symmetric scenario, i.e. all channels between BS and users have the same average gain [123, 129]. Although the network geometry is non-symmetric in this work, SLNR precoder has been considered mainly for its tractability.

Stochastic geometry has been intensively used for cellular network performance analysis during the past decade with the work of Baccelli, Andrews or Haenggi among others [28, 131]. An important amount of works has used stochastic geometry with maximum ratio transmission or ZF precoder, mainly for their tractability, to study network performance metrics such as ASE or EE [109, 132, 133] or coverage probability [110, 111].

Our contribution in this part has been to investigate the performance of the SLNR precoder in terms of EE-ASE tradeoff for MU-MISO cellular network with random topology taking into account non-homogeneous average SNR due to the large scale fading, i.e. path loss, and also the interference created on the other-cell users. In particular, we proposed an analytical expression of the average SINR received by a user conditioned on its distance to BS.

Results

Finding the expression of SLNR precoder is much easier than MMSE precoder, mainly because the precoder weights for a given user do not depends on the precoder of other cells which is not the case for MMSE precoder for instance. The optimal weights maximizing the receive signal power for a user over the leakage power to all other users in the network are obtained by solving:

$$\begin{aligned}\mathbf{w}_{0k} = &\arg \max_{\mathbf{w}_{0k}\in\mathbb{C}^{M\times 1}} \frac{\mathbf{w}_{0k}^H \mathbf{h}_{0k}\mathbf{h}_{0k}^H \mathbf{w}_{0k}}{\mathbf{w}_{0k}^H \left(\bar{\mathbf{H}}_{0k}\bar{\mathbf{D}}_{0k}\bar{\mathbf{H}}_{0k}^H + \frac{\sigma_n^2 u_0}{P_t}\mathbf{I}_M\right)\mathbf{w}_{0k}} \\ &\text{subject to } \mathrm{E}\left[\|\mathbf{w}_{0k}\|^2\right] = 1.\end{aligned} \tag{5.27}$$

where $\bar{\mathbf{H}}_{0k} = \left[\mathbf{h}_{01}, \cdots, \mathbf{h}_{0(k-1)}, \mathbf{h}_{0(k+1)}, \cdots, \mathbf{h}_{0N_{au}}\right]$ represents the concatenated fading channels and $\bar{\mathbf{D}}_{0k} = \mathrm{diag}\left(r_{01}^{-\alpha}, \cdots, r_{0(k-1)}^{-\alpha}, r_{0(k+1)}^{-\alpha}, \cdots, r_{0N_{au}}^{-\alpha}\right)$ is a square diagonal matrix filled by the path losses from the 0-th BS to active users in the network, except the

k-th user. Generally an instantaneous power constraint is imposed on precoder's weights rather than an average power constraint as it is formulated in (5.27). This has been chosen for analytical tractability in the derivation of the average SINR [29]. However, our results are derived for very large number of antennas, i.e. M, and in that case the solution of (5.27) tends toward the same value than the solution of (5.27) but imposing an instantaneous power constraint.

Using the generalized Rayleigh quotient theorem [134], the solution of (5.27) can be proved to be the eigenvector corresponding to the maximum eigenvalue of the matrix $\left(\bar{\mathbf{H}}_{0k}\bar{\mathbf{D}}_{0k}\bar{\mathbf{H}}_{0k}^{H}+\frac{\sigma_n^2 u_0}{P_t}\mathbf{I}_M\right)^{-1}\mathbf{h}_{0k}\mathbf{h}_{0k}^{H}$ which can be written as

$$\mathbf{w}_{0k}=\frac{\left(\bar{\mathbf{H}}_{0k}\bar{\mathbf{D}}_{0k}\bar{\mathbf{H}}_{0k}^{H}+\frac{\sigma_n^2 u_0}{P_t}\mathbf{I}_M\right)^{-1}\mathbf{h}_{0k}}{\sqrt{\mathrm{E}_{\bar{\mathbf{H}}_{0k},\bar{\mathbf{D}}_{0k},\mathbf{h}_{0k}}\left[\left\|\left(\bar{\mathbf{H}}_{0k}\bar{\mathbf{D}}_{0k}\bar{\mathbf{H}}_{0k}^{H}+\frac{\sigma_n^2 u_0}{P_t}\mathbf{I}_M\right)^{-1}\mathbf{h}_{0k}\right\|^2\right]}}. \tag{5.28}$$

We now state our main result in this part on asymptotic average SINR for the typical user in Theorem 4, just after the condition under which the asymptotic analysis holds.

Definition 4 (Asymptotic regime) *Let R_a be the radius of the circular area centered at BS of interest and $\gamma_{au}\in\mathbb{R}^+$ a constant. The asymptotic regime (a.r.) refers to the condition $\lim_{N_{au},M\to+\infty}\frac{N_{au}}{M}=\gamma_{au}$ with $N_{au}\left(R_a\right)\underset{\infty}{\sim}\lambda_{au}\pi R_a^2$ and will be referred as $\overset{a.r.}{\sim}$.*

Theorem 4 (Asymptotic average SINR) *Let a cellular network being made with two independent PPPs for BSs and users deployments with λ_b and λ_u as respective density. Let consider that each BS implement an SLNR precoder with M antennas, then the average SINR in asymptotic regime experienced by user k in a cell with u_0 users, conditioned on BS-user distance, can be expressed as:*

$$\mathrm{E}_{\gamma}\left[\gamma(u_0)|r_{0k}\right]\overset{a.r.}{\sim}\frac{\frac{P_t r_{0k}^{-\alpha}}{u_0}\left(1+\frac{M\bar{m}_{0k}^2(z)}{m'_{0k}(z)}\right)}{\frac{P_t r_{0k}^{-\alpha}\frac{(u_0-1)}{u_0}}{\left(1+M^{\frac{\alpha}{2}}r_{0k}^{-\alpha}\bar{m}_{0k}(z)\right)^2}+\sum_{u=1}^{u_{\max}}\left(f_1(u)-f_2(u,r_{0k})\right)+\sigma_n^2}. \tag{5.29}$$

where $\bar{m}_{0k}(z)$, $m'_{0k}(z)$ are Stieltjes transform and its derivative [135] of the asymptotic distribution of eigenvalues of the random matrix $\frac{1}{M}\bar{\mathbf{H}}_k M^{\frac{\alpha}{2}}\bar{\mathbf{D}}_k\bar{\mathbf{H}}_k^H$, $z=-\frac{M^{\frac{\alpha}{2}-1}\sigma^2 u_0}{P_t}$, f_1 and f_2 are two functions that depend on λ_b, α and $p_N(u)$.

The complete proof of Theorem 4 can be found in [29]. The Stieltjes transforms used in (5.29) can be obtained as unique solution of an equation involving hypergeometric functions, as it has been described in [136] in another context. An upper bound on ergodic rate in asymptotic regime can be computed substituting (5.29) in (5.22) and EE-ASE tradeoff follows using (5.24) and (5.25). There is no closed-form for the integral in (5.22) and the evaluation of (5.29) seems cumbersome. However, this is simply a numerical evaluation of a single integral which requires much less computation resources than Monte-Carlo simulations.

Figs. 5.3(a), 5.3(b) and 5.3(c), 5.3(d) show the behavior of ASE and EE w.r.t. the transmit power P_t labeled on BS-user density ratio and number of antennas respectively. Figs. 5.3(e) and 5.3(f) illustrate the EE-ASE tradeoff for different BS-user density ratios and number of antennas respectively. The values obtained with simulations are compared

with that ones computed with our theoretical result given above. Power consumption of micro BS with multiple antennas is considered, i.e. $P_{\text{RF}} = 35$ W, $c = 34$ W and $a = 3.125$ [132, 137] and α and σ_n^2 are set to 4 and -97.5 dBm respectively. We set $N_u = 5000$ except for the case $\rho = 0.1$, where $N_u = 2500$ was used to reduce the simulation time. Besides, $u_{\max}$ and λ_u are equal to M and $5 \cdot 10^{-4}$ m^{-2} respectively.

First, in all plots in Fig. 5.3, on can remark the very good match of the analytical upper-bound proposed in our analysis w.r.t. simulations despite the use of Jensen's inequality. Second, despite the fact that the analytical expressions for ASE and EE developed from Theorem 4 hold theoretically in asymptotic regime, on may observe a very good match with simulations for M and N_{au} as small as 10 and 2500 respectively, i.e. the maximum value of the relative error does not exceed 3%. The fact that the upper-bounds on ASE and EE using Jensen's inequality provide relatively good match between analytical and simulation results teaches us something: the average performance of large area network is more governed by network topology rather than small scale fading.

The EE-ASE curves in Figs. 5.3(e) and 5.3(f) have a large linear part before a sharp decrease when ASE is increased, as also observed in Section 5.1.1 for hexagonal network for basically the same reasons. Figs. 5.3(a), 5.3(d) and Figs. 5.3(c), 5.3(d) enlighten the EE-ASE curves. Indeed, ASE converges toward a limit when $P_t \to \infty$ while the power consumed per unit area increases without limit. This causes the sharp decrease of EE when P_t is very large in EE-ASE tradeoff curves. The particular value of P_t at which ASE is saturating, depends on the network parameter taken for simulations. Basically, the simulated network corresponds to a (very) low user density area, i.e. 500 users per kilometer square, which is about one and half order of magnitude less than Paris for instance. This choice comes from the very long simulation time needed to run larger network but our results are of course applicable to higher user and BS densities. For the set of parameters taken in this study, one can remark that increasing the BS density, i.e. increasing ρ under fixed λ_u, or increasing the number of antennas, i.e. M, are always beneficial for ASE while keeping the same global EE. However, extreme values of parameters are not necessarily always the optimal choice as it can be observed in Fig. 5.4 where the relative achievable EE-ASE using SLNR and ZF precoders are compared. The ZF precoder used in [109] is implemented as follows

$$\mathbf{w}_{0k} = \frac{[\mathbf{G}_0]_k}{\|[\mathbf{G}_0]_k\|}, \tag{5.30}$$

where $[\mathbf{G}_0]_k$ is the k-th column of $\mathbf{G}_0$ where

$$\mathbf{G}_0 = \mathbf{H}_0 \left[\mathbf{H}_0^H \mathbf{H}_0\right]^{-1}, \tag{5.31}$$

and $\mathbf{H}_0 = [\mathbf{h}_{01}, \cdots, \mathbf{h}_{0k}, \cdots, \mathbf{h}_{0u_0}] \in \mathbb{C}^{M \times u_0}$.

When increasing ρ while keeping $M = 30$ constant, does not lead to an amelioration of EE. Indeed, the static power consumption in RF chains becomes important and increasing the BS density certainly increases ASE but not EE. Same observations when increasing the number of antennas while keeping BS density at a high value, e.g. $\rho = 0.1$. Moreover, ZF performs worse than SLNR due to the nature of the precoder which does not operate an automatic gain control but searches for orthogonalizing the equivalent channel between BS and users. This is done at the cost of desired signal power at user k, resulting in a lower SINR than the one obtained with SLNR. However, ZF precoder is computationally less complex than SLNR which requires to have CSI of *all users at BS of interest*. One can imagine to reduce the complexity by taking into account just the closest cells to the cell of

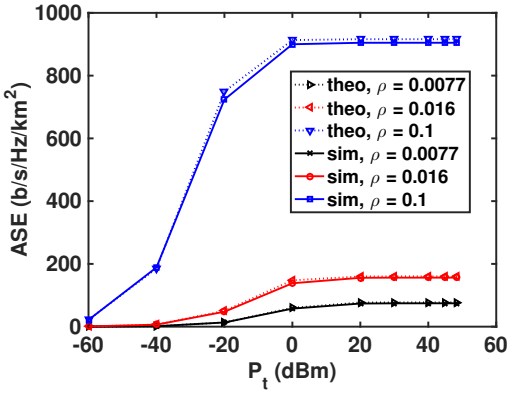

(a) ASE vs P_t, $M = 10$, $\lambda_u = 5 \cdot 10^{-4}\text{m}^{-2}$

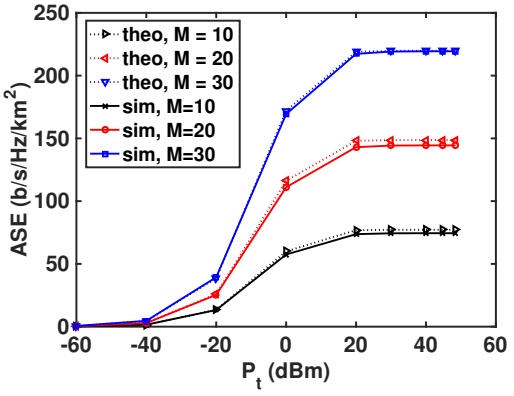

(b) ASE vs P_t, $\rho = 7.7 \cdot 10^{-3}$, $\lambda_u = 5 \cdot 10^{-4}\text{m}^{-2}$

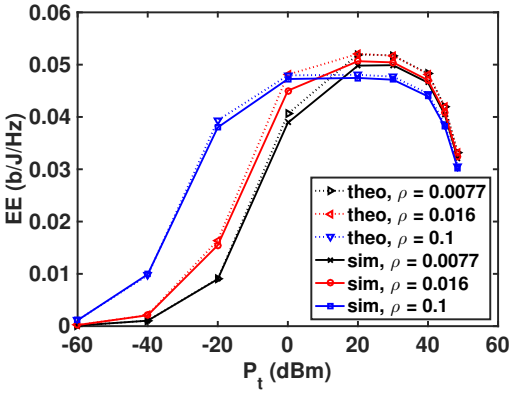

(c) EE vs P_t, $M = 10$, $\lambda_u = 5 \cdot 10^{-4}\text{m}^{-2}$

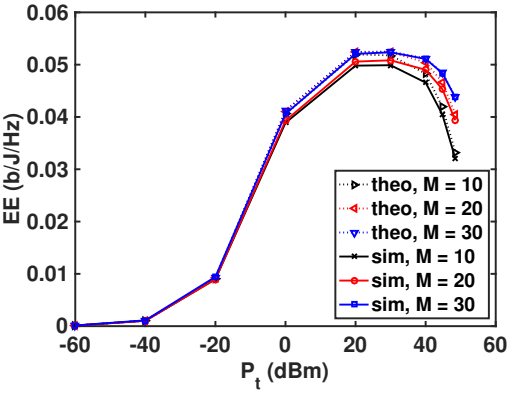

(d) EE vs P_t, $\rho = 7.7 \cdot 10^{-3}$, $\lambda_u = 5 \cdot 10^{-4}\text{m}^{-2}$

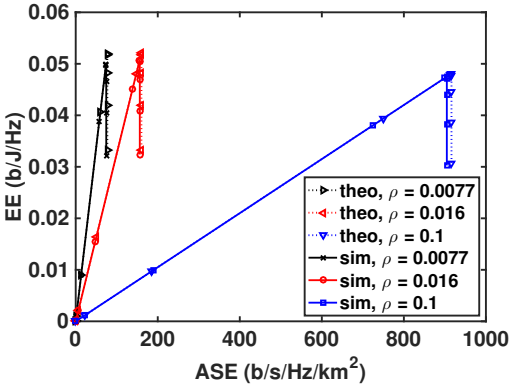

(e) EE vs ASE, $M = 10$, $\lambda_u = 5 \cdot 10^{-4}\text{m}^{-2}$

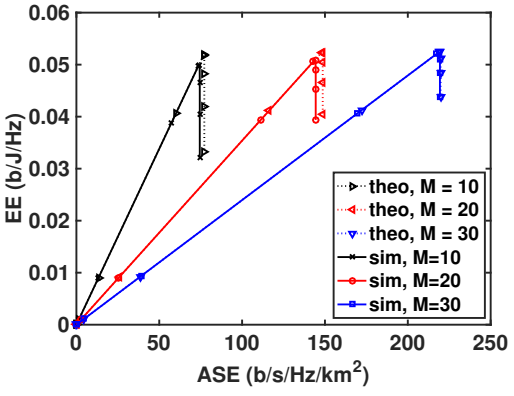

(f) EE vs ASE, $\rho = 7.7 \cdot 10^{-3}$, $\lambda_u = 5 \cdot 10^{-4}\text{m}^{-2}$

Figure 5.3 – ASE, EE characteristics w.r.t. P_t and EE-ASE tradeoff labeled on ρ and M [21]

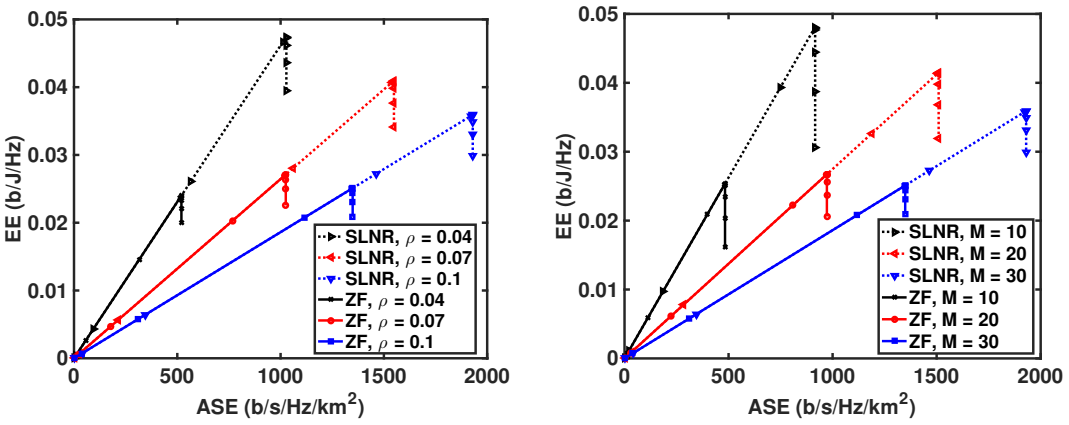

(a) $M = 30$, $\lambda_u = 5 \cdot 10^{-4}\text{m}^{-2}$ (b) $\rho = 0.1$, $\lambda_u = 5 \cdot 10^{-4}\text{m}^{-2}$

Figure 5.4 – Comparison of EE-ASE tradeoff achieved with SLNR and ZF precoders [21]

interest for start and a scheme that listens other-cells terminals when communicating to their respective BS in order to estimate the channel between them and the cell where SLNR precoding has to be done. This can be envisaged only if a certain cooperation between cells is possible.

5.1.3 Summary

Finally, the global behavior of EE-ASE characteristic that has been obtained is the same either considering hexagonal network or random deployment with stochastic geometry, which is logical after all. The difference lies in the methodology where generally, stochastic geometry allows to investigate much more complex scenarii than hexagonal model, at a given cost. This claim is supported by several fundamental theorems of stochastic geometry, e.g. Slivnyak's and Campbell's theorems, which allow to average a network statistic, e.g. SINR, over network realizations and declare that the measured performance metric, e.g. coverage probability, is representative on what happens on the entire network. We have seen that obtaining the EE-SE tradeoff in hexagonal network without resorting to Monte-Carlo simulations, for different set of parameters, e.g. frequency reuse factor, requires a parametric expression of ISR obtained with a curve fitting approach, limiting the universality of expressions. Moreover, the analysis has been done considering only one active user at a time. It is worth noting that is an hypothesis implicitly done in the earlier works in stochastic geometry [28,117], and not sufficiently stated from my personal point of view. Indeed, BSs are considered working in best effort and without considering other users in the cell. In real networks, the transmitted power at each BS depends on the number of users in the cell, which is not uniform, and the resource provisioning should differentiate users at cell-edge than users located close to their BS.

In our work on randomly deployed networks, we dealt with multi-users in each cell however this study did not take into account that adjacent cells may provide different power allocation according to the number of users and their positions in the cell. This is masked by assuming that power is equally divided among users in the cell and the transmitted power at each BS is the same which is not the case in real scenario. A first step toward considering different transmit powers of adjacent cells in PPP has been achieved in [138] where K tiers PPP network is considered and randomly deployed users are separated into cell-edge users and non cell-edge users. Different power allocations are then considered

according to the typical user position: in cell-edge or not. However, to fully addressed the problem of resource allocation in multi-user randomly deployed networks, the joint distribution of a given statistic, e.g. SINR, in a cell should be derived, which is a particular difficult problem, but that deserves to be addressed in the future.

5.2 Machine learning for green communications

5.2.1 Introduction and definitions

In the Cominlabs project framework, I had the opportunity to collaborate with Prof. Christophe Moy from CentraleSupélec Rennes, on reinforcement learning for cognitive radio and networks by co-supervising the PhD work of Navikkumar Modi [22]. The previous studies lead by the team SCEE on cognitive radio have been first focused on reconfiguration issues for software defined equipments and then on reinforcement learning for the OSA problem. In this problem, a set of secondary, or cognitive, users attempts to opportunistically access the licensed bands, i.e. frequencies paid by the operator for its users, when those are not used. In particular, the work of Wassim Jouini dealt with UCB algorithms, a kind of reinforcement learning (RL) policy, to learn the spectrum usage of primary users (PUs) in the network [139]. The available frequency bands are modeled with MAB framework where arms, a.k.a. frequency bands[3], are modeled as a random process with two states, occupy or available.

The goal of any machine learning policy is to learn some statistical characteristics of a process through regular observations of the process output and by taking actions that modify the process output. Fig. 5.5 illustrates the RL concept, where a player observes a state of the environment and gets reward according to the action the player provided on the environment in the previous time instant.

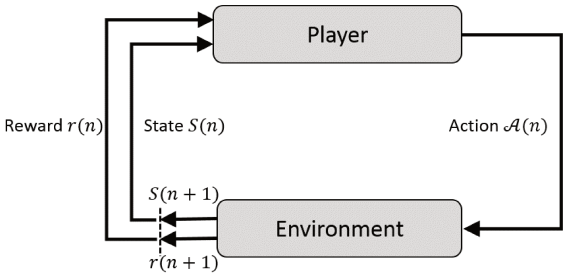

Figure 5.5 – Reinforcement learning principle [22]

Performances of RL algorithms are analyzed with two criteria: convergence and regret [140]. The former is the guarantee that the learning algorithm, at the end, finishes to play *almost* always the optimal arm, and the latter measures the speed at which the convergence is achieved and is defined as the difference between the expected reward obtained using a full knowledge strategy and the selected learning algorithm and will be formally defined in the next section.

When one tries to make a machine learn some random process characteristics on a given problem, one may ask in a first place: *is there something to learn?* This question can be re-formulated as: *does a given policy make better than a random choice on the actions?* Once a policy has been decided for a given problem, this convergence should be proved formally and its regret characterized. In this research work, a contribution has been provided on these issues: i) for OSA scenario, an alternative to the Lempel-Ziv complexity [141], named optimal armed identification factor has been proposed which is more suitable to describe which scenario, in terms of channel occupancy probabilities, is *a priori* favorable for applying a learning algorithm. ii) In OSA and multiple secondary

3. The terms *arm* and *band* refer to the same thing, the latter being related to the application context of the former, and could be interchangeably used in the following.

users (SUs) context, we proposed a RL policy, based on UCB, that takes into account not only the channel availability as a reward but also its quality. Although several previous works have also dealt with channel quality, see the state of the art below, our contribution separately weights the availability and quality of the channel in the learning process. This is of particular importance in CR framework where these both characteristics may be wanted to be separated. The logarithmic behavior of the regret has been assessed theoretically and the achievable data rate of the proposed policy numerically compared to existing algorithms in literature demonstrating the interest of the proposed method. iii) We then modified and applied the proposed policy to the problem of maximizing the network energy efficiency by turn OFF underloaded BSs in order to save energy. All these contributions will not be summarized hereafter, but I will rather focus on the main results in OSA scenario and optimal BS deployment problems.

5.2.2 RL policy for multi-user OSA problem

Problem statement

Let us consider a set of K independent channels, i.e. $\mathcal{K} = \{1, \cdots, K\}$, belonging to a primary network and a set of U SUs, i.e. $\mathcal{U} = \{1, \cdots, U\}$ attempting to access the primary spectrum when no PU uses it, and $K \geq U$. Hence, to be allowed to access a particular band an SU must declare, after a sensing process, the band available or not. Several sensing techniques have been studied in literature, from the simplest energy detector to signal classifiers [142, 143] all with different characteristics. Whatever the detector considered, a hard decision has to be taken in order to decide if the band is free or not. However, the soft metric measuring the energy level in the band can be recorded and may serve to rate the quality of a given channel. Due to the frequency reuse factor and partial utilisation of the frequency band i by PUs in the neighboring cells, the interference level is not the same for all bands which leads to a varying quality according to the band considered. Figure 5.6 illustrates the OSA problem with two possible channel qualities associated to a free channel state, i.e. low and high. It is worth noting that channel quality may be associated to the real SINR, or any other metric, experienced by the point-to-point secondary communication for instance, the results in this part would remain valid.

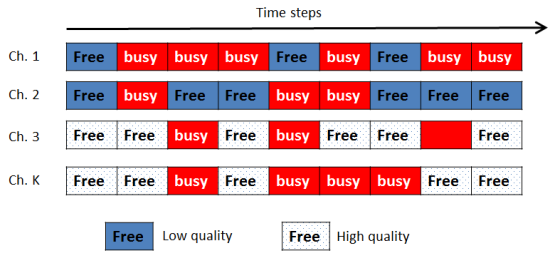

Figure 5.6 – Opportunistic spectrum access problem with different channel qualities [144]

In our work, we considered Markovian MAB framework, where each band is modeled as an aperiodic, irreducible and discrete time Markov chain with two states, i.e. occupy and free. For a band i, user j, the evolution of the associated Markov chain is according to the transition probability matrix $P^{i,j} = \left\{p_{kl}^{i,j}, k, l \in \mathcal{S}^{i,j}\right\}$, where $p_{kl}^{i,j}$ is the $i-$th band's transition probability for user j from state k to state l and $\mathcal{S}^{i,j}$ is the state space of band i and user j. In the following, we assume that state space and transition probability matrices

are the same for all users and so will not be indexed w.r.t. users. Each Markov chain is independent from each other and $\boldsymbol{\pi}^i$ is the stationary distribution of the $i-$th Markov chain with $\pi_q^i(n) = \pi_q^i \ \forall n, \forall q \in \mathcal{S}^i$.

Let a learning policy be defined as a one-to-one mapping $\mathcal{A}$ such as at each time n, a channel i is selected:

$$\begin{array}{rccc} \mathcal{A} : & \mathbb{N} & \longrightarrow & \mathcal{K} \\ & n & \longmapsto & i \end{array}$$

At time slot n, player $j \in \mathcal{U}$ selects a band $i \in \mathcal{K}$ according to some policy $\mathcal{A}$, assuming to be the same for all users. Once band i has been selected by player j at time n, the user collects the random reward $r_q^{i,j}(n)$ associated to the state $q \in \mathcal{S}^i$. The mean reward $\mu_{i,j}$ of the $i-$th band for user j is the expectation of the random variable $r_q^{i,j}(n)$:

$$\mu_{i,j} = \mathrm{E}\left[r_q^{i,j}(n)\right] = \sum_{q \in \mathcal{S}^i} r_q^{i,j} \pi_q^i \tag{5.32}$$

where the process is assumed to be stationary at wide sense. Without loss of generality, let assume that $\mu_{1,j} > \mu_{2,j} > \cdots > \mu_{K,j}, \forall j \in \mathcal{U}$. The regret notion allows to evaluate the gap, in the long run, of a given policy $\mathcal{A}$ to an ideal policy selecting the best channel all the time. The cumulative regret is the summation of the regret for all users:

$$\Phi^{\mathcal{A}}(n) = n \sum_{j=1}^{U} \mu_j - \sum_{j=1}^{U} \sum_{t=1}^{n} \mathrm{E}^{\mathcal{A}} \left[r_{q_{\mathcal{A}(t)}}^{\mathcal{A}(t),j}(t) \right]. \tag{5.33}$$

Since $U \leq K$, μ_j should be understood as the best average reward that could be obtained for user j on the set of channels. Moreover $\mathrm{E}^{\mathcal{A}}$ is the expectation given the policy $\mathcal{A}$ and $q_{\mathcal{A}(t)}$ is the state observed by using the policy $\mathcal{A}$ at time t. Bands whose mean rewards are strictly less than μ_j are referred as suboptimal bands. The goal of any RL policy is to minimize the regret in (5.33).

In Markovian framework, arm is considered having two modes, i.e. *active* and *passive*. An arm is referred as in active mode if it is selected by a player at current time step, otherwise it is in passive mode. Markovian MAB problems are further classified in rested and restless:

— **Rested Markovian MAB:** The state of only active arm evolves according to a Markov process. However the state of arms which are in passive mode remains frozen, i.e. it does not change [31, 145].

— **Restless Markovian MAB:** State of each arm evolves dynamically following unknown stochastic processes no matter it is played or not, and state evolution of arms in passive mode is independent of the player's actions [146, 147].

In OSA scenario, rested MAB is not a valid assumption. Indeed, PUs' activity is an independent process from SUs actions and hence channel states evolve even if frequency bands are not played by SUs, making restless hypothesis more adapted to OSA context. In this research, we aimed at proposing a RL policy able to learn which bands are the best in terms of availability and quality as well.

Related works

OSA scenario has been addressed with several different tools and models. In [148, 149], authors utilized UCB1 policy, initially proposed in [150], as a MAB learning algorithm in OSA scenario considering only one SU and i.i.d. rewards. Then come contributions on multiple SUs and other distributions for rewards. In [151], the authors tackled the problem

of MAB with Markovian rewards, which is a model particularly relevant for OSA scenario because the probability to observe a free band at a given time probably depends on the state of the band at the previous time instant. However, the study was limited to a single player. The multiplayer case has been addressed under different strategies, e.g. stochastic games [152, 153], or Q-learning e.g. [154, 155] but their theoretical performances are barely addressed. The authors in [156] have studied the multi-users OSA scenario under imperfect sensing tasks and proved that the distributed algorithm achieves logarithmic regret order like the centralized policy. The multiplayer Markovian MAB problem has been dealt with in [147, 157] by considering the rested and restless cases and centralized and distributed learning settings as well.

A certain amount of works dealing with continuous rewards rating the quality of the secondary network communications can be reported. The authors of [158, 159] have considered the problem of access the channel that gives the best data rate when the sates of the bands are i.i.d. and Gilbert-Elliot distributed, i.e. Markovian. The proposed policy is index-based and achieves logarithmic order regret but applies for single user. In [159], the authors considered reward as a combination of both channel quality (data rate) and availability statistics, defined as:

$$r^i(n) = (1 - S^i(n))R^i(n),$$

where $S^i(n)$ is the observed state of channel i and R^i is a reward function associated to throughput for instance. Recently, the authors in [33] modeled the OSA problem with a partially observable Markov decision process which considers channel quality along with availability statistics to decide about the channel to sense. However, there is no theoretical guarantee on the convergence of proposed policies.

In all these works, channel quality and availability have not been considered separately. On the contrary, we considered them as separate rewards with "tunable" coefficients for learning process. In wireless communication field, the separation of both functionalities, i.e. availability and quality, is necessary for applications where a certain level of QoS is requisite. Indeed, by separating the engine on the decision and on the quality, we can choose to emphasize on one or the other criterium.

RL policy for OSA taking into account channel quality

We define the global mean reward taking into account channel quality as in (5.32) with $r_q^{i,j} = qG_q^{i,j}$ such that

$$\mu_{i,j} = \sum_{q \in \mathcal{S}^i} qG_q^{i,j}\pi_q^i \tag{5.34}$$

where

$$G_q^{i,j}(T^{i,j}(n)) = \frac{1}{T^{i,j}(n)} \sum_{k=1}^{T^{i,j}(n)} R_q^{i,j}(k) \tag{5.35}$$

denotes the empirical mean of quality observations $R_q^{i,j}$ collected from band i by SU j in state q, $T^{i,j}(n)$ denotes the total number of times band i has been sensed up to time n by SU j. Furthermore, the band quality $R_q^{i,j}$ is rated according to the interference temperature recorded on it and it is assumed to be stationary in wide sense. Finally, q is the value of the state S^i of band i taken as the reward of the state, i.e. 0 or 1 according band i is occupy or free respectively. The global mean reward can be seen as a weighting of the channel availability reward by a random variable reflecting its quality, i.e. $G_q^{i,j}$.

A slotted frame structure is considered for cognitive users as illustrated in Fig. 5.7. The interest of index-based learning policies is that they do not consume bandwidth, since this phase can be done in parallel of transmission. Indeed, in CR context, transmission opportunities are exploited once a free channel is detected, irrespective to the fact that the channel is, in average, the best channel or not.

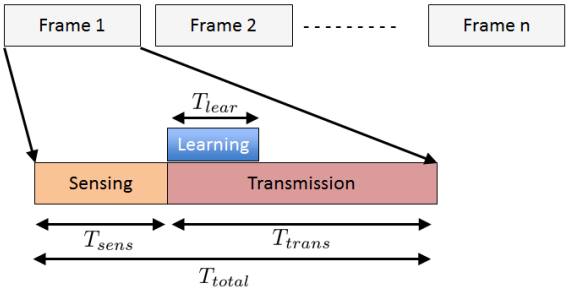

Figure 5.7 – Slotted frame structure for SUs with sensing, learning and transmission phases [22]

The spectrum sensing part of user j should decide between two hypothesis if channel i is free or not:

$$\mathcal{H}_0^j : y_{q_0}^{i,j}[m] = p^i[m] + u^{i,j}[m], \tag{5.36}$$

$$\mathcal{H}_1^j : y_{q_1}^{i,j}[m] = u^{i,j}[m] \tag{5.37}$$

where, $p^i[m]$ and $u^{i,j}[m]$ are the PU signal in the $i-$th channel and noise component in the $i-$th channel seen by SU j, respectively. These signals are assumed to be zero mean i.i.d. random processes with variance $\mathrm{E}[|p^i[m]|^2] = \sigma_{p,i}^2$ and $\mathrm{E}[|u^{i,j}[m]|^2] = \sigma_{u,i,j}^2$ respectively. The signal $u^{i,j}[m]$ counts for the other cells interference and background noise assumed to be gaussian distributed and independent from the primary users' signal p^i. Theoretically, SU should transmit only when no PU occupies channel i. However, it may miss the detection of a primary user and transmits anyway. Under both hypothesis $\mathcal{H}_0^j$ and $\mathcal{H}_1^j$, the received signal at SU Rx when SU Tx transmits is

$$\mathcal{H}_0 : z_{q_0}^{i,j}[m] = s^{i,j}[m] + p^i[m] + u^{i,j}[m], \text{ under } P_{\mathrm{md}} \tag{5.38}$$

$$\mathcal{H}_1 : z_{q_1}^{i,j}[m] = s^{i,j}[m] + u^{i,j}[m], \text{ under } 1 - P_f \tag{5.39}$$

with $s^{i,j}[m]$ being the signal of SU j, zero mean and i.i.d. with variance $\mathrm{E}[|s^{i,j}[m]|^2] = \sigma_{s,i,j}^2$. P_{md} in (5.38) means the probability of miss detection and P_f in (5.39) is the false alarm probability. If a miss detection occurs in the $i-$th channel, SU j transmits under SINR $\Gamma_0^{i,j} = \sigma_{s,i,j}^2 / \left(\sigma_{p,i}^2 + \sigma_{u,i,j}^2\right)$. On the other hand, if channel i is available, SU j transmits under SINR $\Gamma_1^{i,j} = \sigma_{s,i,j}^2 / \sigma_{u,i,j}^2$.

The average achievable throughput of SU j in the $i-$th channel, $\Xi^{i,j}$, is given by the sum of the achievable throughput under $\mathcal{H}_0^j$ and the achievable throughput under $\mathcal{H}_1^j$, which can be written as:

$$\Xi^{i,j} = \frac{T_{\mathrm{total}} - T_{\mathrm{sens}}}{T_{\mathrm{total}}} \left(\pi_{q_0}^i C\left(\Gamma_0^{i,j}\right) P_{\mathrm{md}} + \pi_{q_1}^i C\left(\Gamma_1^{i,j}\right)(1 - P_f)\right), \tag{5.40}$$

where $C(\Gamma)$ denotes the channel capacity with SINR Γ, i.e. $C(\Gamma) = \log_2(1+\Gamma)$. Hence, $C\left(\Gamma_1^{i,j}\right)$ is the achievable rate in the $i-$th channel without any PU and $C\left(\Gamma_0^{i,j}\right)$ is the

achievable rate in the $i-$th channel when a PU has not been detected. The achievable throughput under hypothesis $\mathcal{H}_1$ is hence $C\left(\Gamma_1^{i,j}\right)$ multiplied by the probability channel i is available, i.e. $\pi_{q_1}^i$, and the probability not to generate a false alarm, i.e. $1-P_f$. On the other hand, the achievable throughput under $\mathcal{H}_0$ is $C\left(\Gamma_0^{i,j}\right)$ weighted by the probability channel i is occupied, i.e. $\pi_{q_0}^i$ and the miss detection probability i.e. P_{md}. Both rates are weighted by the effective transmission time ratio, i.e. $\frac{T_{\text{total}}-T_{\text{sens}}}{T_{\text{total}}}$

Our policy, named restless quality of service - upper confidence bound (RQoS-UCB), consists in modifying the classical UCB1 policy [150] to add a correction term linked to the channel quality. The policy computes the index term $B^{i,j}(n,T^{i,j}(n))$ corresponding to the score of the $i-$th channel at time n and updated according to:

$$B^{i,j}(n,T^{i,j}(n)) = \frac{1}{T^{i,j}(n)} \sum_{l=1}^{T^{i,j}(n)} S^{i,j}(l) - Q^{i,j}(n,T^{i,j}(n)) + A^{i,j}(n,T^{i,j}(n)), \forall i,j \quad (5.41)$$

where the first summation term is the empirical mean of the states of the $i-$th channel (occupied or free) observed by user j at time n. The third term, $A^{i,j}(n,T^{i,j}(n))$, is as defined in classical UCB policy [31, 148, 150]:

$$A^{i,j}(n,T^{i,j}(n)) = \sqrt{\frac{\alpha \log(n)}{T^{i,j}(n)}}, \forall i,j. \quad (5.42)$$

This bias forces the algorithm to explore other arms when it finds a channel occupied. The algorithm propensity to explore new arms decreases when it finds good channels. The second term, i.e. $Q^{i,j}(n,T^{i,j}(n))$, is our contribution in this algorithm and represents the quality term and is computed with the observed instantaneous quality $R_{q_1}^{i,j}(n)$ in state q_1.

$$Q^{i,j}(n,T^{i,j}(n)) = \frac{\beta M^{i,j}(n,T^{i,j}(n)) \log(n)}{T^{i,j}(n)}, \forall i,j \quad (5.43)$$

where,

$$M^{i,j}(n,T^{i,j}(n)) = G_{\max}^j(n) - G_{q_1}^{i,j}(T^{i,j}(n)), \ \ \forall i,j$$

and $G_{\max}^j(n) = \max_{i\in\mathcal{K}} G_{q_1}^{i,j}(T^{i,j}(n))$ is the maximum expected quality within the set of channels. Thanks to this formulation, RQoS-UCB tends to select a channel with the highest quality and probability to be vacant. Parameter α in (5.42) forces the exploration of other channels to check their availability while the new parameter β in (5.43) forces the algorithm to give some weight to the quality in the index computation. If α and β increase, exploration is preferred in order to search for channels with better quality and higher availability. However, if α and β decrease, the empirical mean of observed states, i.e. $\bar{S}^i(T^i(n))$ of channel i, dominates the learning process and forces to exploit the best available channel found in previous iterations. The algorithms implementing the single and multi-user policies are not reproduced here not to clutter the exposure but can be found in [34].

Due to the restless nature of the problem, the index computation cannot be done when one just starts observing a Markov chain after being selected. Indeed, arms evolve independently of SUs' actions, i.e. *restless* MAB, and the probability distribution of rewards SU j gets from an arm i is a function of the time elapsed since the last time user j played this arm. The sequence of observations of an arm that is not continuously played does

not correspond to a Markov chain. To overcome this issue, when user j observes a given band, algorithm waits for encountering a predefined state, named *regenerative state* e.g. ξ^i, [146]. Once ξ^i is encountered, rewards are started to be recorded until ξ^i be observed a second time and the policy index $B^{i,j}$ is computed and another band selected according to the result. This structure is necessary to deal with the restless nature of arms in order to re-create the condition of continuous observation of Markov chain. It is worth mentioning, however, that exploitation in CR context occurs all the time that a free band is detected. This particular structure is done only for mathematical proof purposes.

Moreover, the multi-player setting makes the problem rather involved since collisions between SUs need to be handled. The random rank idea from [160] has been adapted in this work. Considering that each user maintains an ordering set of channel indexes, i.e. $\mathcal{K}_j = \sigma_j(\mathcal{K})$, where σ_j is a permutation of $\{1, \cdots, K\}$ for user j, with $\sigma_j(1) > \cdots > \sigma_j(K)$ from the best to the worst rated. The rank r for user j corresponds to the $r-$th entry in the set $\mathcal{K}_j$. If users i and j choose the same channel to sense the next time slot, they collide. In that case, they draw a random number from their respective sets $\mathcal{K}_i$ and $\mathcal{K}_j$ as their new rank and go for these new channels in the next time slot.

As theoretical contributions, we have proved in [34] that the single and multi-user policy regrets behave logarithmically with time and do not depend on the regenerative state chosen for the regenerative path. We state in the following theorem the upper-bound on the regret of multi-user policy.

Theorem 5 (Regret of multi-player distributed RQoS-UCB policy) *Access to primary spectrum bands is modeled as a MAB problem where all arms are finite state, irreducible, aperiodic Markov chains whose transition probability matrices have irreducible multiplicative symmetrization. If* $G_q^i \geq \frac{1}{\hat{\pi}_{\max}+\pi_q^i}$ *and* $\beta \geq 84 S_{\max}^2 G_{\max}^2 \hat{\pi}_{\max}^2 / \left(\gamma_{\min} \Delta\mu_i M_{\min}^j\right)$*, then, the regret of the distributed RQoS-UCB policy can be bounded by*

$$\Phi^M(n) \quad \leq \quad X_1 \log n + X_2 \tag{5.44}$$

where $\hat{\pi}_{\max} = \max_{q \in \mathcal{S}^i, i \in \mathcal{K}} \hat{\pi}_q^i$ *with* $\hat{\pi}_q^i = \max\left\{\pi_q^i, 1 - \pi_q^i\right\}$*. Moreover* $\Delta\mu_i = \mu_1 - \mu_i$*,* $M_{\min}^j = \min_{i \in \mathcal{K}} M^{i,j}\left(n, T^{i,j}(n)\right)$*,* $\gamma_{\min} = \min_{i \in \mathcal{K}} \gamma^i$ *where* γ^i *is the eigenvalue gap of the* $i-$*th arm. Finally,* X_1 *and* X_2 *are two constants depending on the number of users, channels, stationary distributions of Markov chains representing the bands and some other constants.*

The proof is skipped so are the expressions of X_1 and X_2 which are rather complex but reported in [34]. The major outcome of this theorem is that the quality term we added to learn separately on channel quality does not prevent regret from behaving logarithmically with time like classical UCB.

Numerical results

To conclude this section, I provide some simulation results of the proposed policy in multi-user context in terms of percentage of transmission opportunities, Figs. 5.8(a) and 5.8(b), and in terms of achievable throughput in Figs. 5.8(c) and 5.8(d). The number of PUs' bands is 10 and number of SUs varies from 1 to 10. The characteristics of PUs' bands are given in Table 5.2, i.e. transition probabilities P^i selected arbitrarily, for each channel on the first and second rows, the vacancy probability $\pi_{q_1}^i$ calculated from P^i on the third row, the band quality G^i as defined above on the fourth row and the global mean reward, μ_i calculated with (5.34) taking into account availability and quality on the fifth row.

The proposed policy, RQoS-UCB, is compared to some existing policies in literature:

— Distributed Regenerative Cycle Algorithm (RCA) [146]: It is the distributed and restless version of baseline UCB1 policy (in [31, 148, 150]) taking into account regenerative cycle behavior.
— *Restless Upper Confidence Bound (RUCB)* [147]: restless version of baseline UCB1 policy taking into account increasing exploration and exploitation epochs.
— Best channel selection: This policy always selects the optimal channel in terms of availability and quality, i.e. channel with the highest mean reward, and if the selected optimal channel is occupied, it does not transmit.
— Best opportunistic selection: This is a "god driven" policy which knows *a priori* all spectrum holes and the ordering of channels mean reward as well, considering availability and quality.
— Round-Robin perfect order: Deterministic sequence of trials in channel sensing for each user without suffering from collisions. This method needs to deploy a complete network with heavy signalization.

RCA and RCUB policies have been modified to take into account the channel quality in a single reward, i.e. $R_q^{i,j} r_q^{i,j}$, where $r_q^{i,j}$ is a fixed reward associated to the channel state, e.g. 0 or 1, and $R_q^{i,j}$ is the channel quality drawn from Bernouilli distribution for each channel.

The best opportunistic selection logically upper-bounds the performances, followed by the best channel selection policy in Fig. 5.8. Figs. 5.8(a) and 5.8(c) illustrate the convergence property of all policies in terms of transmission opportunities and achievable throughput for two users respectively. One can remark that RQoS-UCB has almost converged at 2000 frames while more than 10000 are needed for distributed RCA to achieve the same values. Moreover, RUCB does not allow to converge as faster than RQoS-UCB to the best channel in terms of quality and availability, i.e. channel 3 in this scenario, preventing RCUB from achieving comparable number of transmission opportunities or throughput than our proposal.

Figs. 5.8(b) and 5.8(d) show the behavior of policies when the number of SUs is varying. The percentage of transmission opportunities and achievable throughput decrease when the number of SUs increases due to higher number of collisions between SUs. RQoS-UCB is almost stick to the best channel selection policy performance whatever the number of users. When the number of SUs increases, all policies end up doing worse than round-robin strategy, i.e. 9 users for RQoS-UCB and RCA and 6 users for RUCB. It is worth noting than these values are not absolute but depend on the total number of PUs' channels w.r.t. the number of SUs. The larger the number of PUs' channels, the larger the number of SUs for which learning is interesting over non-intelligent approach, e.g. round-robin.

Weighting separately channel quality and state does not only prevent regret from growing logarithmically, but also ensures an increased convergence rate as it can be inferred from Fig. 5.8. This comes from the possibility to tune the coefficients α and β, as long as β satisfies some conditions, according to the weights to be granted to availability or quality, in order to accelerate the convergence rate.

5.2.3 Learning the optimal BS deployment for energy-efficient communications

In the TEPN project context, the energy efficiency of global network was of primary interest and this issue has not been tackled directly in the previous section. It is worth mentioning however that the quality measure discussed in the previous section can be anything else than the interference temperature. It could be a measure of the consumed power in a given band for a transmitter to communicate with its receiver at a given rate

channel	1	2	3	4	5	6	7	8	9	10
$p^i_{q_0q_1}$	0.3	0.65	0.75	0.6	0.8	0.4	0.2	0.65	0.45	0.35
$p^i_{q_1q_0}$	0.7	0.35	0.25	0.4	0.2	0.6	0.8	0.35	0.55	0.65
$\pi^i_{q_1}$	0.3	0.65	0.75	0.6	0.8	0.4	0.2	0.65	0.45	0.35
G^i	0.67	0.64	0.79	0.77	0.70	0.80	0.67	0.63	0.64	0.79
μ_i	0.31	0.48	0.60	0.47	0.58	0.33	0.26	0.46	0.39	0.29

Table 5.2 – State transition probabilities, mean availability, empirical mean quality and global mean reward [22, 34]

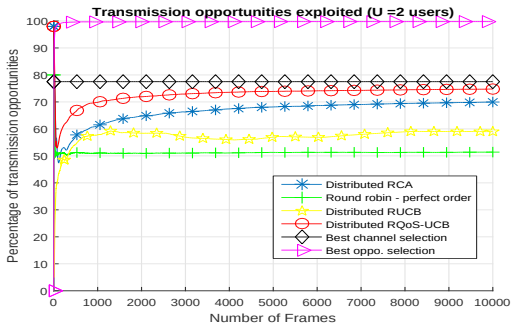

(a) Opportunities w.r.t. the number of frames

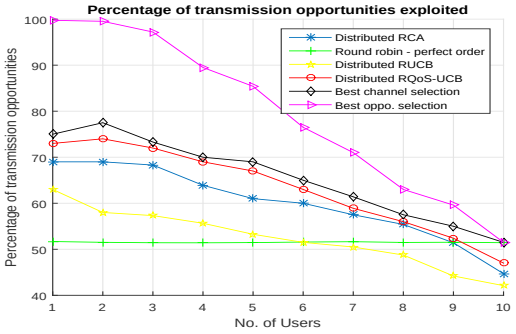

(b) Opportunities w.r.t. the number of SUs

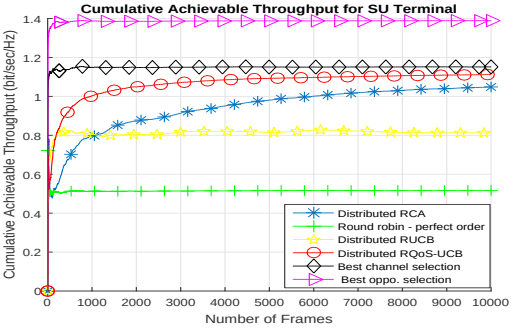

(c) Throughput w.r.t. the number of frames

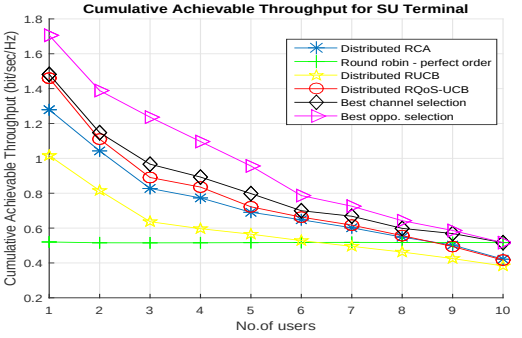

(d) Throughput w.r.t. the number of SUs

Figure 5.8 – Percentage of transmissions and achievable throughput of RQoS-UCB compared to different RL policies in literature [22, 34]

for instance.

Reinforcement learning can also be applied to switch ON and OFF BSs in order to save energy. Indeed, traffic load varies with time in a cellular network and a full BS deployment is not always necessary to satisfy the demand and some BSs may be switched OFF from time to time. Experimental results on voice call informations, recorded from an operator during one week, have shown that traffic load variations were periodic [161]. Since all radio ressources may not be used at their full regime, dynamically putting BSs into sleep mode is one of the effective way to reduce the energy-consumption of the network. Authors in [162, 163] proposed to dynamically switch ON or OFF BSs according to the predicted spatio-temporal traffic load variations, using either a compressed sensing method, in [162], or centralized and distributed optimization algorithm in [163]. The set of BSs to be switched OFF should be chosen with care while maintaining a sufficient quality of service for users. The maximization of energy efficiency by selecting a set of transmitting BSs is an NP-hard problem and then authors of [164] adopted fixed BSs switching patterns to evaluate QoS metrics, e.g. call blocking probability, outage probability, and they chose the BSs switching pattern according to the traffic load encountered in the network.

Machine learning allows to deal with the computational complexity induced by the discrete optimization problem of EE maximization by dynamic deployment. Indeed, one can view the choice of the set of active BSs as a configuration giving a certain reward as a function of the current traffic load in the network. The authors in [165] modeled the traffic load variation as a Markov decision process and attempt to minimize the energy consumption with actor-critic algorithm [166], a RL approach. Moreover, the authors use the *transfer learning* concept that uses the knowledge acquired in historical periods or neighboring geographical regions in order to accelerate the learning phase of a policy to new configuration [167]. Recently, distributed schemes for learning the optimal BSs configuration appeared as solutions of energy consumption minimization problems [161, 168], or using reinforcement learning method [169]. However, theoretical analysis of convergence property is missing in these works.

In this part, we adapt our previous algorithm designed for OSA problem to network EE maximization through the learning of the optimal BSs deployment, i.e. select the set of active BSs and put the remaining ones into sleep mode.

System model

Let us consider an heterogeneous wireless cellular network made of macro and small cells where the set of BSs $\mathcal{Y} = \{1, 2, \cdots, Y\}$ lies in a two dimensional area in $\mathbb{R}^2$ like represented in Fig. 5.9. Downlink communication is considered here, as the primary usage for the mobile Internet application. The decision to switch ON or OFF BSs is taken by a central controller that has the knowledge of the traffic load at the current time instant and which is able to compute the energy efficiency of each cell. This is not a strong assumption, each BS only needs to report to controller the data rate it is providing and at which transmit power cost. The transmission request at position x and time instant n is assumed to be Poisson distributed, with average arrival rate $\Lambda(x, n)$ and the associated file size is exponentially distributed with mean $1/h(x, n)$. The instantaneous traffic load at location x is hence $L(x, n) = \Lambda(x, n)/h(x, n)$ [161, 165]. A mobile station is active when it asks for a file transfer and when call ends, mobile station is considered to be inactive and to be departed from the network.

Let denote $\mathcal{Y}^{on}(n)$ the set of BSs that are switched ON at iteration n, the instantaneous

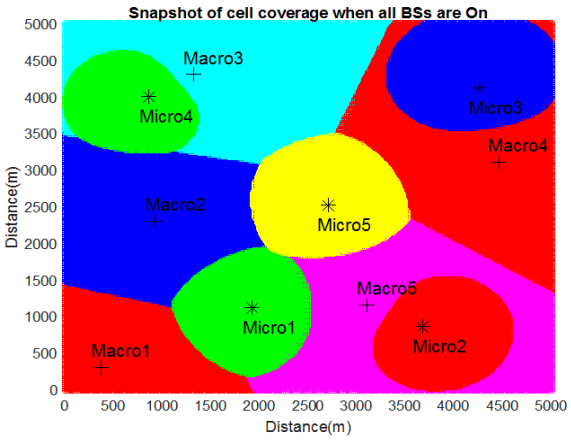

Figure 5.9 – A realization of BS deployment $\mathcal{Y}$ with 5 macro celles and 5 micro cells [22]

traffic load served by BS $k \in \mathcal{Y}^{on}(n)$ can be expressed as:

$$L_k(n) = \sum_{x \in \mathcal{I}_k(n)} \frac{\Lambda(x,n)}{h(x,n)}$$

where $\mathcal{I}_k(n)$, $k = \{1, \cdots Y\}$ denotes the coverage of cell k at iteration n. The instantaneous traffic load is zero, i.e. $L_k(n) = 0$, when BS k is switched OFF on the other hand. The traffic load of a BS can be seen as the number of active mobile stations.

Signal model. The SINR at a mobile station in x and time n in cell k is expressed as

$$\mathrm{SINR}_k(x,n) = \frac{g_k(x,n)\, P_k^{tx}(n)}{\kappa \cdot g_k(x,n)\, P_k^{tx}(n) + \sum\limits_{m \in \mathcal{Y}^{on}(n) \setminus \{k\}} g_m(x,n)\, P_m^{tx}(n) + \sigma^2} \tag{5.45}$$

with σ^2 the noise variance, $g_k(x,n)$ stands for the average channel gain between BS k and user x at time n, $P_k^{tx}(n)$ is the transmit power of BS k at time n. Moreover, $\sum_{m \in \mathcal{Y}^{on}(n) \setminus \{k\}} g_m(x,n)\, P_m^{tx}(n)$ accounts for the power received from interfering BSs and $\kappa \cdot g_k(x,n)\, P_k^{tx}(n)$ is the intra-cell interference, where $\kappa \in [0,1]$ stands for the amount of interference a user located at x received due to the transmit power intended to other users in the cell. By noting B_a the bandwidth used by a user, the service rate for this user is taken equal to the Shannon capacity:

$$\Theta_k(x,n) = B_a \cdot \log_2\left(1 + \mathrm{SINR}_k(x,n)\right)) \tag{5.46}$$

Power consumption. A linear model for power consumption at BSs is used like in previous sections. The total power consumed $P_T(n)$ by each BS k at time n is:

$$P_T^k(n) = a_k P_k^{tx}(n) + P_f^k \tag{5.47}$$

where P_f^k denotes the static power consumption independent of $P_k^{tx}(n)$ and includes all electronic circuit power dissipation due to site cooling, signal processing hardware and battery backup systems as well. a_k is a BS power scaling factor which reflects both amplifier and feeder losses. In the following, we assume that transmit power of cell k is either set to its maximal value or equated to zero when BS is switched OFF.

System load. This quantity is defined as the time required to serve the whole traffic demand in the cell. System load of BS k at the $n-$th iteration is:

$$\rho_k(n) = \sum_{x \in \mathcal{I}_k(n)} \frac{L(x,n)}{\Theta_k(x,n)} \tag{5.48}$$

Switching BSs ON and OFF as a MAB problem

The major contribution in this part has been to model the energy efficiency maximization as a MAB problem for which the policy proposed in Section 5.2.2 can be applied. Let first sate the problem to solve:

$$\begin{array}{lll} \mathcal{Y}^{on^*}(n) = & \arg\max\limits_{\mathcal{Y}^{on}(n)} \left[\sum\limits_{k \in \mathcal{Y}^{on}(n)} \frac{\sum\limits_{x \in \mathcal{I}_k(n)} \Theta_k(x,n)}{P_T^k(n)} \right] \text{ s.t.} \\ (c_1) & 0 \leq \rho_k(n) \leq \rho_{th}, \forall k \in \mathcal{Y}^{on}(n) \\ (c_2) & \Theta_k(x,n) \geq \Theta^{\min}, \forall x \in \mathcal{I}_k(n), \forall k \in \mathcal{Y}^{on}(n) \\ (c_3) & \mathcal{Y}^{on}(n) \neq \emptyset \end{array} \tag{5.49}$$

The optimization problem in (5.49) aims at selecting the set of BSs maximizing the network EE under constraints (c_1) to (c_3). Constraints (c_2) and (c_3) impose a minimal data rate per user and the selected BS set should not be empty, respectively. Constraint (c_1) imposes a threshold on system load to maintain a tradeoff between EE and system stability [161, 165]. Indeed, EE maximization tends to limit the data rate offered to users, once they satisfy their rate contraint, but a too low service rate implies an increasing system load.

This problem is NP-hard and an exhaustive search for optimal configuration requires too much computational resources since the optimal BS active set belongs to a set of $2^Y - 1$ combinations. Without exploring all combinations, we rather propose to learn the best ones in a finite time analysis. The problem of learning the optimal configurations can be modeled with MAB framework as illustrated on Fig. 5.10 where an arm is considered to be a configuration of BSs' status, i.e. ON or OFF. Let consider a tuple $\mathcal{T} =< \mathcal{S}, \mathcal{K}, \mathcal{P}, R >$, where $\mathcal{S}$ denotes the state space, $\mathcal{K}$ denotes the action space, $\mathcal{P}$ denotes a state transition probability matrix, and finally R is a reward function associated with $\mathcal{S}$, $\mathcal{K}$ and $\mathcal{P}$. At each iteration, the central controller chooses an action i among $|\mathcal{K}| = 2^Y - 1$ possible actions, i.e. $\mathbf{a}^i(n) = \left[a_1^i(n), \cdots, a_Y^i(n)\right]^T$ with $a_k^i(n) = 1$ if BS k is switched ON at n and 0 otherwise. This particular action leads to an observable state of the network, $S^i(n) \in \{0, 1\}$ where $S^i(n) = 1$ if all constraints in (5.49) are satisfied and 0 otherwise, in other words the reward on the state of the Markov chain i relies on the fact that the selected action is a feasible solution of (5.49). Due to the random process governing the traffic load of the network, the network state $S^i(n)$ transforms to $S^i(n+1)$ at the next time instant according to a transition probability measure for arm i: $\mathcal{P}^i = \{P_{k,l}^i, k, l \in \mathcal{S}, i \in \mathcal{K}\}$. Considering that the defined Markov process is stationary, over the short term, the distribution of the Markov chain i is $\pi_S^i(n) = \pi_S^i$. Finally, the reward associated to the "quality" of the action taken, $R_S^i(n)$, is EE of the network, defined as the function to be maximized in (5.49).

The goal of our policy is hence to maximize the mean reward on the long run, i.e. $\mu^i = \sum\limits_{S \in \mathcal{S}^i} S \cdot G_S^i \pi_S^i$ such that the weak regret is minimized:

$$\Phi^{\mathcal{A}}(n) = n\mu^* - \sum_{t=1}^{n} \mathrm{E}\left[S^{\mathcal{A}(t)}(t) G_{S^{\mathcal{A}(t)}}^{\mathcal{A}(t)}(t) \right] \tag{5.50}$$

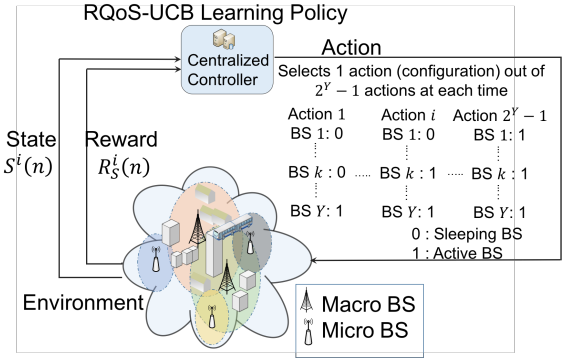

Figure 5.10 – RL framework for BS switching operation [22]

where $S^{\mathcal{A}(t)}$ being the value of the state observed by using the policy $\mathcal{A}$ at iteration t and G_S^i is defined as in (5.35). Like previously, μ^* is the optimal mean reward obtained by always selecting the best action at each time step t.

The policy proposed in Section 5.2.2 can be applied to the BS ON / OFF switching problem. At a given iteration n, the policy $\mathcal{A}$ selects a BS switching operation i with the highest index $B^i(n, T^i(n))$ composed with the same three terms as in (5.41). The execution of a BS switching operation i provides to the central controller a new state $S^i(n+1)$ and a new reward $R_S^i(n+1)$, i.e. energy efficiency. Then policy $\mathcal{A}$ updates the index $B^i(n, T^i(n))$ according to these new inputs and repeats the procedure until convergence to the optimal BS configuration during each hour of operation.

Speed up convergence rate with transfer learning. Traffic load can be seen as a random process that can be modeled with a sinusoidal behavior [170, 171]:

$$L\left(n, V, \Phi, M\right) = V \cos\left(2\pi \frac{n}{T} + \Phi\right) + M$$

where T is the fluctuation period, assumed to be constant, V, Φ, M are random variables representing the amplitude, the phase and the average arrival rate of the random process. This model corresponds relatively well to what it is observed in practice, e.g. [161]. Each day can be seen as a realization of the random process where parameters of the process vary. Hence, the configuration that has been learned at a given hour the day before, may not be the optimal one for the same hour the current day. Learning from scratch each day may be prejudicial to the convergence of the policy to a stable solution in a finite time. We then proposed to use the TL concept from [167] to accelerate the convergence rate of the learning phase. The TL concept is illustrated in Fig. 5.11 where "source task" represents the knowledge acquired in historical periods and target task the configuration to be learned currently. A a given period of time, the policy begins with the BS configuration that has been learned previously in order to achieve faster the best configuration the present day. In order the policy to use the knowledge acquired in previous periods of time, the first term in (5.41) and (5.42), (5.43) should be modified in order to take into account the number of

times action i has been selected in all previous periods h, i.e. H^i such as:

$$\bar{S}^{i,h}(T^i(n)) = \frac{\sum_{t=1}^{T^i(n)} S^i(t) + \sum_{t=1}^{H^i} S^{i,h}(t)}{T^i(n) + H^i}, \forall i. \tag{5.51}$$

$$Q^{i,h}(n, T^i(n)) = \frac{\beta M^{i,h}(n, T^i(n)) \log(n + H^i)}{T^i(n) + H^i}, \forall i, \tag{5.52}$$

$$A^{i,h}(n, T^i(n)) = \sqrt{\frac{\alpha \log(n + H^i)}{T^i(n) + H^i}}, \forall i. \tag{5.53}$$

where,

$$M^{i,h}(n, T^i(n)) = G^S_{\max} - G^{i,h}_S(T^i(n)), \ \ \forall i,$$

and $G^{i,h}_S(T^i(n)) = \frac{1}{T^i(n)} \sum_{k=1}^{T^i(n)} R^i_S(k) + \frac{1}{H^i} \sum_{k=1}^{H^i} R^{i,h}_S(k)$ denotes the empirical mean of reward R^i_S collected by applying BS switching operation i in state S up to current iteration $T^i(n)$ plus total source task iteration H^i. Moreover, $G^S_{\max} = \max_{i \in \mathcal{K}} G^{i,h}_S(T^i(n))$ is the maximum reward within the set of BS switching operations from current and historical observations in state S.

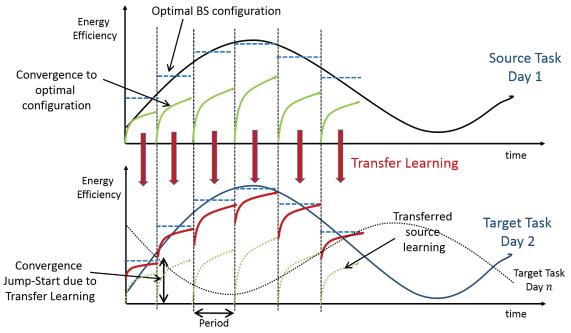

Figure 5.11 – Transfer learning concept for TRQoS-UCB policy [22]

We have proved that the average number of sub-optimal plays, $\mathrm{E}\left[T^{i,h}\right]$, with $i \neq i^*$ is bounded and does not grow faster than a logarithmic function of time [22, 35].

Simulation results

The cellular network described in Fig. 5.9 is simulated with the parameters given in Table 5.3. Fig. 5.12 illustrates the convergence, in terms of cumulative energy efficiency ratio, of the proposed policy with and without TL, i.e. TRQoS-UCB and RQoS-UCB respectively. This metric is simply the energy efficiency achieved with a policy normalized by the energy efficiency when all BSs are ON. Figures from 5.12(a) to 5.12(d) show the result of 3000 iterations of algorithms when the arrival rates in source and target tasks are the same, i.e. $5 \cdot 10^{-6}$ and when the target task arrival rate is 40 times larger than the one of the source task, respectively. Our policy is compared with actor-critic algorithms without and with TL, i.e. ACT, TACT [165] respectively, and a decentralized greedy algorithm [168]. The result of the exhaustive search, which can be done for the simulated network i.e. 10 BSs, is also given as benchmark and is referred as *ideal policy*.

Parameter description	Value
Simulation area	5km × 5km
Maximum transmission power	Macro BS: 20W, Micro BS: 1W
Maximum operational power	Macro BS: 865W, Micro BS: 38W
BS Height	Macro BS: 32m, Micro BS: 12.5m
Intra-cell interference factor	0.01
Channel bandwidth	1.25MHz
Path loss model	COST 231
Arrival rate $\Lambda(x)$ in source task	0.05×10^{-4}
Arrival rate $\Lambda(x)$ in target task	from 0.05×10^{-4} to 2×10^{-4}
MSs call holding time $1/h(x]$	100Kbyte
System load threshold ρ^{th}	0.6
Minimum bit rate requirement $\Theta^{\min}$	122kbps
Exploration parameters of RQoS-UCB	$\alpha = 0.25$ and $\beta = 0.32$

Table 5.3 – Simulation Parameters

Our policy with TL converges toward the best configuration rather quickly compared to other policies when arrival rates of source and target tasks are not so different. The reason has to do with the fact that the more different the realizations of source and target tasks, the more useless for a policy to start with a prior. It can even be a disability as it can be observed in Fig. 5.12(d) where the policy without TL performs better than the one with TL. By doing an iteration every second, our policy learns a good configuration in one hour.

Finally, Fig. 5.13 illustrates EE achieved by the previous algorithms during one day. The sinusoidal-like behavior can be inferred from this figure and we remark that the maximal energy efficiency is achieved during low traffic load periods, i.e. night time to early morning. On the other hand, during peak traffic loads, i.e. from noon to 22h, low EE can be expected and all policies behave the same, except the greedy policy which consists in saving the maximum amount of energy, without any care of efficiency. This is because all BSs need to be ON to absorbe the intense traffic and hence there is *nothing* to learn. On the contrary, during low traffic period, EE depends on user positions and demands and hence learning the best set of active BSs makes sense.

5.2.4 Summary

MAB offers a general framework in which many wireless communication problems, occurring with cognitive systems, may be addressed by reinforcement learning approaches. UCB policies are index-based RL techniques that are order-optimal in regret and very simple to implement, requiring minimal computational ressources and they are particularly well adapted to i.i.d. or Markovian MAB formulation. In these research works, we have been interested in improving existing UCB policies by allowing them to learn on two different criteria. Our investigations lead us to first focus on OSA scenario in which a cognitive user is not only interested by finding free bands in a spectrum but also by selecting the one with the best quality. The quality in our policy may be any random observable, e.g. experienced SINR between a secondary Tx and Rx, power consumed by an SU to transmit at given QoS. The main difference with existing literature has been to separate the reward related to the Markov chains, e.g. state of the channels, and the reward related to the so-called quality in order to emphasize on one or another characteristic. Our formulation does

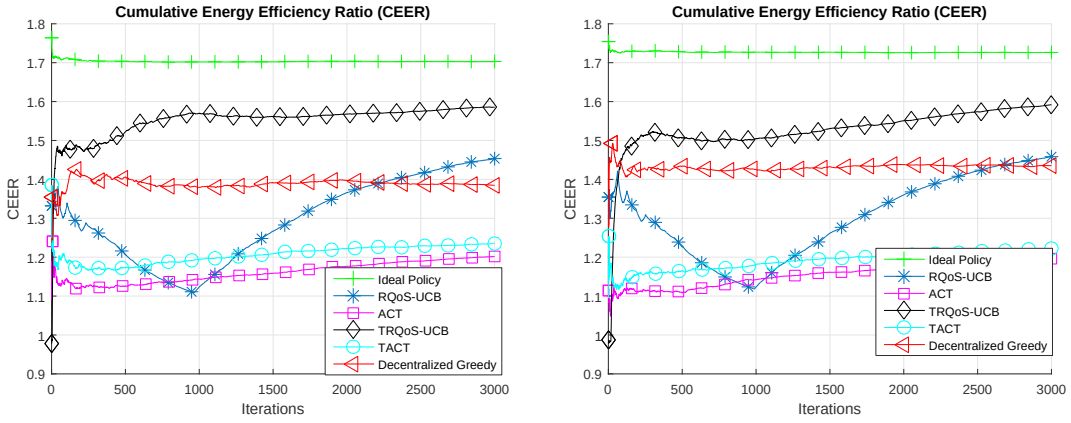

(a) $\Lambda^{\text{target}} = 0.05 \cdot 10^{-4}$ (b) $\Lambda^{\text{target}} = 0.5 \cdot 10^{-4}$

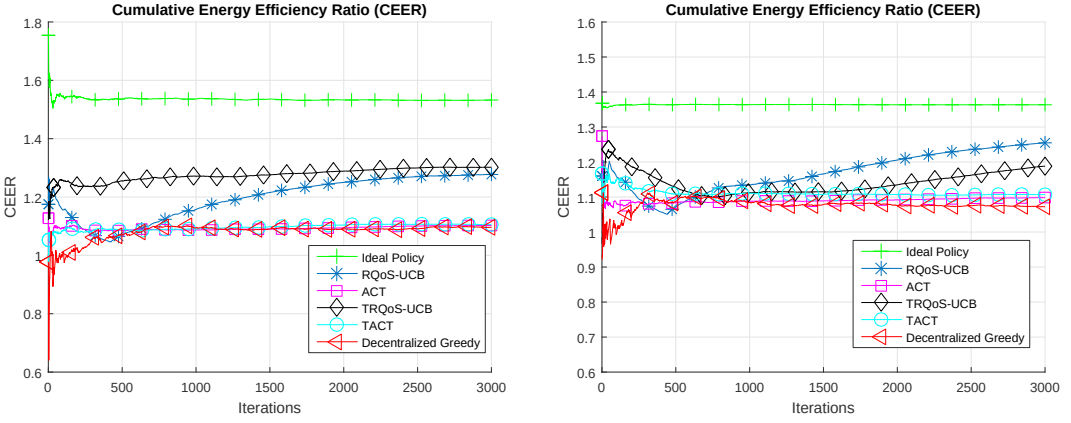

(c) $\Lambda^{\text{target}} = 10^{-4}$ (d) $\Lambda^{\text{target}} = 2 \cdot 10^{-4}$

Figure 5.12 – Convergence comparison of various policies w/wo TL in terms of CEER for $\Lambda^{\text{source}} = 0.05 \cdot 10^{-4}$ [22]

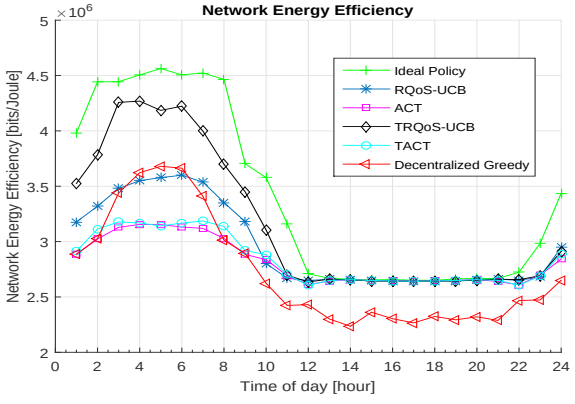

Figure 5.13 – EE with several RL policies w.r.t. the time of the day [22]

not prevent the regret from growing at most logarithmically which is the best behavior that a policy may have. Finally, the problem of network EE that has been studied via PPP in Section 5.1 has been reformulated to fit with a machine learning problem where our policy can be applied. In that case, our policy performs close to the exhaustive search when the number of possible actions is not too important.

5.3 Conclusions, on-going work and perspectives

In this chapter, the problem of network energy-efficiency has been tackled more directly under two perspectives, i.e. stochastic geometry and machine learning respectively. These works have been conducted with the supervision of two former PhD students: Dr. Ahmad Mahbubul Alam for stochastic geometry aspect and Dr. Navikkumar Modi for machine learning aspect. Our main contributions in this chapter can be summarized as follows:

— **Stochastic geometry for wireless networks:** The derivation of the ergodic data rate, averaged over small scale fadings and network geometry, when the SLNR precoder is considered at BS has been conducted. The average desired signal power and the inter and intra-cell interference power have been derived as functions of the Stieltjes transform of the eigenvalues distribution of a matrix of the form $\frac{1}{M}\bar{\mathbf{H}}_k M^{\frac{\alpha}{2}} \bar{\mathbf{D}}_k \bar{\mathbf{H}}_k^H$ when the number of users in the network and number of antennas tend to infinity, where $\bar{\mathbf{H}}_k$ and $\bar{\mathbf{D}}_k$ are matrices gathering the channel and the path loss gain, respectively, from a given BS to users except user k. The analytical expression, although derived in asymptotic regime, reveals to be accurate even for moderate values of the number of antennas and users. Moreover and despite the fact that the theoretical expression implies to solve integral equations to find the value of the Stieltjes transforms, it is much more faster than running lengthly Monte-Carlo simulations. These findings have been published in [29, 172, 173].

— **Multi-armed bandit:** Reinforcement learning has found a nice application in cognitive radio and network. In that context, a radio or a network able to learn on several *distinct* criteria could be particularly interesting for agility purpose. Our contributions in that field remain in proposing an index-based policy, hence very simple to implement, able to learn on two different metrics, e.g. primary bands availability and channel quality. The proposed policy computes, at a given time, an index made up with two coefficients relative to the both criteria to be learned. Moreover, the regret of the policy has been shown not to grow faster than logarithmically with time. This concept has been successfully extended to the best BS deployment learning problem in order to maximize the network energy efficiency. These researches have been published in several conferences and journals including [34, 144, 174–177].

Concerning the performance of large networks with stochastic geometry, one limitation of our previous study is the non consideration of resource provisioning in the average SINR characterization. Indeed, our performance studies are based on the SINR experienced by a user at r_0 with the same resources, e.g. transmit power, whatever the value of r_0. This is obviously a drawback of the approach, and a user in cell-edge will ask again for supplementary resources since it will have been less served in average compared to users closer from BS. The distribution of joint events in PPP network is a difficult issue, however this aspect should be taken into account in a further work. Moreover, the switching ON/OFF operation for underutilized BSs is generally assessed with a random thinning process. This allows to derive some results but this is far from being a realistic use-case. Indeed, the decision to put a BS into sleep mode will likely rely on the traffic demand associated

to the considered cell. A first clue is to model the variability of the traffic load as a random process and switch ON or OFF some cells according to their internal traffic. The resulting thinning process will be dependent on the user-demand and will probably not remain a Poisson point process. Hence, the classical tools used to derive the ergodic rate and coverage probability need to be revised. I have launched with Dr. Jean-Yves Baudais an application call for a PhD on this topic that should start in 2018.

Following the work of Dr. Navikkumar Modi, several research paths have also been raised. On our last contribution, when the number of BSs increases, the policy may take a while before converging to an acceptable configuration due to the important number of possible actions. One research path to investigate would be to apply the RL strategy to several clusters of limited number of BSs. The issue to overcome however would be dealing with the distributed problem nature and to ensure the convergence of the learning process. There exists some works on distributed learning in MAB context, as listed above in this chapter included our contribution in multi-user OSA, and one could try to firstly express the distributed network EE maximization in this context. Each cell or cluster of cells may attempt to find the best suitable configuration to reduce EE of its own group of cells. However, without a minimum information on what the others clusters do, the learning process will likely not lead to the best possible configuration. The remaining question is *which amount of coordination a cluster of cells needs?* In that sense, the insights proposed in the project PERFUME, the ERC of Prof. David Gesbert will be valuable [4]. In a more fundamental perspectives, I would like to investigate the learning on multiple rewards under Bayesian framework. The approach proposed in the PhD of Dr. Modi relies on a frequentist approach, as UCB-based algorithms do. The research for explicit policies, relying on Bayesian models for separate rewards, e.g. Bayes-UCB or Thomson sampling, would be very interesting from my point of view because of their better theoretical performance than the simple UCB policy.

4. http://www.eurecom.fr/cm/gesbert/erc

CHAPTER

6 Protocols for network coding

In this chapter, I leave aside my studies on signal processing and PHY layer to focus on some network coding aspects. In this research work, we did not contribute to the NC theory, but we have been more interested in protocols to make NC work. In particular, we have proposed new schemes that would operate between layers 2 and 3. Network protocol is not my main research field, but I have been interested in this research issue through an international collaboration with Dr. Ayman Khalil from Libanese International University with the PhD work of Samih Abdul-Nabi, that I have co-supervised, and who is now Associate Professor at LIU.

In this Chapter, I first explain the ACNC protocol in Section 6.2 then a study of message cardinality and buffering is conducted when decoding at end and intermediate nodes in Section 6.3. In particular, the notion of aging, preventing a packet from being involved in too many coding operations, is introduced. Finally, the impact of packet losses with NC is investigated in Section 6.4 and some techniques to recover from loss are introduced. Finally Section 6.5 draws the conclusions of the Chapter and summarizes my contributions.

6.1 Introduction

Since the milestone paper of Ahlswede *et al.* on "Network information flow" 17 years ago [178], a lot of contributions emerged in NC which is now in the spotlight since the creation of the network coding research group in 2013 by the internet research task force. The principle of network coding is to allow linear operations on packets travelling into a network. Fig. 6.1 illustrates NC principle over a random network where P^i and g_i, $i = 1, 2$ are respectively the packets and coefficients chosen in a Galois Field of dimension 2 or higher dimensions, e.g. $\mathbb{F}_{2^m}$ for some integer m. In this figure, both source nodes s_1 and s_2 send their own packet information, P^1 and P^2, to the destination nodes, t_1, t_2 and t_3. In this network, NC is possible at nodes 2 and 5 allowing to save one transmission on each link departing from 2 or 5. Since the min-cut [179] between the set of sources and each destination is 2, NC allows to transmit 2 packets to all destinations in one flow, assuming a capacity of 1 on each link.

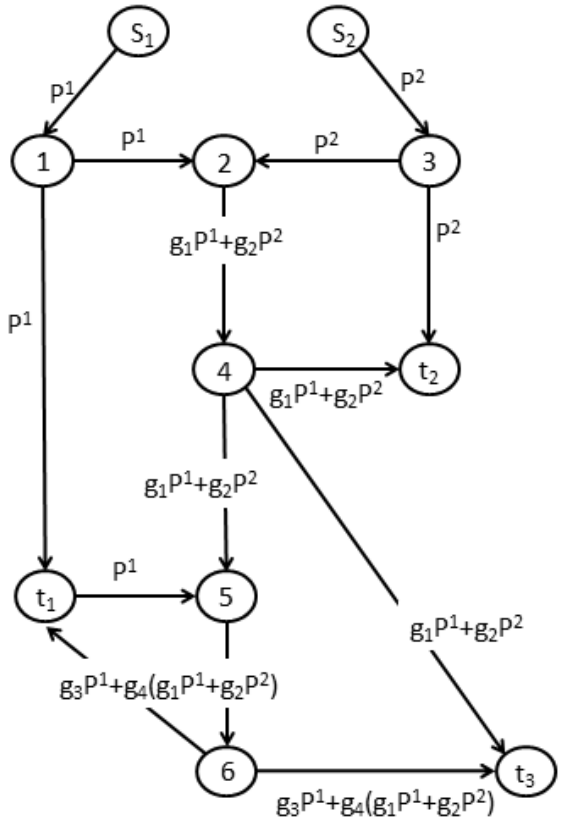

Figure 6.1 – Linear network coding principle [36]

The linear network coding (LNC) has been introduced in [180] and authors proved that LNC, in multicast context, achieves the max-flow bound, i.e. the rate at which a message reaches each destination node. Koetter and Médard in [181] have formulated the NC problem as an algebraic problem by introducing the network transfer matrix $\mathbf{M}$ between a couple of nodes u and v. By concatenating the set of vectors received by u in matrix $\mathbf{X}$ and the ones received by v in matrix $\mathbf{Y}$ such that $\mathbf{Y} = \mathbf{MX}$, they searched for algebraic properties of $\mathbf{M}$ in order to maximize the network flow by linking these properties to the max-flow min-cut theorem. In [182], the authors proposed algorithms to select the coding

vectors to be used in LNC. Ho *et al.* in [183] have proved that if each node randomly chooses coding vectors over a finite field, respecting some conditions, the error probability at destinations nodes, i.e. probability not to decode a message due to the random coding, is exponentially decreasing with the code length.

Besides theoretical works on NC, some authors have also been interested in practical issues induced by NC. Two researchers from Microsoft laboratories, proposed a new peer-to-peer protocol for software and very large files sharing, named *Avalanche* [184]. This protocol uses the NC principle by splitting the file into smaller blocks and transmitting linear random combinations of these blocks. Simulations have shown that the downloading time is reduced up to 2 to 3 times compared to non-encoded transmissions. Katti *et al.* published a complete NC-based protocol named COPE [185]. This protocols inserts a coding layer, between the layers 2 and 3 of OSI model, which is used to identify the coding opportunities available for saving transmissions. COPE has been originally designed for wireless mesh networks but authors argue that it can be applied to various kinds of networks. However, nodes cannot completely rely on the reception reports because they might be lost in a severe congestion or delivered late due to network traffic which affects the decoding probability.

NC can be done at each layer of OSI model; from the application layer [186] to physical layer with the so-called physical layer network coding [187] passing by the transport [188], network [189] and data-link [190] layers. In our work, the protocols we proposed are located between the layers 2 and 3.

6.2 Address correlated network coding and decoding

6.2.1 Problem

In this work, we essentially focused on linear networks because this is the structure of connection-oriented networks and NC at intermediate nodes can substantially improves the bandwidth usage [191]. We hence consider a linear network with n intermediate nodes as a graph $\mathcal{G} = (E, V)$, where the set of vertices is made of two end nodes, i.e. A, B and a collection of intermediate nodes IN_i, $i \in \{1, \cdots, n\}$, and the set of edges is such as $E = \{(A, IN_1), (IN_i, IN_j), (IN_n, B), \forall (i,j) : |i - j| = 1\}$.

In the following, a *packet* refers to a non-coded piece of information and a coded *message*, or simply a *message*, is a network coded piece of information made of two or more packets coded together.

Definition 5 (Address Correlation) *Two packets are said to be address correlated if the destination of any of the two packets is the source of the other one.*

One of the prior question when it comes with NC implementation is *which packets in the flow should be coded first?* In each queue of intermediate nodes, a timer t_i associated to packet i indicates how long the packet has been in the queue. Moreover, a priority indicator, $P_r(i)$ is set to packet i and can be extracted from packet header. Priority can be set by end users according to the application or by the relay according the packet characteristics. A binary variable y_i, initially set to 0, is also associated to each arriving packet; it is set to 1 when packet i is selected to be coded. The selection of packets to be coded and released into the network is completed in two phases. In the first phase, high priority packets are selected to be coded. If very few packets are chosen, then additional packets can be selected to be coded with the first selected set in order to improve the bandwidth usage in a second phase. Once enough packets are selected in both phases,

coded messages are built and sent into the network. The process then repeats itself with the time out value of a new packet in the queue.

The selection in both phases can be modeled with two optimization problems as in (6.1) and (6.2). The objective function of the first problem contains two terms, i.e. $-P_r(i)$ and $E_w(i)$, being respectively the priority and expiry weights for packet i. The expiry weight is a linear function of the timer t_i and the maximum delay allowed for packet i, $T(P_r(i))$. Hence, objective function of problem (6.1) searches for selecting packets to be coded with the highest priority and the lowest expiry weight. Constraint (c_1) in (6.1) is related to the decoding capacity of the network, i.e. maximal number of coded packets that a given node can decode. In other words, among the n packets in the queue, a maximum of M_d packets can be used to make a coded message. The number M_d may be updated dynamically by the node, however, as it will be seen later, each packet in coded message increases the size of the header of few bytes. Hence in practice, there is a limit on the number of packets in a message depending on the lower layers in charge to transmit those messages over the medium. Constraint (c_2) deals with priority management by forcing the selection of expired packets. If $t_i - T(P_r(i)) \leq 0$ then y_i can be 0 or 1 but if $t_i - T(P_r(i)) > 0$ then y_i should be 1. The constant C is taken large enough to ensure the validity of the constraint when $t_i - T(P_r(i))$ is larger than 1. Hence, two packets i and j such as $P_r(i) < P_r(j)$ but $t_i - T(P_r(i)) = t_j - T(P_r(j))$ are treated equally by (c_2) but objective function forces to select the packet with the highest priority. Moreover, the closer a packet is from time out, the lower the value of $E_w(i)$. Once phase 1 completes, packets are divided in two sets: i) the set of packets already selected to be coded together and ii) the set of packets that may be selected to take part of the coding process.

$$
\begin{aligned}
&\min_{y_i} \quad \sum_{i=1}^{n} \left(-P_r(i) + E_w(i)\right) y_i \text{ s.t.} \\
&(c_1) \quad \sum_{i=1}^{n} y_i \leq M_d \\
&(c_2) \quad t_i - T(P_r(i)) \leq y_i \times C, \ \forall i \\
&(c_3) \quad y_i \in \{0,1\} \ \forall i
\end{aligned}
\tag{6.1}
$$

$$
\begin{aligned}
&\max_{y_i} \quad \sum_{i=1}^{n} y_i \text{ s.t.} \\
&(c_1) \quad \sum_{i=1}^{n} y_i \leq M_d \\
&(c_2) \quad \sum_{i=1}^{n} \min(1, |S_j - D_i| \times y_i y_j) < \sum_{i=1}^{n} y_i, \ \forall j \\
&(c_3) \quad y_i \in \{0,1\} \ \forall i
\end{aligned}
\tag{6.2}
$$

Phase 2 consists in solving the problem in (6.2). Phase 2 aims at increasing the set of coded packets resulting from phase 1 by adding more packets, i.e. objective function. The first constraint is the same than in phase 1 and the second constraint forces to select packets that are address correlated in order to reduce the number of transmissions of coded messages. Let denote by S_j and D_i the addresses of the source of packet j and destination of packet i respectively. Hence, the system searches for selecting packets such as $|S_j - D_i| y_i y_j = 0$, that is to say, if $|S_j - D_i| = 0$, i.e. packets i and j are address correlated, or $y_i y_j = 0$, i.e. packet i or j has not been selected yet.

The problem in (6.1) is a binary integer programming problem since the optimization variables are $y_i \in \{0,1\}, \forall i$. This problem can be solved efficiently with branch and bound

algorithms, as it has been discussed in Chapter 4. On the other hand, phase 2 in (6.2) is a non-linear optimization problem because of constraint (c_2). In that case, we proposed an iterative procedure to find a good set of packets to be coded together [36].

6.2.2 Implementation

ACNC adds a layer between data link and network layers of OSI model. Coded messages can be produced by using XOR operation over the bits or with another general linear coding scheme. Without giving all implementation details, let us illustrate how ACNC works, with a simple example.

Intermediate node IN_i receives two packets, 123 and 124, from nodes IN_{i-1} and IN_{i+1} respectively. The header of both packets are as represented in Table 6.1. When constructing a new coded message, header fields such as *unicast*, *exist at destination* and *next hop* has to be updated. The field *unicast* is set to true if at most one packet is unknown to destination and set to false otherwise. The next hops of packets 123 and 124 are IN_{i+1} and IN_{i-1} respectively. The field *exist at destination* is set by comparing the value of the field *coming from* of the received message to the value of the field *next hop* in the generated message. After being coded together, 123⊕124, are broadcasted by node IN_i as shown on Fig. 6.2. The header of the coded message 123⊕124, is updated as in Table 6.2

Unicast	Yes	Unicast	Yes
Addr1	A	Addr1	B
Addr2	B	Addr2	A
Coming from	IN_{i-1}	Coming from	IN_{i+1}
Nb. of packets	1	Nb. of packets	1
ID	123	ID	124
Source	A	Source	B
Exist at dest.	No	Exist at dest.	No
Next hop	- - - -	Next hop	- - - -

Table 6.1 – Packets to be coded by node IN_i [36]

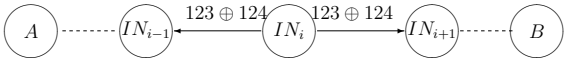

Figure 6.2 – A coding opportunity in a linear network [36]

The coded message contains now 2 packets, neither packet 123 nor packet 124 exist at destination since both packets come from a node that does not correspond to their respective destination. The coded message is no longer *unicast* since both packets do not exist at their destination. The same procedure is repeated at each node and can be done between a packet and a coded message or two coded messages. Of course, header is updated according to the situation encountered but not detailed here. It can also be observed that header size increases with the number of coded packets in a message. This typically is a practical issue that it is skipped in literature in general. NC undoubtedly can improve the bandwidth usage, however the overhead implied by the header size increase should be controlled in order to keep benefits of NC.

Unicast	No
Addr1	A
Addr2	B
Coming from	IN_i
Nb. of packets	2
ID	123
Source	A
Exist at dest.	No
Next hop	IN_{i+1}
ID	124
Source	B
Exist at dest.	No
Next hop	IN_{i-1}

Table 6.2 – Updated header of the coded message before transmission [36]

6.3 Decoding at end and intermediate nodes

6.3.1 Decoding at end nodes

A node is modeled as a server with two queues: one for receiving messages and another for releasing them in the network. Nodes are modeled with a state diagram as represented in Fig. 6.3(a) and Fig. 6.3(b) for intermediate and end nodes respectively. Server can perform one of the following activity: packet generation, coding, sending message and decoding denoted by g, c, s and d respectively. Node activity assignments are constructed according to the node role in the following scheme: sending node activity set $\{g, s\}$, intermediate node activity set $\{c, s\}$, receiving node activity set $\{d\}$.

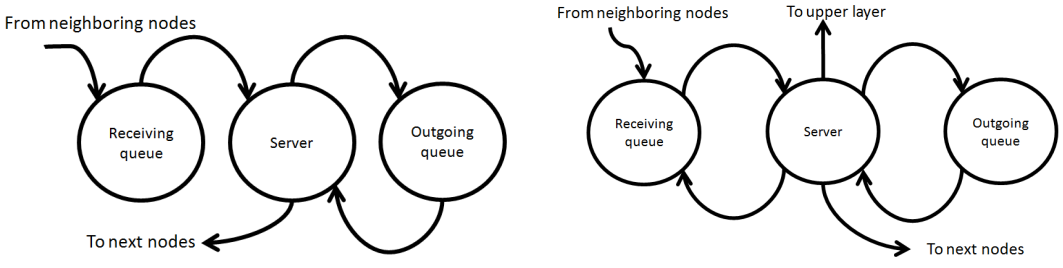

(a) State diagram of intermediate node (b) State diagram of end node

Figure 6.3 – State diagram of nodes [36]

The activity decision at intermediate nodes is either coding or sending a message. This decision depends on the number of packets in the queues and should be taken in order to balance the load in receiving and outgoing queues. To achieve this task, we proposed and

solved the following integer programming problem [39]:

$$\begin{array}{ll} \max\limits_{y_c,y_s} & y_c \sum\limits_{i=1}^{x_r(t)} m_{r_i}(t) + y_s \sum\limits_{j=1}^{x_o(t)} m_{o_j}(t) \text{ s.t.} \\ (c_1) & y_c + y_s = 1 \\ (c_2) & y_c \geq \frac{x_r(t)-x_o(t)-d_{ro}}{C_r} \\ (c_3) & y_s \geq \frac{x_o(t)-x_r(t)-d_{or}}{C_o} \\ (c_4) & y_s, y_c \in \{0,1\} \end{array} \tag{6.3}$$

where $m_{r_i}(t)$, $m_{o_j}(t)$ are the amount of time messages i and j have been spent in receiving and outgoing queues at time t, respectively. Moreover, $x_r(t)$, $x_o(t)$ are the number of messages to be further coded and to be transmitted at time t, respectively. The binary variables y_c and y_s are set to 1 if the coding and sending activities respectively are chosen and 0 otherwise. These activities are exclusive as formulated in constraint (c_1). Constraints (c_2) and (c_3) are set to balance the receiving and outgoing queue respectively. For instance in (c_2), coding will be chosen if the difference between receiving and outgoing queue lengths is larger than an acceptable value, i.e. d_{ro}. Constant C_r, is chosen large enough to ensure that the right hand side of (c_2) does not exceed 1 with high probability. Constraint (c_3) and constants d_{or}, C_o are read in the same way. Objective function tends to select the activity that corresponds to the largest value among the time packets spent in receiving and outgoing queues. This problem can be efficiently solved with a branch and bound algorithm.

End nodes, on the other hand can perform more activities than intermediate nodes, except coding activity, that is to say decode, send or generate a packet. Since the packet generation is a random process, end node activity is chosen according to a probabilistic model, as suggested in [192], such that the probabilities to set the decoding and sending activities, at end nodes, are respectively:

$$P(d) = \frac{e^{-\beta x_o(t)}}{e^{-\beta x_o(t)} + e^{-\beta x_r(t)}} \tag{6.4}$$

$$P(s) = \frac{e^{-\beta x_r(t)}}{e^{-\beta x_o(t)} + e^{-\beta x_r(t)}} \tag{6.5}$$

where $P(d) + P(s) = 1$ and β is a control parameter set to make the decision more or less random according to the values of $x_r(t)$ and $x_o(t)$. If $\beta \to 0$ both activities have the same probability to be selected, i.e. 1/2, but if $\beta \to \infty$ then decoding activity is almost sure if the receiving queue is more fulfilled than the outgoing queue, i.e. $x_r(t) > x_o(t)$ while sending probability goes to zero, and opposite behavior if $x_r(t) < x_o(t)$. For all other values of β, end node has a non-zero probability to chose decoding or sending activity whatever the status of its queues.

We already mentioned that increasing too much the number of packets in a coded message may unreasonably increase the overhead of NC protocols. We set a definition that will be used in the notion of aging.

Definition 6 (Message cardinality [38]) *The cardinality $|C_i|$ of a coded message C_i is the number of packets coded within the message.*

The cardinality of a message is important regarding the decoding capacity of the network. The maximal cardinality of a coded message that can be decoded by a node, given hardware and software constraints, is noted Ç. Actually, if packets and messages are continuously

coded at each node, the message cardinality is continuously increasing with the number of transmissions at each end nodes as it can be observed on Fig. 6.4. The simulated network contains 7 nodes with 5 intermediate nodes. Time to time, cardinality decreases due to absorbing effect, i.e. a packet is removed from the coded messages because it was present in the both incoming messages to the node. However, the general tendency is the growth of cardinality and network architecture cannot be control to favor this absorbing effect. In order to limit this tendency, we introduced the notion of aging and maturity as following:

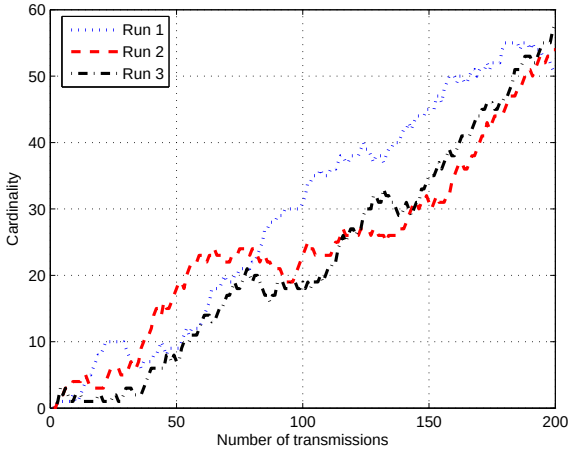

Figure 6.4 – Message cardinality vs the number of transmissions [36]

Definition 7 (Age of a packet [38]) *The age of a packet is the number of times the packet contributes to a coded message and the age of a coded message is defined as the age of the oldest packet in the coded message.*

Definition 8 (Maturity [38]) *The maturity of a network is the highest allowed age for all the packets in the network.*

The aging concept is illustrated on Fig. 6.5 where 2 intermediate nodes are emulated, the maturity is set to 2 and each packet is upper-scripted by its age. For instance at time $t_0 + 4T$, IN_2 receives $3^1 \oplus 1^2 \oplus b^2$ and d^0 and performs a procedure to check the age of each packet in messages the node received. Packets b and 1 achieve the maturity and hence no more packets are allowed to be coded with this message. This implies naturally a throughput loss since packet d^0 and message $3^1 \oplus 1^2 \oplus b^2$ need to be sent in two channel uses, however it saves buffering resources at end nodes.

By introducing the notion of coding graph [36, 38], we were able to state two theorems on message cardinality and the number of transmissions needed to exchange P packets between two end nodes [38]:

Theorem 6 (Message cardinality with aging) *Given a network $G = (V, E)$, a coding capacity $\c{C}$ and a maturity scalar μ in $\mathbb{N}^+$, the cardinality of any coded message in the network is bounded by $\c{C}^{\mu}$.*

Theorem 7 (Maximum number of transmissions with aging) *Given a linear network $G = (V, E)$ with two end nodes and a maturity scalar $\mu \in \mathbb{N}^+$, the number of transmissions needed to exchange a total of P packets between the two end nodes is given by*

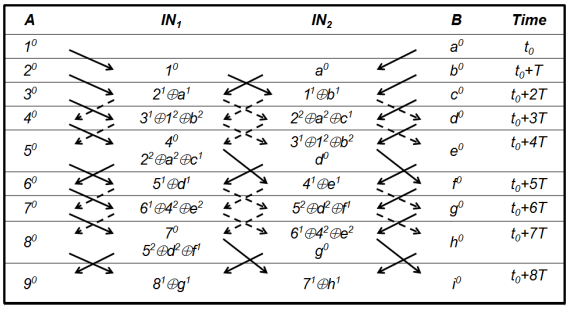

Figure 6.5 – Aging effect with two intermediate nodes [36]

$$T(N,\mu,P) = (N-1)P - P\frac{\frac{\mu(\mu+1)}{2} - 2\sum_{i=1}^{\mu}\max\left(0,\left\lceil\frac{i-\lceil\frac{N-2}{2}\rceil}{2}\right\rceil\right)}{2\min\left(\mu,\lceil\frac{N-2}{2}\rceil\right) + 2\max\left(0,\left\lceil\frac{\mu-\lceil\frac{N-2}{2}\rceil+1}{2}\right\rceil\right)} \tag{6.6}$$

where N is the total number of nodes in the network.

Figs 6.6(a) and 6.6(b) show the cardinality and the total number of transmissions respectively when aging is applied. In Fig. 6.6(a) the cardinality obtained by simulation is polynomially fitted to smooth the plots. The figure shows the cardinality of coded messages in the queue of an intermediate node for three different values of maturity with a coding capacity Ç set to 2. According to Theorem 6, the maximum cardinality is well bounded by $Ç^{\mu}$. Fig. 6.6(b) compares the expression obtained in Theorem 7 with simulations according to the maturity age and in function of the number of nodes in the network for $P = 1000$ packets exchanged between end nodes. A perfect agreement between theory and simulation can be first remarked and the number of transmissions reduces when the maturity increases, as expected.

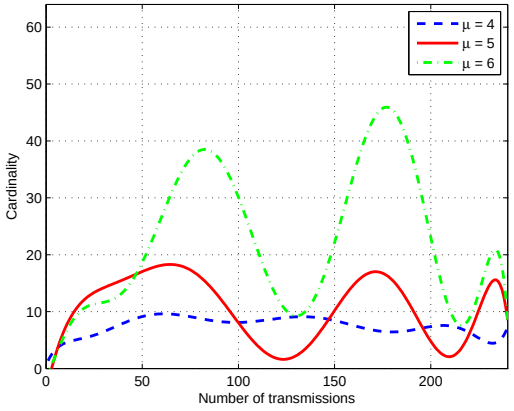

(a) Cardinality with aging in 7 nodes network [36]

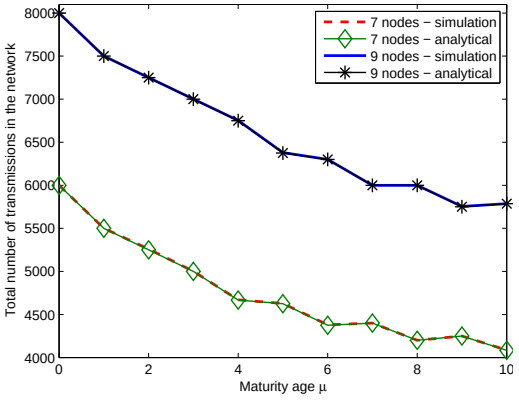

(b) Number of transmissions vs. maturity [36]

Figure 6.6 – Effect of aging on message cardinality and on number of transmissions

The take-home message here is the proposition of a practical implementable notion that can make NC viable with practical hardware and software constraints in real networks and supported by theorems.

6.3.2 Decoding at intermediate nodes

Several NC protocols rely on buffering received packets to forward linear combinations of these packets. The authors of the work in [193] have studied distributed implementations of random linear physical network coding and have proved that their solution allows to keep minimal buffer sizes while maintaining optimal performance in terms of bandwidth utilization. A buffer-aware cross-layered approach for NC has been discussed in [194]. In their solution, some packets are transmitted without NC to reduce the delay of a packet. Reliable data storage over a long period of time using a distributed collection, maybe unreliable, of storage nodes has been investigated in [195].

With NC, packets injected into the network are duplicated by mean of coding and broadcasting making very difficult to control packet redundancy. The aging concept introduced earlier allows to limit the number of times a packet is used in a message but does not limit the redundancy of packets traveling into the network. To this end, intermediate nodes may have to handle themselves the packet redundancy without compromising the decidability at end nodes. Let us consider the flowchart of a two intermediate nodes network in Fig. 6.7 where the received and transmitted messages are shown at each iteration in the first and second line respectively. At $t_0 + 2T$, IN_1 receives packets P_{a2} and P_{b1} in unicast and broadcasts the coded message $P_{a2} \oplus P_{b1}$. Both packets P_{a2} and P_{b1} are moreover buffered in IN_1 instead of being removed from the queues as it was previously the case. At iteration $t_0 + 4T$, P_{a2} is received back at IN_1 through the coded message $P_{a2} \oplus P_{b3}$. This message has to be delivered also at destination B with broadcast and hence P_{a2} is redundant and can be safely removed from the network since it has already been delivered to B, if no packet loss occurred.

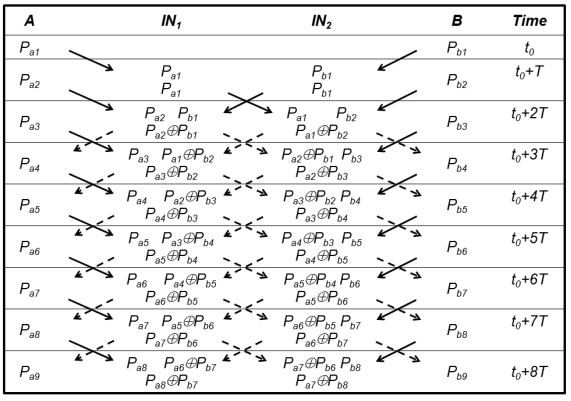

Figure 6.7 – Decoding at intermediate nodes [36]

Each intermediate node is equipped with a buffer used to store received packets. When a node receives a message, it performs a simple procedure consisting in comparing the packets in the coded message to packets buffered [37]. If a match is found, that indicates this packet has already reached this node in previous transmissions and is now on its way to destination. The presence of this packet in the coded message is a consequence of NC and can be safely removed from the message.

This procedure implies to buffer some packets at each intermediate node and the buffering time a packet is hold in the buffer is an important characteristic for end-to-end QoS. We have proved the following theorem on buffering time, $B_t(i)$, at node i.

Theorem 8 (Buffering time [37]) *Let consider a linear network. The maximal buffering time $B_t(i)$ at node i can be upper-bounded as*

$$B_t(i) \leq q_s(i)t_m(i) + \max_j \{q_s(j)t_m(j)\}\, j \in \mathcal{N}_i^+ \tag{6.7}$$

where $q_s(i)$ is the queue size at node i, $t_m(i)$ is the average time between two transmissions and $\mathcal{N}_i^+$ is the set of nodes neighboring node i.

Figs 6.8(a) and 6.8(b) show the average and maximal percentage of buffering time when decoding at end and intermediate nodes respectively. The percentage is computed w.r.t. the total communication time. When decoding at end nodes, Fig. 6.8(a), buffering at end nodes only is needed, however it requires an important amount of storage resource. In average, packets need to be buffered half of the total communication duration and almost all the communication time in the worst case for a network with 8 nodes. This is because early generated packets might remain in coded messages during all communication time.

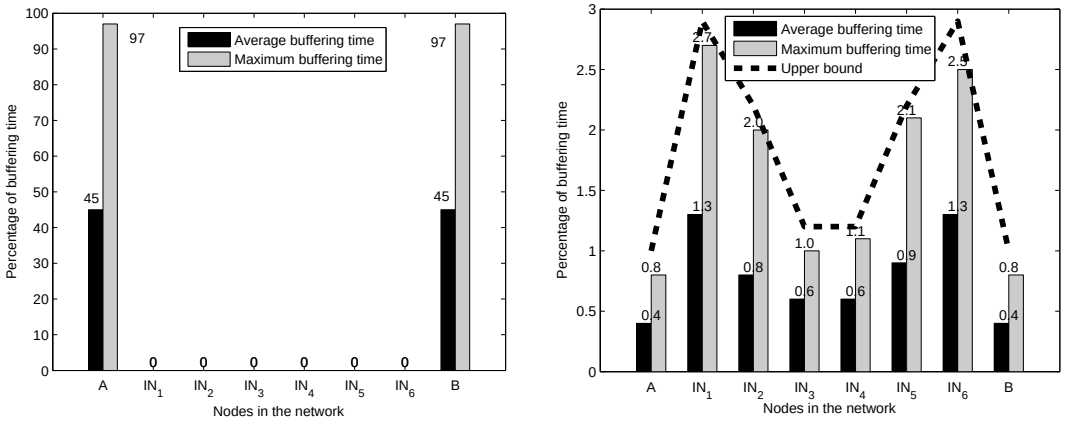

(a) Decoding at end nodes

(b) Decoding at intermediate nodes

Figure 6.8 – Average and maximal buffering time for decoding at end, Fig. 6.8(a), and intermediate nodes, Fig. 6.8(b), when exchanging 1000 packets in a 8 nodes network [36]

Figure 6.8(b), on the other hand, shows that decoding at intermediate nodes allows to save a lot of storage resources. First, the buffer size at end nodes is largely reduced and second, even if intermediate nodes need to store packets, the total buffering time does not exceed 6.3% in average and 13% in the worst case. Moreover our upper-bound in Theorem 8 gives a good estimation of the maximal buffering time at each node.

When it comes with practical implementation of NC, the overhead implies by the protocols needs to be assessed in terms of the number of exchanged bytes in the network. This depends on the message cardinality, the number of nodes, i.e. N, the number of exchanged packets by the two end nodes, i.e. P, and the payload and header sizes, i.e. P_a and P_h respectively. One can obtain that the number of extra-bytes exchanged due to coding activity of three protocols, i.e. traditional store and forward, NC-decoding at end nodes and NC-distributed decoding, is at least as in Table 6.3 [37].

Figure 6.9 shows the number of exchanged bytes in the network according to the number of exchanged packets for the three protocols of Table 6.3. The packet size is $P_a = 1500$ bytes, which is typically used in Ethernet-based networks. Header size is set to $P_h = 15$ bytes and $P = 1000$ packets are exchanged between two end nodes, i.e. 500 each. The expressions given in Table 6.3 constitute good lower bounds on the number of transmitted

Protocol	Transmissions	Exchanged bytes	
Traditional store and forward	$(N-1)P$	$(N-1)PP_a$	(6.8)
NC-decoding at end nodes	$N\frac{P}{2}$	$N\frac{P}{2}P_a + P_h(N-2)\frac{P(P+2)}{8}$	(6.9)
NC-distributed decoding	$N\frac{P}{2}$	$N\frac{P}{2}P_a + P_h(N-2)P$	(6.10)

Table 6.3 – Lower bound on the number of bytes exchanged with each protocol [37]

bytes for NC with decoding at end or intermediate nodes. One can remark that decoding at end nodes implies a quadratic behavior on the number of exchanged bytes as suggested by (6.9) and verified in Fig. 6.9. The direct consequence in that case is that NC is no more interesting compared to a simple store and forward relaying scheme once the number of exchanged packets exceeds 400. This is due to the increase of message cardinality and the addition of header at each coding activity. On the other hand, with distributed decoding, number of exchanged bytes grows linearly with P and makes NC an interesting technology compared to nodes with just store and forward ability.

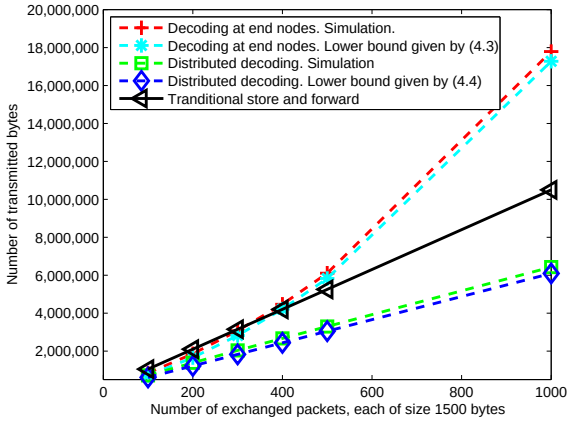

Figure 6.9 – Number of bytes transmitted in the network for different protocols with $P_a = 1500$ bytes [36, 37]

It is worth mentioning that this practical aspects of NC are barely taken into account in literature but are of primary importance to make NC a viable technology. Links were considered error-free so far, i.e. no packet loss occurred when messages are transmitted. In the next section, the impact of packet loss in NC performance is discussed.

6.4 Recovery from packet loss

In traditional store and forward networks, the loss of a packet does not impact the decoding of other packets. With NC, when a message is lost, and thus a certain number of packets, it may affect the decoding of subsequent messages. In that case, the lost packets will be asked to be transmitted again. The delivery delay is not only compromised but also the bandwidth usage is increased. Let us consider a 5-nodes network and let us investigate what happens when a loss occurred in a transmission in Fig. 6.10 where

dash and solid arrows stand for broadcast and unicast transmissions respectively. In this example, maturity is set to 3 and each packet is superscripted by its age. At iteration 7, message $P_{a5}^2 \oplus P_{b5}^2$ is lost and this creates a discrepancy with a situation where no lost occurs. Not only, packet P_{a5} cannot be decoded at B at iteration 9, but also P_{b7} cannot be coded with a message at iteration 8 in IN_3. This implies two channel uses at iteration 9 from IN_2. The effect of packet loss lasts till iteration 13, without talking about that some packets have been lost.

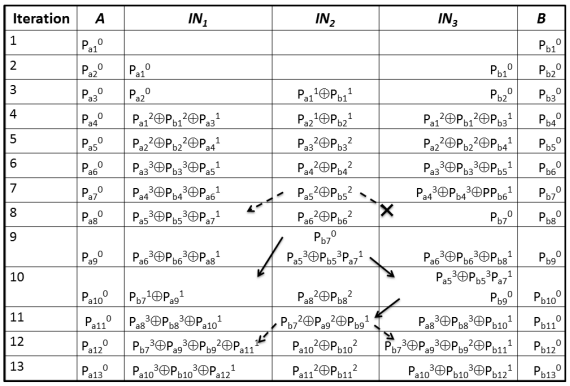

Figure 6.10 – Impact of packet loss in a 5-nodes network with NC [36]

6.4.1 Decoding at end nodes

In traditional communication protocols, end-to-end reliability relies on the transport layer that uses ARQ protocol to ensure the packet delivery from source to destination. Moreover, hop by hop reliability is ensure at data-link and PHY layer with HARQ protocols. In this work, ARQ refers to a level-4 request. In order to deal with packet loss, two recovery procedures have been proposed, named immediate retransmission request (IRR) and basic covering set discovery (BCSD) [39].

Immediate retransmission request. End nodes buffer packets for decoding purpose. When an end node receives an undecodable message, it is able to identify, by reading the message header, those packets that exist at destination and compares those with packets in its buffer. The packets that are not present in the buffer are immediately requested for retransmission without waiting for a demand from layer 4. Due to delay and unordered arrivals of messages at the receiver, a single message that is not decodable is not a sign of packet loss. One might suspect that a loss occurred when undecodable message remains undecoded during a specific duration or when receiving a certain amount of undecodable messages. The request for packet retransmissions is incorporated in the header of a newly generated packet or with a specific packet, just asking for retransmission, if no new packet has to be generated. IRR is different from end-to-end ARQ protocol of the transport layer and IRR does not replace ARQ. Indeed, IRR is performed when an undecodable message arrives at destination. However, a packet might be lost with no impact on decoding process. Hence, ARQ of layer-4 takes the lead to request for this specific packet.

Basic covering set discovery. Before summarizing how BCSD works, let us define the closures and covering sets. Let denote by $\mathcal{S}$ and $\mathcal{C}$ the sets of packets and coded messages respectively.

Definition 9 (Simple closure [39]) *Considering NC by XORing packets together, the simple closure of $\mathcal{S}$, denoted by $\mathcal{S}_C^+$, is the set of packets that can be decoded from $\mathcal{C}$ using packets in $\mathcal{S}$.*

Let illustrate this definition by an example. Let $\mathcal{S} = \{p_1, p_2, p_3\}$ the set of packets and $\mathcal{C} = \{p_1p_4, p_1p_3p_5, p_4p_5p_7, p_5p_6p_7, p_6p_8p_9, p_7p_8p_9\}$ the set of coded messages. The simple closure of $\mathcal{S}$ is built as follows:

$$\begin{array}{lll}
\mathcal{S}_C^+ = \{p_1, p_2, p_3\} & & \\
\mathcal{S}_C^+ = \{p_1, p_2, p_3, p_4\} & \text{using} & p_1p_4 \\
\mathcal{S}_C^+ = \{p_1, p_2, p_3, p_4, p_5\} & \text{using} & p_1p_3p_5 \\
\mathcal{S}_C^+ = \{p_1, p_2, p_3, p_4, p_5, p_7\} & \text{using} & p_4p_5p_7 \\
\mathcal{S}_C^+ = \{p_1, p_2, p_3, p_4, p_5, p_7, p_6\} & \text{using} & p_5p_6p_7
\end{array}$$

Definition 10 (Covering set [39]) *$\mathcal{S}^c$ is a covering set of $\mathcal{C}$ if the closure of $\mathcal{S}$ includes all packets that are part of the coded messages in $\mathcal{C}$.*

In the previous example, $\mathcal{S}_C^+$ is not a covering set of $\mathcal{C}$.

Definition 11 (Basic covering set [39]) *A basic covering set $\mathcal{B}$ of $\mathcal{C}$ is a covering set of $\mathcal{C}$ with minimal cardinality.*

The recovery mechanism consists in finding a basic covering set of undecodable messages set $\mathcal{C}$ and packets in the covering set are requested from the sender. When an undecodable message is received, a period of gathering undecodable messages is launched. This period is an application specific parameter that depends on the type of application. It can vary from milliseconds in case of instant messaging where messages need to be delivered sorted to the upper layer, to seconds in case of file exchange where only the complete file needs to be sorted. When the timer times out, the recovery mechanism is launched. For the set $\mathcal{C}$ given as example above, the algorithm builds the incident matrix M such as:

$$M = \begin{array}{c} \\ p_1p_4 \\ p_1p_3p_5 \\ p_4p_5p_7 \\ p_5p_6p_7 \\ p_6p_8p_9 \\ p_7p_8p_9 \end{array} \begin{array}{c} \begin{array}{cccccccc} p_1 & p_3 & p_4 & p_5 & p_6 & p_7 & p_8 & p_9 \end{array} \\ \begin{pmatrix} 1 & & 1 & & & & & \\ 1 & 1 & & 1 & & & & \\ & & 1 & 1 & & 1 & & \\ & & & 1 & 1 & 1 & & \\ & & & & 1 & & 1 & 1 \\ & & & & & 1 & 1 & 1 \end{pmatrix} \end{array}$$

where columns identify the packets in $\mathcal{C}$ and rows represent undecodable chunks of messages sorted by receiving time. An entry equal to 1 indicates that the packet is contained in the undecodable message and the other entries are set to 0. The basic covering set $\mathcal{B}$ is first empty. At each iteration, the column containing the highest number of ones is selected, i.e. highest number of occurrences of undecodable messages, and the corresponding packet is added to the covering set $\mathcal{B}$. In the example above, packet P_5 is first added then the corresponding column is removed. If the resulting matrix contains a row with a single one, then the row is removed with the corresponding column since the corresponding packet can be decoded. If more than one column contain the same number of one, then any one of these columns can be selected. This procedure is repeated until M is empty. In that case, the covering set found is $\mathcal{B} = \{p_5, p_7, p_8\}$

Figure 6.11 compares the delivery time of three protocols for recovering from packet loss, i.e. IRR, BSCD and a revised version of linear network coding [180] in order to be

adapted to our linear network. Figure 6.11(a) investigates the total delivery time for 10^4 packets exchanged in a 6-nodes network according to the loss probability on each link. Total delivery time is computed as the time elapsed between the transmission of the first packet and the reception of the last one. Delivery time increases with packet loss probability but both BCSD and IRR are more efficient that LNC to deliver, in a short time, all packets.

Figure 6.11(b) on the other hand, shows the average delivery time for a packet, computed as the time elapsed between the first transmission of this packet and its reception. In this case, LNC is more robust than IRR and BCSD for large packet loss probability. This is because no transmission is requested in LNC and the increase of average delivery time is due to the time needed at end nodes to gather enough number of messages in order to decode the packets in a block. Moreover, IRR reacts instantaneously to a packet loss while BCSD waits longer to gather sufficient number of undecodable messages to reduce the size of the covering set.

BCSD may be more interesting than the other protocols in case of file exchange application while LNC may be of interest when the average delivery time per packet is the important measure. However, some applications are sensitive to the jitter, i.e. standard deviation of the packet delivery time seen as a random variable. The robustness of these protocols to the jitter has not been investigated but could be an interesting way to pursue.

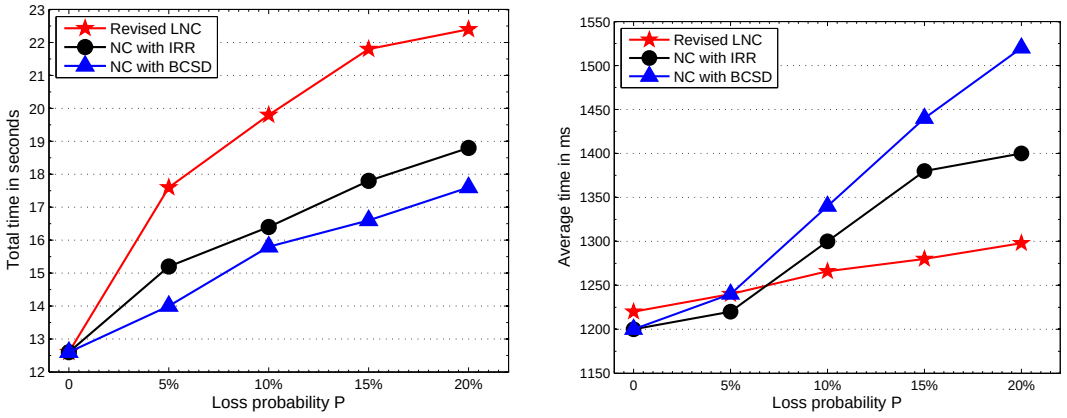

(a) Total delivery time

(b) Average delivery time

Figure 6.11 – Total and average delivery time, Figs. 6.11(a) and 6.11(b) respectively, for a 6-nodes network exchanging 10^4 packets [36, 39]

6.4.2 Decoding at intermediate nodes

A protocol has also been proposed in case where decoding is done at intermediate node [196] but will not be reported here. When decoding is allowing at intermediate nodes, those are required to buffer some packets to remove redundancy in the network. This characteristic can be exploited to detect a loss and recover from it without ACK/NACK messages or requesting for retransmission.

6.5 Conclusion, on-going work and perspective

Although this field was not my main research interest, I found interesting to address the problem of protocols that could make NC work. Finally, my skills acquired in optimization

found also an application in this work by formulating the choice of node activity as the solution of binary integer programming problem for instance. The supervision of Dr. Abdul-Nabi's PhD allowed me to understand how upper-layers of OSI model work and gave me background on protocols at level above the data-link layer. The main contributions in this part can be summarized as follows:

— A practical layer defining which packets could be coded together at a given node has been proposed and named address correlated network coding. This protocol has been tested in the linear network case but easily works in a more general network topology. Moreover based on packets buffering, practical procedures to decode at the end or intermediate nodes have been proposed.

— In a linear network, decoding at the end nodes requires to buffer all transmitted packets until the end of communication if network coding is done at each intermediate node. In order to limit the cardinality of a message, i.e. number of times a packet is used in xoring operations, the concept of **aging** has been introduced. This allows an important amount of storage resources to be saved in the network [38].

— Network coding schemes are more affected by non-reliable links compared to traditional store-and-forward schemes because several packets are lost when a message transmission fails. In order a receiving node to find which packets need to be retransmitted after receiving an undecodable message, we proposed the *basic set covering discovery* procedure. The algorithm aims at finding the smallest set of packets to be retransmitted in order to decode all messages. Simulations showed that BCSD is a good candidate to minimize the total communication completion time [39].

At this time, I have no longer activities on these issues. In the near future, I will investigate more closely information theory and coding as it will be detailed in my research perspectives in the next chapter. Even if NC is not the primary objective of my researches in information theory for IoT, it constitutes a possible solution for some scenarii that could be investigated in ARBurst project.

CHAPTER

7 Research perspectives

In previous chapters, I summarized my scientific contributions through the PhDs I had the luck to co-supervise during the last seven years. I believe I developed solid theoretical background in mathematical optimization through my researches around resource allocations for energy efficient wireless communications. Recently, I have extended my research interests to stochastic geometry and machine learning to characterize large scale networks.

In this chapter, I give the research paths I intend to follow during the next 5 to 10 years. Scientific issues related to the researches developed in previous chapters that will, or may, be pursued have been given at the end of each previous chapters and will not be repeated here. In Section 7.1, I expose the scientific issues of finite block length information theory applied to IoT context that will be investigated in the next 5 years. In Section 7.2, some research paths on machine learning are given and section 7.3 details what could be done in orbital angular momentum (OAM) based communications.

7.1 Models and information theoretic tools for IoT networks

IoT, myth or reality, is in intensive development phase and, if we believe public and technical media, is going to take a major place in telecommunications industry [1, 2]. Whatever it be, no one would deny that IoT has already taken roots in research and development activities both among academics and industrial researchers. Indeed, recent or well established industrial actors have already started deploying IoT networks, such like the french company Sigfox [3], Worldsensing [4] that aims at providing smart cities, but also big companies like Orange, Bouygues, IBM, etc. have invested in the LoRa alliance [5] to build services on this new paradigm. The enthusiasm is so important that IEEE launched the IoT initiative group in 2014 [6] to organize the scientific community and forecast technical issues around IoT technology. The 3GPP working group is intensively involved in the upcoming fifth wireless system generation and plans to standardize IoT technologies [7].

IoT and machine-to-machine (M2M) terms are often equally used in literature. From a technical point of view, IoT refers to a system providing objects with a connection to the Internet, hence requiring a radio infrastructure. On the other hand, M2M refers to an *ad-hoc* communication between two objects without infrastructure. 5G networks could offer these two kinds of communication modes, each having their own constraints and characteristics. From a scientific point of view, future IoT/M2M networks will be characterized by three main features:

— short packet length communications,
— bursty communications,
— high density of nodes.

While the first point invalidates the use of the classical Shannon capacity as performance indicator, the second limits the applicability of the Gaussian assumption to model the interference distribution. As a consequence, stochastic geometry used since years to model interference distribution of large scale networks, [28], should be adapted to take into account the two first characteristics. The traditional energy-capacity tradeoff may not be the more relevant metric to analyze the fundamental bounds of dense IoT/M2M networks as also suggested by some seminal papers [197–199]. In consequence, the fundamental bounds on dense IoT/M2M networks are neither well known nor even well formulated due to the lack of complete theoretical tools. Of course, this state of affairs does not prevent from engineering IoT networks, however we face today the same challenges than those have been met in pre-Shannon era, when engineers tried to optimize communications over noisy channels without knowing if current techniques were close to a fundamental limit or even if such a limit existed. Some important questions that IoT networks may rise and that could be of interest for network operators are: *what is the maximal number of nodes we may deploy in a given scenario at a given packet length? At which energetic cost? With which reliability or latency?*

The short packet length characteristic should be addressed using the non asymptotic information theory background developed by Polyanskiy at Princeton in [40]. Actually,

1. http://www.silicon.fr/linternet-des-objets-un-marche-a-1300-milliards-de-dollars-en-2019-133885.html
2. http://www.silicon.fr/philippe-keryer-organiser-lossature-numerique-des-reseaux-de-demain-133185.html
3. https://www.sigfox.com/en
4. http://www.worldsensing.com
5. https://www.lora-alliance.org
6. http://iot.ieee.org
7. http://www.3gpp.org/news-events/3gpp-news/1785-nb_iot_complete

the development of fundamental bounds when codeword length remains finite can be dated back to Feinstein and Shannon himself around 50's who gave achievability results on the rate. But it was only recently that a complete set of results has been reformulated and rigorously proved. One of the main achievement of this work is the development of a tight approximation of achievability rate that holds in finite block length as:

$$\frac{1}{n}\log_2 M^*(n,\epsilon) = C - \sqrt{\frac{V}{n}}Q^{-1}(\epsilon) + O(\log n) \tag{7.1}$$

where n is the codeword length, C stands for the asymptotic channel capacity, i.e. when $n \to \infty$, ϵ is the error probability, M is the message set cardinality, Q is the gaussian error function and V is the channel dispersion defined as:

$$V = \lim_{\epsilon \to 0} \limsup_{n \to \infty} \frac{1}{n} \left(\frac{nC - \log_2 M^*(n,\epsilon)}{Q^{-1}(\epsilon)} \right)^2 \tag{7.2}$$

which can also be viewed as the variance of the information density $i(X;Y) = \log \frac{dP_{Y|X}}{dP_Y}$ averaged over the joint distribution of (X,Y), where $\frac{dP_{Y|X}}{dP_Y}$ should be understood in the sense of Radon-Nikodym derivative. Expression in (7.1) is the achievable rate when n remains bounded and is a second-order result. The dispersion term in (7.2) is the rate penalty from Shannon capacity for a system operating at $n < \infty$. Non asymptotic information theory is at this time a very hot topic, not only from a theoretical perspective with dedicated sessions in information theory conferences, e.g. ISIT [8], ITW [9], but also from practical point of view with its insights in short packet length communications. Polyanskiy derived achievability and converse bounds in finite block length regime in binary symmetric channel, binary erasure channel, Gilbert-Elliot channel, AWGN channel and communications with feedback. Since then, some authors have addressed the fundamental bounds of finite block-length multi-user communication problems, i.e. multiple access channel (MAC), broadcast channel (BC) and AWGN or fading environments, e.g. [105, 200]. However, several problems are still opened that I would like to deal with in the next years, in the framework of the ARburst ANR project in collaboration with Prof. Jean-Marie Gorce, CITI, INSA Lyon and Prof. Laurent Clavier, IRCICA, Telecom Lille.

Multi-objective framework for IoT. The first important step to characterize the fundamental bounds for IoT network is to define which relevant criteria should be used for this purpose. As mentioned above, spectral efficiency is not the only criterium to be optimized in dense IoT networks since few bytes of information have to be sent time-to-time. However, the number of nodes that can be deployed in a given area for a given error probability for a finite block length n makes more sense. Moreover, the latency induced by the massive multi-users characteristic, in MAC or BC scenarii, is another important criteria and does not only rely on channel block length n. Indeed, in asymptotic regime, users' information can be spread out over infinite block length, i.e. $n \to \infty$ which allows to derive, via superposition coding technique, the achievable rates of dense BC and MAC scenarii [201]. However, when finite block length is considered, there is a finite number of users that can be scheduled at a given time which impacts the latency of global system. This issue is actually under investigation with the PhD of Dadja Toussaint Anade Akpo that I co-supervise with Prof. Jean-Marie Gorce.

8. International symposium on information theory
9. Information theory wokshop

Fundamental bounds in dense MAC and BC scenarii. We refer to *network asymptotic regime* the case where a very dense network is considered such that nodes can be approximated with a continuum [201]. On the other hand *packet non-asymptotic regime* refers to finite block length channel codeword hypothesis. Although some authors have addressed the problem of achievable rate and converse for MAC and BC in packet non-asymptotic regime, e.g. [200], the derived bounds often rely on union of convex sets that is already difficult to evaluate for 2 users but for which no relevant insights can be drawn for K users. Hence from my point of view, this approach will not give practical insights for a scenario with hundreds, or more, nodes. The spatial continuum notion, introduced in [201], for MAC and BC seems a good starting point. Can a channel dispersion for spatial continuum MAC and BC be defined? Answering that question would allow to assess not only the gap between packet asymptotic and non-asymptotic regime but also between network asymptotic and non asymptotic regime, i.e. bounded number of users in the cell. This study will also be conducted within the PhD thesis mentioned above.

Fundamental bounds in dense bursty communications. The non-fully coordinated feature of IoT networks makes communications bursty by essence. This would be even more the case for M2M scenario leading to the interference channel (IC) in information theory problems. In uncoordinated IoT/M2M networks, interference experienced at a given receiving node may not be Gaussian. Even if the large number of nodes suggests that central limit theorem may apply, a few strong interferers are enough to invalidate the Gaussian assumption on the interference distribution. One may use $\alpha-$stable distributions to model these rare events or other kind of distributions able to capture impulsiveness property, e.g. Gaussian mixture. While studying the dispersion matrix of Gaussian channel, some authors concluded that i.i.d. Gaussian input, although capacity-achieving, is not second order-rate optimal, i.e. in finite block-length scenario, it is hence interesting to wonder what happens in additive $\alpha-$stable noise. In packet asymptotic regime, outer bound can be at least simulated by maximizing $I(X;Y)$ under average power constraint on input, but this does not lead to a closed-form solution for capacity in $\alpha-$stable noise for $\alpha < 2$. However, adapting the input constraint cost can lead to a lower bound on capacity in packet asymptotic regime [202]. But more important, in packet non-asymptotic regime, one can still impose the codewords x^n of length n to be on a *power shell* $\mathcal{F}_n = \left\{x^n \in \mathbb{R}^n : ||x^n||^2 = nP\right\}$, or any other cost constraint, and try to investigate the approach of [203]. This relies on the definition of a *modified information density* $\tilde{i}(X^n, Y^n) = \log \frac{P_{Y^n|X^n}(Y^n|X^n)}{Q_{Y^n}(Y^n)}$ where Q_{Y^n} is an arbitrary distribution chosen to minimize an error probability on a binary hypothesis testing problem. The first challenge is to determine at which conditions the capacity result in [202] can be considered as the first moment of the modified information density, i.e. $\mathrm{E}_{Q_{Y^n}} \tilde{i}(x^n, Y^n)$ for a given entry x^n and the second is to define a dispersion for the additive stable noise channel which cannot be, *a priori*, the second order moment of the modified information density. These studies will be led in collaboration with Profs. Laurent Clavier and Jean-Marie Gorce.

Design of coding schemes and protocols for dense IoT networks. Besides the fundamental bounds discussed above, performance of practical short length coding schemes and protocols should be evaluated in the framework defined above. In our recent work in [41], we investigated the practical impact of finite-block length communication on some criteria used to rate the performance of wireless systems in various environments, e.g. EE-SE tradeoff, outage probability and average error probability in fading channels. Moreover,

finite-block length has already been successfully employed to characterize the performance of practical retransmission schemes [104]. I believe that it could be interesting to study the behavior according to n of some coding schemes known to be asymptotically efficient, e.g. polar codes, in finite block length regime. Moreover, superposition coding is known to be capacity-achieving of BC and MAC (with transferable power). However, in finite block length, this is not proved yet and hence the research for the best protocol achieving the fundamental bounds discussed above would be interesting. The performance of fountain codes could also be interesting to assess in case of high density of nodes in BC scenario when a set of files or parameters should be shared with all nodes. In particular random linear coding can get arbitrary close to the Shannon limit when the number of packets to encode tends toward infinity, this should be studied in finite block length hypothesis.

7.2 Machine learning

As described in Chapter 5, reinforcement learning techniques consist for an agent in choosing a policy that maximizes its long term reward according to its past actions and the state observations of the environment. There are basically two ways to tackle MAB settings, i.e. the Bayesian and frequentist approaches. In parametric MAB, bandits are parameterized by an unknown set of parameters which is assumed to be drawn from *a prior* distribution in Bayesian approach and to be unknown but deterministic in frequentist formulation. In Bayesian approach, we search for characterizing the *a posteriori* law of the parameter θ_a of arm a conditioned on the past observations on this arm while in the frequentist approach θ_a is estimated thanks to some estimators, e.g. maximum likelihood, or with confidence bounds [204]. The Bayesian algorithms have been first designed to maximize the long term reward and frequentist algorithms to minimize the average regret. However, one should separate the performance measures to the statistical approaches, i.e. frequentist or Bayesian, and one can show that Bayesian algorithms can be relevant in a frequentist framework [204]. Recent theoretical advances in MAB issues have allowed to show that index-based policies, e.g. KL-UCB, Bayes-UCB, are asymptotically optimal in terms of regret, i.e. they achieve the lower bound on the regret when the number of plays goes to infinity, but also in finite horizon setup. I think that interesting links can be made between finite block length information theory and reinforcement learning and MAB problems in particular.

Finite block length learning. Let consider the interaction of an agent with its environment as a Markov decision process $(\mathcal{X}, \mathcal{A}, \mathcal{P}, \mathcal{R})$, where calligraphed letters are the space of states, the space of actions, the transition state kernel, i.e. $\mathcal{P} : \mathcal{X}, \mathcal{A} \to \mathcal{X}$, and the reward function, i.e. $\mathcal{R} : \mathcal{X}, \mathcal{A} \to \mathbb{R}$ respectively. The bandit problem may be viewed as a compression problem, where return is a measure of a quality and action is a lossy or lossless representation of the state. Among the policies with the same return, one may choose the most compact one. Tackling *machine learning* problems with information-theoretic tools is not new and has been investigated in [205–207]. For instance, [205] investigated the minimization of average cost under infinite horizon using Lempel-Ziv coding concept. The approach of [207] consists in defining the information that action A carries about the state X under policy π as the mutual information between these two random variables, i.e. $I^{\pi}(A; X)$. Based on that, they proposed a formulation to maximize the expected reward under constant mutual information. These works, however, considered *asymptotic* information-theoretic tools and it would have been interesting to compare the insights of the formulation given in these papers to the so-called regret notion used by the machine

learning community. I think that the formalism of finite block length information theory could bring interesting insights for the finite horizon analysis of RL. Indeed, it could be interesting to start from the formalism of [207] by defining for instance the *information density* carried by action A about the state X under policy π, i.e. $i^{\pi}(A;X) = \log \frac{dP_{A|X}}{dP_A}$ and try to derive second-order results when the description length of these random variables remains bounded. In the particular context of MAB, the best arm identification problem that has been dealt with in [204], could be tackled with information-theoretic tool and compared to the complexity measure proposed in [204].

7.3 Orbital angular momentum based communications

In 2014, I submitted a junior researcher project at ANR for funding on OAM based communications that has unfortunately not been funded at this period. Since then I did not work a lot on this topic due to the lack of resources, but I think that some issues in particular scenarii could be addressed. OAM is one physical observable quantity in electromagnetic (EM) radiation. Nowadays, only linear momentum carried out by the Poynting vector is used to transport informations over long distances. In addition to linear momentum, EM waves have an angular momentum [208] which can be split into two parts : the intrinsic and the extrinsic angular momentum. The first one is related to the polarization [209], the second one is related to OAM of the photon. Contrary to the polarization which can only take two distinct values, OAM is characterized by the topological charge l which can take an infinite number of discrete values.

From a wave point of view, one of the characteristic of OAM is an helical phase front, depending on the azimuthal angle and the topological charge l, contrary to the plane wave for which the phase front is uniform, as illustrated on Fig. 7.1 for $l = +3$. This phenomena can theoretically lead to orthogonal channels which can be used for the transmission of the information. Recently, Thidé *et al.* have been interested in OAM in the radio frequency band [210, 211] and have shown that EM waves carrying an OAM can be generated using a circular antenna array. From the receiving side, the topological charge l can be detected by phase gradient method in the propagation front [212]. Recently, Edfors and Johansson have proved that OAM is a subset of the singular value decomposition (SVD) of MIMO systems in free space propagation scenario [213]. From this paper followed a rather tough discussion between the authors and Thidé; the former claiming that nothing new was revealed by OAM compared to MIMO and the later claims that the former did not fully understand what OAM physically is. Without entering into such a polemic, both are rights from their own perspective. Indeed, physicists have well described angular momentum as an observable quantity on its own right since almost a century [208]. Thidé and his co-workers, who are physicists and not researchers in electrical engineering, wanted to show that it is possible to generate EM wave carrying out OAM with a circular antenna array made of elementary dipoles and they conclude, maybe a little bit too fast, that it can increase the capacity of wireless communications. If wireless systems used this classical array technique, it is clear that it cannot give any additional degrees of freedom compared to MIMO and overall OAM is the spatial multiplexing solution of the MIMO free space scenario, which is an interesting result for itself. It is also interesting to note that even with fancy antenna design as the one presented in [214] with an helical dish, the communication system still remains a MIMO channel. The difference is that orthogonality is intrinsic to the propagation mode, hence no digital baseband processing is needed. The problem however, is the donut-shape power profile of OAM modes $l \neq 0$ with a null power in the propagation direction. Moreover, the signal amplitude falls in $r^{|l|+1}$ which makes very difficult to gather

enough energy on these modes in far-field region. According to physicists however, OAM seems to be *more* than an helical phase front. Actually, this phase front is a manifestation of OAM but measured by means of linear momentum only, i.e. with antenna elements only sensitive to the force produced by the linear momentum on the electrons. OAM is able to produce a force on electrons which is distinct from the translation movement produced by the linear momentum on an antenna. In particular, OAM is able to create a mechanical torque on physical objects that has been experimentally demonstrated by a team from IETR in part [215]. Physicists claim that if we were able to detect this effect and separate this from the classical translation movement of electrons, we could create another degree of freedom to carry the information. The remaining question is *can we?* Some researchers are enthusiastic others are sceptic [216], but the question seems not to be definitively answered. From my point of view, and at this stage of state of the art, OAM cannot increase the

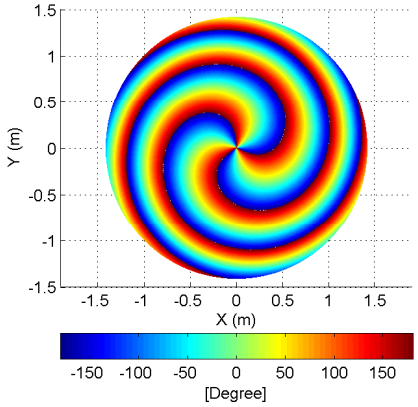

Figure 7.1 – Phase front of an EM wave carrying an OAM $l = +3$

MIMO channel capacity.

In my previous work, without increasing capacity of wireless channels, I have been interested in the error probability on symbols encoded in the spatial phase gradient [217, 218]. If the interest of OAM in radio frequency remains to be still demonstrated, one can envisage this technique for free space optical (FSO) communications for instance where some works have been done but mostly by simulations [219].

OAM for FSO communications. The works in [219, 220] have dealt with multi-dimensional constellation choice for LDPC-OAM based communications in free space optical (FSO) channel. However, no theoretical approach on fundamental performance bounds has been provided. A first interesting research would be to theoretically investigate the achievable rate of FSO communication using OAM with standard MIMO theory by studying how atmospheric disturbance and crosstalk impact the channel capacity in FSO channel. Moreover, the comparison of optical communications using OAM modes with lens-based MIMO systems [221], but transposed in optics, could be an interesting research path.

Encoding in higher algebra structure for OAM communications. As per been done for polarized MIMO channels [222], I think that an interesting research path would be to investigate space-time encoding schemes on higher algebra structure, like quaternion and octonion, for FSO communications. By modeling the extra-dimensional space, but spatially co-located, induced by OAM with hypercomplex numbers, we could assess the

fundamental performance of OAM-based communications without CSI at transmitter. We can start from the works of Belfiore *et al.* on space-time encoding using numbers theory and investigate how this could be applied to FSO channel when using Laguerre-Gauss vortex beams for instance.

Bibliography

[1] H. Shin and J. H. Lee, "On the Error Probability of Binary and M-ary Signals in Nakagami-m Fading Channels," *IEEE Transactions on Communications*, vol. 52, no. 4, pp. 536–539, Apr. 2004.

[2] ——, "Performance Analysis of Space-Time Block Codes Over Keyhole Nakagami-m Fading Channels," *IEEE Transactions on Vehicular Technology*, vol. 53, no. 2, pp. 351–362, Mar. 2004.

[3] P. Mary, M. Dohler, J. M. Gorce, G. Villemaud, and M. Arndt, "BPSK Bit Error Outage over Nakagami-m Fading Channels in Lognormal Shadowing Environments," *IEEE Communications Letters*, vol. 11, no. 7, pp. 565–567, July 2007.

[4] ——, "Estimation du taux de coupure d'une liaison radio MIMO dans un canal de nakagami avec effet de masque," in *Actes du colloque GRETSI*, September 2007.

[5] ——, "M-ary symbol error outage over nakagami-m fading channels in shadowing environments," *IEEE Transactions on Communications*, vol. 57, no. 10, pp. 2876–2879, October 2009.

[6] P. Mary, M. Dohler, J. M. Gorce, and G. Villemaud, "Symbol error outage for spatial multiplexing systems in rayleigh fading channel and lognormal shadowing," in *2009 IEEE 10th Workshop on Signal Processing Advances in Wireless Communications*, June 2009, pp. 349–353.

[7] ——, "Symbol Error Outage Analysis of MIMO OSTBC Systems over Rice Fading Channels in Shadowing Environments," *IEEE Transactions on Wireless Communications*, vol. 10, no. 4, pp. 1009–1014, April 2011.

[8] ——, "Packet Error Outage for Coded Systems Experiencing Fast Fading and Shadowing," *IEEE Transactions on Wireless Communications*, vol. 12, no. 2, pp. 574–585, February 2013.

[9] P. Mary, J. M. Gorce, G. Villemaud, M. Dohler, and M. Arndt, "Performance Analysis of Mitigated Asynchronous Spectrally-Overlapping WLAN Interference," in *2007 IEEE Wireless Communications and Networking Conference*, March 2007, pp. 2097–2102.

[10] ——, "Reduced Complexity MUD-MLSE Receiver for Partially-Overlapping WLAN-Like Interference," in *2007 IEEE 65th Vehicular Technology Conference - VTC2007-Spring*, April 2007, pp. 1876–1880.

[11] P.-F. Morlat, P. Mary, G. Villemaud, J. M. Gorce, and M. Arndt, "Performance Validation of a Multi-Standard and Multi-Antenna Receiver," in *The European Conference on Antennas and Propagation : EuCAP 2006 (ESA SP-626)*, 2006.

[12] E. Oh, B. Krishnamachari, X. Liu, and Z. Niu, "Toward dynamic energy-efficient operation of cellular network infrastructure," *IEEE Communications Magazine*, vol. 49, no. 6, pp. 56–61, June 2011.

[13] B. Gergely, J. Malmodin, and F. Albrecht, "Economic and Ecological Impact of ICT," EARTH project deliverable D2.1, Tech. Rep., 2012.

[14] M. Maaz, "Resource allocation and performance metrics analysis in cooperative cellular networks," PhD dissertation, INSA de Rennes, Dec. 2013.

[15] H. Bawab, "Power allocation in overlaid DVB-LTE systems," PhD dissertation, INSA de Rennes, Dec. 2015.

[16] C. J. L. Martret, A. L. Deleuze, and P. Ciblat, "Optimal time-hopping codes for multi-user interference mitigation in ultra-wide bandwidth impulse radio," *IEEE Transactions on Wireless Communications*, vol. 5, no. 6, pp. 1516–1525, June 2006.

[17] P. Mary, I. Fijalkow, and C. Poulliat, "Multi-Rate Resource Allocations for TH-UWB Wireless Communications," *IEEE Trans. Wireless Commun.*, vol. 11, no. 12, pp. 4470–4481, Dec. 2012.

[18] M. Maaz, P. Mary, and M. Helard, "Energy Minimization in HARQ-I Relay-Assisted Networks with Delay-limited Users," *IEEE Transactions on Vehicular Technology*, vol. PP, no. 99, pp. 1–1, January 2017.

[19] M. Maaz, J. Lorandel, P. Mary, J.-C. Prévotet, and M. Hélard, "Energy efficiency analysis of hybrid-ARQ relay-assisted schemes in LTE-based systems," *EURASIP Journal on Wireless Communications and Networking*, vol. 2016, no. 1, p. 22, Jan 2016.

[20] H. Bawab, P. Mary, J. Hélard, Y. Nasser, and O. Bazzi, "Spectral Overlap Optimization for DVB-T2 and LTE Coexistence," *Submitted to IEEE Transactions on Broadcasting*, 2017.

[21] A. M. Alam, "Energy efficiency-spectral efficiency tradeoff in interference limited wireless networks," PhD dissertation, INSA de Rennes, March 2017.

[22] N. Modi, "Machine Learning and Statistical Decision Making for Green Radio," PhD dissertation, CentraleSupélec, May 2017.

[23] P. Gupta and P. R. Kumar, "The capacity of wireless networks," *IEEE Transactions on Information Theory*, vol. 46, no. 2, pp. 388–404, Mar 2000.

[24] A. Ozgur, O. Leveque, and D. N. C. Tse, "Hierarchical cooperation achieves optimal capacity scaling in ad hoc networks," *IEEE Transactions on Information Theory*, vol. 53, no. 10, pp. 3549–3572, Oct 2007.

[25] V. Rodoplu and T. H. Meng, "Bits-per-joule capacity of energy-limited wireless networks," *IEEE Transactions on Wireless Communications*, vol. 6, no. 3, pp. 857–865, March 2007.

[26] J.-M. Kelif, M. Coupechoux, and P. Godlewski, "A Fluid Model for Performance Analysis in Cellular Networks," *EURASIP Journal on Wireless Comm. and Networking*, no. 435189, pp. 1–11, August 2010.

[27] A. M. Alam, P. Mary, J. Y. Baudais, and X. Lagrange, "Energy Efficiency-Spectral Efficiency Tradeoff in Interference-Limited Wireless Networks with Shadowing," in *2015 IEEE 82nd Vehicular Technology Conference (VTC2015-Fall)*, Sept 2015, pp. 1–5.

[28] J. G. Andrews, F. Baccelli, and R. K. Ganti, "A tractable approach to coverage and rate in cellular networks," *IEEE Transactions on Communications*, vol. 59, no. 11, pp. 3122–3134, 2011.

[29] A. M. Alam, P. Mary, J. Y. Baudais, and X. Lagrange, "Asymptotic analysis of area spectral efficiency and energy efficiency in ppp networks with slnr precoder," *IEEE Transactions on Communications*, vol. PP, no. 99, pp. 1–1, 2017.

[30] J. Mitola and G. Q. Maguire, "Cognitive radio: making software radios more personal," *IEEE Personal Communications*, vol. 6, no. 4, pp. 13–18, Aug 1999.

[31] C. Tekin and M. Liu, "Online algorithms for the multi-armed bandit problem with markovian rewards," in *Communication, Control, and Computing (Allerton), 2010 48th Annual Allerton Conference on.* IEEE, 2010, pp. 1675–1682.

[32] J. Lunden, V. Koivunen, and H. V. Poor, "Spectrum exploration and exploitation for cognitive radio: Recent advances," *IEEE Signal Processing Magazine*, vol. 32, no. 3, pp. 123–140, May 2015.

[33] Y. Wang, Y. Xu, L. Shen, C. Xu, and Y. Cheng, "Two-dimensional pomdp-based opportunistic spectrum access in time-varying environment with fading channels," *Journal of Communications and Networks*, vol. 16, no. 2, pp. 217–226, April 2014.

[34] N. Modi, P. Mary, and C. Moy, "QoS Driven Channel Selection Algorithm for Cognitive Radio Network: Multi-User Multi-Armed Bandit Approach," *IEEE Transactions on Cognitive Communications and Networking*, vol. 3, no. 1, pp. 49–66, March 2017.

[35] ——, "TRQoS-UCB: A Transfer Restless QoS-UCB Policy for Energy Efficient Heterogeneous Cellular Networks," *Submitted to IET Communications*, 2017.

[36] S. Abdul-Nabi, "Centralized and distributed address correlated network coding protocols," PhD dissertation, INSA de Rennes, Sep. 2015.

[37] S. Abdul-Nabi, P. Mary, A. Khalil, and J. F. Hélard, "Novel distributed decoding scheme for efficient resource utilization in network coding," in *2015 IEEE Wireless Communications and Networking Conference (WCNC)*, March 2015, pp. 1012–1017.

[38] S. Abdul-Nabi, A. Khalil, P. Mary, and J. F. Hélard, "Aging in Network Coding," *IEEE Wireless Communications Letters*, vol. 4, no. 1, pp. 78–81, Feb 2015.

[39] S. Abdul-Nabi, A. Khalil, P. Mary, and J.-F. Hélard, "Efficient network coding solutions for limiting the effect of packet loss," *EURASIP Journal on Wireless Communications and Networking*, vol. 2017, no. 1, p. 35, Feb 2017.

[40] Y. Polyanskiy, H. Poor, and S. Verdu, "Channel Coding Rate in the Finite Blocklength Regime," *IEEE Transactions on Information Theory*, vol. 56, no. 5, pp. 2307–2359, May 2010.

[41] P. Mary, J. M. Gorce, A. Unsal, and H. V. Poor, "Finite Blocklength Information Theory: What Is the Practical Impact on Wireless Communications?" in *2016 IEEE Globecom Workshops (GC Wkshps)*, Dec 2016, pp. 1–6.

[42] T. M. Cover and J. A. Thomas, *Elements of Information Theory*, 2nd ed. Wiley, 2006.

[43] P. Mary, I. Fijalkow, and C. Poulliat, "Time slot allocation for tdma/cdma th-uwb ad-hoc networks," in *2010 IEEE 11th International Workshop on Signal Processing Advances in Wireless Communications (SPAWC)*, June 2010, pp. 1–5.

[44] S. A. Jafar and A. Goldsmith, "Adaptive Multirate CDMA for Uplink Throughput Maximization," *IEEE Transactions on Wireless Communications*, vol. 2, no. 3, pp. 218–228, Mar. 2003.

[45] Y. Guo and B. Aazhang, "Capacity of Multi-Class Traffic CDMA System with Multiuser Receiver ," in *IEEE Wireless Communications and Networking Conference (WCNC)*, 1999, pp. 500–504.

[46] H. Wymeersch, G. Zussman, and M. Z. Win, "SNR Analysis for MultiRate UWB-IR," *IEEE Communications Letters*, vol. 11, pp. 49–51, 2007.

[47] M. Nasiri-Kenari and M. G. Shayesteh, "Performance Analysis and Comparison of Different Multirate TH-UWB Systems: Uncoded and Coded Schemes," *IEE Proceedings - Communications*, vol. 152, no. 6, pp. 833–844, 2005.

[48] M. Z. Win and R. A. Scholtz, "Ultra-Wide Bandwidth Time-Hopping Spread-Spectrum Impulse Radio for Wireless Multiple-Access Communications," *IEEE Transactions on Communications*, vol. 48, no. 4, pp. 679–689, Apr. 2000.

[49] F. Kharrat-Kammoun, C. J. Le Martret, and P. Ciblat, "Performance analysis of ir-uwb in a multi-user environment," *IEEE Transactions on Wireless Communications*, vol. 8, no. 11, pp. 5552 –5563, nov. 2009.

[50] A. F. Molisch, J. R. Foerster, and M. Pendergrass, "Channel models for ultrawideband personal area networks," *IEEE Wireless Communications*, vol. 10, no. 6, pp. 14–21, Dec. 2003.

[51] A.-L. Deleuze, C. J. Le Martret, P. Ciblat, and E. Serpedin, "Cramer-Rao Bound for Channel Parameters in Ultra-Wide Band Based System," in *IEEE 5th Workshop on Signal Processing Advances in Wireless Communications (SPAWC)*, july 2004.

[52] P. Mary, I. Fijalkow, and C. Poulliat, "Adaptive Rate Allocation Scheme for Uplink TH-UWB Networks," in *IEEE International Conference on Communications (ICC)*, June 2011.

[53] S. Boyd, S.-J. Kim, L. Vandenberghe, and A. Hassibi, "A tutorial on geometric programming," *Optimization and Engineering*, vol. 8, no. 1, pp. 67–127, 2007.

[54] M. Dohler, "Virtual Antenna Arrays," Ph.D. dissertation, King's College London, 2003.

[55] J. N. Laneman, "Cooperative diversity in wireless networks: Algorithms and architectures," Dissertation, MASSACHUSETTS INSTITUTE OF TECHNOLOGY, 2002.

[56] M. Dohler and Y. Li, *Cooperative Communications: Hardware, Channel and PHY*. Wiley, 2010.

[57] J. N. Laneman and G. W. Wornell, "Distributed Space-Time Coded Protocols for Exploiting Cooperative Diversity in Wireless Networks," *IEEE Transactions on Information Theory*, vol. 49, no. 10, pp. 2415–2425, Oct. 2003.

[58] J. N. Laneman, D. N. C. Tse, and G. W. Wornell, "Cooperative Diversity in Wireless Networks: Efficient Protocols and Outage Behavior," *IEEE Transactions on Information Theory*, vol. 50, no. 12, pp. 3062–3080, dec. 2004.

[59] A. Ribeiro, X. Cai, and G. B. Giannakis, "Symbol Error Probabilities for General Cooperative Links," *IEEE Transactions on Wireless Communications*, vol. 4, no. 3, pp. 1264–1273, May 2005.

[60] T. Cover and A. Gamal, "Capacity theorems for the relay channel," *Information Theory, IEEE Transactions on*, vol. 25, no. 5, pp. 572–584, 1979.

[61] B. Nazer and M. Gastpar, "Compute-and-Forward: Harnessing Interference Through Structured Codes," *IEEE Transactions on Information Theory*, vol. 57, no. 10, pp. 6463–6486, Oct 2011.

[62] W. Nam, W. Chang, S.-Y. Chung, and Y. Lee, "Transmit Optimization for Relay-Based Cellular OFDMA Systems," in *Communications, 2007. ICC '07. IEEE International Conference on*, june 2007, pp. 5714 –5719.

[63] T. Wang and L. Vandendorpe, "WSR Maximized Resource Allocation in Multiple DF Relays Aided OFDMA Downlink Transmission," *IEEE Transactions on Signal Processing*, vol. 59, no. 8, pp. 3964–3976, Aug 2011.

[64] K. Vardhe, D. Reynolds, and B. Woerner, "Joint power allocation and relay selection for multiuser cooperative communication," *IEEE Transactions on Wireless Communications*, vol. 9, no. 4, pp. 1255 –1260, april 2010.

[65] A. Le Duc, "Performance Closed-form Derivations and Analysis of Hybrid ARQ Retransmission Schemes in a Cross-layer Context," Ph.D. dissertation, Telecom ParisTech, 2010.

[66] D. Chase, "Code Combining–A Maximum-Likelihood Decoding Approach for Combining an Arbitrary Number of Noisy Packets," *IEEE Transactions on Communications*, vol. 33, no. 5, pp. 385–393, 1985.

[67] J. Hagenauer, "Rate-compatible punctured convolutional codes (RCPC codes) and their applications," *IEEE Transactions on Communications*, vol. 36, no. 4, pp. 389–400, 1988.

[68] D. Hui, V. Lau, and W. H. Lam, "Cross-Layer Design for OFDMA Wireless Systems With Heterogeneous Delay Requirements," *IEEE Transactions on Wireless Communications*, vol. 6, no. 8, pp. 2872 –2880, august 2007.

[69] S. Boyd and L. Vandenberghe, *Convex Optimization*. New York, NY, USA: Cambridge University Press, 2004.

[70] M. Maaz, P. Mary, and M. Hélard, "Resource allocation for qos aware relay-assisted ofdma cellular networks," in *2011 Third International Workshop on Cross Layer Design*, Nov 2011, pp. 1–6.

[71] Q. Zhang, W. Cao, and A. Nallanathan, "Cramer-rao lower bounds for uwb localization with antenna array," in *IEEE International Conference on Communications (ICC) 2010*, may 2010.

[72] O. Blume *et al.*, "Most promising tracks of green network technologies," INFSO-ICT-247733 EARTH, Tech. Rep., Dec. 2011.

[73] G. Miao, N. Himayat, G. Li, and S. Talwar, "Distributed interference-aware energy-efficient power optimization," *IEEE Trans. Wireless Commun.,*, vol. 10, no. 4, pp. 1323 –1333, April 2011.

[74] E. V. Belmega, S. Lasaulce, and M. Debbah, "A survey on energy-efficient communications," in *IEEE 22nd Int. Symp. on Personal Indoor and Mobile Radio Commun. (PIMRC), 2011*, Sept. 2011, pp. 1–5.

[75] R. G. Gallager, "Energy limited channels: Coding, multiaccess and spread spectrum," Massachusetts Institute of Technology, LIDS, Tech. Rep., 1987.

[76] S. Verdu, "On channel capacity per unit cost," *IEEE Transactions on Information Theory*, vol. 36, no. 5, pp. 1019–1030, Sep 1990.

[77] B. Hajek and V. G. Subramanian, "Capacity and reliability function per fourth moment cost for wssus fading channels," in *Proceedings of the 1999 IEEE Information Theory and Communications Workshop*, 1999, pp. 42–44.

[78] A. El Gamal and S. Zahedi, "Minimum energy communication over a relay channel," in *Proc. on IEEE Int. Symp. Inf. Theo.*, June-July 2003.

[79] A. El Gamal, M. Mohseni, and S. Zahedi, "Bounds on capacity and minimum energy-per-bit for awgn relay channels," *IEEE Trans. Inf. Theory*, vol. 52, no. 4, pp. 1545–1561, April 2006.

[80] I. Stanojev, O. Simeone, Y. Bar-Ness, and K. Dong Ho, "Energy efficiency of non-collaborative and collaborative Hybrid-ARQ protocols," *IEEE Trans. Wireless Commun.*, vol. 8, no. 1, pp. 326–335, Jan. 2009.

[81] Y. Qi, R. Hoshyar, M. Imran, and R. Tafazolli, "H2-ARQ-relaying: Spectrum and energy efficiency perspectives," *IEEE J. Sel. Areas Commun.*, vol. 29, no. 8, pp. 1547 –1558, Sept. 2011.

[82] R. Zhang, J.-M. Gorce, and K. Jaffres-Runser, "Low bound of energy-latency tradeoff of opportunistic routing in multi-hop networks," in *ICC '09. IEEE Int. Conf. on Comm., 2009.*, June 2009, pp. 1–6.

[83] D. Mackay and C. P. Hesketh, "Performance of Low Density Parity Check Codes as a Function of Actual and Assumed Noise Levels," *Electronic Notes in Theoretical Computer Science*, vol. 74, pp. 89 – 96, 2003.

[84] X. Lagrange, "Throughput of HARQ protocols on a block fading channel," *IEEE Communications Letters*, vol. 14, no. 3, pp. 257–259, 2010.

[85] G. Auer, O. Blume, V. Giannini *et al.*, "Energy efficiency analysis of the reference systems, areas of improvements and target breakdown," EARTH, Deliverable D2.3 INFSO-ICT-247733, 2010.

[86] M. Grant and S. Boyd, "CVX: Matlab software for disciplined convex programming, version 2.1," http://cvxr.com/cvx, Mar. 2014.

[87] ——, "Graph implementations for nonsmooth convex programs," in *Recent Advances in Learning and Control*, ser. Lecture Notes in Control and Information Sciences, V. Blondel, S. Boyd, and H. Kimura, Eds. Springer-Verlag Limited, 2008, pp. 95–110.

[88] "3rd Generation Partnership Project; Technical Specification Group Radio Access Network; Evolved Universal Terrestrial Radio Access (E-UTRA); Relay architectures for E-UTRA (LTE-Advanced) (Release 9)," march 2010.

[89] V. Asghari and S. Aissa, "Adaptive Rate and Power Transmission in Spectrum-Sharing Systems," *IEEE Transactions on Wireless Communications*, vol. 9, no. 10, pp. 3272–3280, 2010.

[90] ——, "Resource Management in Spectrum-Sharing Cognitive Radio Broadcast Channels: Adaptive Time and Power Allocation," *IEEE Transactions on Communications*, vol. 59, no. 5, pp. 1446–1457, 2011.

[91] S. Srinivasa and S. Jafar, "How much spectrum sharing is optimal in cognitive radio networks?" *IEEE Transactions on Wireless Communications*, vol. 7, no. 10, pp. 4010–4018, 2008.

[92] A. T. Hoang and Y.-C. Liang, "Downlink Channel Assignment and Power Control for Cognitive Radio Networks," *IEEE Transactions on Wireless Communications*, vol. 7, no. 8, pp. 3106–3117, 2008.

[93] H. Yao, Z. Zhou, H. Liu, and L. Zhang, "Optimal power allocation in joint spectrum underlay and overlay cognitive radio networks," in *Cognitive Radio Oriented Wireless Networks and Communications, 2009. CROWNCOM '09. 4th International Conference on*, 2009, pp. 1–5.

[94] J. Mietzner, L. Lampe, and R. Schober, "Distributed transmit power allocation for multihop cognitive-radio systems," *IEEE Transactions on Wireless Communications*, vol. 8, no. 10, pp. 5187–5201, 2009.

[95] L. Li and A. Goldsmith, "Capacity and optimal resource allocation for fading broadcast channels – Part I: Ergodic capacity," *IEEE Transactions on Information Theory*, vol. 47, no. 3, pp. 1083–1102, 2001.

[96] R. Zhang, S. Cui, and Y.-C. Liang, "On Ergodic Sum Capacity of Fading Cognitive Multiple-Access and Broadcast Channels," *IEEE Transactions on Information Theory*, vol. 55, no. 11, pp. 5161–5178, 2009.

[97] H. Bawab, P. Mary, J. F. Helard, Y. Nasser, and O. Bazzi, "Global Ergodic Capacity Closed-Form Expression of Coexisting DVB-LTE-Like Systems," in *2014 IEEE 79th Vehicular Technology Conference (VTC Spring)*, May 2014, pp. 1–5.

[98] H. Bawab, P. Mary, J. F. Hélard, Y. Nasser, and O. Bazzi, "Ergodic capacity optimization in coexisting dvb-lte-like systems," in *2014 6th International Congress on Ultra Modern Telecommunications and Control Systems and Workshops (ICUMT)*, Oct 2014, pp. 54–59.

[99] N. Ksairi, P. Bianchi, P. Ciblat, and W. Hachem, "Resource Allocation for Downlink Cellular OFDMA Systems - Part I: Optimal Allocation," *IEEE Transactions on Signal Processing*, vol. 58, no. 2, pp. 720–734, Feb 2010.

[100] ——, "Resource Allocation for Downlink Cellular OFDMA Systems - Part II: Practical Algorithms and Optimal Reuse Factor," *IEEE Transactions on Signal Processing*, vol. 58, no. 2, pp. 735–749, Feb 2010.

[101] T. Han and K. Kobayashi, "A new achievable rate region for the interference channel," *IEEE Transactions on Information Theory*, vol. 27, no. 1, pp. 49–60, Jan 1981.

[102] A. Yuille and A. Rangarajan, "The Concave-Convex Procedure," *Neural Computation*, vol. 15, no. 15, pp. 915–936, April 2003.

[103] M. Maaz, P. Mary, and M. Hélard, "Energy efficiency analysis in relay assisted hybrid-ARQ communications," in *PIMRC*. IEEE, 2012, pp. 2263–2268.

[104] B. Makki, T. Svensson, and M. Zorzi, "Finite Block-Length Analysis of the Incremental Redundancy HARQ," *IEEE Wireless Communications Letters*, vol. 3, no. 5, pp. 529–532, Oct 2014.

[105] W. Yang, G. Durisi, T. Koch, and Y. Polyanskiy, "Quasi-static multiple-antenna fading channels at finite blocklength," *IEEE Transactions on Information Theory*, vol. 60, no. 7, pp. 4232–4265, July 2014.

[106] E. Pollakis, R. L. Cavalcante, and S. Stańczak, "Base station selection for energy efficient network operation with the majorization-minimization algorithm," in *IEEE 13th International Workshop on Signal Processing Advances in Wireless Communications (SPAWC)*, 2012, pp. 219–223.

[107] J. Gong, J. S. Thompson, S. Zhou, and Z. Niu, "Base station sleeping and resource allocation in renewable energy powered cellular networks," *IEEE Transactions on Communications*, vol. 62, no. 11, pp. 3801–3813, 2014.

[108] J. M. Gorce, D. Tsilimantos, P. Ferrand, and V. H. Poor, "Energy-Capacity Tradeoff Bounds in a Downlink Typical Cell," in *IEEE 25th International Symposium on Personal Indoor and Mobile Radio Communications (PIMRC)*, September 2014, pp. 1–6.

[109] C. Li, J. Zhang, and K. Letaief, "Performance analysis of SDMA in multicell wireless networks," in *IEEE Global Communications Conference (GLOBECOM)*, 2013, pp. 3867–3872.

[110] A. K. Gupta, H. S. Dhillon, S. Vishwanath, and J. G. Andrews, "Downlink coverage probability in MIMO HetNets with flexible cell selection," in *IEEE Global Communications Conference (GLOBECOM)*, 2014, pp. 1534–1539.

[111] H. S. Dhillon, M. Kountouris, and J. G. Andrews, "Downlink MIMO HetNets: Modeling, ordering results and performance analysis," *IEEE Transactions on Wireless Communications*, vol. 12, no. 10, pp. 5208–5222, 2013.

[112] J. M. Kelif, M. Coupechoux, and P. Godlewski, "Effect of shadowing on outage probability in fluid cellular radio networks," in *2008 6th International Symposium on Modeling and Optimization in Mobile, Ad Hoc, and Wireless Networks and Workshops*, April 2008, pp. 141–150.

[113] G. Auer, V. Giannini, M. Olsson, M. J. Gonzalez, and C. Desset, "Framework for Energy Efficiency Analysis of Wireless Networks," in *2nd International Conference on Wireless VITAE*, February 2011, pp. 1–5.

[114] S. Verdu and T. S. Han, "A general formula for channel capacity," *IEEE Transactions on Information Theory*, vol. 40, no. 4, pp. 1147–1157, Jul 1994.

[115] L. Fenton, "The Sum of Log-Normal Probability Distributions in Scatter Transmission Systems," *IRE Transactions on Communications Systems*, vol. 8, no. 1, pp. 57–67, March 1960.

[116] D. B. Cheikh, J.-M. Kelif, M. Coupechoux, and P. Godlewski, "SIR Distribution Analysis in Cellular Networks Considering the Joint Impact of Path-Loss, Shadowing and Fast Fading," *EURASIP Journal on Wireless Comm. and Networking*, no. 137, pp. 1–10, October 2011.

[117] M. Haenggi, *Stochastic geometry for wireless networks*. Cambridge University Press, 2012.

[118] F. Aurenhammer, "Voronoi diagrams-a survey of a fundamental geometric data structure," *ACM Computing Surveys (CSUR)*, vol. 23, no. 3, pp. 345–405, 1991.

[119] P. Calka, "Precise formulae for the distributions of the principal geometric characteristics of the typical cells of a two-dimensional poisson-voronoi tessellation and a poisson line process," *Advances in Applied Probability*, vol. 35, no. 03, pp. 551–562, 2003.

[120] J.-S. Ferenc and Z. Néda, "On the size distribution of Poisson Voronoi cells," *Physica A: Statistical Mechanics and its Applications*, vol. 385, no. 2, pp. 518–526, 2007.

[121] R. Wang, J. Zhang, S. Song, and K. B. Letaief, "Average throughput analysis of downlink cellular networks with multi-antenna base stations," in *IEEE 25th Annual International Symposium on Personal, Indoor, and Mobile Radio Communication (PIMRC)*, 2014, pp. 1892–1896.

[122] M. Di Renzo, A. Guidotti, and G. E. Corazza, "Average rate of downlink heterogeneous cellular networks over generalized fading channels: A stochastic geometry approach," *IEEE Transactions on Communications*, vol. 61, no. 7, pp. 3050–3071, 2013.

[123] E. Björnson, M. Bengtsson, and B. Ottersten, "Optimal multiuser transmit beamforming: A difficult problem with a simple solution structure," *IEEE Signal Processing Magazine*, vol. 31, no. 4, pp. 142–148, 2014.

[124] D. H. Nguyen and T. Le-Ngoc, "MMSE precoding for multiuser MISO downlink transmission with non-homogeneous user SNR conditions," *EURASIP Journal on Advances in Signal Processing*, no. 1, pp. 1–12, 2014.

[125] S. S. Christensen, R. Agarwal, E. De Carvalho, and J. M. Cioffi, "Weighted sum-rate maximization using weighted MMSE for MIMO-BC beamforming design," *IEEE Transactions on Wireless Communications*, vol. 7, no. 12, pp. 4792–4799, 2008.

[126] P. Cheng, M. Tao, and W. Zhang, "A new SLNR-based linear precoding for downlink multi-user multi-stream MIMO systems," *IEEE Communications Letters*, vol. 14, no. 11, pp. 1008–1010, 2010.

[127] I. Sohn, H. Lee, and K. B. Lee, "Generalized MMSE beamforming for multicell MIMO systems with random user geometry and channel feedback latency," *EURASIP Journal on Wireless Communications and Networking*, vol. 2014, no. 1, pp. 1–10, 2014.

[128] M. Sadek, A. Tarighat, and A. H. Sayed, "A leakage-based precoding scheme for downlink multi-user MIMO channels," *IEEE Transactions on Wireless Communications*, vol. 6, no. 5, pp. 1711–1721, 2007.

[129] P. Patcharamaneepakorn, S. Armour, and A. Doufexi, "On the Equivalence Between SLNR and MMSE Precoding Schemes with Single-Antenna Receivers," *IEEE Communications Letters*, vol. 16, no. 7, pp. 1034–1037, July 2012.

[130] A. Tarighat, M. Sadek, and A. H. Sayed, "A multi user beamforming scheme for downlink MIMO channels based on maximizing signal-to-leakage ratios," in *IEEE International Conference on Acoustics, Speech, and Signal Processing (ICASSP'05)*, vol. 3, 2005.

[131] M. Haenggi and R. K. Ganti, *Interference in large wireless networks*. Now Publishers Inc, 2009.

[132] C. Li, J. Zhang, and K. B. Letaief, "Energy efficiency analysis of small cell networks," in *IEEE International Conference on Communications (ICC)*, 2013, pp. 4404–4408.

[133] E. Bjornson, L. Sanguinetti, and M. Kountouris, "Designing wireless broadband access for energy efficiency: Are small cells the only answer?" in *IEEE International Conference on Communication Workshop (ICCW)*, 2015, pp. 136–141.

[134] G. H. Golub and C. F. Van Loan, *Matrix computations*. JHU Press, 2012, vol. 3.

[135] R. Couillet and M. Debbah, *Random matrix methods for wireless communications*. Cambridge University Press, 2011.

[136] S. Govindasamy, D. W. Bliss, and D. H. Staelin, "Spectral Efficiency in Single-Hop Ad-Hoc Wireless Networks with Interference Using Adaptive Antenna Arrays," *IEEE Journal on Selected Areas in Communications*, vol. 25, no. 7, pp. 1358–1369, September 2007.

[137] C. Li, J. Zhang, and K. Letaief, "Throughput and energy efficiency analysis of small cell networks with multi-antenna base stations," *IEEE Transactions on Wireless Communications*, vol. 13, no. 5, pp. 2505–2517, 2014.

[138] H. Zhuang and T. Ohtsuki, "A Model Based on Poisson Point Process for Analyzing MIMO Heterogeneous Networks Utilizing Fractional Frequency Reuse," *IEEE Transactions on Wireless Communications*, vol. 13, no. 12, pp. 6839–6850, Dec 2014.

[139] W. Jouini, "Contribution to learning and decision making under uncertainty for Cognitive Radio." Ph.D. dissertation, CentraleSupélec, Jun. 2012.

[140] N. Cesa-Bianchi and G. Lugosi, *Prediction, Learning, and Games*. New York, NY, USA: Cambridge University Press, 2006.

[141] A. Lempel and J. Ziv, "On the complexity of finite sequences," *IEEE Trans. Inf. Theor.*, vol. 22, no. 1, pp. 75–81, Sep. 2006. [Online]. Available: http://dx.doi.org/10.1109/TIT.1976.1055501

[142] H. Urkowitz, "Energy detection of unknown deterministic signals," *Proceedings of the IEEE*, vol. 55, no. 4, pp. 523–531, April 1967.

[143] W. A. Gardner, "Signal interception: a unifying theoretical framework for feature detection," *IEEE Transactions on Communications*, vol. 36, no. 8, pp. 897–906, Aug 1988.

[144] N. Modi, P. Mary, and C. Moy, "Apprentissage machine orienté QoS pour l'accès opportuniste au spectre," in *XXVe Colloque GRETSI 2015*, Lyon, France, Sep. 2015, p. 4 pages.

[145] V. Anantharam, P. Varaiya, and J. Walrand, "Asymptotically efficient allocation rules for the multiarmed bandit problem with multiple plays-part ii: Markovian rewards," *Automatic Control, IEEE Transactions on*, vol. 32, no. 11, pp. 977–982, Nov 1987.

[146] C. Tekin and M. Liu, "Online learning in opportunistic spectrum access: A restless bandit approach," in *INFOCOM, 2011 Proceedings IEEE*. IEEE, 2011, pp. 2462–2470.

[147] H. Liu, K. Liu, and Q. Zhao, "Learning in a changing world: Restless multiarmed bandit with unknown dynamics," *IEEE Transactions on Information Theory*, vol. 59, no. 3, pp. 1902–1916, 2013.

[148] W. Jouini, D. Ernst, C. Moy, and J. Palicot, "Upper confidence bound based decision making strategies and dynamic spectrum access," in *International Conference on Communications, ICC'10*, May 2010.

[149] W. Jouini, C. Moy, and J. Palicot, "Decision making for cognitive radio equipment: analysis of the first 10 years of exploration," *EURASIP Journal on Wireless Communications and Networking*, vol. 2012, no. 26, Jan. 2012.

[150] P. Auer, N. Cesa-Bianchi, and P. Fischer, "Finite-time analysis of the multiarmed bandit problem," *Machine Learning*, vol. 47, no. 2-3, pp. 235–256, May 2002. [Online]. Available: http://dx.doi.org/10.1023/A:1013689704352

[151] C. Tekin and M. Liu, "Online learning of rested and restless bandits," *IEEE Transactions on Information Theory*, vol. 58, no. 8, pp. 5588–5611, Aug 2012.

[152] F. Fu and M. van der Schaar, "Learning to compete for resources in wireless stochastic games," *IEEE Transactions on Vehicular Technology*, vol. 58, no. 4, pp. 1904–1919, May 2009.

[153] Y. Xu, J. Wang, Q. Wu, A. Anpalagan, and Y. D. Yao, "Opportunistic spectrum access in unknown dynamic environment: A game-theoretic stochastic learning solution," *IEEE Transactions on Wireless Communications*, vol. 11, no. 4, pp. 1380–1391, April 2012.

[154] O. van den Biggelaar, J.-M. Dricot, P. De Doncker, and F. Horlin, "Sensing time and power allocation for cognitive radios using distributed q-learning," *EURASIP Journal on Wireless Communications and Networking*, vol. 2012, no. 1, pp. 1–12, 2012.

[155] N. Morozs, T. Clarke, D. Grace, and Q. Zhao, "Distributed q-learning based dynamic spectrum management in cognitive cellular systems: Choosing the right learning rate," in *2014 IEEE Symposium on Computers and Communications (ISCC)*, June 2014, pp. 1–6.

[156] K. Liu and Q. Zhao, "Cooperative game in dynamic spectrum access with unknown model and imperfect sensing," *IEEE Transactions on Wireless Communications*, vol. 11, no. 4, pp. 1596–1604, April 2012.

[157] D. Kalathil, N. Nayyar, and R. Jain, "Decentralized learning for multiplayer multiarmed bandits," *IEEE Transactions on Information Theory*, vol. 60, no. 4, pp. 2331–2345, April 2014.

[158] J. Oksanen and V. Koivunen, "An order optimal policy for exploiting idle spectrum in cognitive radio networks," *IEEE Transactions on Signal Processing*, vol. 63, no. 5, pp. 1214–1227, March 2015.

[159] J. Oksanen, V. Koivunen, and H. V. Poor, "A sensing policy based on confidence bounds and a restless multi-armed bandit model," *CoRR*, vol. abs/1211.4384, 2012.

[160] A. Anandkumar, N. Michael, A. K. Tang, and A. Swami, "Distributed algorithms for learning and cognitive medium access with logarithmic regret," *IEEE Journal on Selected Areas in Communications*, vol. 29, no. 4, pp. 731–745, April 2011.

[161] E. Oh, K. Son, and B. Krishnamachari, "Dynamic base station switching-on/off strategies for green cellular networks," *IEEE Transactions on Wireless Communications*, vol. 12, no. 5, pp. 2126–2136, May 2013.

[162] R. Li, Z. Zhao, Y. Wei, X. Zhou, and H. Zhang, "Gm-pab: A grid-based energy saving scheme with predicted traffic load guidance for cellular networks," in *2012 IEEE International Conference on Communications (ICC)*, June 2012, pp. 1160–1164.

[163] J. Gong, S. Zhou, and Z. Niu, "A Dynamic Programming Approach for Base Station Sleeping in Cellular Networks," *IEICE Transactions on Communications*, vol. 95, pp. 551–562, 2012.

[164] F. Han, Z. Safar, and K. J. R. Liu, "Energy-efficient base-station cooperative operation with guaranteed QoS," *IEEE Transactions on Communications*, vol. 61, no. 8, pp. 3505–3517, August 2013.

[165] R. Li, Z. Zhao, X. Chen, J. Palicot, and H. Zhang, "TACT: A transfer actor-critic learning framework for energy saving in cellular radio access networks," *IEEE Transactions on Wireless Communications*, vol. 13, no. 4, pp. 2000–2011, April 2014.

[166] V. R. Konda and V. S. Borkar, "Actor-critic–type learning algorithms for markov decision processes," *SIAM Journal on Control and Optimization*, vol. 38, no. 1, pp. 94–123, 1999.

[167] M. E. Taylor and P. Stone, "Transfer Learning for Reinforcement Learning Domains: A Survey," *Journal of Machine Learning Research*, vol. 10, no. 1, pp. 1633–1685, 2009.

[168] W.-T. Wong, Y.-J. Yu, and A.-C. Pang, "Decentralized energy-efficient base station operation for green cellular networks," in *Global Communications Conference (GLOBECOM), 2012 IEEE*, Dec 2012, pp. 5194–5200.

[169] W. Guo and T. O'Farrell, "Dynamic cell expansion with self-organizing cooperation," *IEEE Journal on Selected Areas in Communications*, vol. 31, no. 5, pp. 851–860, May 2013.

[170] E. Oh, B. Krishnamachari, X. Liu, and Z. Niu, "Toward dynamic energy-efficient operation of cellular network infrastructure," *IEEE Communications Magazine*, vol. 49, no. 6, pp. 56–61, June 2011.

[171] A. S. Alam, L. S. Dooley, and A. S. Poulton, "Traffic-and-interference aware base station switching for green cellular networks," in *2013 IEEE 18th International Workshop on Computer Aided Modeling and Design of Communication Links and Networks (CAMAD)*, Sept 2013, pp. 63–67.

[172] A. M. Alam, P. Mary, J.-Y. Baudais, and X. Lagrange, "Energy Efficiency-Area Spectral Efficiency Tradeoff in PPP Network with SLNR Precoder," in *The 17th IEEE International Workshop on Signal Processing Advances in Wireless Communications (SPAWC)*, vol. 17, 2016, p. 6.

[173] A.-M. Alam, P. Mary, J.-Y. Baudais, and X. Lagrange, "Compromis efficacités énergétique et spectrale du précodeur SLNR dans un réseau cellulaire aléatoire," in *XXVIe Colloque GRETSI 2017*, Juan-Les-Pins, France, Sep. 2017, p. 4 pages.

[174] N. Modi, P. Mary, and C. Moy, "Efficient learning in stationary and non-stationary osa scenario with qos guaranty," *EAI Endorsed Transactions on Wireless Spectrum*, vol. 17, no. 11, 1 2017.

[175] ——, "QoS driven channel selection algorithm for opportunistic spectrum access," in *IEEE Globecom 2015 Workshop on Advances in Software Defined Radio Access Networks and Context-aware Cognitive Networks (IEEE SDRANCAN 2015)*, San Diego, USA, Dec. 2015.

[176] N. Modi, C. Moy, P. Mary, and J. Palicot, *A New Evaluation Criteria for Learning Capability in OSA Context*. Cham: Springer International Publishing, 2016, pp. 3–14. [Online]. Available: http://dx.doi.org/10.1007/978-3-319-40352-6_1

[177] N. Modi, P. Mary, and C. Moy, "Apprentissage machine pour l'optimisation des réseaux cellulaires hétérogènes sans-fil : une approche bandit à bras multiples," in *XXVIe Colloque GRETSI 2017*, Juan-Les-Pins, France, Sep. 2017, p. 4 pages.

[178] R. Ahlswede, N. Cai, S.-Y. R. Li, and R. W. Yeung, "Network information flow," *IEEE Transactions on Information Theory*, vol. 46, no. 4, pp. 1204–1216, 2000.

[179] R. K. Ahuja, T. L. Magnanti, and J. B. Orlin, "Network flows," DTIC Document, Tech. Rep., 1988.

[180] S.-Y. R. Li, R. W. Yeung, and N. Cai, "Linear network coding," *IEEE Transactions on Information Theory*, vol. 49, no. 2, pp. 371–381, 2003.

[181] R. Koetter and M. Médard, "An algebraic approach to network coding," *IEEE/ACM Transactions on Networking (TON)*, vol. 11, no. 5, pp. 782–795, 2003.

[182] S. Jaggi, P. Sanders, P. Chou, M. Effros, S. Egner, K. Jain, L. M. Tolhuizen *et al.*, "Polynomial time algorithms for multicast network code construction," *IEEE Transactions on Information Theory*, vol. 51, no. 6, pp. 1973–1982, 2005.

[183] T. Ho, M. Médard, R. Koetter, D. R. Karger, M. Effros, J. Shi, and B. Leong, "A random linear network coding approach to multicast," *IEEE Transactions on Information Theory*, vol. 52, no. 10, pp. 4413–4430, 2006.

[184] C. Gkantsidis and P. R. Rodriguez, "Network coding for large scale content distribution," in *INFOCOM 2005. 24th Annual Joint Conference of the IEEE Computer and Communications Societies. Proceedings IEEE*, vol. 4. IEEE, 2005, pp. 2235–2245.

[185] S. Katti, H. Rahul, W. Hu, D. Katabi, M. Médard, and J. Crowcroft, "Xors in the air: practical wireless network coding," *IEEE/ACM Transactions on Networking (ToN)*, vol. 16, no. 3, pp. 497–510, 2008.

[186] Y. Zhu, B. Li, and J. Guo, "Multicast with network coding in application-layer overlay networks," *Selected Areas in Communications, IEEE Journal on*, vol. 22, no. 1, pp. 107–120, 2004.

[187] S. C. Liew, S. Zhang, and L. Lu, "Physical-layer network coding: Tutorial, survey, and beyond," *Physical Communication*, vol. 6, pp. 4–42, 2013.

[188] C. Robinson and P. Kumar, "Sending the most recent observation is not optimal in networked control: Linear temporal coding and towards the design of a control specific transport protocol," in *Decision and Control, 2007 46th IEEE Conference on*. IEEE, 2007, pp. 334–339.

[189] S. Ahmed and S. S. Kanhere, "Vanetcode: network coding to enhance cooperative downloading in vehicular ad-hoc networks," in *Proceedings of the 2006 international conference on Wireless communications and mobile computing*. ACM, 2006, pp. 527–532.

[190] L. Scalia, F. Soldo, and M. Gerla, "Piggycode: a mac layer network coding scheme to improve tcp performance over wireless networks," in *IEEE Global Telecommunications Conference, 2007. GLOBECOM'07*. IEEE, 2007, pp. 3672–3677.

[191] H. Guo, Y. Qian, K. Lu, and N. Moayeri, "The benefits of network coding over a wireless backbone," in *Global Telecommunications Conference, 2009. GLOBECOM 2009. IEEE*. IEEE, 2009, pp. 1–6.

[192] T. Ohira and R. Sawatari, "Phase transition in a computer network traffic model," *Physical Review E*, vol. 58, no. 1, p. 193, 1998.

[193] B. Haeupler, M. Kim, and M. Médard, "Optimality of network coding with buffers," *IEEE Information Theory Workshop (ITW)*, pp. 533–537, 2011.

[194] W. Chen, K. B. Letaief, and Z. Cao, "Buffer-aware network coding for wireless networks," *IEEE/ACM Transactions on Networking*, vol. 20, no. 5, pp. 1389–1401, 2012.

[195] A. G. Dimakis, P. Godfrey, Y. Wu, M. J. Wainwright, and K. Ramchandran, "Network coding for distributed storage systems," *IEEE Transactions on Information Theory*, vol. 56, no. 9, pp. 4539–4551, 2010.

[196] S. Abdul-Nabi, P. Mary, J. F. Hélard, and A. Khalil, "Fault-tolerant minimal retransmission mechanism with network coding," in *2015 23rd International Conference on Software, Telecommunications and Computer Networks (SoftCOM)*, Sept 2015, pp. 148–152.

[197] S. Weber and J. Andrews, "Transmission capacity of wireless networks," in *Foundations and Trends in Networking*. NOW Publishers, 2012, vol. 5.

[198] J. Andrews *et al.*, "Rethinking information theory for mobile ad hoc networks," *Communications Magazine, IEEE*, vol. 46, no. 12, pp. 94–101, 2008.

[199] A. Goldsmith, M. Effros, R. Koetter, M. Médard, A. Ozdaglar, and L. Zheng, "Beyond shannon: the quest for fundamental performance limits of wireless ad hoc networks," *Communications Magazine, IEEE*, vol. 49, no. 5, pp. 195–205, 2011.

[200] V. Y. Tan and O. Kosut, "On the dispersions of three network information theory problems," *Information Theory, IEEE Transactions on*, vol. 60, no. 2, pp. 881–903, 2014.

[201] J. M. Gorce, H. V. Poor, and J. M. Kelif, "Spatial Continuum Model: Toward the Fundamental Limits of Dense Wireless Networks," in *2016 IEEE Global Communications Conference (GLOBECOM)*, Dec 2016, pp. 1–6.

[202] M. Egan, M. de Freitas, L. Clavier, A. Goupil, G. Peters, and N. Azzaoui, "Achievable rates for additive isotropic α-stable noise channels," in *2016 IEEE International Symposium on Information Theory (ISIT) (ISIT'2016)*, Barcelona, Spain, Jul. 2016.

[203] E. MolavianJazi, "A unified approach to gaussian channels with finite blocklength," Ph.D. dissertation, University of Notre Dame, July 2014.

[204] E. Kaufmann, "Analysis of bayesian and frequentist strategies for sequential resource allocation," Theses, Télécom ParisTech, Oct. 2014.

[205] V. F. Farias, C. C. Moallemi, B. V. Roy, and T. Weissman, "Universal Reinforcement Learning," *IEEE Transactions on Information Theory*, vol. 56, no. 5, pp. 2441–2454, May 2010.

[206] S. Still and D. Precup, "An information-theoretic approach to curiosity-driven reinforcement learning," *Theory in Biosciences*, vol. 131, no. 3, pp. 139–148, Sep 2012.

[207] N. Tishby and D. Polani, *Information Theory of Decisions and Actions*. New York, NY: Springer New York, 2011, pp. 601–636.

[208] J. D. Jackson, *Classical Electrodynamics*, 4th ed. New York, USA: Wiley, 1965.

[209] R. A. Beth, "Mechanical detection and measurement of the angular momentum of light," *Phys. Rev.*, vol. 50, no. 2, pp. 115–125, 1936.

[210] B. Thidé, H. Then, J. Sjöholm, K. Palmer, J. E. S. Bergman, T. D. Carozzi, Y. N. Istomin, N. H. Ibragimov, and R. Khamitova, "Utilization of photon orbital angular momentum in the low frequency radio domain," *Physical Review Letters*, vol. 99, no. 8, Aug. 2007.

[211] S. M. Mohammadi, L. K. S. Daldorff, J. E. S. Bergman, R. L. Karlsson, B. Thidé, K. Forozesh, T. D. Carozzi, and B. Isham, "Orbital angular momentum in radio – a system study," *IEEE Transactions on Antennas and Propagation*, vol. 58, no. 2, pp. 565–572, Feb. 2010.

[212] S. M. Mohammadi, L. K. S. Daldorff, K. Forozesh, B. Thidé, J. E. S. Bergman, B. Isham, R. L. Karlsson, and T. D. Carozzi, "Orbital angular momentum in radio: Measurement methods," *Radio Science*, vol. 45, Jul. 2010.

[213] O. Edfors and A. J. Johansson, "Is orbital angular momentum (OAM) based radio communication an unexploited area?" *IEEE Transactions on Antennas and Propagation*, vol. 60, no. 2, Feb. 2012.

[214] F. Tamburini, E. Mari, A. Sponselli, B. ThidÃľ, A. Bianchini, and F. Romanato, "Encoding many channels on the same frequency through radio vorticity: first experimental test," *New Journal of Physics*, vol. 14, no. 3, p. 033001, 2012.

[215] O. Emile, C. Brousseau, J. Emile, R. Niemiec, K. Madhjoubi, and B. Thidé, "Electromagnetically induced torque on a large ring in the microwave range," *Phys. Rev. Lett.*, vol. 112, no. 5, p. 053902, February 2014.

[216] M. Tamagnone, J. S. Silva, S. Capdevila, J. R. Mosig, and J. Perruisseau-Carrier, "The orbital angular momentum (OAM) multiplexing controversy: OAM as a subset of MIMO," in *2015 9th European Conference on Antennas and Propagation (EuCAP)*, May 2015, pp. 1–5.

[217] A. Haskou, P. Mary, and M. Hélard, "Error probability on the orbital angular momentum detection," in *2014 IEEE 25th Annual International Symposium on Personal, Indoor, and Mobile Radio Communication (PIMRC)*, Sept 2014, pp. 302–307.

[218] P. Mary, A. Haskou, and C. Brousseau, "Method for Transmitting a Sequence of Data Symbols, Transmission Device, Signal, Receiving Method, Corresponding Receiving Device and Corresponding Computer Program," November 2013, patent, no WO2015079020A1; FR3014271A1.

[219] I. B. Djordjevic, "LDPC-coded OAM modulation and multiplexing for deep-space and near-Earth optical communications," in *2011 International Conference on Space Optical Systems and Applications (ICSOS)*, May 2011, pp. 325–333.

[220] I. B. Djordjevic and M. Arabaci, "LDPC-coded orbital angular momentum (OAM) modulation for free-space optical communication," *Opt. Express*, vol. 18, no. 24, pp. 24 722–24 728, Nov 2010.

[221] Y. Zeng and R. Zhang, "Millimeter Wave MIMO With Lens Antenna Array: A New Path Division Multiplexing Paradigm," *IEEE Transactions on Communications*, vol. 64, no. 4, pp. 1557–1571, April 2016.

[222] O. Ertug, "Communication over Hypercomplex Kähler Manifolds: Capacity of Dual-Polarized Multidimensional-MIMO Channels," in *2006 International Symposium on Information Theory and Its Applications (ISITA)*, Oct 2016, pp. 106–110.